

# **From natural scaffolds to detailed drug-target interactions on biogenic amines**

Inaugural-Dissertation

zur Erlangung des Doktorgrades  
der Mathematisch-Naturwissenschaftlichen Fakultät  
der Heinrich-Heine-Universität Düsseldorf

vorgelegt von

**Annika Frank**  
aus Bergisch Gladbach

Düsseldorf, Oktober 2019

---

aus dem Institut für Pharmazeutische und Medizinische Chemie  
der Heinrich-Heine-Universität Düsseldorf

Gedruckt mit der Genehmigung der  
Mathematisch-Naturwissenschaftlichen Fakultät der  
Heinrich-Heine-Universität Düsseldorf

Berichterstatter:

1. Prof Dr. Dr. h.c. Holger Stark

2. Prof. Dr. Holger Gohlke

Tag der mündlichen Prüfung:

17.12.2019



---

*Devoted to*

*my parents*

*Angelika and Detlev Schank*

*and to*

*my husband*

*Marian Frank*

---

*„Die Neugier ist die mächtigste Antriebskraft im Universum, weil sie die beiden größten Bremskräfte im Universum überwinden kann: die Vernunft und die Angst.“*

*-Walter Moers*

## Table of contents

Table of contents .....	I
A Abstract .....	1
A Zusammenfassung .....	2
1 General introduction and theoretical background .....	3
1.1 Biogenic amines in drug development .....	3
1.1.1 Drug-target interactions of biogenic amines at GPCRs .....	5
1.1.2 Scaffold evaluation in the field of biogenic amines .....	8
1.2 Selected biogenic amines .....	10
1.2.1 Histamine and its receptors .....	10
1.2.2 Dopamine and its receptors .....	15
1.3 Biogenic amines in Parkinson's disease .....	20
1.4 Novel aspects of drug-target interactions at the example of schizophrenia .....	22
1.5 Drug-target residence time in schizophrenia .....	24
2 Scope and objectives .....	26
3 From medicinal plant extracts to defined chemical compounds targeting the histamine H <sub>4</sub> receptor: Curcuma longa in the treatment of inflammation .....	27
4 New lead elements for histamine H <sub>3</sub> receptor ligands in the pyrrolo[2,3-d]pyrimidine class...	35
5 Nature-inspired pyrrolo[2,3-d]pyrimidines targeting the histamine H <sub>3</sub> receptor .....	61
6 Studies on anticonvulsant effects of novel histamine H <sub>3</sub> R antagonists in electrically and chemically induced seizures in rats .....	91
7 Talipexole variations as novel bitopic dopamine D <sub>2</sub> and D <sub>3</sub> receptor ligands .....	116
8 Prior activation of 5-HT <sub>7</sub> receptors modulates the conditioned place preference with methylphenidate .....	121
9 Binding kinetics of cariprazine and aripiprazole at the dopamine D <sub>3</sub> receptor .....	136
10 Conclusions and prospects .....	148
11 List of abbreviations .....	155
12 Research contributions .....	158
13 References for chapters 1-2 & 10 .....	160
14 Acknowledgement .....	177
15 Declaration of academic honesty .....	180
16 Curriculum vitae .....	181
17 Published research .....	183

## A Abstract

Neurodegenerative diseases gathered high attention, although limited knowledge regarding pathogenesis, drug-target interactions and limited scaffold variations present a serious challenge for drug development. This cumulative thesis describes the preclinical evaluation of novel compounds directed at aminergic G protein-coupled receptors and the development of a novel *in vitro* evaluation tool for drug-target interactions. Compounds include natural products as well as synthetic small molecules that were tested for *in vitro* affinity at histamine, dopamine and serotonin receptor subtypes in radioligand displacement assays.

The therapeutic utility of curcumin extracts for the treatment of inflammatory diseases was evaluated at the so far neglected histamine H<sub>4</sub> receptor (H<sub>4</sub>R) and three natural compounds were found as rare non-amine scaffolds (chapter 3). By screening of a series of novel pyrrolo[2,3*d*]pyrimidines, inspired by natural products, their selectivity for the histamine H<sub>3</sub> receptor (H<sub>3</sub>R) became apparent and was supported by *in silico* studies (chapter 4). Because this is a novel scaffold class for the target, structural modifications based on known H<sub>3</sub>R ligands were performed. The new series displayed improved receptor affinity and provides a novel lead class of H<sub>3</sub>R ligands (chapter 5). *In vitro* evaluation of (homo)piperidine ether derivatives confirmed affinity at the H<sub>3</sub>R and the compounds were thus considered for *in vivo* testing that revealed a promising preclinical agent for the treatment of epilepsy (chapter 6).

The combination of a known dopamine receptor scaffold (in this case talipexole) with derivatization patterns such as (2,3-dichlorophenyl)piperazines or (2-methoxyphenyl)piperazines resulted in a small series of novel bitopic ligands targeting the dopamine D<sub>2</sub> and D<sub>3</sub> receptors (D<sub>2</sub>/D<sub>3</sub>Rs) (chapter 7). They were designed with bioisosteric exchange of catechol moieties with aminothiazoles in mind and two compounds displayed improved binding affinity at D<sub>2</sub>/D<sub>3</sub>Rs compared to talipexole. A 1-(5-fluoro-4'-methoxy-[1,1'-biphenyl]-2-yl)piperazine derivative (TP-22) was recently discovered as serotonin 5-HT<sub>7</sub> receptor agonist and was now identified to be a potent ligand at dopamine D<sub>1</sub> and D<sub>5</sub> receptors, contributing to mode of action studies (chapter 8). To complement *in vitro* drug profiling of novel compounds, a drug-target residence time assay at D<sub>2</sub>/D<sub>3</sub>R was developed (chapter 9). Evaluation at the D<sub>3</sub>R revealed unusual dissociation of the recently marketed cariprazine, which was confirmed via dynamic modelling *in silico*.

The evaluated compounds expand their respective scaffold libraries and will ultimately increase discovery chances for successful clinical agents. Most importantly, the exploration of novel drug design approaches such as specific residence times grants pharmacological tools to improve our understanding of drug-target interactions.

### A Zusammenfassung

Neurodegenerative Erkrankungen gewinnen an Interesse, obwohl begrenztes Wissen in Bezug auf Pathogenese, Arzneistoff-Zielstruktur-Interaktionen und eingeschränkte Arzneistoffgerüst-Variationen eine ernst zu nehmende Hürde für die Arzneistoffentwicklung darstellt. Diese kumulative Dissertation beschreibt die präklinische Evaluierung neuer Verbindungen, die gegen aminerge G-Protein-gekoppelte Rezeptoren gerichtet sind und die Entwicklung eines neuartigen *in vitro* Evaluierungstools von Arzneistoff-Zielstruktur-Interaktionen. Die Verbindungen beinhalten Naturstoffe und synthetische niedermolekulare Verbindungen, die in Radioliganden-Bindungsstudien auf *in vitro* Affinität zu Histamin-, Dopamin- und Serotonin-Rezeptor-Subtypen getestet wurden.

Der therapeutische Einsatz von Curcumin Extrakten in der Behandlung inflammatorischer Erkrankungen wurde am bisher vernachlässigten Histamin-H<sub>4</sub>-Rezeptor (H<sub>4</sub>R) evaluiert und drei Naturstoffe wurden als seltene, nicht-Amin-Grundgerüst identifiziert (Kapitel 3). Testung einer Reihe neuartiger Pyrrolo[2,3d]pyrimidine, inspiriert durch Naturstoffe, zeigte H<sub>3</sub>-Rezeptor (H<sub>3</sub>R)-Selektivität, was durch *in silico* Studien bestätigt wurde (Kapitel 4). Da dies ein neues Grundgerüst für diese Zielstruktur darstellt, wurden Strukturmodifikationen anhand bekannter H<sub>3</sub>R-Liganden durchgeführt. Die neue Serie wies verbesserte Rezeptor-Affinität auf und liefert eine neue Leitstruktur für H<sub>3</sub>R-Liganden (Kapitel 5). *In vitro* Evaluierung von (homo)Piperidine-Ether-Derivaten bestätigte H<sub>3</sub>R-Affinität und die Verbindungen wurden für *in vivo* Testung vorgeschlagen, die einen vielversprechenden präklinischen Kandidaten zur Therapie der Epilepsie hervorbrachten (Kapitel 6).

Die Kombination bekannter Dopamin-Rezeptor-Ligandengerüste (in diesem Fall Talipexol) mit Derivatisierungs-Mustern wie (2,3-Dichlorophenyl)piperazinen oder (2-Methoxyphenyl)piperazinen resultierte in einer kleinen Reihe neuartiger bitopischer Liganden, die sich gegen Dopamin D<sub>2</sub>- und D<sub>3</sub>-Rezeptoren (D<sub>2</sub>/D<sub>3</sub>R) richten (Kapitel 7). Sie wurden vor dem Hintergrund des bioisosteren Austauschs der Catechol-Struktur durch Amino-thiazole entwickelt und zwei Verbindungen zeigten erhöhte D<sub>2</sub>/D<sub>3</sub>R-Affinität im Vergleich zu Talipexol. Ein 1-(5-Fluoro-4'-methoxy-[1,1'-biphenyl]-2-yl)piperazine-Derivat (TP-22) wurde kürzlich als Serotonin 5-HT<sub>7</sub>-Rezeptor-Agonist entdeckt und nun als potenter Ligand an D<sub>1</sub>- und D<sub>5</sub>-Rezeptoren identifiziert, was Wirkmechanismus-Studien unterstützt (Kapitel 8). Um *in vitro* Evaluierung neuartiger Verbindungen zu ergänzen, wurde ein Assay zur Bestimmung der Arzneistoff-Zielstruktur-Besetzungsdauer an D<sub>2</sub>/D<sub>3</sub>R entwickelt (Kapitel 9). Evaluierung am D<sub>3</sub>R zeigte eine ungewöhnliche Dissoziation des kürzlich zugelassenen Arzneistoffs Cariprazin, die durch dynamische Simulation *in silico* bestätigt werden konnte.

Die evaluierten Verbindungen bereichern ihre jeweilige Grundgerüst-Bibliothek und erhöhen letztlich die Entdeckungschance erfolgreicher klinischer Liganden. Vor Allem ermöglicht die Erforschung neuartiger Entwicklungs-Ansätze, wie spezifischer Besetzungsdauern, pharmakologische Werkzeuge die unser Verständnis der Arzneistoff-Zielstruktur-Interaktionen vertiefen.

## 1 General introduction and theoretical background

### 1.1 Biogenic amines in drug development

Biogenic amines are a heterogeneous group consisting of amines, derived from *de-novo* synthesis, (endogenic amines), decarboxylation of endogenic amino acids or from decarboxylation of exogenic amino acids (exogenic amines) (Jairath et al., 2015). They include heterocyclic and/or aromatic amines such as histamine, tryptamine, serotonin, dopamine, tyramine and phenylethylamine (Figure 1) as well as aliphatic amines (e. g. spermidine, cadaverine, ethylamine) (Erdag et al., 2018; Jairath et al., 2015). Biogenic amines can have precursor functions for essential biochemical structures (e. g. dopamine for noradrenaline) (Meiser et al., 2013) or can be products of protein catabolism (e. g. cadaverine) (Ioan et al., 2017). Besides involvement in metabolism, they can also display biological activities (Schildkraut, Kety, 1967). This work will focus on biogenic amines that act as neurotransmitters. Dopamine was originally considered to be the precursor for adrenaline and noradrenaline (Fahn, 2008). Its function as neurotransmitter was only discovered in the 1960s and today it is a neurophysiological key player (Fahn, 2008; Jaber et al., 1996). Histamine was identified early as a bioactive amine involved in peripheral and central processes. The discovery of the histamine H<sub>3</sub> receptor, mainly expressed in the central nervous system (CNS), emphasized histamine's regulatory function (Arrang et al., 1983; Emanuel, 1999; Haas et al., 2008). Bioactive biogenic amines evoke their pharmacological effects through interaction with a variety of targets such as G protein-coupled receptors (GPCRs), ion channels or metabolic enzymes such as monoamine oxidases (Frederick, Stanwood, 2009; Rudnick, Clark, 1993). Imbalances in biogenic amine levels are a key factor in many pathophysiological processes, e.g. dopamine in schizophrenia (Abi-Dargham et al., 2000) or histamine in inflammation (Kubes, Kanwar, 1994). Hence, they provide valid targets for drug development in numerous application fields (Aral et al., 1984; Frederick, Stanwood, 2009; Maas, 1975). By designing structural analogues, it is possible to compensate pathophysiological imbalances or modulate their pharmacological responses. Most of these analogous compounds are small molecules, as they mimic the naturally occurring biogenic amines (Figure 1).

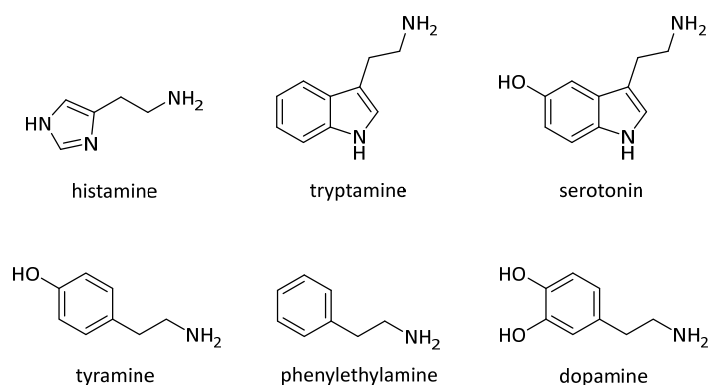


Figure 1: Chemical structures of selected biogenic amines.

## 1.1 Biogenic amines in drug development

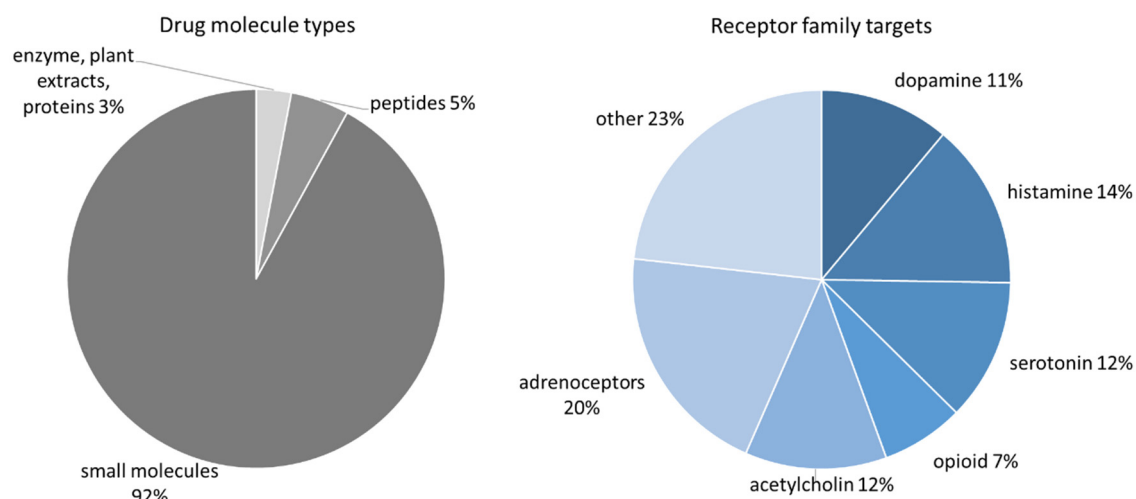


Figure 2: Approved drug's molecule types and receptor family targets among GPCRs. Modulated after GPCRdb and Hauser (Hauser et al., 2017).

Design and synthesis of small molecules is rather straightforward and they constitute a rewarding outcome in drug development approaches (Schreiber, 2000). Additionally they promise good biological activity and display high drug-likeness (Lipinski et al., 2001). For those reasons more than 90% of approved drugs, targeted towards GPCRs, are small molecules and 37% of those target dopamine, histamine or serotonin receptor subtypes (Figure 2) (Hauser et al., 2017). Through the advances in X-ray crystallography, many molecular targets were identified and elucidated from a structural point of view (Cherezov et al., 2007; Shimamura et al., 2011; Wang et al., 2018). This gave novel insights into drug-target interactions (Chien et al., 2010) and allowed for more accurate “virtual screenings” (Lionta et al., 2014; Sabatucci et al., 2018). When combined with comprehensive *in vitro* hit-compound libraries, these studies grant useful information for the evaluation of structure-activity relationships (SARs), the design of novel scaffolds and on the basics of target modulation by biogenic amines.

### 1.1.1 Drug-target interactions of biogenic amines at GPCRs

Modulating biological responses by targeting aminergic GPCRs has become a major aspect in drug design, with 35% market share for this target class (Sriram, Insel, 2018). Based on the evaluation of genetic and structural homology, they are divided in class A (rhodopsin-like), class B (secretin-like), class C (glutamate-like) and Adhesion and Frizzled/Taste GPCRs (Fredriksson et al., 2003). This work will focus on the most common class A. Structurally, they consist of seven transmembrane domains (TMDs, Figure 3) that usually form a pore, where ligands can enter towards the orthosteric binding site (OBS) and other interaction sites (Venkatakrishnan et al., 2013). The OBS in aminergic GPCRs offers a highly conserved aspartate residue in TMD3 that interacts with the biogenic amines, which are positively charged under physiological conditions (Huang, 2003). A so-called “ionic lock”, polar interactions between the E/DRY motif (glutamic acid/aspartic acid, arginine, tyrosine) of TMD3 and amino acids on TMD6, stabilizes the inactive receptor state (Vogel et al., 2008). The TMDs are connected by three extracellular loops (ECLs), three intracellular loops (ICLs) as well as an extracellular amino and an intracellular carboxyl terminus (Figure 3) (Latorraca et al., 2017). The ECLs, especially ECL2, contribute to binding interactions in a distinctive way for each receptor families (Venkatakrishnan et al., 2013; Wheatley et al., 2012). So far only a disulfide bond between ECL2 and Cys<sup>3.25</sup> in TMD3 was discovered as a common feature (Shi, Javitch, 2004; Wheatley et al., 2012). This high structural diversity is probably one of the reasons for ligand specificity among GPCRs as there is evidence for its modulation of drug-target interactions (Wheatley et al., 2012). Among the ICLs ICL3 stands out, as it provides most structural diversity and is thought as one of the modulators of G protein selectivity for different GPCRs (Katritch et al., 2012). Binding of activating ligands results in conformational changes of the receptor (e.g. outward shift of TMD6). This leads to intracellular recruitment of G proteins, which consist of one  $\alpha$ -subunit ( $G\alpha$ ) and a dimeric  $\beta\gamma$ -subunit ( $G\beta\gamma$ ) (Hilger et al., 2018). Both subunits are responsible for further intracellular signal cascades after receptor activation, following their dissociation and exchange of guanosine di- by triphosphate (GDP/GTP) (Hilger et al., 2018).

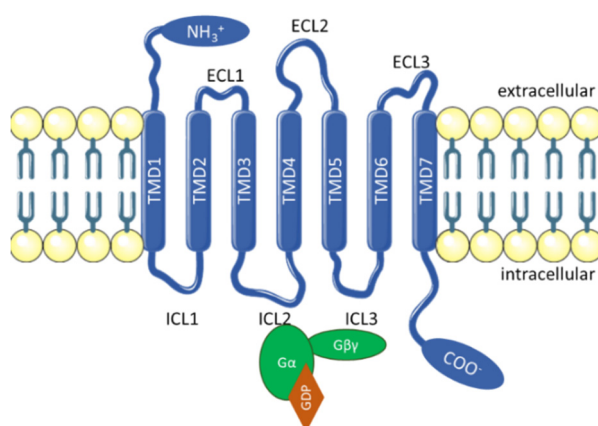


Figure 3: Schematic representation of GPCRs and G proteins



### 1.1.1 Drug-target interactions of biogenic amines at GPCRs

G proteins are divided into  $G_s$ ,  $G_i/G_o$ ,  $G_q$  and  $G_{12/13}$  (Elefsinioti et al., 2004; Syrovatkina et al., 2016).  $G_s$  coupled proteins stimulate the adenylyl cyclase (AC), leading to an increase in 3',5'-cyclic adenosine monophosphate (cAMP) concentration, thereby increasing the activity of protein kinase A (PKA) (Milligan, Kostenis, 2006).  $G_i$  coupled proteins lead to a decreased activity of the AC and hence a less activated PKA (Marinissen, Gutkind, 2001). By addressing  $G_q$ , the phospholipase C- $\beta$  (PLC $\beta$ ) is activated, increasing levels of inositol (1,4,5)-trisphosphate (IP3) and diacylglycerol (DAG), followed by calcium ion ( $Ca^{2+}$ ) release and protein kinase C (PKC) activation, respectively (Billups et al., 2006).  $G_{12/13}$  proteins are less common (Syrovatkina et al., 2016).  $G\beta\gamma$  are able to influence  $Ca^{2+}$  and potassium ion ( $K^+$ ) channels, AC and PLC $\beta$  (Hilger et al., 2018). This signal diversity is amplified, because the biological effects of GPCRs are also controlled by G protein independent mechanisms such as  $\beta$ -arrestin recruitment (DeWire et al., 2007). In order to prevent overexcitation, intracellular receptor sides can be phosphorylated by GPCR kinases, tagging the receptor for  $\beta$ -arrestin recruitment that leads to disruption of the GPCR-G protein complex (Grady et al., 1997) and receptor internalization (Grady et al., 1997; Marinissen, Gutkind, 2001). Latest research revealed that  $\beta$ -arrestins are also able to coordinate members of the mitogen-activated protein kinase (MAPK) pathway. By recruiting a tyrosine kinase (c-SRC) to the receptor, they can indirectly initiate the activation of ERK (DeWire et al., 2007; Luttrell et al., 1999). The two known isoforms  $\beta$ -arrestin 1 and 2 act as chaperone molecules that facilitate interaction of members of the ERK, JNK3 or p38 pathways by spatial orientation or initiate activation by direct phosphorylation (DeWire et al., 2007). The spectrum of known targets that are influenced by  $\beta$ -arrestins is rapidly increasing, including other kinases and even nuclear responses (DeWire et al., 2007; Povsic et al., 2003; Witherow et al., 2004). An implication of these  $\beta$ -arrestin mediated pathways in drug action was shown for example with antipsychotic agents (Allen et al., 2011). However, the applicability for drug design remains a topic of high interest.

The sheer diversity of GPCRs and proteins involved in the signal cascade is challenging for the evaluation of drug-target interactions, but gets more complex by the existence of different ligand types. Receptor agonists bind to the receptor and evoke the same response as the endogenous ligand. Neutral antagonists block the receptor's binding site, so that the endogenous ligand is unable to evoke its physiological response (Pleuvry, 2004). Either way, a pathophysiological dysregulation can be compensated. While agonists preferably stabilize an active state of the receptor and shift the active/inactive population ratio towards more active receptors (Figure 4A), antagonists prevent binding of other ligands without altering the ratio (Weis, Kobilka, 2018). Several GPCRs exhibit a basal receptor activity even in absence of agonists, a term referred to as constitutive activity (Sadée et al., 2005; Smit et al., 1996). Ligands that reverse this basal activity, stabilize an inactive receptor state and shift the population ratio accordingly are considered inverse agonists (Figure 4A) (Weis, Kobilka, 2018).

### 1.1.1 Drug-target interactions of biogenic amines at GPCRs

Many ligands, which have been formerly described as antagonists are now considered inverse agonists (Bakker et al., 2000; Chidiac et al., 1994). Partial agonists lead to an activation of the receptor, but do not evoke full receptor response, when compared to the endogenous ligand (lower intrinsic activity) (Lawler et al., 1999). However, when directly competing with a full agonist, they behave as functional antagonist due to competition for the binding site (Lieberman, 2004). Biased agonist can activate different signal cascades (GPCR dependent and independent) with different intensity and functionality (Berg, Clarke, 2018). It has to be noted that these classifications can depend on the assay conditions and different set-ups can yield different results for a given ligand (Berg, Clarke, 2018).

The evaluation of GPCR crystal structures (Chien et al., 2010; Shimamura et al., 2011; Wang et al., 2018) confirmed the existence of allosteric binding sites (ABSs) and secondary binding pockets (SBPs). ABSs are regions of a protein where ligands can bind and change receptor confirmation, thereby positively or negatively influencing other ligands in their binding to the OBS (Figure 4B) (Changeux et al., 1984). SBPs are binding pockets on the extracellular side of the protein or in proximity to the OBS that can further contribute to drug-target interactions (Ludlow et al., 2015). Compounds directed at the ABS or the SBP instead of the highly conserved OBS, are discussed to have increased chances of displaying higher selectivity and subtype specificity (Fronik et al., 2017; Lane et al., 2013). This can be realised by designing ligands that address the OBS and SBP simultaneously (bitopic ligands, Figure 4C) (Kühhorn et al., 2011). The presented drug-target interactions are not only valuable for the design of new compounds, but also require re-evaluation of currently used evaluation methods.

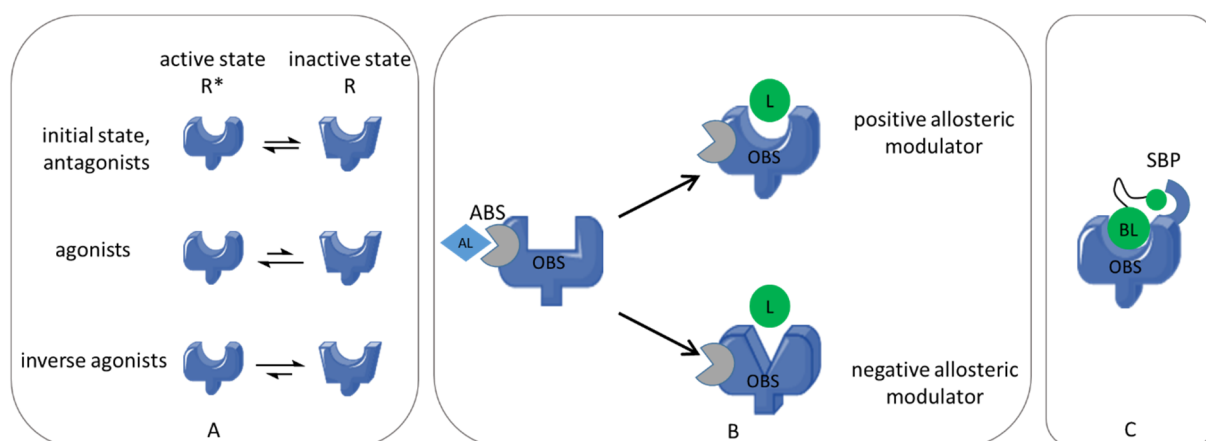


Figure 4: Schematic aspects of drug-target interactions at GPCRs. (A) Influence on receptor states by agonists, inverse agonists and antagonist. (B) Allosteric modulation, ABS: allosteric binding site, AL: allosteric ligand, L: ligand, OBS: orthosteric binding site,. (C) Representation of a secondary binding pocket (SBP), BL: bitopic ligand.

### 1.1.2 Scaffold evaluation in the field of biogenic amines

Because insights into crystal structures, binding behaviour and target modulation are rapidly growing, a constant need exists to expand scaffold libraries of clinically active compounds and to understand underlying biomolecular mechanisms via pharmacological tools. Early stages of aminergic drug development can be inspired by the scaffold of the endogenous ligands themselves (Bleicher et al., 2003; Mocking et al., 2016). Derivatization of serotonin resulted for example in sumatriptan, used in the treatment of migraines (Figure 5) (McCrory, Gray, 2003). However, such compounds may be prone to adverse drug effects due to a high analogy to the endogenous ligands and poor receptor selectivity. Furthermore, endogenous ligands can display metabolic weak points (e.g. susceptibility to oxidation of the catechol structure in dopamine (Segura-Aguilar et al., 2014)) that usually limit therapeutic application of closely related derivatives. Hence, moieties with improved binding affinity or selectivity, optimized pharmacokinetics as well as superior clinical efficacy and safety are emphasized. Natural compounds display large structural heterogeneity, are easily accessible and provide high hit rates in *in vitro* screenings as they inherit a biological activity for their hosts (Breinbauer et al., 2002). For example, ergotamine, isolated from *Claviceps purpurea*, interacts with serotonin and dopamine receptors and its vasoactive properties have been successfully used in the treatment of migraine (Graham, Wolff, 1938). Nowadays, therapy limiting cardiac effects call a use of this drug into question (Meyler, 1996). The synthetic derivatization towards bromocriptine (Figure 5) led to a dopamine and serotonin receptor agonist, still used in the treatment of Parkinson's disease (Lieberman et al., 1976). The combination of endogenous scaffolds, natural compound libraries and the possibilities of synthetic derivatization yields a reasonable approach to expand compound libraries at a given target (Bleicher et al., 2003). It has to be noted that many diseases are not exclusively related to one specific biogenic amine but are rather multifactorial in nature (de Strooper, 2010; Riess, Krüger, 1999). Hence, for some applications, the research became focused on compounds that act on a particular set of different targets (Morphy et al., 2004). The fusion of two pharmacophores (Figure 5) generates a novel scaffold that requires affinity at the selected receptors and selectivity towards adverse targets. However, this attempt displays new challenges, as the design and evaluation of these drugs can take more effort than previously, as seen with the extensive evaluation for bromocriptine (Figure 5) (Morphy, Rankovic, 2006).

In order to find new clinical entities, initial leads can be found in high- to medium-throughput assays of (natural) compound libraries (Bleicher et al., 2003) or by rational re-evaluation of plant extracts and drugs that are known for their action in another application field (drug repositioning) (Pushpakom et al., 2018). By combining the results of *in vitro* screenings with *in silico* structure-based drug design, hit compounds can be optimized and characterized once more *in vitro* for novel leads in an iterative

### 1.1.2 Scaffold evaluation in the field of biogenic amines

process (Klebe, 2000). Preclinical lead compounds should then be evaluated in appropriate *in vivo* models. The joined expertise of drug researchers results in the development of a preclinical agent awaiting its clinical prospects. The better knowledge on drug-target interactions is gathered, the higher are the demands for clinical agents and pharmacological tools. Hence, assay design, scaffold design and evaluation are major topics for researchers in drug development as well as in basic target research.

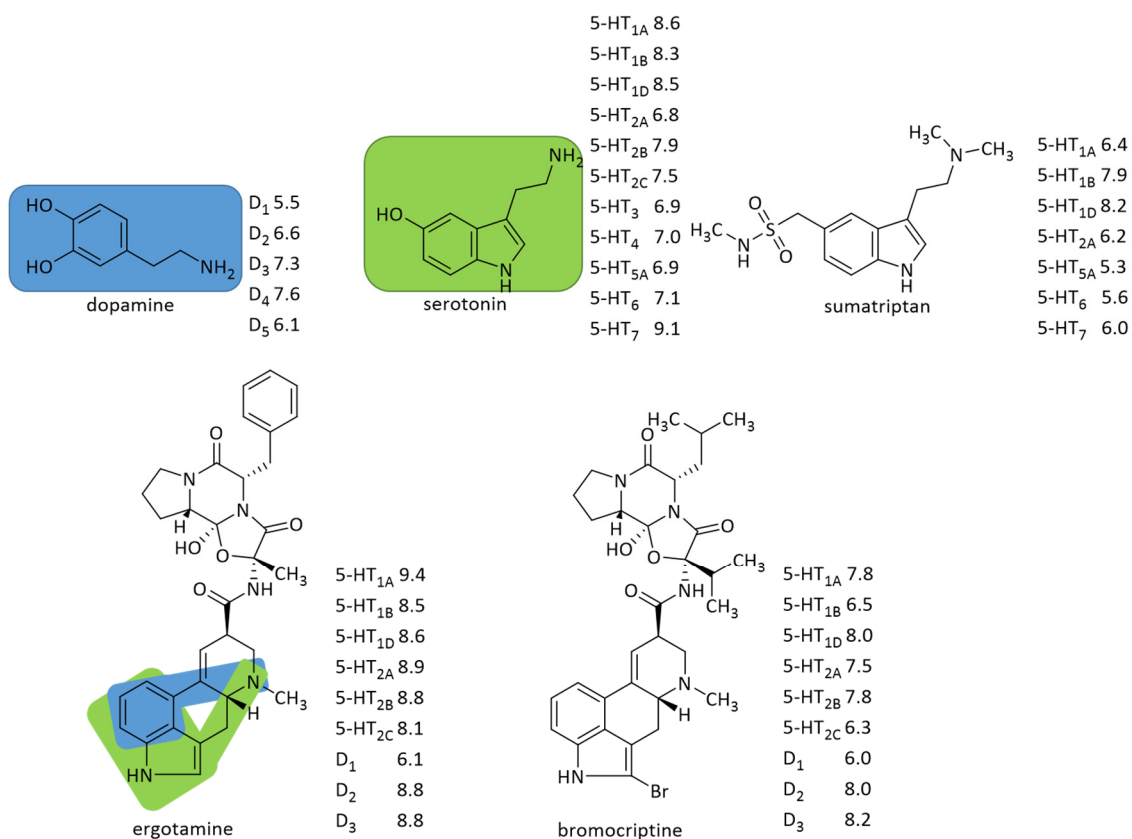


Figure 5: Structures of natural products and synthetic derivatives. Values are median  $pK_i$  values at the respective targets obtained from the IUPHAR DB (Harding et al., 2018). Blue and green boxes represent respective scaffolds that can be found in multi-target-directed ligands.

## 1.2 Selected biogenic amines

### 1.2.1 Histamine and its receptors

Histamine (2-(1*H*-imidazol-4-yl)ethan-1-amine) orchestrates a wide array of effects, taking an active part in the CNS, immune modulation and peripheral processes. It is derived by decarboxylation of the amino acid L-histidine exclusively via the L-histidine decarboxylase (Figure 6) and is metabolized by *N*-methyltransferase to *N*<sup>ε</sup>-methylhistamine (Shahid et al., 2009). Monoamine oxidase lead to subsequent oxidative deamination in the CNS, while diamine oxidase is mainly responsible for peripheral metabolism of histamine (Green et al., 1987; Mondovi et al., 2013). It exerts its pharmacological effects via four class A GPCRs (Table 1) (Bongers et al., 2010). While H<sub>1</sub>, H<sub>2</sub> and H<sub>3</sub> receptors are expressed in various brain regions, the existence of H<sub>4</sub> receptors (H<sub>4</sub>Rs) in the brain is still a topic of debate (Connelly et al., 2009; Haas, Panula, 2016). However, all four receptors are abundantly expressed in the periphery (Mocking et al., 2016), contributing to their diverse application fields (Table 1). The histamine H<sub>1</sub> receptor represents a major target for antihistaminergic agents in the treatment of allergic symptoms, motion sickness and sleep disorders, while H<sub>2</sub> receptor antagonists are widely known for their action against esophageal reflux and gastrointestinal ulcers (Blandina, Passani, 2016). As the histamine H<sub>3</sub> and H<sub>4</sub>Rs are rather novel targets compared to the H<sub>1</sub> and H<sub>2</sub> receptors, their therapeutic potential is still underexplored. The H<sub>3</sub> receptor (H<sub>3</sub>R) is mainly localised in the CNS, where the constitutively active autoreceptor modulates the synthesis and release of histamine via negative feedback loops (Arrang et al., 1983). H<sub>3</sub>Rs are G<sub>i</sub> coupled, but also initiate PLC, MAPK, phosphatidylinositol 3-kinase and phospholipase A2 pathways via Gβγ (Nieto-Alamilla et al., 2016). Additionally, H<sub>3</sub>Rs have been linked to the release of other neurotransmitters such as dopamine, acetylcholine and serotonin, etc. (Nieto-Alamilla et al., 2016). These effects are likely caused by inhibition of voltage-gated Ca<sup>2+</sup> channels and activation of G protein-gated inwardly rectifying K<sup>+</sup> (GIRK) channels via Gβγ (Nieto-Alamilla et al., 2016; Sander et al., 2008; Torrent et al., 2005). By its abundant receptor distribution and neurotransmitter modulation, histamine takes an active part in the regulation of sleep-wake cycles as well as social and cognitive behaviours. This profile presents the H<sub>3</sub>R as an interesting target for multifactorial neurological disorders, such as Parkinson's disease (PD), Alzheimer's disease and schizophrenia (Hu, Chen, 2017) that are characterized by an imbalance of several neurotransmitters.

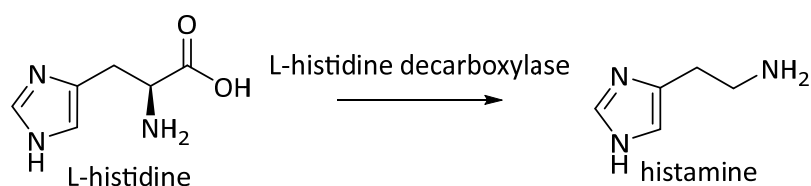


Figure 6: Chemical structures of L-histidine and histamine.

### 1.2.1 Histamine and its receptors

Table 1: Properties of histamine receptor subtypes. The  $pK_i$  values are medians derived by the IUPHAR Database.

	H <sub>1</sub> R	H <sub>2</sub> R	H <sub>3</sub> R	H <sub>4</sub> R
Coupling (Hough, 2001)	G <sub>q</sub>	G <sub>s</sub>	G <sub>i/o</sub>	G <sub>i/o</sub>
Histamine $pK_i$ (Harding et al., 2018)	4.2	4.3	8.0	7.8
Established applications and research fields (*) (Hu, Chen, 2017; Panula et al., 2015)	Allergy, sleep disorders, motion sickness	Esophageal reflux, gastrointestinal ulcer	Sleep disorders, schizophrenia*, PD*, epilepsy*, Alzheimer's disease*	Inflammation*, asthma*, allergy*, pruritus*, immune modulation*
Tissue distribution (Panula et al., 2015)	Ubiquitously (immune cells, CNS, lung, blood vessels)	Ubiquitously (gastrointestinal, smooth muscle cells, heart, uterus, CNS)	Ubiquitously (CNS, peripheral system, lung, heart, gastrointestinal)	Immune system, mast cells, colon, bone marrow, liver, lung

Currently H<sub>3</sub>R agonists as well as inverse agonists/antagonists are under investigation for their application in given research fields (Nieto-Alamilla et al., 2016). The H<sub>3</sub>R challenges researchers with species differences in receptor structure and isoform specific pharmacology. Most prominently the protein sequence of rodents (rats, mouse, guinea pig) differs to those of humans or monkeys in two amino acids (residues 119, 122), located in proximity to Asp114 in TMD3 (Nieto-Alamilla et al., 2016; Stark et al., 2001). Additionally, the human H<sub>3</sub>R displays a variety of splicing-based isoforms that inherit characteristic coupling behaviour and ligand binding (Nieto-Alamilla et al., 2016). These differences resulted in discrepant *in vitro* studies and unsuccessful translation to *in vivo* models, which is one of the reasons why many ligands required re-evaluation after their initial discovery (Hancock, 2006; Sander et al., 2008). In addition, the H<sub>4</sub>R displays a high sequence similarity to the H<sub>3</sub>R (58% in the TMD) (Mocking et al., 2016), causing a lack of pharmacological discrimination between H<sub>3</sub>R and H<sub>4</sub>R binding. This led to misinterpretations of H<sub>3</sub>R binding affinities, as the H<sub>4</sub>R existence was still unknown in the beginning of H<sub>3</sub>R drug development. Thus compounds regarded as selective were later found to be unselective or only slightly preferring the H<sub>3</sub>R (Liu et al., 2001). Early agonists (e.g.  $\alpha$ -methylhistamine, imetit) constitute of 4-monosubstituted imidazoles, designed based on the scaffold of histamine itself (Figure 7) (Mocking et al., 2016). With initial antagonist (e.g. clobenpropit, thioperamide) substitution patterns of the imidazole are more variable (Nieto-Alamilla et al., 2016). The presence of Glu206 in the OBS of H<sub>3</sub>R as well as the H<sub>4</sub>R (not in H<sub>1</sub>Rs and H<sub>2</sub>Rs), is considered as one reason for poor subtype selectivity, reported with imidazole-based compounds (Axe et al., 2006; Nieto-Alamilla et al., 2016). Furthermore, the imidazole may be afflicted with insufficient

### 1.2.1 Histamine and its receptors

pharmacokinetic properties such as poor blood-brain barrier penetration and CYP interactions (Ishikawa et al., 2010; Nieto-Alamilla et al., 2016; Young et al., 1988). To improve selectivity and pharmacokinetic properties of novel antagonists, research focuses on non-imidazolic compounds (Sander et al., 2008). The imidazole moiety was thought to be necessary for agonists (Leurs et al., 1995), but recent research suggests otherwise (Ghoshal et al., 2018). Modern scaffolds contain a basic, aliphatic amine (blue, Figure 7) that is connected to a lipophilic region and usually an electron-rich aromatic core. The basic part interacts with Asp114, while the lipophilic moiety modulates selectivity and pharmacokinetic features (Sander et al., 2008). It has to be noted, that in some instances, e.g. pitolisant, the basic amine was reported to bind to other motifs than the aspartate (Ghamari et al., 2019b). The two parts are connected by an alkyl linker (red, Figure 7) often comprising additional hydrophilic characteristics (green, Figure 7) (Sander et al., 2008), as seen with one of the first potent, non-imidazole-based  $H_3R$  antagonists, UCL-1972 (Figure 7). The natural compound aplysamine-1 (Figure 7) was also evaluated as  $H_3R$  antagonist and based on the proposed scaffold, further derivatization of this basic pharmacophore resulted in promising novel  $H_3R$  antagonists, supporting the use of natural compounds in drug development at GPCRs (Swanson et al., 2006). To date only one compound surpassed the clinical evaluation, despite a large substance library with suitable *in vitro* receptor affinities. The inverse agonist/antagonist pitolisant (Wakix®) is approved for the treatment of narcolepsy with and without cataplexy (Dauvilliers et al., 2019; Syed, 2016) and was just recently approved for its use in excessive daytime sleepiness in adults with narcolepsy by the FDA.

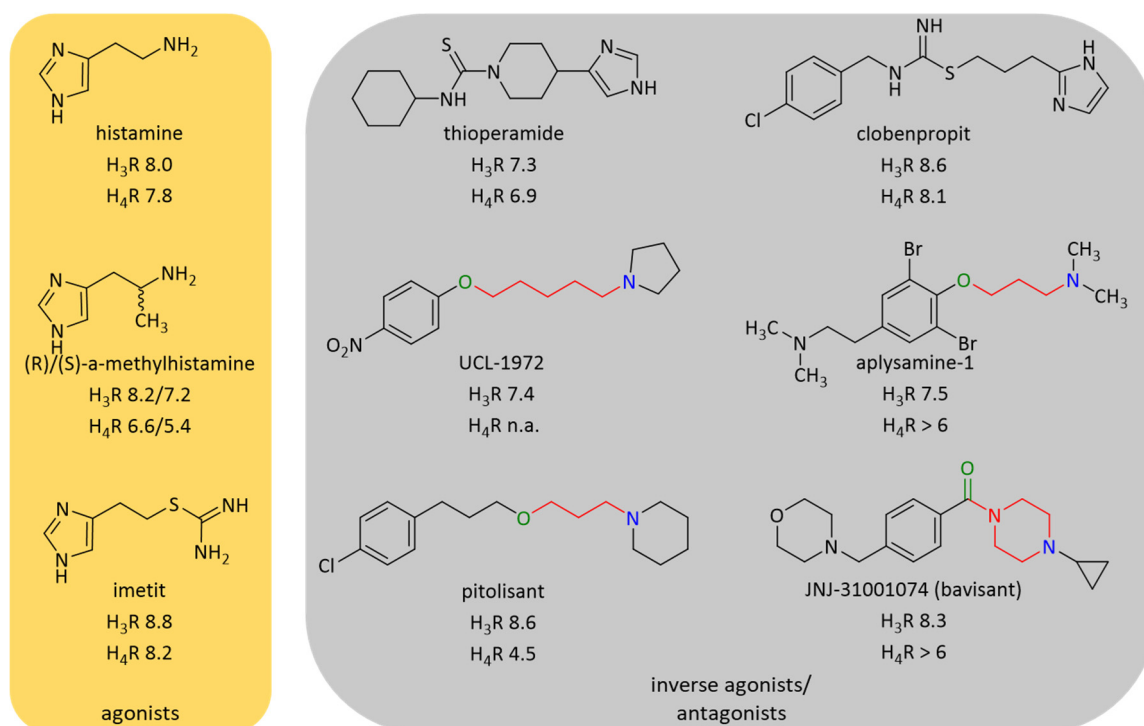


Figure 7: Reported scaffolds of  $H_3R$  ligands. The  $pK_i$  values are medians from (Harding et al., 2018; Letavic et al., 2015; Lim et al., 2005; Panula et al., 2015; Swanson et al., 2006). N.a. not available.

### 1.2.1 Histamine and its receptors

As H<sub>3</sub>R modulation was found to be beneficial in sleep disorders and cognitive impairments that accompany neurodegenerative disorders (Sadek et al., 2016b), pitolisant is currently under investigation for the adjuvant treatment of other neurodegenerative diseases (NCT01072968, NCT01066442) and single-patient case studies for its use in Prader-Willi syndrome are ongoing (Pullen et al., 2019). Currently about 20 H<sub>3</sub>R selective antagonists/inverse agonists are in clinical evaluation, mostly related to sleep disorders, allergic rhinitis, Alzheimer's disease and attention deficit hyperactivity disorder (ADHD) (Ghamari et al., 2019a). In addition to pitolisant, JNJ-31001074 (bavisant) (Figure 7) is currently under investigation for excessive daytime sleepiness in PD (NCT03194217), while a study for ADHD revealed no effectivity (Ghamari et al., 2019a). Several of the reported ligands have no disclosed results so far, or trials were terminated without information or due to a lack of *in vivo* activity (Egan et al., 2012; Griebel et al., 2012; Herring et al., 2012). The interest in H<sub>3</sub>R agonists and inverse agonists/antagonists was increased by the pioneering nature of pitolisant and related compounds. However, drug development lacks novel scaffolds to bring forth additional clinical candidates to further validate the H<sub>3</sub>R as clinical target.

In 1994 Raible et al. postulated the existence of a fourth histamine receptor subtype localised on eosinophils (Raible et al., 1994), which eventually led to the cloning of the H<sub>4</sub>R (Liu et al., 2001; Nakamura et al., 2000; Oda et al., 2000). It is mainly located in the periphery and in cells of the immune system (mast cells, eosinophils, haematopoietic stem cells), contributing to inflammatory events and immune modulation (Zampeli, Tiligada, 2009). A high expression on special cancer cell lines, especially in breast cancer (Medina et al., 2011), constitutes a possible target for cancer therapy or the overcoming of chemotherapy resistance (Nicoud et al., 2019). Due to uncertain pharmacological implications and the modulatory effects of the receptor it is still discussed whether inverse agonists/antagonist or agonist possess higher therapeutic applicability, although antagonists are nowadays favoured by drug development (Thurmond, 2015). The blueprint for H<sub>4</sub>R is not as extensively studied as for other histaminergic receptors, given its rather recent discovery. However, due to the high sequence similarity between H<sub>4</sub>Rs and H<sub>3</sub>Rs, selectivity evaluation is standard procedure for novel ligands at both receptors nowadays. As already discussed, imidazole-containing compounds mostly lack the required binding selectivity (Mocking et al., 2016), but neither H<sub>4</sub>R agonist nor antagonists require imidazole-based scaffolds (Smits et al., 2009). To allow for interaction with aspartate in the OBS, antagonists can be designed with a basic amine within an aliphatic ring that is connected to a heteroaromatic group, further substituted with lipophilic residues for hydrophobic interaction in the receptor (Mocking et al., 2016). To date JNJ-777120 (Figure 8) is one of the few selective compounds for the H<sub>4</sub>R. It never proceeded towards the clinical market due to poor pharmacokinetics, despite *in vitro* and *in vivo* results suggesting anti-inflammatory, analgesic and antipruritic properties (Corrêa,



### 1.2.1 Histamine and its receptors

dos Santos Fernandes, 2015). Nevertheless, it is of great relevance as reference compound and pharmacological tool due to its biased action as inverse agonist/antagonist on [ $^{35}$ S]GTP $\gamma$ S binding and partial agonist at the  $\beta$ -arrestin/ERK pathway (Rosethorne, Charlton, 2011). Heterocyclic analogues of JNJ-7777120 (e.g. benzothiophenes, Figure 8) displayed significantly reduced  $H_4R$  activity (Karcz et al., 2010), while 2-methyloctahydropyrrolo[3,4-c]pyrroles could improve affinity at the  $H_4R$  but display poor pharmacokinetics as well (Lane et al., 2012). The compound JNJ-39758979 (Figure 8) went into clinical trial for histamine-induced pruritus (NCT01068223) and moderate atopic dermatitis (NCT01497119) (Thurmond, 2015). While the trial for histamine-induced pruritus completed with promising results (Kollmeier et al., 2014), the trial on moderate atopic dermatitis had to be terminated due to events of agranulocytosis (Murata et al., 2015; Thurmond, 2015). A trial in asthmatic patients (NCT00946569) failed to meet its defined endpoint, but the authors recommend further evaluation of  $H_4R$  antagonist in eosinophilic asthma based on their subgroup analysis (Kollmeier et al., 2018). Toreforant (Figure 8) just recently completed several phase II studies on rheumatoid patients. A phase IIa study was terminated early due to a serious adverse event (NCT00941707) (Thurmond et al., 2016). Another study on toreforant's mode of action was terminated before reaching the endpoint (Boyle et al., 2019), due to its lack of significant efficacy in a previously phase IIb study (NCT01679951) (Thurmond et al., 2016). Promising clinical candidates for the  $H_4R$  are sparse, impeding evaluation of the receptors pharmacological potential. Major challenges arise by poor selectivity, poor pharmacokinetics and a difficult translation of *in vitro* findings, mostly from rodents, to the clinics.

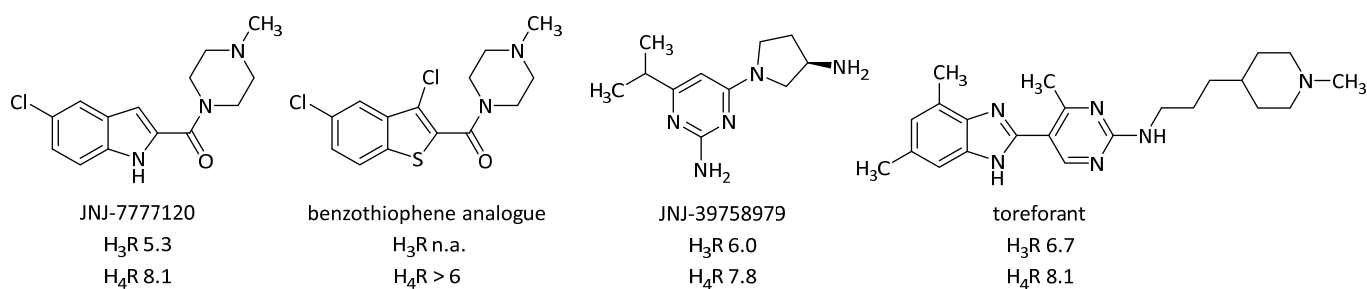


Figure 8: Selected  $H_4R$  ligands. The  $pK_i$  values are reported as medians (Harding et al., 2018; Thurmond et al., 2017). N.a. not available.

### 1.2.2 Dopamine and its receptors

Dopamine (4-(2-aminoethyl)catechol), a catecholic biogenic amine, is one of the key players in the CNS as well as the vegetative nervous system. Its bioformation in the CNS starts with the hydroxylation of L-tyrosine via tyrosine-3-hydroxylase (TH) to form levodopa (L-DOPA, L-3,4-dihydroxyphenylalanine) in neurons of the substantia nigra and the ventral tegmentum (Ayano, 2016; Meiser et al., 2013). Subsequent decarboxylation by the DOPA decarboxylase (DDC, aromatic L-amino acid decarboxylase, Figure 9) leads to dopamine that can be stored in synaptic vesicles (Fahn, 2008; Meiser et al., 2013). Latest results suggest the existence of another pathway, that involves oxidation of tyramine by CYP2D6 enzymes (Wang et al., 2014). Dopamine transporters (DAT) are responsible for synaptic reuptake of released neurotransmitter, while mitochondria associated monoamine oxidase (MAO) and catechol-*O*-methyltransferase (COMT) in surrounding glia cells catalyse its further metabolization (Figure 9, 10) in collaboration with alcohol and aldehyde dehydrogenases (Lindemann, Hoener, 2005; Meiser et al., 2013). These proteins are also prominent targets for treatment of dopamine related diseases. Once released into the synaptic cleft, dopamine acts via five class A GPCRs (Table 2), of which presynaptic D<sub>2</sub> autoreceptors initiate a negative feedback loop, thereby regulating dopamine transmission (Figure 10) (Ford, 2014). Dopamine receptors are divided into two groups characterized by their signaling cascades and protein sequences (Kebabian et al., 1972). The D<sub>2</sub>-like receptor subfamily comprises G<sub>i/o</sub> coupled G proteins and includes the D<sub>2</sub>, D<sub>3</sub> and the D<sub>4</sub> receptors (Jackson, Westlind-Danielsson, 1994; Kebabian et al., 1972).

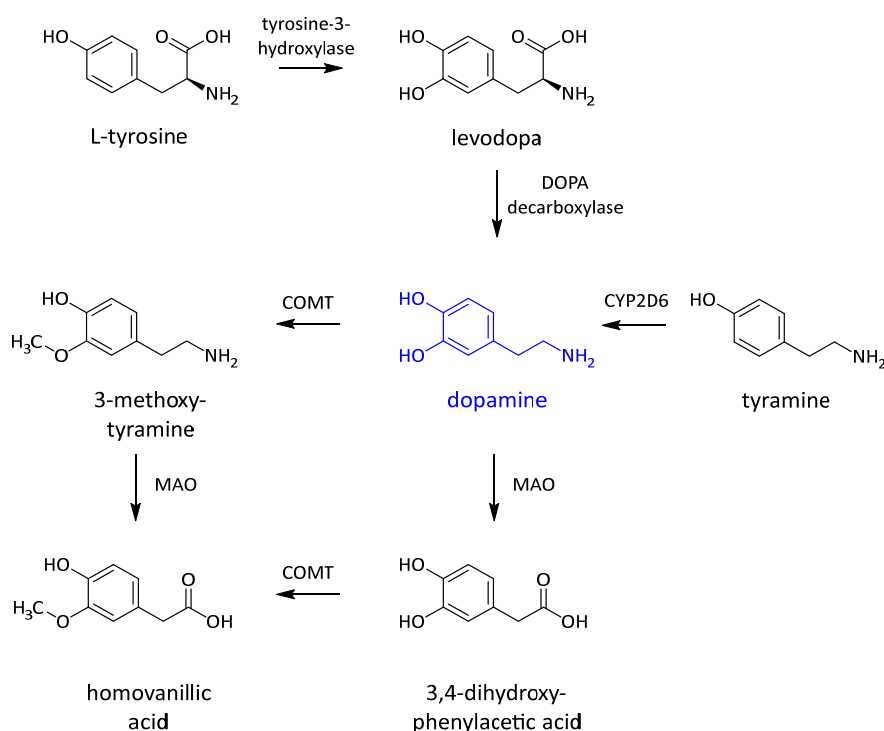


Figure 9: Formation, biometabolization and -degradation of dopamine.

### 1.2.2 Dopamine and its receptors

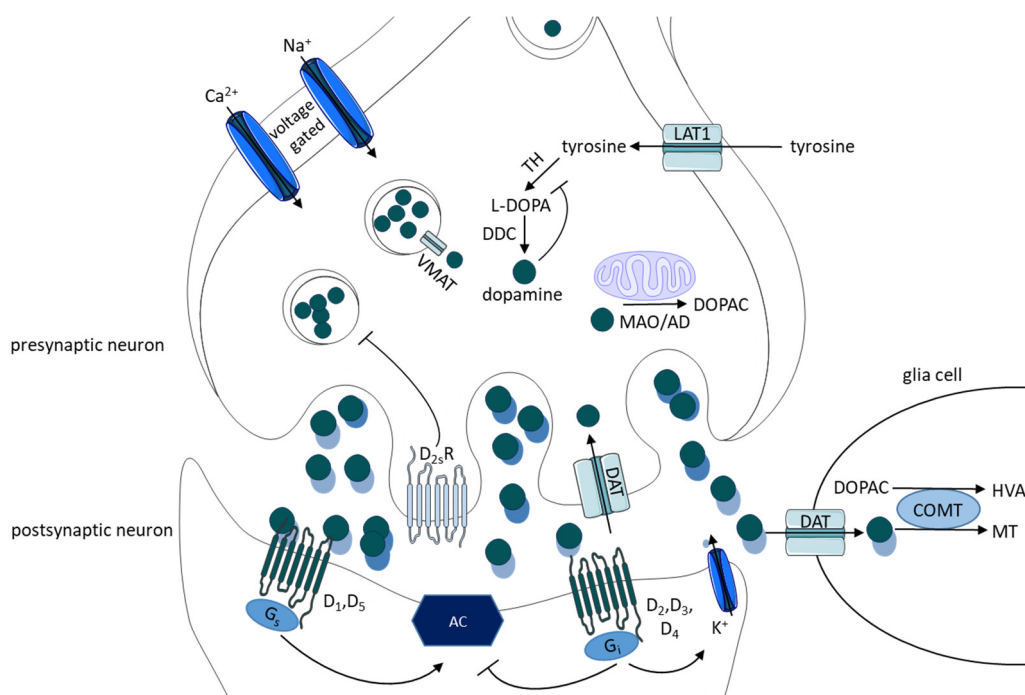


Figure 10: Dopamine formation, metabolism and signal transduction. Modified after (Knab, Lightfoot, 2010; Meiser et al., 2013). AC: adenylyl cyclase; AD: aldehyde dehydrogenase; COMT: catechol-O-methyltransferase; DAT: dopamine transporter; DDC: DOPA decarboxylase; DOPAC: 3,4-dihydroxyphenylacetic acid; HVA: homovanillic acid; LAT: L-amino acid transporter; MAO: monoamine oxidase; MT: 3-methoxy-tyramine; TH: tyrosine-3-hydroxylase; VMAT: vesicular monoamine transporter.

The D<sub>2</sub>R and the D<sub>3</sub>R display a sequence identity of around 50% in the total sequence and 79% in the TMD (Sokoloff et al., 1990), but different tissue distribution, receptor density and pharmacology. The high similarity requires thorough selectivity evaluation of novel compounds, to distinguish pharmacological contributions. Sequence identity of the D<sub>4</sub>R with the D<sub>2</sub>R and D<sub>3</sub>R is far lower with around 50% in the TMDs (Civelli et al., 1991). Differences in dopamine's signaling are not only caused by different couplings and tissue distributions, but also by existing splicing homologues in the D<sub>2</sub>-like family (Gingrich, Caron, 1993). Although reported for all receptor subtypes, pharmacological significant differences were most prominently found for the human D<sub>2</sub>-short (*hD<sub>2s</sub>R*) and D<sub>2</sub>-long (*hD<sub>2l</sub>R*) splicing variants that differ in 29 amino acids in ICL3 (Grandy et al., 1989). Based on a mainly presynaptic localisation, the D<sub>2s</sub>R is suggested to be the autoreceptor, responsible for the negative feedback loop on dopamine release. The D<sub>2l</sub>R is primarily localised postsynaptically and seems to be the target of several antipsychotic agents (Centonze et al., 2002; Usiello et al., 2000). The ability to differentiate these contributions *in vivo* remains controversial. High- and low-affinity states of dopamine receptors challenge drug-target evaluations even further, as both receptor states are differently favoured and influenced by agonists and antagonists and are modulated differently by signal transducers, leading to conflicting assay results (de Lean et al., 1982; Sibley et al., 1982). The D<sub>1</sub> and D<sub>5</sub> receptors belong to the D<sub>1</sub>-like subfamily, distinguished by a G<sub>s</sub> coupling protein (Table 2) (Jackson, Westlind-Danielsson, 1994). Similar to the D<sub>2</sub>/D<sub>3</sub>Rs, they share a sequence identity of 79% in the TMDs (Demchyshyn et al., 2000) with variations in tissue distribution and receptor density, alike.

### 1.2.2 Dopamine and its receptors

Dopaminergic transmission is most commonly subdivided in the mesolimbic, mesocortical, nigrostriatal and tubero-infundibular pathways (Figure 11) (Ayano, 2016; Butini et al., 2016). While mesolimbic projections are related to reward, emotion and perception, mesocortical areas influence cognition, memory, attention and emotional behaviour (Ayano, 2016). Accordingly, these pathways are under investigation for the treatment of drug abuse, schizophrenia and ADHD. The nigrostriatal pathway is best known for its involvement in the planning and execution of movements (Ayano, 2016), hence a target for PD, restless-legs syndrome (RLS) or chorea Huntington. In contrast to these, the tubero-infundibular projection is a common off-target of dopaminergic treatment strategies, resulting in some of its adverse drug effects (ADE) (Butini et al., 2016). The D<sub>1</sub>R is widely represented in all brain areas (Jaber et al., 1996; Meador-Woodruff et al., 1996; Mishra et al., 2018; Palacios et al., 1988). It is involved in emotion, memory/learning, reward, attention, cognition and motoric activity (Kim et al., 2015; Koob et al., 1998; Lynch, 1992; Mishra et al., 2018). CNS distributions of the D<sub>5</sub>R are far more limited (Ayano, 2016; Mishra et al., 2018). Participation of the receptor in memory and learning processes is highly probable (Mishra et al., 2018; Missale et al., 1998). The D<sub>2</sub>R is found in nearly every part of the brain, with high expression in the striatum (Meador-Woodruff et al., 1996), but also in the substantia nigra, ventral tegmental area, olfactory bulb and the amygdala (Ayano, 2016; Mishra et al., 2018; Takahashi et al., 2010). Given its high density in different areas, the receptor is involved in emotion, learning, behaviour and motoric activity. Receptor distribution of the D<sub>3</sub>R is more distinct, mainly localised in the islands of calleja and the striatum, which is why the receptor is suggested to be involved in limbic functions (Meador-Woodruff et al., 1996). Receptor density of the D<sub>4</sub>R in the CNS is not as abundant and ligands are mainly investigated for use in cognitive disorders (Mishra et al., 2018).

Table 2: Properties of dopamine receptor subtypes. Values of the pK<sub>i</sub> are derived by the IUPHAR Database (Harding et al., 2018) and are reported as medians.

	D <sub>1</sub> R	D <sub>2</sub> R	D <sub>3</sub> R	D <sub>4</sub> R	D <sub>5</sub> R
Coupling	G <sub>s</sub>	G <sub>i/o</sub>	G <sub>i/o</sub>	G <sub>i/o</sub>	G <sub>s</sub>
Dopamine pK <sub>i</sub>	5.5	6.6	7.3	7.6	6.1
Established application for antagonists (°) and agonists (°) and promising research fields (*)	Schizophrenia*, substance abuse*	Schizophrenia <sup>§</sup> , emesis <sup>§</sup> , motor disorders°, depression*	Schizophrenia <sup>§</sup> , depression*, substance abuse*, motor disorders°	Schizophrenia*, substance abuse*	Substance abuse*

### 1.2.2 Dopamine and its receptors

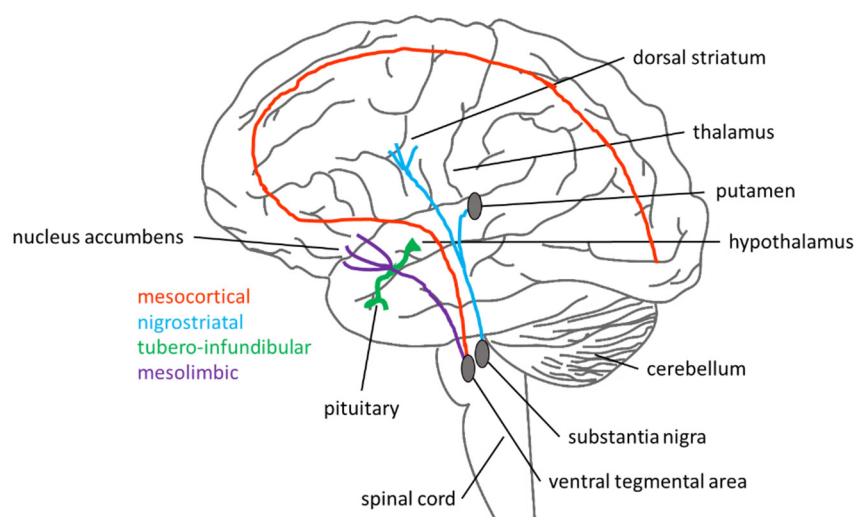


Figure 11: Schematic representation of dopaminergic pathways in the brain. Modified after creative commons CC BY-SA 4.0.

Given the resolved crystal structure of the D<sub>2</sub>R and the D<sub>3</sub>R, drug design focuses on these two receptors and approaches the challenges depicted by their high similarity. Clinical candidates and applied ligands for the D<sub>2</sub>R are numerous. Antagonists such as chlorpromazine and haloperidol or domperidone and metoclopramide are applied in the treatment of schizophrenia and nausea, respectively (Figure 12) (Kovac, 2000; Leucht et al., 2008). Agonists such as rotigotine and ropinirole are used in the treatment of PD (Figure 12) (Fox et al., 2011). However, most of the compounds targeting the D<sub>2</sub>R lack reasonable selectivity profiles towards other dopamine receptors and even show considerable affinity towards other neurotransmitter receptors (Butini et al., 2016). Although in some instances specific off-target activity may aid multifactorial approaches (Butini et al., 2016), the design of D<sub>2</sub>/D<sub>3</sub>R selective ligands, is a major goal to evaluate neurobiological mechanisms specific to the receptor subtypes. Sumanrole (Figure 12) was one of the first highly selective agonists designed for the D<sub>2</sub>R (McCall et al., 2005) and even proceeded to phase III clinical trial in PD (NCT00036218). However, it failed to excel over the existing therapeutic approaches and thus further evaluations were terminated (Barone et al., 2007). The design of D<sub>3</sub>R selective compounds experienced progression in the last years (Blagg et al., 2007; Cao et al., 2018). Cariprazine (Figure 12) was the first ligand on the market that displayed significant D<sub>3</sub>R preference and appears highly promising for an innovative treatment of schizophrenia and depression (Kiss et al., 2010). The D<sub>2</sub>R and the D<sub>3</sub>R were successfully crystallised in complex with risperidone and eticlopride (Figure 12), respectively (Chien et al., 2010; Wang et al., 2018). This allowed structural insights into ligand binding to the receptors, aiding rational drug design of selective ligands. Typical dopaminergic ligands contain a basic amine for interacting with Asp110<sup>3.32</sup> (Asp114<sup>3.32</sup> in D<sub>2</sub>R) in TMD3. The amine is connected via an alkyl linker to an aromatic core with hydrogen-bond acceptor capacities. Hydrophobic interactions with phenylalanine (Phe345,346), valine (Val111,189) and serine (Ser192,193) in TMD3/5/6 contribute to the binding of eticlopride in the D<sub>3</sub>R (Chien et al., 2010).

## 1.2.2 Dopamine and its receptors

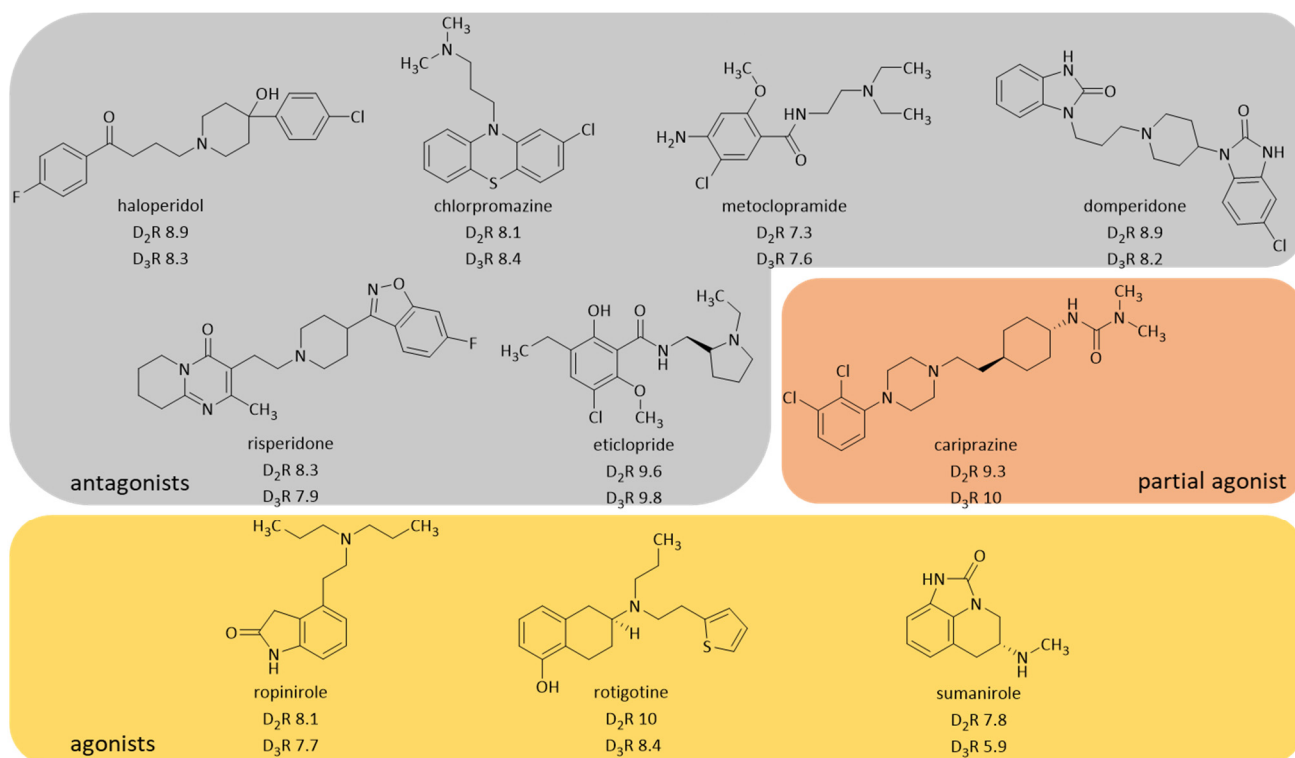


Figure 12: Structures of selected D<sub>2</sub>/D<sub>3</sub>R ligands. pK<sub>i</sub> values are reported as medians derived from the IUPHAR Database (Harding et al., 2018).

The hydrophobic pocket formed by isoleucine (Ile183 in D<sub>3</sub>R, Ile184 in D<sub>2</sub>R) in ECL2 contribute to the binding of both ligands (Chien et al., 2010; Wang et al., 2018). The elucidation of a SBP near the extracellular regions of the D<sub>3</sub>R and different orientation of the SBP in the D<sub>2</sub>R promises advances in subtype selective drug design (Chien et al., 2010; Wang et al., 2018). As the SBPs are not as highly conserved as the OBS and display different spatial orientation, the design of bitopic ligands, extended towards the SBP became a promising strategy to improve selectivity at D<sub>2</sub>/D<sub>3</sub>Rs (Newman et al., 2012; Omran et al., 2018). While a 2,3-dichloro-4-phenylpiperazine was implemented successfully in D<sub>2</sub>R as well as in D<sub>3</sub>R ligands, an aryl amide with a 4-carbon linker is used to increase D<sub>3</sub>R selectivity (Newman et al., 2012). However, the determination of a SBP also reinforces the need for careful evaluation of binding data, as previous assays have rarely been evaluated with regards to this topic. The lack of selective radiolabelled ligands for the D<sub>2</sub>R and D<sub>3</sub>R impedes further evaluation of pharmacological differences. A lack of selectivity among dopamine receptor ligands results in major ADE in the treatment of PD and schizophrenia (Seeman, 2006). In the case of schizophrenia, the treatment with primarily D<sub>2</sub>R selective antagonist is unable to address all symptoms sufficiently and requires researchers to re-evaluate treatment approaches. Hence, the receptor's SBP supplies interesting drug-target interactions for exploration by novel assays and pharmacological tools.

### 1.3 Biogenic amines in Parkinson's disease

Parkinson's disease (PD) is a highly multifactorial disease within the neurodegenerative cluster. A progressive loss of dopaminergic cells in the pars compacta of the substantia nigra (SN), leads to an imbalanced transmission in the basal ganglia (Moore et al., 2005). This results in typical movement disorders with cardinal symptoms such as tremor, rigor, bradykinesia and postural instability (Bereczki, 2010). They can be accompanied by cognitive, vegetative or psychiatric symptoms (Chaudhuri, Schapira, 2009). PD's pathophysiology is not conclusively elucidated but certainly multifactorial in nature. Neurodegenerative inclusions ("Lewy Bodies") (Moore et al., 2005), oxidative stress, neuroinflammation and mitochondrial dysfunction greatly contribute to the loss of dopaminergic cells (Segura-Aguilar et al., 2014). Notably the products of dopamine's oxidation itself (quinones, aminochromes) are discussed to be neurotoxic (Segura-Aguilar et al., 2014). This is one of the reasons for increased development of dopaminergic ligands, lacking a catechol scaffold. Up until today motor symptoms in PD are treated mostly symptomatically and this thesis reports on the dopaminergic approaches among those. Researchers were able to link dopamine to PD and found striatal dopamine deficiency responsible for the motor symptoms only in the 1960s (Ehringer, Hornykiewicz, 1960; Fahn, 2008; Hornykiewicz, 1966). The application of levodopa (Madopar®) for PD in 1973 was ground breaking and is still one of the most effective treatments for the motor symptoms (Fox et al., 2011). Dopamine itself is unable to penetrate the blood-brain barrier, while levodopa, as precursor, is taken up through an active carrier. To prevent peripheral metabolism of the prodrug, DDC inhibitors (e.g. benserazid, carbidopa) or COMT inhibitors (e.g. entacapone, tolcapone) are usually co-administered (Rinne, Mölsä, 1979; Seeberger, Hauser, 2009). However, levodopa is discussed to display negative effects on disease progression (Lipski et al., 2011), inter- and intra-individual pharmacokinetics (Nomoto et al., 2009) and evokes levodopa-induced dyskinesia (Ahlskog, Muenter, 2001). Because symptomatic treatment of PD requires a lifelong therapy, drug development requires agents with similar efficacy to levodopa, but without its drawbacks. Dopamine receptor agonists display high, but unselective affinity at D<sub>2</sub>/D<sub>3</sub>Rs as well as activity at other aminergic receptors. Ergoline derivatives (e.g. bromocriptine, lisuride) display off-target interactions and questionable safety profiles and have been superseded by non-ergoline dopamine receptor ligands like pramipexole, rotigotine, talipexole, piribedil, ropinirole and apomorphin (Figure 13) (Davie, 2008). To overcome unselective dopaminergic activation, the D<sub>3</sub>R gathered interest. The receptor was found to be downregulated in PD patients (Ryoo et al., 1998), while animal models confirmed a link between D<sub>3</sub>R upregulation and levodopa-induced dyskinesia (Bézard et al., 2003; Bordet et al., 1997). *In vivo* studies with a D<sub>3</sub>R selective partial agonist (BP 897, Figure 13), revealed a reduction of levodopa-induced dyskinesia (Bézard et al., 2003), but also non-motor symptoms may be addressed by D<sub>3</sub>R agonists

### 1.3 Biogenic amines in Parkinson's disease

(Carnicella et al., 2014). Novel scaffolds are required to improve D<sub>3</sub>R selectivity and catechol's poor pharmacokinetic. D<sub>3</sub>R selectivity could be achieved by extension and derivatization of the linker chain length in bitopic ligands (Newman et al., 2012), while a bioisosteric exchange of catechol moieties may decrease metabolism steps by COMT and CYP enzymes (Segura-Aguilar et al., 2014). Typical exchanges include (aromatic) heterocycles, containing an amino or hydroxyl moiety (Boeckler, Gmeiner, 2006) and were performed with pyrroles, pyrazoles and aminothiazoles (Bach et al., 1980; McQuaid et al., 1989; Schneider, Mierau, 1987), among others. However, profound SAR studies on hydrogen-bond donor and acceptor capacities in catechol bioisosteres are sparse to date.

Dopaminergic treatment significantly reduces typical motor symptoms, but is not able to treat associated symptoms that reduce quality of life likewise. Psychological non-motor symptoms include depression, cognitive impairments and sleep disorders (Seppi et al., 2011). New evidence supports involvement of the H<sub>3</sub>R in the progression of PD and non-motor symptoms. While histamine levels in PD patients were found to be increased, levels of a corresponding metabolite (*N*<sup>r</sup>-methylhistamine) were not increased (Rinne et al., 2002). An increased H<sub>3</sub>R expression was also shown by mRNA levels and radioligand binding studies (Anichtchik et al., 2001), although these findings were not confirmed by other investigations (Goodchild et al., 1999). However, researchers proved an H<sub>3</sub>R mediated D<sub>1</sub>/D<sub>2</sub>R modulation and even presented data suggesting the existence of H<sub>3</sub>-D<sub>2</sub>R heteromers *in vitro* with an inhibitory relationship (Ferrada et al., 2008). This substantiates the involvement of H<sub>3</sub>R signal transduction on dopamine-mediated transmission. Together with the clinical potential of pitolisant and JNJ-31001074 for excessive daytime sleepiness in PD, the recent results indicate high applicability of H<sub>3</sub>R ligands in the treatment of PD and related cognitive impairments. Due to the multifactorial scale of the disease and the need for lifelong treatment, it is necessary to expand and improve pharmacophore scaffolds for dopamine as well as histamine receptor subtypes.

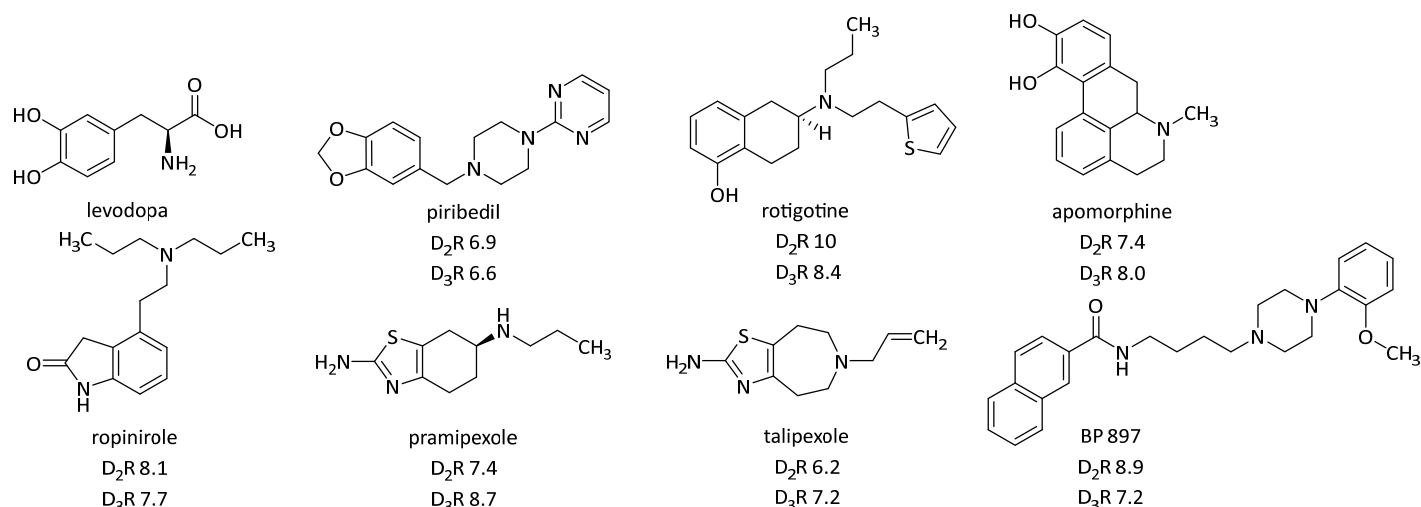


Figure 13: Structures and receptor affinities of selected dopamine receptor agonists, used in the treatment of PD. The pK<sub>i</sub> values are reported as medians derived by the IUPHAR DB (Garcia-Ladona, Cox, 2003; Harding et al., 2018; Millan et al., 2002).



### 1.4 Novel aspects of drug-target interactions at the example of schizophrenia

Schizophrenia is one of the most prominent psychotic disorders regarding inner experience, emotions and behaviour. As it represents a complex syndrome, pathophysiological evaluation is impeded (Fischer, Carpenter, 2009). Dopamine's involvement in the pathogenesis ("dopamine hypothesis") was originally postulated as high doses of antipsychotic agents evoked PD-like symptoms (Meltzer, Stahl, 1976; Seeman, 2006; Shen et al., 2012) and was later confirmed by binding assays at D<sub>2</sub>Rs (Seeman et al., 1976; Seeman, 2006). However, the dopamine hypothesis fails to explain insufficient treatment, despite sufficient D<sub>2</sub>R blockade in some patients and especially fails to elucidate clozapine's high clinical efficacy, although its D<sub>2</sub>R affinity is only moderate (Pilowsky et al., 1992). Today there is evidence that a hyperactivity of D<sub>2</sub>Rs in the mesolimbic pathway (Meltzer, Stahl, 1976) is combined with a disturbance in D<sub>1</sub>R and D<sub>3</sub>R signal transduction (Okubo et al., 1997; Simpson et al., 2014). However, evidence for D<sub>1</sub>R involvement is contradictory (Abi-Dargham et al., 2002; Karlsson et al., 2002). In addition imbalances in serotonin and glutamate/GABA transmission may also evoke psychosis (Stahl, 2013; 2016). Due to the lack of specific tracers, the disorder is diagnosed and characterized by the occurrence of specific symptoms, divided into positive and negative symptoms. Positive symptoms include behaviours and perceptions that are intensified in patients (e.g. hallucinations or delusions). They are linked, although not exclusively, to increased dopaminergic transmission in mesolimbic brain regions (Stahl, 2018). Negative symptoms are characterized by a lack of perception or behaviour (social withdrawal, depression or cognitive impairments) (Cerveri et al., 2019). Their origin is the topic of recent research and is discussed to be highly multifactorial. D<sub>3</sub>R imbalances, serotonin-dopamine interactions, D<sub>1</sub>R hypotransmission and reduced activity of the nucleus caudate were all shown as possible targets (Meltzer et al., 2003; O'Donnell, Grace, 1998; Shen et al., 2012; Simpson et al., 2014).

Accordingly, antipsychotics can be divided in two classes, characterized by their clinical profile. Typical antipsychotic agents (Figure 14, e.g. chlorpromazine) reduce positive symptoms by D<sub>2</sub>/D<sub>3</sub>R antagonism in mesolimbic areas, but display an increased risk for extrapyramidal side effects (EPS, characteristic motoric facial and limb disorders) (Stahl, 2018). Clozapine (Figure 14) was the first antipsychotic agent with significantly less EPS (Stille, Hippus, 1971) and thereby introduced the class of "atypical" antipsychotic agents (Gründer et al., 2009). The reason for this lower incidence is not fully elucidated but focuses on dopaminergic, serotonergic and adrenergic transmission (Gründer et al., 2009; Kapur, Seeman, 2001; Meltzer et al., 1989; Pilowsky et al., 1997; Wadenberg et al., 2007). A second generation of atypical antipsychotic agents entered the market with aripiprazole (Abilify®, Figure 14) in 2004. It displays characteristic partial agonism at D<sub>2</sub>/D<sub>3</sub> and 5-HT<sub>1A</sub>Rs, combined with antagonism at 5-HT<sub>2A</sub>Rs. Partial agonists are thought to stabilize neurotransmitter fluctuations, while

## 1.4 Novel aspects of drug-target interactions at the example of schizophrenia

simultaneously allowing essential receptor activation by peaks in dopamine levels, which presumably decreases ADE (Gründer et al., 2009; Pulvirenti, Koob, 2002).

Negative symptoms show poor response to most of the antipsychotic agents. Up to now, only cariprazine, amisulpride, olanzapine (Figure 14) and quetiapine show clinical efficacy on negative symptoms (Cerveri et al., 2019). The pharmacological profiles differ remarkably and no common mechanism was found responsible for their action. Cariprazine (Vraylar®, Reagila®) was approved 2015 in the USA for the treatment of schizophrenia and acute manic or mixed episodes associated with bipolar I disorder. In 2017 the European commission approved it for the use in schizophrenia as well (Ragguett, McIntyre, 2019). It acts as partial agonists at D<sub>2</sub>/D<sub>3</sub>Rs and 5-HT<sub>1A</sub>Rs, while showing antagonism on 5-HT<sub>2A</sub> and 5-HT<sub>2B</sub>Rs (Calabrese et al., 2019) and possesses similar structural features to aripiprazole. However, aripiprazole does not work significantly well on negative symptoms. This difference, gave a new stimulus to evaluate structural features and pharmacological mechanisms responsible for action against negative symptoms. Although both ligands are partial agonists, cariprazine displays an increased D<sub>3</sub>R preference, which raises interest for mode of action studies. D<sub>3</sub>R modulation was linked to improved cognitive functions in several studies (Laszy et al., 2005; Millan et al., 2007; Nakajima et al., 2013), although these findings were majorly concluded by antagonism at the receptor. Long-term cariprazine administration was able to increase D<sub>3</sub>R expressions (Calabrese et al., 2019; Choi et al., 2014) but did not influence 5-HT<sub>2A</sub>R levels as strong as aripiprazole (Calabrese et al., 2019; Choi et al., 2014; Tarazi et al., 2001). Such receptor regulations are strongly linked to  $\beta$ -arrestin. The involvement of  $\beta$ -arrestin recruitment in antipsychotic activity was shown *in vitro* and in mice models (Allen et al., 2011; Masri et al., 2008), although the *in vivo* study found agonistic actions responsible, while *in vitro* results suggest an antagonism as mode of action. Hence, the therapeutic effects of D<sub>3</sub>R or  $\beta$ -arrestin biased targeting are contradictory or not conceivable yet, but motivate further investigation in clinical profiles of antipsychotic agents.

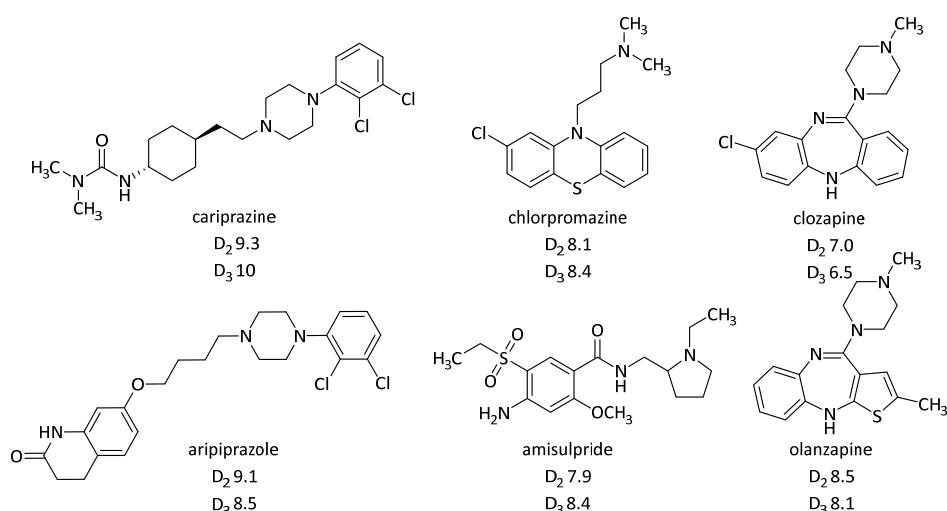


Figure 14: Structures and pK<sub>i</sub> values of selected antipsychotic agents (Harding et al., 2018; Seeman, Tallerico, 1998).

### 1.5 Drug-target residence time in schizophrenia

The “fast-off hypothesis” of antipsychotics was originally discussed for EPS and atypicality (Kapur, Seeman, 2001), but may reveal new insights for negative symptoms as well. As neurotransmitter levels underlie a steady fluctuation *in vivo*, the binding period of active agents *in vitro* seems to be a reasonable surrogate parameter to assess their pharmacological impact on neurotransmitter regulation. The aim of drug-target residence time (DTRT) evaluations is to mimic physiological conditions and to translate pharmacokinetic *in vitro* profiles to *in vivo* clinical profiles (Guo et al., 2014). Ligand binding to its receptor is a constant association and dissociation *in vivo* but usually reaches a steady state *in vitro*. The time that it takes a given ligand to dissociate from 50% of the initial receptor occupancy ( $t_{1/2\text{dissociation}}$ , Figure 15) can be transformed into its dissociation rate constant ( $k_{\text{off}}$ , eq. 1,  $RT = 1/k_{\text{off}}$ ) (Guo et al., 2014). The observed kinetic rate constant ( $k_{\text{obs}}$ ) is derived from the time it takes the ligand to reach 50% receptor occupancy ( $t_{1/2\text{association}}$ , Figure 15, eq. 2) (Bosma et al., 2017). Its association rate constant ( $k_{\text{on}}$ ), is derived from  $k_{\text{obs}}$  taking the drug’s concentration [L] and its  $k_{\text{off}}$  into account (eq. 3) (Bosma et al., 2017). As  $k_{\text{on}}$  is affected by the ligand’s concentration and a steady dissociation, it has only limited information value *in vivo*. Additionally, the association of a drug is influenced by tissue distribution or clearance *in vivo* and limited by diffusion rates of the target and ligand *in vitro* (Copeland et al., 2006). The  $k_{\text{off}}$  on the other hand is not biased by these parameters and depicts a cleaner surrogate for drug-target interactions (Copeland et al., 2006). Usually a prolonged RT offers a prolonged pharmacological effect, as long as it exceeds the pharmacokinetic elimination half-life (Vauquelin, van Liefde, 2006). In the case of schizophrenia, a long RT could be beneficial to stabilize neurotransmitter fluctuations continuously (Vauquelin, van Liefde, 2006), but at the same time a lasting receptor blockade is linked to the occurrence of EPS (Gründer et al., 2009; Guo et al., 2014). An inverse correlation between this mechanism-based toxicity and a short RT at the D<sub>2</sub>R was shown, as typical antipsychotic agents displayed long RT at the D<sub>2</sub>, while most of the atypical agents dissociated rapidly from the receptor (Kapur, Seeman, 2000). A fast off-rate of atypical agents such as clozapine (Langlois et al., 2012) could allow receptor activation in response to sudden peaks in dopamine levels that would lead to EPS, if the receptor was still blocked.

$$\text{Equation 1} \quad k_{\text{off}} = \frac{\ln 2}{t_{1/2\text{dissociation}}} [\text{min}^{-1}]$$

$$\text{Equation 2} \quad k_{\text{obs}} = \frac{\ln 2}{t_{1/2\text{association}}} [\text{min}^{-1}]$$

$$\text{Equation 3} \quad k_{\text{obs}} = k_{\text{on}} * [L] + k_{\text{off}}$$

## 1.5 Drug-target residence time in schizophrenia

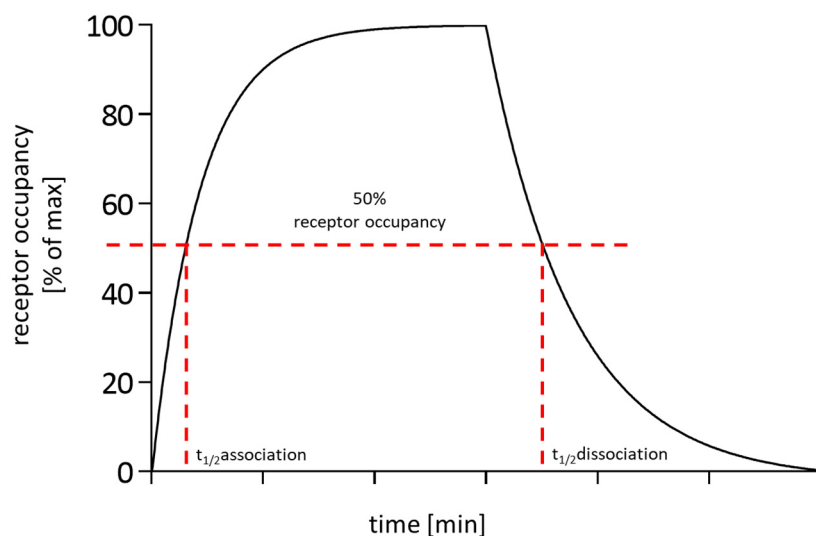


Figure 15: Schematic representation of  $t_{1/2}$  of association and dissociation.

*In vivo* data of the atypical agent clozapine and the typical agent haloperidol did support these *in vitro* findings (Jones et al., 2000). Accordingly, JNJ-37822681 is reported as specific  $D_2R$  antagonist, that displays *in vitro* dissociation kinetics comparable to clozapine and was found as promising antipsychotic agent, with low EPS incidence (Langlois et al., 2012). The “fast-off theory” at the  $D_2R$  is however unable to explain cariprazine’s and aripiprazole’s differences as comparison revealed only little variation in RT at the  $D_2R$  so far ( $0.49 \text{ min}^{-1}$  and  $0.14 \text{ min}^{-1}$ ) (Klein Herenbrink et al., 2016). However, data on  $D_3R$  RT is only sparse and underexplored to date. Furthermore, evaluation of DTRT at the dopamine receptors could be insufficient, as the published assays and results did apply mathematical methods for monomolecular reaction steps only. Considering the reported SBP and different receptor states, dopamine receptor-drug interactions are more likely steps of higher order and recent evaluations might have been oversimplified. Although the  $D_2R$  doesn’t seem as likely target, the  $D_3R$  might reveal novel insights into the mode of action for negative symptoms. Evaluating DTRT requires novel assays and demands close collaboration of *in vitro*, *in silico* and *in vivo* specialist to interpret and assess its clinical impact (Schuetz et al., 2017).

## 2 Scope and objectives

Scaffold evaluation represents one of the main tasks in preclinical drug development. This work aims to improve the existing drug design at aminergic GPCRs, by evaluating natural products and natural product inspired compounds as well as drug-target interactions that were recently underexplored.

The H<sub>4</sub>R represents a target at which only few compounds show considerable affinity and the evaluation of novel scaffolds is necessary to improve clinical recognition of this target. Thorough SARs investigation will be possible, by more active compounds. In this work natural compounds will be evaluated at the H<sub>4</sub>R to generate inspiration for novel scaffolds.

In this work natural product inspired compounds will be evaluated at the H<sub>3</sub>R and derivatized, based on recent SAR studies to increase the number of H<sub>3</sub>R active ligands. A larger substance library may increase the chance to overcome insufficient *in vivo* efficacy and advance this target in the awareness of neurological drug designers. Therefore a series of non-imidazole-based compounds will be pharmacologically characterized for their histamine receptor subtype affinity, to forward them into preclinical evaluation.

The design and evaluation of bitopic D<sub>2</sub>/D<sub>3</sub>R ligands and the exploration of bioisosteric exchange in dopamine receptor ligands can further contribute to the treatment of dopamine related neurological disorders. This work will report on the pharmacological characterization of a small series of bitopic dopamine receptor ligands to contribute to this topic. Given a high overlap of dopamine and serotonin receptor subtypes a preclinical serotonin receptor agonist will also be evaluated at the dopamine receptor subtypes to complement its pharmacological characterization. New binding pockets in the dopamine receptor subtypes require novel *in vitro* investigation tools, as recently used assays are not sufficient to describe non-monomolecular binding interactions into detail. One aspect of this thesis will be the evaluation of a novel drug-target residence time assay to address this and to complement preclinical drug evaluation of novel compounds.

This cumulative thesis aims to expand scaffold libraries of histamine and dopamine receptor ligands by natural compounds, natural compound inspired motifs, bitopic ligands and ligands with more than one target. As the preclinical *in vitro* evaluation of novel compounds requires innovative assays, a focus was set on the design and evaluation of a new, indirect radioligand displacement assay to assess the DTRT of dopamine D<sub>2</sub>/D<sub>3</sub> receptor ligands.

3 From medicinal plant extracts to defined chemical compounds targeting the histamine H<sub>4</sub> receptor: Curcuma longa in the treatment of inflammation

### **3 From medicinal plant extracts to defined chemical compounds targeting the histamine H<sub>4</sub> receptor: Curcuma longa in the treatment of inflammation**

Frank A<sup>1</sup>, Abu-Lafi S<sup>2</sup>, Adawi A<sup>3</sup>, Schwed JS<sup>1</sup>, Stark H<sup>1</sup>, Rayan A<sup>3,4</sup>, **2017**.

<sup>1</sup>Institute of Pharmaceutical and Medicinal Chemistry, Heinrich Heine University Düsseldorf, 40225, Düsseldorf, Germany.

<sup>2</sup>Faculty of Pharmacy, Al-Quds University, P.O. Box 20002, Abu-Dies, Palestine.

<sup>3</sup>Institute of Applied Research, The Galilee Society, P.O. Box 437, 20200, Shefa-'Amr, Israel.

<sup>4</sup>Drug Discovery Informatics Lab, Qasemi Research Center, Al-Qasemi Academic College, P.O. Box 124, 30100, Baka EL-Garbya, Israel

Published in: *Inflammation Research*, **66**: 923-929.

DOI: 10.1007/s00011-017-1075-x.

Research contribution: Pharmacological evaluation of majority of extracts and compounds at the H<sub>4</sub> receptor, interpretation of data and preparation of manuscript.

Reprinted by permission from Springer Nature Customer Service Centre GmbH: Springer Nature, Inflammation Research, From medicinal plant extracts to defined chemical compounds targeting the histamine H<sub>4</sub> receptor: Curcuma longa in the treatment of inflammation, Annika Frank, Saleh Abu-Lafi, Azmi Adawi, Johannes S. Schwed, Holger Stark, Anwar Rayan, 2017, *Inflammation Research*, 66: 923-929, DOI: 10.1007/s00011-017-1075-x. Copyright Springer Nature Customer Service Centre GmbH, 2017.

### 3 From medicinal plant extracts to defined chemical compounds targeting the histamine H<sub>4</sub> receptor: *Curcuma longa* in the treatment of inflammation

Inflamm. Res. (2017) 66:923–929  
DOI 10.1007/s00011-017-1075-x

Inflammation Research

ORIGINAL RESEARCH PAPER



## From medicinal plant extracts to defined chemical compounds targeting the histamine H<sub>4</sub> receptor: *Curcuma longa* in the treatment of inflammation

Annika Frank<sup>1</sup> · Saleh Abu-Lafi<sup>2</sup> · Azmi Adawi<sup>3</sup> · Johannes S. Schwed<sup>1</sup> · Holger Stark<sup>1</sup> · Anwar Rayan<sup>3,4</sup>

Received: 27 April 2017 / Revised: 2 June 2017 / Accepted: 21 June 2017 / Published online: 24 June 2017  
© Springer International Publishing AG 2017

### Abstract

**Objectives** The aim was to evaluate the activity of seven medicinal, anti-inflammatory plants at the hH<sub>4</sub>R with focus on defined chemical compounds from *Curcuma longa*.

**Materials** Activities were analyzed with membrane preparations from Sf9 cells, transiently expressing the hH<sub>4</sub>R, G<sub>α12</sub> and G<sub>β1γ2</sub> subunits.

**Methods** From the methanolic extract of *C. longa* curcumin (1), demethoxycurcumin (2) and bis(4-hydroxycinnamoyl)methane (3) were isolated, purified with HPLC (elution-time 10.20, 9.66, 9.20 min, respectively) and together with six additional extracts, were characterized via radioligand binding studies at the hH<sub>4</sub>R.

**Results** Compounds from *C. longa* were the most potent ligands at the hH<sub>4</sub>R. They exhibited estimated *K<sub>i</sub>* values of 4.26–6.26 μM (1.57–2.31 μg/mL) (1); 6.66–8.97 μM (2.26–3.04 μg/mL) (2) and 10.24–14.57 μM (3.16–4.49 μg/mL) (3) (95% CI). The estimated *K<sub>i</sub>* value of the crude extract of curcuma was 0.50–0.81 μg/mL. Fractionated curcumin and the crude extract surpassed the effect of pure curcumin with a

*K<sub>i</sub>* value of 5.54 μM or 2.04 μg/mL [95% CI (4.47–6.86 μM), (1.65–2.53 μg/mL)].

**Conclusion** Within this study, defined compounds of *C. longa* were recognized as potential ligands and reasonable lead structures at the hH<sub>4</sub>R. The mode of anti-inflammatory action of curcumin was further elucidated and the role of extracts in traditional phytomedicine was strengthened.

**Keywords** *Curcuma longa* · Natural compounds · hH<sub>4</sub>R · Inflammatory diseases · Phenylpropanoids

### Introduction

The evaluation of the fourth human histamine receptor subtype (hH<sub>4</sub>R) revealed its crucial role in chemotaxis, inflammation and autoimmune disorders [1]. Drug research on the hH<sub>4</sub>R is highly interested in antagonists, due to their suggested potential in the treatment of inflammatory diseases [2].

Natural products have been a source for therapeutic agents for ages [3] and a high amount of currently used biologically active agents are natural product inspired compounds or their derivatives [4]. They are a well-studied source for pharmaceutical development and provide high hit rates in pharmacological screenings as lead-compounds [5]. Therefore, drug discovery and development are highly interested in novel drugs and bioactive lead-compounds out of nature's kitchen [6]. Plants and spices like curcuma, thyme, saffron, cumin, and ephedra species are well reported for their use in traditional medicine, especially against inflammatory events [7–11] and could meet the demands for drug development by supporting natural-based compounds for treating inflammatory diseases. A well investigated representative of these plants is *Curcuma*

Responsible Editor: Bernhard Gibbs.

✉ Holger Stark  
stark@hhu.de

<sup>1</sup> Institute of Pharmaceutical and Medicinal Chemistry, Heinrich Heine University Düsseldorf, 40225 Düsseldorf, Germany

<sup>2</sup> Faculty of Pharmacy, Al-Quds University, P.O. Box 20002, Abu-Dies, Palestine

<sup>3</sup> Institute of Applied Research, The Galilee Society, P.O. Box 437, 20200 Shefa-Amr, Israel

<sup>4</sup> Drug Discovery Informatics Lab, Qasemi Research Center, Al-Qasemi Academic College, P.O. Box 124, 30100 Baka EL-Garbya, Israel

### 3 From medicinal plant extracts to defined chemical compounds targeting the histamine H<sub>4</sub> receptor: *Curcuma longa* in the treatment of inflammation

924

A. Frank et al.

*longa* L., a perennial herb of the *Zingiberaceae* (ginger) family [12]. It has traditionally been used to treat various conditions [13] and extensive research in vitro and in vivo during the last few decades revealed that *C. longa* possesses anti-inflammatory effects [14]. Its inhibition of NF- $\kappa$ B (nuclear factor 'kappa-light-chain-enhancer' of activated B-cells), Akt-phosphorylation (protein kinase B), m-TOR activation (mechanistic target of rapamycin) and in contrast an activation of AMPK (5' AMP-activated protein kinase) in inflammatory events are well reported, but its mode of action is still not conclusively investigated [15].

The aim of the current study is to evaluate the activity of different plant extracts from traditional phytomedicine approaches at the hH<sub>4</sub>R with a focus on defined chemical structures from *C. longa*. All seven plants were investigated because of their traditional use against inflammatory events and could support the treatment of those. Especially curcuma's purified and isolated compounds display different structural features from any previously known ligands and may provide new directions for selective and specific scaffolds for the hH<sub>4</sub>R, opening new ways in treating inflammatory diseases. In doing so the anti-inflammatory mode of action of curcuma can be further elucidated, supporting its rational use in the adjuvant treatment of inflammatory diseases.

#### Materials and methods

*Curcuma longa* L. for the first extract was purchased from Al Alim-Medicinal Herb Center (Zippori, Israel), all other herbs and *C. longa* for the repeated measurement were gathered by the Institute of the Qasemi Research Centre (Baka EL-Garbya, Israel). Pure curcumin was kindly provided by Prof. Dr. Gunter Eckert, Frankfurt/Germany, another batch as curcumin 2 was purchased from Sigma Aldrich.

#### Plant extract preparation

Each extract stems from one plant sample, except for *C. longa*, that was extracted from two different samples. The respective plant parts were chosen, because of their most common use in traditional phytomedicine. 20 mL of methanol were added to 2 g of the dried plant material. Samples were sonicated for 120 min at 45 °C and left for 2 h. The liquid was made to pass through a 0.4  $\mu$ m filter and concentrated by a rotary vacuum evaporator.

#### HPLC experiments

The analytical HPLC (High performance liquid chromatography) was a Waters Alliance (e2695 separations

module) with a 2998 Photodiode Array detector (PDA). The preparative HPLC system consisted of a 3535 quaternary gradient module with a 996 PDA detector. The analytical experiments were run on an ODS column of Waters (XBridge, 4.6 ID  $\times$  150 mm, 5  $\mu$ m, guard column of Xbridge ODS, 20 mm  $\times$  4.6 mm ID, 5  $\mu$ m). The mobile phase consisted of acidified water at pH 3 adjusted with phosphoric acid (A) and acetonitrile (B). Linear gradient started at 55% of (A) and 45% of (B) to reach 30% (A) and 70% (B) in 13 min then to 100% (B) in 1 min keeping it at 100% (B) for 5 min and back to 55% (A) in 1 min. PDA wavelengths ranged from 200 to 600 nm. The flow rate was set to 1 mL/min, the injection volume was 10  $\mu$ L and the column temperature was at room temperature. The three major fractions were reinjected to the prep-HPLC with an ODS column (Agilent PrepHT C18, 22.2  $\times$  250 mm, 10  $\mu$ m). The elution program was set as in the analytical mode, the flow rate was 20 mL/min and 1 mL injection volume. Fractionation of the methanolic crude extract of *C. longa* by preparative HPLC lead to isolation of three purified compounds (**1**, **2**, **3**) (purity >90%). The isolated compounds were further determined by HR-ESI-MS (High-resolution electrospray ionization mass spectrometry) in positive mode (LTQ-Orbitrap XL hybrid ion trap with a high resolution Orbitrap detection system, Thermo Scientific, USA).

#### Membrane preparation

Cell culture and membrane preparation were performed according to Schneider and Seifert [16] to gain membrane preparations from Sf9 cells transiently expressing the hH<sub>4</sub>R, the G<sub>αi2</sub> and G<sub>β1γ2</sub> subunits. Briefly, Sf9 cells were cultured in spinner flasks at 28 °C and 100 rpm in Sf9 medium [with 5% (v/v) fetal bovine serum and 10  $\mu$ L/mL penicillin/streptomycin].  $3 \times 10^6$  cells/mL was infected with a baculovirus solution (1:100), containing the human histamine H<sub>4</sub> receptor and the G<sub>αi2</sub> and G<sub>β1γ2</sub> subunits. 48 h after infection cells were harvested and membrane preparation was performed at 4 °C. The infected Sf9 cells were centrifuged at 1000 rpm for 10 min. The resulting pellet was resuspended in phosphate buffered saline (PBS) and centrifuged again at 1000 rpm for 10 min. Afterwards the pellet was resuspended in 15 mL lysis buffer [80  $\mu$ M benzamidine, 20  $\mu$ M leupeptin, 200  $\mu$ M phenylmethyl sulfonylfluoride (PMSF), in H<sub>4</sub> binding buffer (13 mM MgCl<sub>2</sub>, 1 mM EDTA and 75 mM Tris/HCl, pH 7.4)] per 100 mL cell suspension. After homogenization in a hand potter the suspension was centrifuged at 500 rpm for 5 min and the supernatant was centrifuged for 20 min at 18,000 rpm. The resulting pellet was resuspended in lysis buffer, homogenized and centrifuged for 20 min at 18,000 rpm. The pellet was



resuspended in 12 mL H<sub>4</sub> binding buffer per 100 mL cell suspension, homogenized and stored as 1 mL aliquots at −70 °C.

[<sup>3</sup>H]Histamine competition binding assay

The assays were performed as published recently [17]. The extracts (A)–(F) were tested at fixed concentrations of 5 µg/mL in two independent experiments to allow a rough screening. The crude extract of curcuma and its three isolated compounds were tested at 10 µg/mL in three independent experiments, performed in triplicates for one-point measurements. For concentration–response curves, the curcuma extract and compounds (2)–(3) were tested at four concentrations ranging from 0.3 to 10 µg/mL allowing an estimation of the 95% confidence intervals of the *K<sub>i</sub>* values. Compound (1) and pure curcumin were tested at six and eight distinct concentrations, respectively (0.01 ng/mL–100 µg/mL). A second crude extract of curcuma was tested at eleven concentrations (0.01 ng/mL–100 µg/mL) and the testing of pure curcumin (curcumin 2) was repeated in ten concentrations (0.01–10 ng/mL), allowing determination of the *K<sub>i</sub>* values for the latter four substances. The used concentrations were chosen as standard logarithmic or half-logarithmic concentrations, limited by the solubility of the given compounds in the assay buffer. Bound radioligand was separated from free radioligand by filtration with a cell harvester (Inotech, Brandon, FL). The amount of bound radioactive ligand collected on the filtermats was determined by liquid scintillation counting with a Betacounter Trilux (Perkin Elmer, Waltham, MA, USA).

Data

HPLC Data acquisition used Empower 3 chromatography data software (Waters, Eschborn, Germany). Values of one-point measurements were calculated relative to specific binding. Concentration–response competition binding data were analyzed with Prism 6 (GraphPad

**Table 1** Composition of plant extracts tested at the hH4R

Plant	Part of the plant	Abbreviation
<i>Crocus sativus</i>	Flower	(A)
<i>Cuminum cyminum</i>	Seed	(B)
<i>Nigella sativa</i>	Seed	(C)
<i>Thymus serpyllum</i>	Leaf	(D)
<i>Cuminum karamani</i>	Seed	(E)
<i>Ephedra foeminea</i>	Stem	(F)
<i>Curcuma longa</i>	Rhizome	Crude extract

**Table 2** Percentual inhibition of radioligand binding at hH<sub>4</sub>R of extracts (A)–(F) (5 µg/mL), the extract of curcuma and the compounds (1)–(3) (10 µg/mL)

Inhibition (%)	Extract (A)	Extract (B)	Extract (C)	Extract (D)	Extract (E)	Extract (F)	Curcuma extract	Compound (1)	Compound (2)	Compound (3)
Mean	2.99	7.71	8.11	8.86	11.05	20.62	102.00	88.50	76.93	71.40
Lower limit to upper limit	−2.60 to 7.60	−2.60 to 26.67	−8.00 to 19.73	5.20 to 11.80	4.60 to 23.20	10.60 to 33.62	98.03 to 106.00	86.26 to 90.74	68.86 to 85.01	53.02 to 89.78
<i>n</i>	2	2	2	2	2	2	3	3	3	3

*n* = number of independent experiments performed with the same extract, each performed in triplicates

### 3 From medicinal plant extracts to defined chemical compounds targeting the histamine H4 receptor: *Curcuma longa* in the treatment of inflammation

926

A. Frank et al.

Software Inc., San Diego, CA, USA). The  $K_i$  values were calculated from the  $IC_{50}$  values using the Cheng–Prusoff equation [18]. Values of binding data obtained are means of three experiments, each performed as triplicates. Values of binding data obtained by eleven and ten point measurements are means of three independent experiments run in at least duplicates. Binding data is given as 95% confidence intervals and are complemented by means for six, eight, ten and eleven point measurements. One-point measurements are reported as means with the respective ranges.

#### Results

The methanolic extracts of *C. longa*, *Crocus sativus*, *Nigella sativa*, *Thymus serpyllum*, *Cuminum karamani* (*Carvon coptikum*), *Cuminum cyminum* and *Ephedra foeminea* (Table 1) were tested for their inhibition of radioligand binding at the hH<sub>4</sub>R from purified membrane preparations.

The plant extracts displayed poor activity at the receptor (<50% inhibition at 5  $\mu$ g/mL), with the exception of the methanolic extract of *C. longa* that showed strong activity (complete inhibition at 10  $\mu$ g/mL) (Table 2). As extracts (A)–(F) showed low affinities, their further evaluation was discontinued after two independent experiments in this rough pre-screening.

Due to its superior affinity the methanolic curcuma extract was further purified, which resulted in three chemically defined compounds (1–3). Curcumin (1), demethoxycurcumin (2), and bis-(4-hydroxycinnamoyl)methane (3), 1,7-bis(4-hydroxyphenyl)hepta-1,6-diene-3,5-dione (Fig. 1) were collected using a preparative HPLC, eluting at 10.20 (1), 9.66 (2) and 9.20 min (3), respectively (purity >90%), and showing UV–Vis spectra with  $\lambda_{max}$  at 425 nm (1), 421 nm (2) and 416 nm (3).

The compounds and the crude extract were able to inhibit radioligand binding at the hH<sub>4</sub>R by more than 70% in measurements at 10  $\mu$ g/mL. Compound (1) showed highest inhibition of the three isolated compounds with 89% (1) >77% (2) >71% (3) inhibition, while the strongest activity was shown for the crude extract with a complete inhibition of radioligand binding (adjusted  $p$  value <0.05) (Fig. 2; Table 2). Statistical analysis showed, that the comparison of the crude extracts activity against the three compounds (1)–(3) was significant (adjusted  $p$  values <0.05), activity comparison of compound (1) against (2) was significant (adjusted  $p$  value = 0.03) and comparisons of activities from compound (1) against (3) and compound (3) against (2) were not significant.

The tested compounds and the crude extract showed clear concentration–response effects in radioligand binding studies. Competition binding assays resulted in 95% confidence intervals for the estimated  $K_i$  values ranging

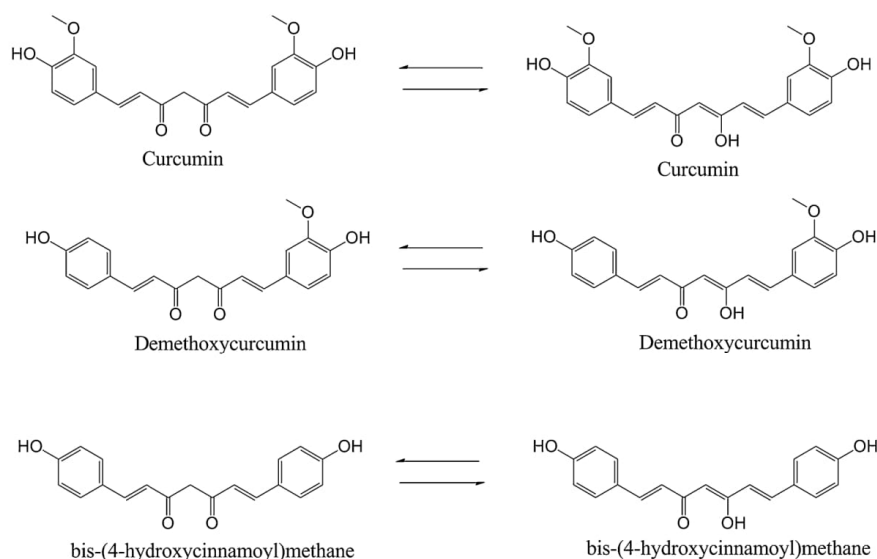


**Fig. 1** Chemical structures of the fractionated compounds, curcumin, demethoxycurcumin, and bis-(4-hydroxycinnamoyl)methane

### 3 From medicinal plant extracts to defined chemical compounds targeting the histamine H<sub>4</sub> receptor: *Curcuma longa* in the treatment of inflammation

From medicinal plant extracts to defined chemical compounds targeting the histamine H<sub>4</sub>...

927

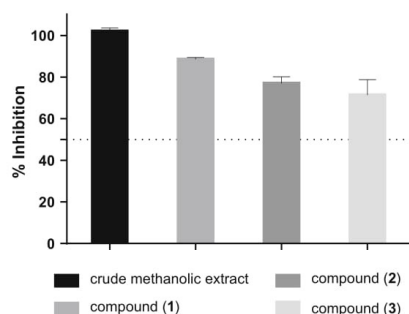


**Fig. 2** Percentual inhibition of radioligand binding at hH<sub>4</sub>R of curcumas extract and fractions (1)–(3) (10 µg/mL)  $n = 3$  independent experiments each performed in triplicates. Data are given as mean with the respective ranges

between 1.57–2.31 µg/mL (1), 2.26–3.04 µg/mL (2) and 3.16–4.49 µg/mL (3). This led to molar values of 4.26–6.26 µM (1), 6.66–8.97 µM (2) and 10.24–14.57 µM (3), respectively (Table 3), for the purified compounds. Highest activity was shown for the crude extract with an estimated 95% confidence interval for the  $K_i$  value spanning 0.50–0.81 µg/mL, indicating a synergistic effect of all compounds.

It is noteworthy that the crude extract as well as the isolated curcumin (1) showed stronger binding to the hH<sub>4</sub>R than pure curcumin with a  $K_i$  value of 5.54 µM [95% CI (4.47–6.86 µM)] or 2.04 µg/mL [95% CI (1.65–2.53 µg/mL)]. For verification, the evaluation was repeated with a second extract preparation from *Curcuma longa*. It displayed a  $K_i$  value of 9.36 µg/mL [95% CI (4.96–17.68 µg/mL)], while a second batch of pure curcumin (curcumin 2) confirmed the first measurement with a measured  $K_i$  value of 4.97 µM [95% CI (3.26–7.57 µM)] or 1.83 µg/mL [95% CI (1.20–2.79 µg/mL)] (Fig. 3; Table 3).

#### Discussion

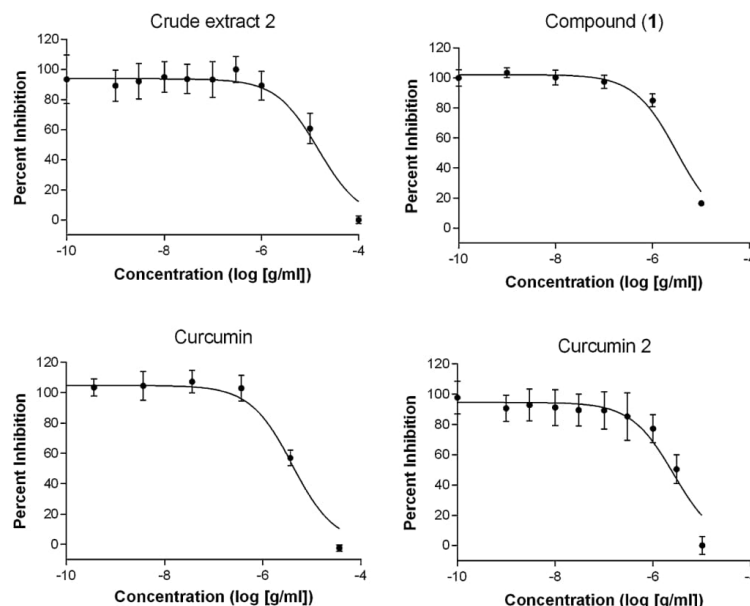
The study showed a superiority of *C. longa* crude extract and isolated curcumin in contrast to pure curcumin. This could be due to the presence of glycosides, complex carbohydrates or associated plant compounds like other

polyphenols, that are not detectable in the used detector system, but are known for inheriting anti-inflammatory effects [19]. Although not yet tested at the hH<sub>4</sub>R, their attendance could result in synergistic effects in the in vitro testing-systems. The superiority of extracts in comparison to purified compounds is well reported [20] and could be one reason why clinical studies that used pure curcumin instead of extracts cannot confirm the in vitro activity often reported. The discrepancy in activity between different batches of the same extract may be caused by the natural deviation of compound composition in plants. The compounds concentration and composition strongly depends on the environmental conditions, gathering seasons and extraction conditions. Though a thorough standardization method is essential for the therapies success when using plant extracts. Although JNJ-777120, a well-studied reference hH<sub>4</sub>R antagonist, displays a  $K_i$  value of 22.26 nM, compounds showing activity in low micromolar concentrations could serve as potential lead structures for designing optimized and structurally novel hH<sub>4</sub>R ligands [21]. Achievable plasma concentrations of curcumin in in vivo testings are in the same range as affinities in our in vitro H<sub>4</sub> studies of curcumins methanolic extracts and isolated compounds. Thus, an interaction with the H<sub>4</sub> receptor has to be considered when assessing anti-inflammatory effects of curcumin and its extracts. In humans peak plasma levels of curcumin after the oral dosing of 8 g were 1.77 µM [22]. The simultaneous application of piper alkaloids (2 g/kg curcumin + 20 mg/kg alkaloids) resulted in maximal serum concentrations of 0.18 µg/mL [23] and special formulations like nanocurcumin [24] or poly lactic-co-glycolic acid encapsulated curcumin [25] are on the rise to improve its bioavailability. Complex carbohydrates that are attendant in most extracts could further enhance bioavailability of the extracts [26]. At the same time curcumin displays very low toxicity even at high doses up to 12 g per day [22] allowing application of reasonable therapeutic doses in anti-inflammatory treatment. Although curcumin has traditionally been used against inflammatory diseases and in vitro as well as in vivo data supports the anti-inflammatory effects, the clinical effectiveness as well as the main molecular target still needs to be proven. This led to a wide discussion whether or not the pharmacological use of curcumin and its derivatives should be

**Table 3** Estimated 95% CI and  $K_i$  values of curcumas crude extract, the compounds (1)–(3) and pure curcumin

	Crude extract	Crude extract 2	Curcumin	Curcumin 2	Compound (1)	Compound (2)	Compound (3)
$K_i$	–	9.36	2.04	1.83	1.90	–	–
(95% CI) µg/mL	(0.50–0.81)	(4.96–17.68)	(1.65–2.53)	(1.20–2.79)	(1.57–2.31)	(2.26–3.04)	(3.16–4.49)
MW g/mol	–	–	368.39	368.39	368.39	338.36	308.33
$K_i$	–	–	5.54	4.97	5.17	–	–
(95% CI) µM	–	–	(4.47–6.86)	(3.26–7.57)	(4.26–6.26)	(6.66–8.97)	(10.24–14.57)

**Fig. 3** Concentration–response curves for the crude extract 2, compound (1), curcumin and curcumin 2. Data are given as mean with the respective 95% CI. All assays were performed in three experiments, each run at least in duplicates



recommended and how in vitro investigations may be interpreted [27]. Certainly pure curcumin will not be the miracle cure of inflammations, but considering the comprehensive scientific data of its activity against inflammatory targets [15] the adjuvant treatment of inflammation with curcumin can be considered. Thereby, the bioavailability of a given formulation, the composition of bioactive compounds in an extract or capsule and a potential affinity optimization of the lead-compounds could be taken into account.

In conclusion, our research reveals that among other inactive plant extracts, *C. longa* and three of its isolated compounds display affinity at the hH<sub>4</sub>R, despite not showing typical structure motifs [28]. They are not positively charged at physiological pH value and do not contain the aminergic structure of typical imidazole or non-imidazole hH<sub>4</sub>R ligands. Thus, dicinnamoyl methanes might depict reasonable lead structures for novel scaffolds in hH<sub>4</sub>R targeting. Further evaluation of different derivatives will be necessary to allow a thorough structure–activity relationship evaluation, as there are only minor structure differences between the three compounds.

Although the hH<sub>4</sub>R plays an important role in chemotaxis, inflammation and autoimmune disorders, at recent date there are no approved drugs on the market, leaving the development of new ligands at this receptor highly desired. We found

that the crude extract of *C. longa* displays higher potency than its purified compounds. This illustrates the advantages of using complex extracts in pharmaceutical therapy as they sometimes surpass their isolated compounds in therapeutic potency due to synergistic effects [29]. When using extracts in pharmacotherapy it is important to take care of the naturally deviating compound concentrations in plants and a thorough standardization method of extracts is essential for a phytotherapy's success. The conclusive data of in vitro as well as in vivo results of pharmacologic investigations can support the use of *C. longa*, especially extracts, in the adjuvant treatment of inflammatory diseases when combined with modern, orthodox medicine.

Within this study, we were able to evaluate seven different natural extracts at the hH<sub>4</sub>R and identified curcumin derivatives as potential lead for future drug development. Thereby, we further characterized curcumins mode of action on molecular targets in fighting inflammatory events and extended the lead structure database of biologically active compounds at the hH<sub>4</sub>R.

**Acknowledgements** This study was supported by the Al-Qasemi Research Foundation, the Ministry of Science, Space and Technology, BM0806, CM1204 and CA15125 COST Actions as well as DFG INST 208/664 and GRK2158. We declare that the funders had no role in study design, data collection and analysis, decision to publish, or preparation of the manuscript.



### 3 From medicinal plant extracts to defined chemical compounds targeting the histamine H4 receptor: *Curcuma longa* in the treatment of inflammation

From medicinal plant extracts to defined chemical compounds targeting the histamine H<sub>4</sub>...

929

#### References

1. Dunford PJ, O'Donnell N, Riley JP, Williams KN, Karlsson L, Thurmond RL. The histamine H<sub>4</sub> receptor mediates allergic airway inflammation by regulating the activation of CD4<sup>+</sup> T cells. *J Immunol*. 2006;176:7062–70.
2. Zaid H, Raiyn J, Osman M, Falah M, Srouji S, Rayan A. In silico modeling techniques for predicting the tertiary structure of human H<sub>4</sub> receptor. *Front Biosci*. 2015;21:597–619.
3. Cragg GM, Newman DJ. Medicinals for the millennia. The historical record. *Ann N Y Acad Sci*. 2001;8:2–25.
4. Lee K-H. Discovery and development of natural product-derived chemotherapeutic agents based on a medicinal chemistry approach. *J Nat Prod*. 2010;73:500–16.
5. Lahlou M. The success of natural products in drug discovery. *Pharmacol Pharm*. 2013;4:17–31.
6. Harvey A. The role of natural products in drug discovery and development in the new millennium. *IDrugs*. 2010;13:70–2.
7. Aggarwal BB, Harikumar KB. Potential therapeutic effects of curcumin, the anti-inflammatory agent, against neurodegenerative, cardiovascular, pulmonary, metabolic, autoimmune and neoplastic diseases. *Int J Biochem Cell Biol*. 2009;41:40–59.
8. Mousavi SZ, Bathaie SZ. Historical uses of saffron: identifying potential new avenues for modern research. *AJP*. 2011;1:57–66.
9. Bhat SP, Rizvi W, Kumar A. Effect of *Cuminum cyminum* L. seed extracts on pain and inflammation. *J Neurosci Res*. 2014;14:186–92.
10. Ocana-Fuentes A, Arranz-Gutierrez E, Senorans FJ, Reglero G. Supercritical fluid extraction of oregano (*Origanum vulgare*) essential oils: anti-inflammatory properties based on cytokine response on THP-1 macrophages. *Food Chem Toxicol*. 2010;48:1568–75.
11. Ali-Shtayeh MS, Jamous RM, Salameh NMY, Jamous RM, Hamadeh AMA. Complementary and alternative medicine use among cancer patients in Palestine with special reference to safety-related concerns. *J Ethnopharmacol*. 2016;187:104–22.
12. Ammon HPT, Wahl MA. Pharmacology of *Curcuma longa*. *Planta Med*. 1991;57:1–7.
13. Mahdizadeh S, Ghadiri MK, Gorji A. Avicenna's canon of medicine: a review of analgesics and anti-inflammatory substances. *AJP*. 2015;5:182–202.
14. Jurenka JS. Anti-inflammatory properties of curcumin, a major constituent of *Curcuma longa*. *Altern Med Rev*. 2009;14:141–53.
15. Shehzad A, Lee YS. Molecular mechanisms of curcumin action: signal transduction. *Biofactors*. 2013;39:27–36.
16. Schneider EH, Seifert R. Sf9 cells: a versatile model system to investigate the pharmacological properties of G protein-coupled receptors. *Pharmacol Ther*. 2010;128:387–418.
17. Kottke T, Sander K, Weizel L, Schneider EH, Seifert R, Stark H. Receptor-specific functional efficacies of alkyl imidazoles as dual histamine H<sub>3</sub>/H<sub>4</sub> receptor ligands. *Eur J Pharmacol*. 2011;654:200–8.
18. Yung-Chi C, Prusoff WH. Relationship between the inhibition constant (*K<sub>i</sub>*) and the concentration of inhibitor which causes 50 per cent inhibition (IC<sub>50</sub>) of an enzymatic reaction. *Biochem Pharmacol*. 1973;22:3099–108.
19. Raz O, Rogowski O, Rosenzweig T, Shapira I, Berliner S, Boaz M. Anti inflammatory effect of high complex carbohydrate diet in obese volunteers: gender related effects. *Atherosclerosis*. 2015. doi:10.1016/j.atherosclerosis.2015.04.942.
20. Williamson EM. Synergy and other interactions in phyto-medicines. *Phytomedicine*. 2001;8:401–9.
21. Stark H. Histamine H<sub>4</sub> receptor: a novel drug target for immunoregulation and inflammation. London: Versita; 2013.
22. Cheng A-L, Hsu C-H, Lin J-K, Hsu M-M, Ho Y-F, Shen T-S, et al. Phase I clinical trial of curcumin, a chemopreventive agent, in patients with high-risk or pre-malignant lesions. *Anticancer Res*. 2001;21:2895–900.
23. Shoba G, Joy D, Joseph T, Majeed M, Rajendran R, Srinivas PS. Influence of piperine on the pharmacokinetics of curcumin in animals and human volunteers. *Planta Med*. 1998;64:353–6.
24. Sasaki H, Sunagawa Y, Takahashi K, Imaizumi A, Fukuda H, Hashimoto T, et al. Innovative preparation of curcumin for improved oral bioavailability. *Biol Pharm Bull*. 2011;34:660–5.
25. Tsai Y-M, Chang-Liao W-L, Chien C-F, Lin L-C, Tsai T-H. Effects of polymer molecular weight on relative oral bioavailability of curcumin. *Int J Nanomed*. 2012;7:2957–66.
26. Cho E, Jung S. Supramolecular complexation of carbohydrates for the bioavailability enhancement of poorly soluble drugs. *Molecules*. 2015;20:19620–46.
27. Nelson KM, Dahlin JL, Bisson J, Graham J, Pauli GF, Walters MA, et al. The essential medicinal chemistry of curcumin: miniperspective. *J Med Chem*. 2017;60:1620–37.
28. Pappalardo M, Shachaf N, Basile L, Milardi D, Zeidan M, Raiyn J, et al. Sequential application of ligand and structure based modeling approaches to index chemicals for their hH4R antagonism. *PLoS One*. 2014. doi:10.1371/journal.pone.0109340.
29. Wagner H, Ulrich-Merzenich G. Synergy research: approaching a new generation of phytopharmaceuticals. *Phytomedicine*. 2009;16:97–110.

## 4 New lead elements for histamine H<sub>3</sub> receptor ligands in the pyrrolo[2,3-d]pyrimidine class

Espinosa-Bustos C<sup>1</sup>, Frank A<sup>2</sup>, Arancibia-Opazo S<sup>3</sup>, Salas CO<sup>3</sup>, Fierro A<sup>3</sup>, Stark H<sup>2</sup>, 2018.

<sup>1</sup>Departamento de Farmacia, Facultad de Química, Pontificia Universidad Católica de Chile, Santiago 6094411, Chile.  
Electronic address: ccespino@uc.cl.

<sup>2</sup>Institute of Pharmaceutical and Medicinal Chemistry, Heinrich Heine University Düsseldorf, Universitaetsstr. 1, 40225 Düsseldorf, Germany.

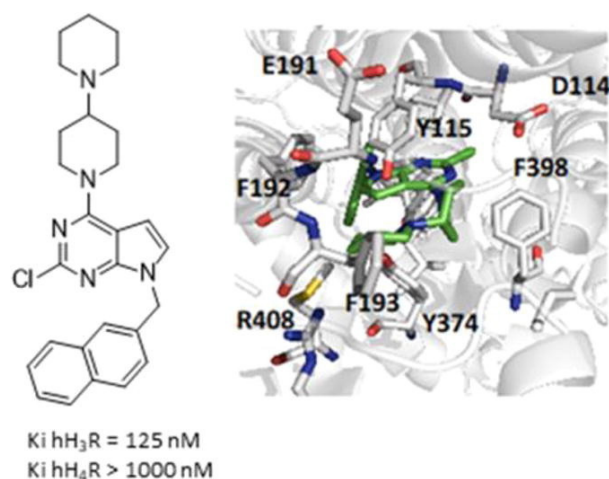
<sup>3</sup>Departamento de Química Orgánica, Facultad de Química, Pontificia Universidad Católica de Chile, Santiago, Chile.

Published in: *Bioorganic & Medicinal Chemistry Letters*, **28**: 2890-2893.

DOI: 10.1016/j.bmcl.2018.07.023

Research contribution: Pharmacological evaluation of compounds at the H<sub>3</sub> and H<sub>4</sub> receptor, interpretation of data and preparation of manuscript.

Graphical abstract:



Reprinted by permission from Elsevier. This article was published in *Bioorganic & Medicinal Chemistry Letters*, 28, Christian Espinosa-Bustos, Annika Frank, Sandra Arancibia-Opazo, Cristian O. Salas, Angelica Fierro, Holger Stark, New lead elements for histamine H<sub>3</sub> receptor ligands in the pyrrolo[2,3 d]pyrimidine class, 2890-2893, Copyright Elsevier Ltd. (2018).



Contents lists available at ScienceDirect

Bioorganic &amp; Medicinal Chemistry Letters

journal homepage: [www.elsevier.com/locate/bmcl](http://www.elsevier.com/locate/bmcl)

## New lead elements for histamine H<sub>3</sub> receptor ligands in the pyrrolo[2,3-*d*]pyrimidine class

Christian Espinosa-Bustos<sup>a,\*</sup>, Annika Frank<sup>b</sup>, Sandra Arancibia-Opazo<sup>c</sup>, Cristian O. Salas<sup>c</sup>, Angelica Fierro<sup>c</sup>, Holger Stark<sup>b</sup>

<sup>a</sup> Departamento de Farmacia, Facultad de Química, Pontificia Universidad Católica de Chile, Santiago 6094411, Chile

<sup>b</sup> Institute of Pharmaceutical and Medicinal Chemistry, Heinrich-Heine-University Düsseldorf, Universitätsstr. 1, 40225 Düsseldorf, Germany

<sup>c</sup> Departamento de Química Orgánica, Facultad de Química, Pontificia Universidad Católica de Chile, Santiago, Chile

### ARTICLE INFO

#### Keywords:

Histamine H<sub>3</sub> receptor  
Pyrrolo[2,3-*d*]pyrimidine derivatives  
Microwave assisted synthesis  
G-protein coupled receptors

### ABSTRACT

This work describes the microwave assisted synthesis of twelve novel histamine H<sub>3</sub> receptor ligands. They display pyrrolo[2,3-*d*]pyrimidine derivatives with rigidized aliphatic amines as warheads. The compounds were screened for H<sub>3</sub>R and H<sub>4</sub>R binding affinities in radioligand displacement assays and the most potent compounds were evaluated for H<sub>3</sub>R binding properties *in vitro* and in docking studies. The combination of a rigidized H<sub>3</sub>R warhead and the pyrrolo[2,3-*d*]pyrimidine scaffold resulted in selective activity at the H<sub>3</sub> receptor with a pK<sub>i</sub> value of 6.90 for the most potent compound. A bipiperidine warhead displayed higher affinity than a piperazine or morpholine motif, while a naphthyl moiety in the arbitrary region increased affinity compared to a phenyl derivative. The compounds can be starting points for novel, simply synthesized histamine H<sub>3</sub> receptor ligands.

The physiological effects of histamine are facilitated by four G protein coupled receptors (GPCRs).<sup>1</sup> H<sub>1</sub>, H<sub>2</sub>, H<sub>3</sub>, and H<sub>4</sub> receptors belong to the same family but differ in their structure, signalling mechanisms, function, tissue distribution and ligand binding. Histamine H<sub>3</sub> receptors (H<sub>3</sub>R) are spread mainly in sympathetic and parasympathetic neurons of the CNS, regulating the release of various neurotransmitters such as histamine, dopamine, serotonin, acetylcholine and noradrenaline.<sup>1</sup> As ligands at the receptor are known for modulating memory functions and arousal, the human H<sub>3</sub>R gained interest of the pharmaceutical industry due to its involvement in pathologies such as schizophrenia, Alzheimer's disease and sleep disorders.<sup>2</sup>

A general pharmacophore for ligands at the H<sub>3</sub>R contains a basic moiety connected by a linker (mostly an alkyl) to a central core, which can be further substituted by an arbitrary region.<sup>3</sup> The basic moiety and the linker display the functional framework, essential for receptor binding, while the arbitrary region is mainly responsible for potency and pharmacokinetic properties.<sup>4</sup> The first generation H<sub>3</sub>R ligands usually contained imidazole-based scaffolds, with regard to histamines structure.<sup>4</sup> Although they displayed high potency, the nucleus resulted in lack of selectivity and pharmacokinetic issues (e.g. interaction with cytochrome P450 enzymes).<sup>5</sup> Hence, several non-imidazolic ligands have been synthesized and successful replacement was accomplished

with piperidine moieties. This led to pitolisant (Fig. 1),<sup>6</sup> which was approved by the EMA for the treatment of narcolepsy in 2016. With JNJ 7737782 (Fig. 1), the alkylspacer was rigidized and a morpholine structure was added in the arbitrary region. The structure displayed beneficial pharmacokinetic properties (e.g. short half-life), affinity remained high and the compound increased wakefulness in rats.<sup>7</sup> Compound I (Fig. 1) was developed as centrally acting antagonist with a bipiperidine structure. It displayed high activity *in vitro* as well as *in vivo* with optimized pharmacokinetic properties.<sup>8</sup>

On the other hand, pyrrolo[2,3-*d*]pyrimidine scaffolds are present in many anti-inflammatory,<sup>9</sup> antitumor<sup>10</sup> and anti-infective compounds.<sup>11,12</sup> Though the combination of the H<sub>3</sub>R pharmacophore and 2,4,7-trisubstituted pyrrolo[2,3-*d*]pyrimidine as central core could be promising for developing H<sub>3</sub>R ligands with additional pharmacological properties. As the pyrrolo[2,3-*d*]pyrimidine scaffold exhibits low micromolar affinity at the H<sub>4</sub> receptor,<sup>13</sup> all compounds were screened for their H<sub>4</sub> receptor binding properties as well.

Thus, we synthesized rigidized modifications of piperidine moieties in this work, as those are reported to deliver high affinities at the H<sub>3</sub>R and provide beneficial pharmacokinetic properties.

In this work, we show the microwave-assisted synthesis of twelve new pyrrolo[2,3-*d*]pyrimidine derivatives with several rigidized aliphatic amines as warheads and different hydrophobic arbitrary

\* Corresponding author.

E-mail address: [ccespino@uc.cl](mailto:ccespino@uc.cl) (C. Espinosa-Bustos).

<https://doi.org/10.1016/j.bmcl.2018.07.023>

Received 17 April 2018; Received in revised form 11 July 2018; Accepted 12 July 2018

Available online 17 July 2018

0960-894X/ © 2018 Elsevier Ltd. All rights reserved.

## 4 New lead elements for histamine H3 receptor ligands in the pyrrolo[2,3-d]pyrimidine class

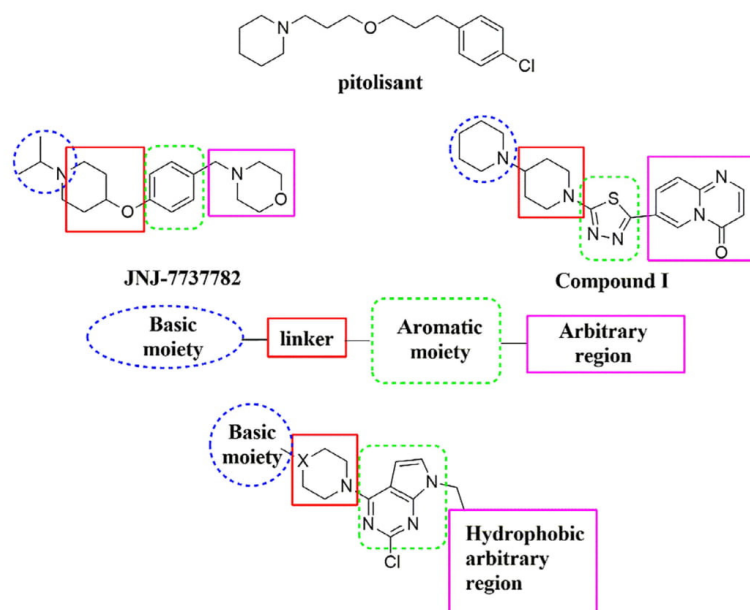
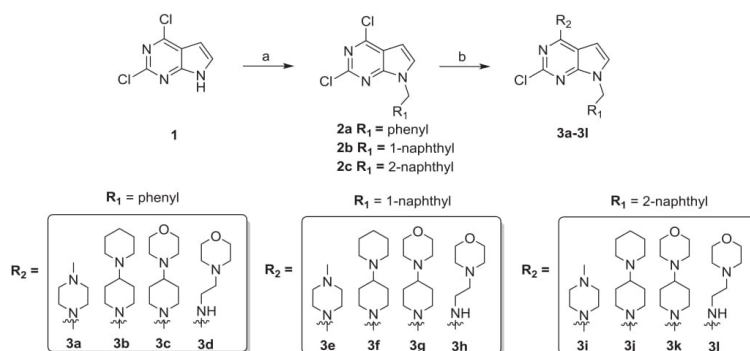


Fig. 1. Chemical structures of H<sub>3</sub> receptor ligands, pharmacophore and proposed structures in this work.



Scheme 1. Reagents and conditions a) Alkyl halides, K<sub>2</sub>CO<sub>3</sub>, DMF, r.t. 6 h, 50–89% b) Amines, NEt<sub>3</sub>, EtOH, 80 °C, MW, 15 min, 62–99%.

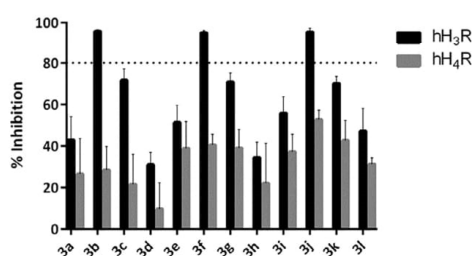


Fig. 2. Inhibition of radioligand binding at the hH<sub>3</sub>R and hH<sub>4</sub>R. Compounds were tested at 1  $\mu$ M in two independent experiments, each as triplicate. Values are calculated relative to specific binding (mean%  $\pm$  range).

Table 1  
pK<sub>i</sub> values of compounds 3b, 3c, 3f and 3j at the hH<sub>3</sub>R determined in radioligand displacement assays. Binding energy determined by molecular modeling approaches.

Compounds	hH <sub>3</sub> R pK <sub>i</sub> $\bar{x} \pm$ SEM	Energy (kcal/mol)
1	7.89 <sup>a</sup>	–6.68
3b	6.31 $\pm$ 0.19	–6.22
3c	5.97 $\pm$ 0.15	–6.18
3f	6.83 $\pm$ 0.23	–8.63
3j	6.90 $\pm$ 0.27	–8.1

Data show mean  $\pm$  standard error of mean (SEM) of five to six independent experiments in duplicates.

<sup>a</sup> Published in 8.



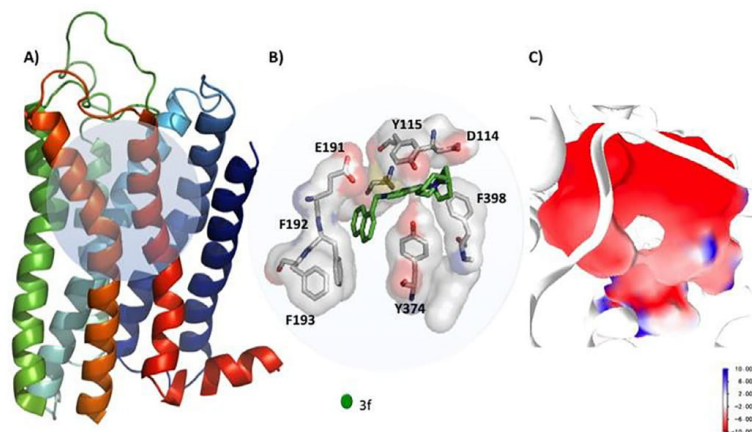


Fig. 3. A) Global structure of H<sub>3</sub>R (homology model) B) Main interactions of **3f** in the binding cavity of H<sub>3</sub>R. C) Electrostatic potential of the binding cavity. Red: negative charge; Blue: positive charge; white: non-charge (color scale values in kT/e).

moieties. As the presence of the pyrrolo[2,3-*d*]pyrimidine scaffold could cause a loss in selectivity all compounds were screened for H<sub>3</sub>R and H<sub>4</sub>R binding affinities. Selected compounds were further evaluated for their H<sub>3</sub>R binding properties *in vitro* and in docking studies. The general synthetic procedure for preparation of 2,4,7-trisubstituted pyrrolo[2,3-*d*]pyrimidine is outlined in Scheme 1. The derivatives **2a–c** were obtained by nucleophilic substitution among the commercially available 2,4-dichloro-7H-pyrrolo[2,3-*d*]pyrimidine **1** and the corresponding alkyl halide, in good yields.<sup>14</sup> In a second step, microwave-assisted reaction, using different cyclic amines, furnished the target compounds **3a–l**, with good yields (> 60%). The chemical structures of the compounds were established based on their spectral properties (IR, <sup>1</sup>H NMR, <sup>13</sup>C NMR and HRMS, see supplementary and ESI).

The compounds **3a** to **3l** were screened for their inhibition of [<sup>3</sup>H] N<sup>α</sup>-methylhistamine binding to the hH<sub>3</sub>R and for their ability to inhibit [<sup>3</sup>H]histamine binding to the hH<sub>4</sub>R at 1 μM. A cut off for further evaluation was set at 80% inhibition. At the H<sub>3</sub>R the compounds **3b**, **3f** and **3j** showed strongest inhibition of radioligand binding with inhibition values of 96% (**3b**) and 95% (**3f**, **3j**) (Fig. 2). No compound showed relevant inhibition at the hH<sub>4</sub>R. As only compounds **3b**, **3f** and **3j** surpassed the threshold, they were further evaluated at the hH<sub>3</sub>R. Although **3c** did not reach the threshold, this compound was investigated as a representative for those below the cut off. The compounds showed clear dose-response effects at the H<sub>3</sub>R with pK<sub>i</sub> values shown in Table 1. Ligand efficiency metrics for assessing as thumb-rule metric on drug-likeness of compounds **3b**, **3c**, **3f** and **3j** were calculated.<sup>15</sup> For novel compounds, lipophilic ligand efficiency (LLE) values should increase, while lipophilicity-corrected ligand efficiency (LELP; also: ligand-efficiency-dependent lipophilicity) values should decrease, ranging between −10 and 10 to optimize drug likeliness (see supplementary). Calculation revealed that improved binding affinity in the compounds comes with a decrease of LLE values (halved from **3c** to **3j**) and an increase of LELP values (nearly doubled from **3c** to **3j**).<sup>15</sup>

To evaluate the main interactions between the hH<sub>3</sub>R and the compounds a three-dimensional model of the receptor was obtained by homology modelling (Fig. 3A). The 3D structure shows interactions between the basic moiety of **3f** and Asp114, which is essential for receptor activation (Fig. 3B).<sup>16</sup> In addition aromatic residues (Tyr115, Tyr374, Phe192, Phe193 and Phe398) stabilized the binding of the ligand with a negative electrostatic potential inside the cavity (Fig. 3C) and both anion/π and cation/π could be generated inside the cavity.

The energy values of the H<sub>3</sub>R and the ligands are listed in Table 1. **3f** and **3j** showed lower values than **3b** and **3c**, which is consistent with experimental results.

In conclusion, using a microwave assisted synthesis allows rapid and easy preparation of different 2,4,7-trisubstituted pyrrolo[2,3-*d*]pyrimidine derivatives. Radioligand binding showed that the combination of typical structure motifs for the H<sub>3</sub>R and the pyrrolo[2,3-*d*]pyrimidine scaffold resulted in selective activity at the hH<sub>3</sub>R. The presence of a piperidine in the warhead increased affinity, compared to a piperazine or morpholine motif. These findings support the activity of bipiperidine moieties at the hH<sub>3</sub>R as in **1**. The addition of a more lipophilic moiety in the arbitrary region revealed improved binding kinetics as shown with compounds **3f** and **3j**. This is also supported by the docking studies, as the binding pocket stabilizes a more lipophilic substituted compound preferably. Although calculated pharmacokinetic values are not favourable for bipiperidine compounds, they substantiate the pharmacokinetic superiority of morpholine structures as reported for JNJ-7737782.<sup>7</sup> The given compounds display moderate, but selective activity at the hH<sub>3</sub>R and can be starting points for novel, simply synthesized ligands. Within this work, the *in vitro* efficiency of piperidine, especially bipiperidine derivatives compared to other aliphatic heterocycles in H<sub>3</sub>R binding was re-affirmed.

#### Acknowledgments

We gratefully acknowledge the financial support of FONDECYT (Post-doctoral fellowship 3150198) and FONDECYT project N° 1161816.

#### References and notes

*General synthetic procedure to obtain N-alkyl pyrrolo[2,3-*d*]pyrimidine 2a–c.* A mixture of 2,4-dichloro-7H-pyrrolo[2,3-*d*]pyrimidine **1** (1.0 mmol), the respective alkyl halide (1.5 mmol) and potassium carbonate (3.0 mmol) in DMF (5 mL) was stirred for 6 h, then the mixture was filtered and evaporated under vacuum. The products were separated by flash chromatography on silica gel eluting with methylene chloride.

*General synthetic procedure to obtain 2,4,7-trisubstituted pyrrolo[2,3-*d*]pyrimidines 3a–l.* The N-alkyl pyrrolo[2,3-*d*]pyrimidine **2a–c** (1.0 mmol), amines (3.0 mmol), triethylamine (4.5 mmol) and ethanol

## 4 New lead elements for histamine H3 receptor ligands in the pyrrolo[2,3-d]pyrimidine class

C. Espinosa-Bustos et al.

Bioorganic & Medicinal Chemistry Letters 28 (2018) 2890–2893

(3 mL) were added to a microwave reaction flask and the reaction mixture was irradiated for 15 min at 80 °C. Then the solvent was evaporated under vacuum and the crude product was purified by column chromatographic on silica gel using chloroform/methanol (10:1) mixture.

### A. Supplementary data

Supplementary data associated with this article can be found, in the online version, at <https://doi.org/10.1016/j.bmcl.2018.07.023>.

### References

1. Parsons ME, Ganellin CR. *Br. J. Pharmacol.* 2006;147:127–135.
2. Tiligada E, Zampeli E, Sander K, Stark H. *Expert Opin. Investig. Drugs.* 2009;18:1519–1531.
3. Labeeuw O, Levoine N, Poupardin-Olivier O, et al. *Bioorg. Med. Chem. Lett.* 2013;23:2548–2554.
4. Wingen K, Stark H. *Drug Discov. Today Technol.* 2013;10:e483–e489.
5. Yang R, Hey JA, Aslanian R, Rizzo CA. *Pharmacology.* 2002;66:128–135.
6. Ligneau X, Perrin D, Landais L, et al. *J. Pharmacol. Exper. Ther.* 2007;320:365–375.
7. Dvorak CA, Apodaca R, Barbier AJ, et al. *J. Med. Chem.* 2005;48:2229–2238.
8. Xiao D, Palani A, Sofolarides M, et al. *Bioorg. Med. Chem. Lett.* 2012;22:3354–3357.
9. Mohamed MS, Mostafa AG, El-hameed RHA. *Pharmacophore.* 2012;3:44–54.
10. Miwa T, Hitaka T, Akimoto H, Nomura H. *J. Med. Chem.* 1991;34:555–560.
11. Mohamed MS, Kamel R, Fatahala SS. *Eur. J. Med. Chem.* 2010;45:2994–3004.
12. Pudlo JS, Nassiri MR, Kern ER, Wotring LL, Drach JC, Townsend LB. *J. Med. Chem.* 1990;33:1984–1992.
13. Gao L-J, Schwed JS, Weizel L, de Jonghe S, Stark H, Herdewijn P. *Bioorganic Med. Chem. Lett.* 2013;23:132–137.
14. Calderón-Arancibia J, Espinosa-Bustos C, Cañete-Molina Á, et al. *Molecules.* 2015;20:6808–6826.
15. Hopkins AL, Keserü GM, Leeson PD, Rees DC, Reynolds CH. *Nat. Rev. Drug Discov.* 2014;13:105–121.
16. Ishikawa M, Watanabe T, Kudo T, et al. *J. Med. Chem.* 2010;53:6445–6456.

**New Lead Elements for  
Histamine H<sub>3</sub> Receptor Ligands in the Pyrrolo[2,3-*d*]pyrimidine Class**

Christian Espinosa-Bustos<sup>a</sup>, Annika Frank<sup>b</sup>, Sandra Arancibia-Opazo<sup>c</sup>, Cristian O. Salas<sup>c</sup>, Angelica Fierro<sup>c</sup>, Holger Stark<sup>b</sup>

<sup>a</sup>Departamento de Farmacia, Facultad de Química, Pontificia Universidad Católica de Chile, Santiago, Chile  
Phone: +56(2)2354-4838, E-mail: ccespino@uc.cl

<sup>b</sup>Institute of Pharmaceutical and Medicinal Chemistry, Heinrich Heine University Düsseldorf, Duesseldorf,  
Phone: +49(0)211-8110478, Fax: +49(0)211-8113359, E-mail: stark@hhu.de.

<sup>c</sup>Departamento de Química Orgánica, Facultad de Química, Pontificia Universidad Católica de Chile,  
Santiago, Chile

**Supporting Information**

NMR Characterization of compounds <b>3a-3l</b>	pages 2-5
NMR spectrums of compounds <b>3a-3l</b>	pages 6-17
Molecular simulations	pages 18-21
Ligand efficiency metrics	pages 21

### General information

Microwave-assisted reactions were carried out in a Microwave Synthesis Reactor Monowave 300 (Anton Paar GmbH, Graz, Austria), in 10 mL sealed vials. Melting points were determined on a Thermogeräte Kofler apparatus (Reichert, Werke A.G., Wien, Austria) and were uncorrected. Nuclear magnetic resonance spectra were recorded on a Bruker AM-400 apparatus using CDCl<sub>3</sub> solutions containing TMS as internal standard. HPLC-MS experiments were performed on an Exactive Plus Orbitrap MS (Bremen, Germany). Mass spectra were obtained on an HP 5988A spectrometer (Hewlett-Packard, Palo Alto, CA, USA). Thin layer chromatography (TLC) was performed using Merck GF-254 type 60 silica gel. Column chromatography was carried out using Merck silica gel 60 (70–230 mesh).

**7-Benzyl-2,4-dichloro-7H-pyrrolo[2,3-d]pyrimidine (2a).** White solid, yield 67 %. <sup>1</sup>H NMR (400 MHz, CDCl<sub>3</sub>) δ 7.38 – 7.28 (m, 3H), 7.24 – 7.20 (m, 2H), 7.17 (d, *J* = 3.6 Hz, 1H), 6.60 (d, *J* = 3.6 Hz, 1H), 5.41 (s, 2H). <sup>13</sup>C NMR (101 MHz, CDCl<sub>3</sub>) δ 152.71, 152.16, 152.10, 135.68, 129.63, 129.05 (2C), 128.41, 127.82 (2C), 116.30, 100.48, 48.60.

**2,4-Dichloro-7-(naphthalen-1-ylmethyl)-7H-pyrrolo[2,3-d]pyrimidine (2b).** White solid, yield 50 %, mp 128 – 130 °C. <sup>1</sup>H NMR (400 MHz, CDCl<sub>3</sub>) δ 7.94 – 7.82 (m, 3H), 7.52 – 7.45 (m, 2H), 7.44 – 7.39 (m, 1H), 7.26 (d, *J* = 7.0 Hz, 1H), 7.01 (d, *J* = 3.6 Hz, 1H), 6.51 (d, *J* = 3.6 Hz, 1H), 5.82 (s, 2H). <sup>13</sup>C NMR (101 MHz, CDCl<sub>3</sub>) δ 152.78, 152.09, 152.04, 133.91, 131.09, 130.80, 129.60, 129.48, 128.99, 127.16 (2C), 126.36, 125.35, 122.77, 116.41, 100.38, 46.50.

**2,4-Dichloro-7-(naphthalen-2-ylmethyl)-7H-pyrrolo[2,3-d]pyrimidine (2c).** White solid, yield 89 %, mp 108 – 110 °C. <sup>1</sup>H NMR (400 MHz, CDCl<sub>3</sub>) δ 7.87 – 7.83 (m, 3H), 7.72 (s, 1H), 7.58 – 7.50 (m, 2H), 7.35 (d, *J* = 8.4 Hz, 1H), 7.23 (d, *J* = 3.5 Hz, 1H), 6.65 (d, *J* = 3.4 Hz, 1H), 5.60 (s, 2H). <sup>13</sup>C NMR (101 MHz, CDCl<sub>3</sub>) δ 152.75, 152.22, 152.15, 133.24, 133.05 (2C), 129.68, 129.09, 127.86, 127.78, 126.94, 126.68, 126.55, 125.34, 116.35, 100.56, 48.75.

**7-Benzyl-2-chloro-4-(4-methylpiperazin-1-yl)-7H-pyrrolo[2,3-d]pyrimidine (3a).** Yellow solid, yield 87 %, mp 108–111 °C. <sup>1</sup>H NMR (400 MHz, CDCl<sub>3</sub>) δ 7.31 – 7.23 (m, 3H), 7.15 (d, *J* = 6.7 Hz, 2H), 6.79 (d, *J* = 3.7 Hz, 1H), 6.43 (d, *J* = 3.7 Hz, 1H), 5.30 (s, 2H), 3.98 – 3.90 (m, 4H), 2.53 – 2.45 (m, 4H), 2.32 (s, 3H). <sup>13</sup>C NMR (101 MHz, CDCl<sub>3</sub>) δ 157.41, 153.43, 152.64, 136.91, 128.77 (2C), 127.85, 127.72 (2C), 123.55, 101.61, 101.28, 54.87 (2C), 47.99, 46.14, 45.49 (2C). HRMS for (C<sub>18</sub>H<sub>21</sub>ClN<sub>5</sub> [M+H]<sup>+</sup>). Calcd: 342.1480. Found: 342.1484.

**4-([1,4'-Bipiperidin]-1'-yl)-7-benzyl-2-chloro-7H-pyrrolo[2,3-d]pyrimidine (3b).** Brown solid, yield 93 %, mp 131–133 °C. <sup>1</sup>H NMR (400 MHz, CDCl<sub>3</sub>) δ 7.31 – 7.21 (m, 3H), 7.16 (d, *J* = 6.7 Hz, 2H), 6.78 (d, *J* = 3.7 Hz, 1H), 6.42 (d, *J* = 3.7 Hz, 1H), 5.30 (s, 2H), 4.76 (d, *J* = 13.3 Hz, 2H), 3.10 – 2.98 (m, 2H), 2.59 (t, *J* = 11.3 Hz, 1H), 2.55 – 2.47 (m, 4H), 1.94 (d, *J* = 12.3 Hz, 2H), 1.67 – 1.50 (m, 6H), 1.50 – 1.36 (m, 2H). <sup>13</sup>C NMR (101 MHz, CDCl<sub>3</sub>) δ 157.17, 153.52,

## 4 New lead elements for histamine H3 receptor ligands in the pyrrolo[2,3-d]pyrimidine class

152.58, 136.97, 128.75 (2C), 127.83, 127.73 (2C), 123.36, 101.72, 101.19, 62.59 (2C), 50.20, 47.97 (2C), 45.59 (2C), 27.90 (2C), 26.21, 24.65. HRMS for (C<sub>23</sub>H<sub>29</sub>ClN<sub>5</sub> [M+H]<sup>+</sup>). Calcd: 410.2106. Found: 410.2109.

**4-{1-(7-Benzyl-2-chloro-7H-pyrrolo[2,3-d]pyrimidin-4-yl)piperidin-4-yl)morpholine (3c).** Brown solid, yield 95 %, mp 126-128 °C. <sup>1</sup>H NMR (400 MHz, CDCl<sub>3</sub>) δ 7.31 – 7.22 (m, 3H), 7.16 (d, *J* = 6.7 Hz, 2H), 6.79 (d, *J* = 3.7 Hz, 1H), 6.42 (d, *J* = 3.7 Hz, 1H), 5.30 (s, 2H), 4.73 (d, *J* = 13.3 Hz, 2H), 3.74 – 3.68 (m, 4H), 3.16 – 3.04 (m, 2H), 2.61 – 2.42 (m, 5H), 1.95 (d, *J* = 12.0 Hz, 2H), 1.55 (ddd, *J* = 15.9, 12.3, 4.0 Hz, 2H). <sup>13</sup>C NMR (101 MHz, CDCl<sub>3</sub>) δ 157.18, 153.50, 152.59, 136.93, 128.76 (2C), 127.85, 127.73 (2C), 123.46, 101.65, 101.22, 67.17 (2C), 61.92, 49.73 (2C), 47.99, 45.14 (2C), 28.16 (2C). HRMS for (C<sub>22</sub>H<sub>27</sub>ClN<sub>5</sub>O [M+H]<sup>+</sup>). Calcd: 412.1899. Found: 412.1902.

**7-Benzyl-2-chloro-N-(2-morpholinoethyl)-7H-pyrrolo[2,3-d]pyrimidin-4-amine (3d).** White solid, yield 92 %, mp 115-117 °C. <sup>1</sup>H NMR (400 MHz, CDCl<sub>3</sub>) δ 7.33 – 7.21 (m, 3H), 7.16 (d, *J* = 6.6 Hz, 2H), 6.79 (d, *J* = 3.6 Hz, 1H), 6.35 (d, *J* = 2.9 Hz, 1H), 5.84 (s, 1H), 5.30 (s, 2H), 3.72 – 3.65 (m, 6H), 2.62 (t, *J* = 5.9 Hz, 2H), 2.52 – 2.44 (m, 4H). <sup>13</sup>C NMR (101 MHz, CDCl<sub>3</sub>) δ 153.97, 136.95, 128.77 (2C), 127.87, 127.69 (2C), 124.08, 66.96 (2C), 56.81, 53.26 (2C), 47.96 (2C). HRMS for (C<sub>19</sub>H<sub>23</sub>ClN<sub>5</sub>O [M+H]<sup>+</sup>). Calcd: 372.1586. Found: 372.1589.

**2-Chloro-4-(4-methylpiperazin-1-yl)-7-(naphthalen-1-ylmethyl)-7H-pyrrolo[2,3-d]pyrimidine (3e).** Yellow solid, yield 62 %, mp 96 – 98 °C. <sup>1</sup>H NMR (400 MHz, CDCl<sub>3</sub>) δ 7.98 – 7.93 (m, 1H), 7.88 – 7.79 (m, 2H), 7.52 – 7.46 (m, 2H), 7.40 (t, *J* = 7.6 Hz, 1H), 7.22 (d, *J* = 6.9 Hz, 1H), 6.68 (d, *J* = 3.5 Hz, 1H), 6.38 (d, *J* = 3.5 Hz, 1H), 5.76 (s, 2H), 3.96 (d, *J* = 4.4 Hz, 4H), 2.55 – 2.48 (m, 4H), 2.33 (s, 3H). <sup>13</sup>C NMR (101 MHz, CDCl<sub>3</sub>) δ 157.44, 153.41, 152.46, 133.82, 132.04, 131.26, 129.03, 128.75, 126.83 (2C), 126.12, 125.32, 123.40, 123.25, 101.50, 101.34, 54.86 (2C), 46.14, 46.04 (2C), 45.47. HRMS for (C<sub>22</sub>H<sub>23</sub>ClN<sub>5</sub> [M+H]<sup>+</sup>). Calcd: 392.1636. Found: 392.1642.

**4-[(1,4'-Bipiperidin)-1'-yl]-2-chloro-7-(naphthalen-1-ylmethyl)-7H-pyrrolo[2,3-d]pyrimidine (3f).** White solid, yield 83%, mp 168 – 169 °C. <sup>1</sup>H NMR (400 MHz, CDCl<sub>3</sub>) δ 7.83 – 7.74 (m, 1H), 7.72 – 7.60 (m, 2H), 7.34 – 7.27 (m, 2H), 7.23 (t, *J* = 7.6 Hz, 1H), 7.04 (d, *J* = 6.9 Hz, 1H), 6.49 (d, *J* = 3.4 Hz, 1H), 6.20 (d, *J* = 3.4 Hz, 1H), 5.58 (s, 2H), 4.60 (d, *J* = 13.0 Hz, 2H), 2.88 (t, *J* = 12.4 Hz, 2H), 2.47 – 2.29 (m, 5H), 1.77 (d, *J* = 12.1 Hz, 2H), 1.46 – 1.41 (br, 6H), 1.31 – 1.22 (m, 2H). <sup>13</sup>C NMR (101 MHz, CDCl<sub>3</sub>) δ 157.21, 153.50, 152.41, 133.81, 132.11, 131.28, 129.00, 128.73, 126.82 (2C), 126.11, 125.32, 123.29, 123.19, 101.63, 101.25, 62.55, 50.21 (2C), 46.03, 45.58 (2C), 27.94 (2C), 26.28 (2C), 24.69. HRMS for (C<sub>27</sub>H<sub>31</sub>ClN<sub>5</sub> [M+H]<sup>+</sup>). Calcd: 460.2263. Found: 460.2269.

**4-{1-(2-Chloro-7-(naphthalen-1-ylmethyl)-7H-pyrrolo[2,3-d]pyrimidin-4-yl)piperidin-4-yl)morpholine (3g).** White solid, yield 77%, mp 148 – 150 °C. <sup>1</sup>H NMR (400 MHz, CDCl<sub>3</sub>) δ 8.01 – 7.93 (m, 1H), 7.91 – 7.73 (m, 2H), 7.51 – 7.45 (m, 2H), 7.40 (t, *J* = 7.6 Hz, 1H), 7.22 (d, *J* = 7.0 Hz, 1H), 6.67 (d, *J* = 3.5 Hz, 1H), 6.37 (d, *J* = 3.5 Hz, 1H), 5.75 (s, 2H), 4.74 (d, *J* = 13.2

Hz, 2H), 3.73 – 3.65 (m, 4H), 3.10 (t,  $J$  = 12.3 Hz, 2H), 2.60 – 2.43 (m, 5H), 1.95 (d,  $J$  = 12.1 Hz, 2H), 1.63 – 1.50 (m, 2H).  $^{13}\text{C}$  NMR (101 MHz,  $\text{CDCl}_3$ )  $\delta$  157.22, 153.49, 152.43, 133.82, 132.08, 131.27, 129.02, 128.74, 126.83 (2C), 126.12, 125.32, 123.27 (2C), 101.55, 101.28, 67.28 (2C), 61.83, 49.78 (2C), 46.04, 45.13 (2C), 28.23 (2C). HRMS for ( $\text{C}_{26}\text{H}_{29}\text{ClN}_5\text{O}$   $[\text{M}+\text{H}]^+$ ). Calcd: 462.2055. Found: 462.2059.

**2-Chloro-N-(2-morpholinoethyl)-7-(naphthalen-1-ylmethyl)-7H-pyrrolo[2,3-d]pyrimidin-4-amine (3h).** White solid, yield 99%, mp 88 – 90 °C.  $^1\text{H}$  NMR (400 MHz,  $\text{CDCl}_3$ )  $\delta$  7.99 – 7.89 (m, 1H), 7.89 – 7.76 (m, 2H), 7.48 – 7.44 (m, 2H), 7.38 (t,  $J$  = 7.6 Hz, 1H), 7.22 (d,  $J$  = 8.8 Hz, 1H), 6.67 (d,  $J$  = 3.3 Hz, 1H), 6.30 (s, 1H), 5.87 (s, 1H), 5.74 (s, 2H), 3.74 – 3.65 (m, 6H), 2.62 (t,  $J$  = 5.7 Hz, 2H), 2.47 (s, 4H).  $^{13}\text{C}$  NMR (101 MHz,  $\text{CDCl}_3$ )  $\delta$  157.28, 153.94, 133.82, 132.09 (2C), 131.23, 129.03, 128.76, 126.83 (2C), 126.75 (2C), 126.13, 125.32, 123.96, 123.20, 66.93 (2C), 56.81 (2C), 53.25 (2C), 45.99. HRMS for ( $\text{C}_{23}\text{H}_{25}\text{ClN}_5\text{O}$   $[\text{M}+\text{H}]^+$ ). Calcd: 422.1742. Found: 422.1746.

**2-Chloro-4-(4-methylpiperazin-1-yl)-7-(naphthalen-2-ylmethyl)-7H-pyrrolo[2,3-d]pyrimidine (3i).** Yellow oil, yield 92%.  $^1\text{H}$  NMR (400 MHz,  $\text{CDCl}_3$ )  $\delta$  7.78 – 7.71 (m, 3H), 7.61 (s, 1H), 7.47 – 7.40 (m, 2H), 7.27 (d,  $J$  = 8.5 Hz, 1H), 6.81 (d,  $J$  = 3.5 Hz, 1H), 6.43 (d,  $J$  = 3.5 Hz, 1H), 5.50 (s, 2H), 4.00 – 3.89 (m, 4H), 2.56 – 2.45 (m, 4H), 2.31 (s, 3H).  $^{13}\text{C}$  NMR (101 MHz,  $\text{CDCl}_3$ )  $\delta$  157.44, 153.48, 152.69, 134.35, 133.28, 132.91, 128.71, 127.84, 127.72, 126.63, 126.39, 126.18, 125.63, 123.59, 101.72, 101.32, 54.87 (2C), 48.15, 46.14, 45.50 (2C). HRMS for ( $\text{C}_{22}\text{H}_{23}\text{ClN}_5$   $[\text{M}+\text{H}]^+$ ). Calcd: 392.1636. Found: 392.1640.

**4-([1,4'-Bipiperidin]-1'-yl)-2-chloro-7-(naphthalen-2-ylmethyl)-7H-pyrrolo[2,3-d]pyrimidine (3j).** White solid, yield 75%, mp 162 – 163 °C.  $^1\text{H}$  NMR (400 MHz,  $\text{CDCl}_3$ )  $\delta$  7.60 – 7.47 (br, 3H), 7.40 (s, 1H), 7.28 – 7.19 (br, 2H), 7.07 (d,  $J$  = 6.5 Hz, 1H), 6.59 (s, 1H), 6.22 (s, 1H), 5.24 (s, 2H), 4.56 (d,  $J$  = 10.9 Hz, 2H), 2.81 (d,  $J$  = 11.1 Hz, 2H), 2.36 – 2.29 (br, 5H), 1.72 (d,  $J$  = 9.5 Hz, 2H), 1.37 – 1.21 (m, 8H).  $^{13}\text{C}$  NMR (101 MHz,  $\text{CDCl}_3$ )  $\delta$  157.18, 153.55, 152.60, 134.42, 133.28, 132.89, 128.68, 127.84, 127.71, 126.62, 126.37, 126.16, 125.65, 123.40, 101.85, 101.23, 62.53, 50.19 (2C), 48.12, 45.58 (2C), 27.92 (2C), 26.26 (2C), 24.68. HRMS for ( $\text{C}_{27}\text{H}_{31}\text{ClN}_5$   $[\text{M}+\text{H}]^+$ ). Calcd: 460.2263. Found: 460.2268.

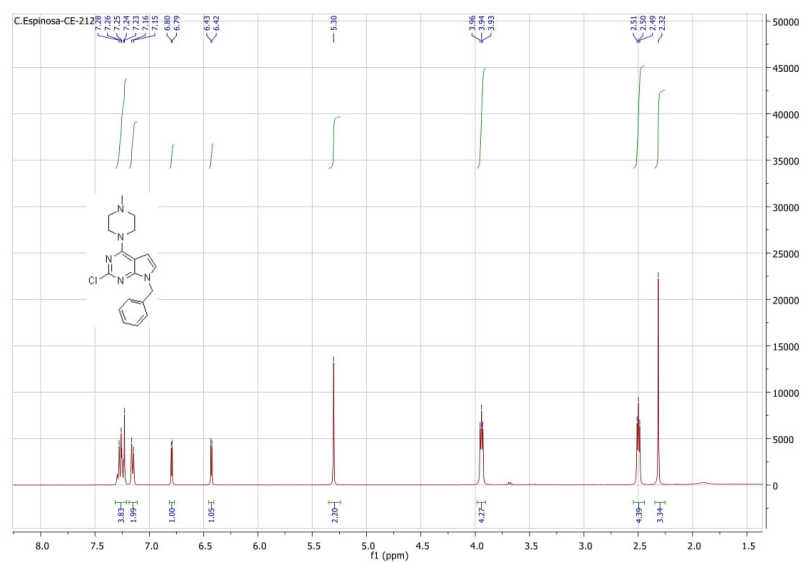
**4-(1-(2-Chloro-7-(naphthalen-2-ylmethyl)-7H-pyrrolo[2,3-d]pyrimidin-4-yl)piperidin-4-yl)morpholine (3k).** White solid, yield 65%, mp 156 – 157 °C.  $^1\text{H}$  NMR (400 MHz,  $\text{CDCl}_3$ )  $\delta$  7.85 – 7.76 (m, 3H), 7.66 (s, 1H), 7.52 – 7.44 (br, 2H), 7.32 (d,  $J$  = 7.9 Hz, 1H), 6.85 (s, 1H), 6.47 (s, 1H), 5.50 (s, 2H), 4.78 (d,  $J$  = 12.3 Hz, 2H), 3.73 (s, 4H), 3.13 (t,  $J$  = 12.1 Hz, 2H), 2.65 – 2.48 (br, 5H), 1.98 (d,  $J$  = 11.2 Hz, 2H), 1.59 (d,  $J$  = 10.5 Hz, 2H).  $^{13}\text{C}$  NMR (101 MHz,  $\text{CDCl}_3$ )  $\delta$  157.20, 153.54, 152.63, 134.40, 133.28, 132.90, 128.70, 127.84, 127.72, 126.63, 126.39, 126.18, 125.65, 123.47, 101.78, 101.26, 67.27 (2C), 61.82, 49.77 (2C), 48.14, 45.15 (2C), 28.23 (2C). HRMS for ( $\text{C}_{26}\text{H}_{29}\text{ClN}_5\text{O}$   $[\text{M}+\text{H}]^+$ ). Calcd: 462.2055. Found: 462.2057.

**2-Chloro-N-(2-morpholinoethyl)-7-(naphthalen-2-ylmethyl)-7H-pyrrolo[2,3-d]pyrimidin-4-amine (3l).** White solid, yield 92 %, mp 161-162 °C.  $^1\text{H}$  NMR (400 MHz,  $\text{CDCl}_3$ )  $\delta$  7.89 –

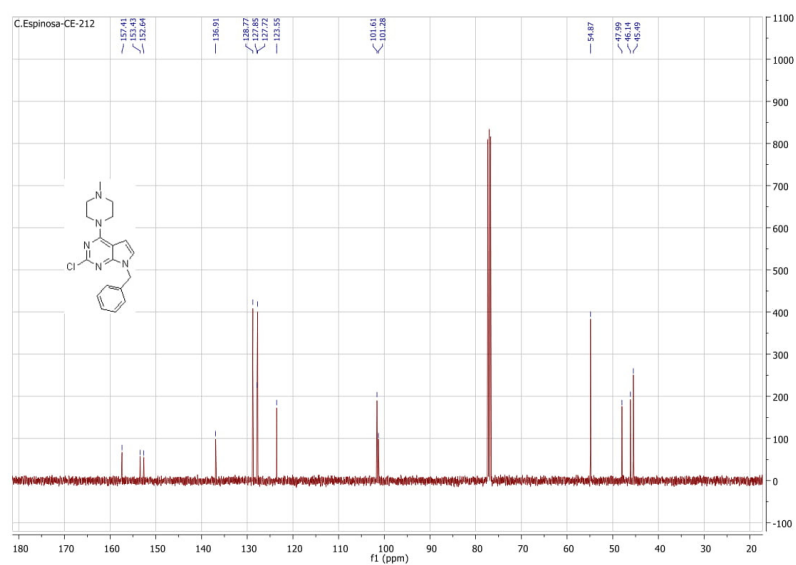
7.75 (m, 3H), 7.66 (s, 1H), 7.56 – 7.44 (m, 2H), 7.33 (dd,  $J = 8.5, 1.2$  Hz, 1H), 6.87 (d,  $J = 3.6$  Hz, 1H), 6.42 (d,  $J = 2.9$  Hz, 1H), 5.93 (s, 1H), 5.51 (s, 2H), 3.85 – 3.73 (m, 6H), 2.68 (t,  $J = 5.9$  Hz, 2H), 2.54 (d,  $J = 4.0$  Hz, 4H).  $^{13}\text{C}$  NMR (101 MHz,  $\text{CDCl}_3$ )  $\delta$  157.24, 154.01, 134.40 (2C), 133.28, 132.91, 128.72, 127.83, 127.73, 126.60 (2C), 126.40 (2C), 126.20, 125.59, 124.12, 66.94 (2C), 56.82, 53.26 (2C), 48.13 (2C). HRMS for  $(\text{C}_{23}\text{H}_{25}\text{ClN}_5\text{O} [\text{M}+\text{H}]^+)$ . Calcd: 422.1742. Found: 422.1746.

#### 4 New lead elements for histamine H3 receptor ligands in the pyrrolo[2,3-d]pyrimidine class

$^1\text{H}$  NMR for **3a**



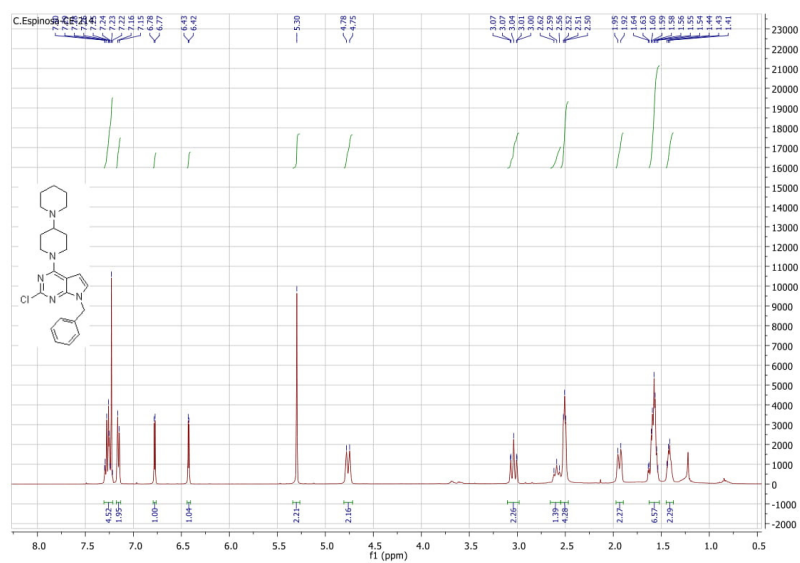
$^{13}\text{C}$  NMR for **3a**



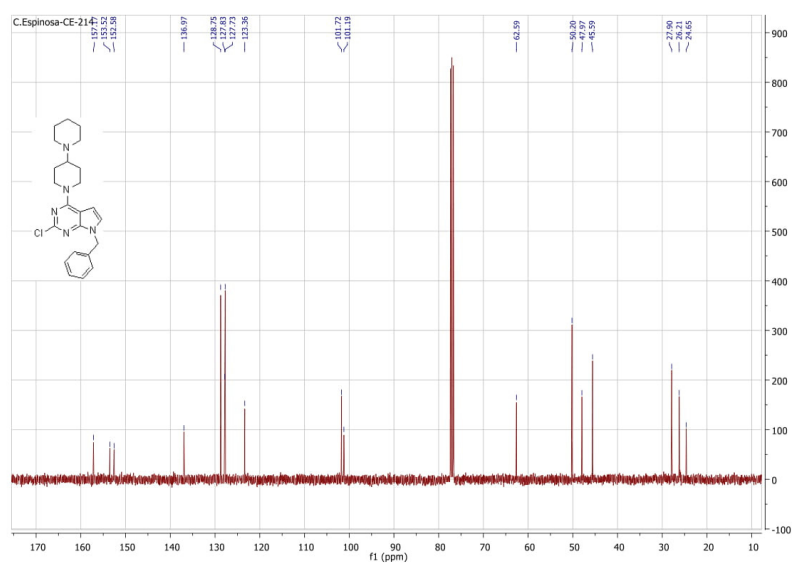


#### 4 New lead elements for histamine H3 receptor ligands in the pyrrolo[2,3-d]pyrimidine class

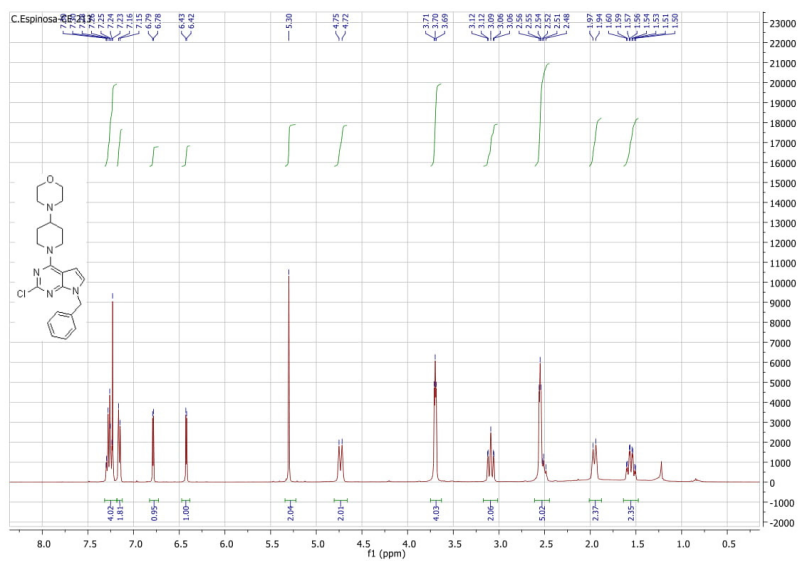
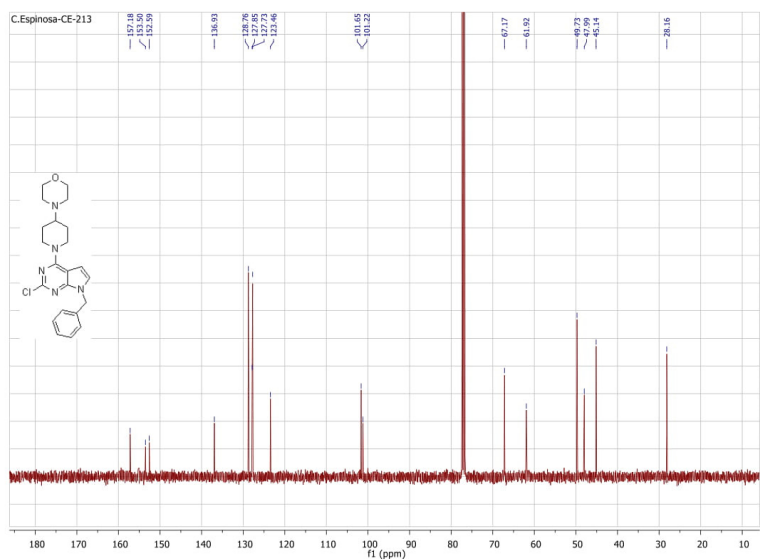
<sup>1</sup>H NMR for **3b**



<sup>13</sup>C NMR for **3b**

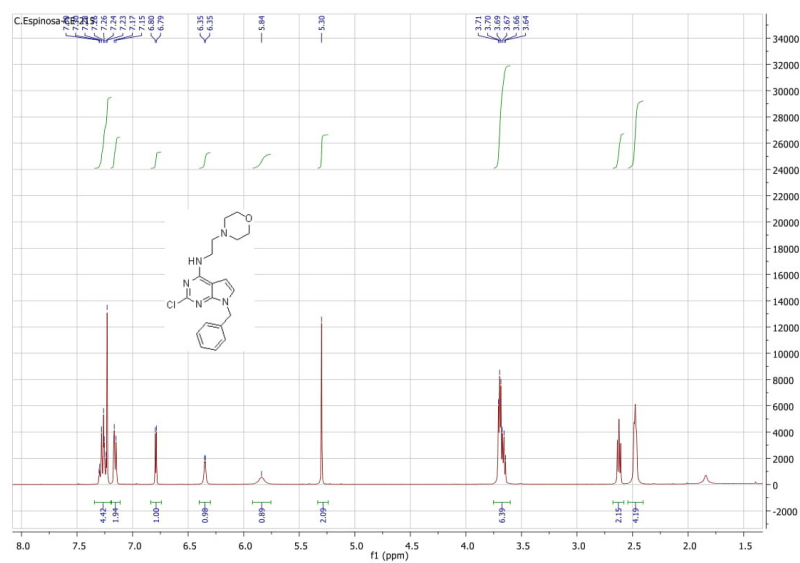


#### 4 New lead elements for histamine H3 receptor ligands in the pyrrolo[2,3-d]pyrimidine class

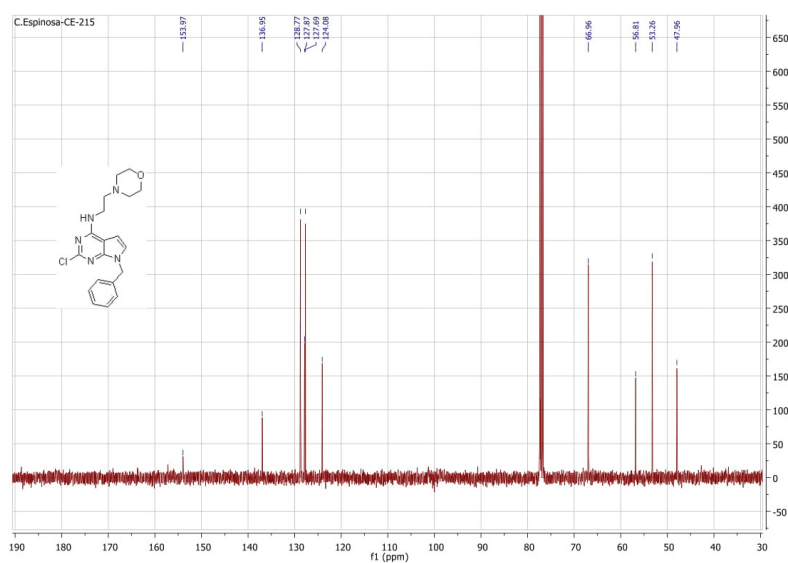
<sup>1</sup>H NMR for **3c** $^{13}\text{C}$  NMR for **3c**

#### 4 New lead elements for histamine H3 receptor ligands in the pyrrolo[2,3-d]pyrimidine class

<sup>1</sup>H NMR for **3d**

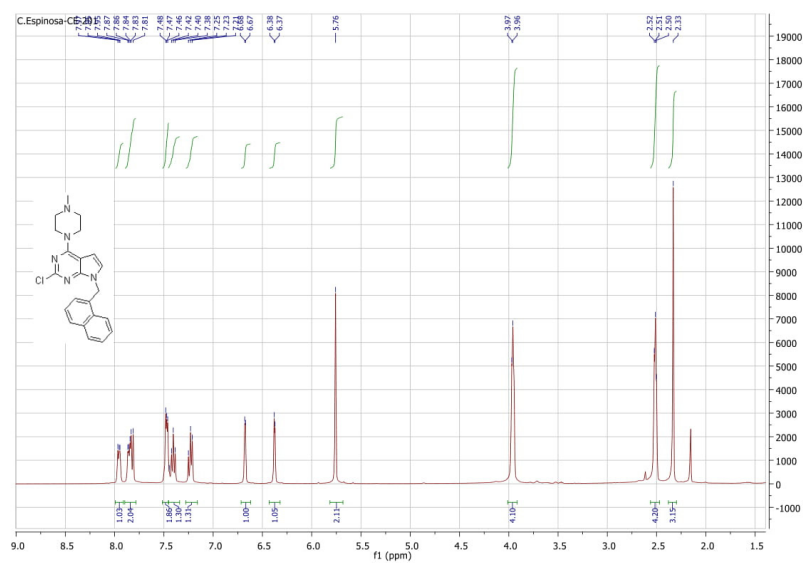


<sup>13</sup>C NMR for **3d**

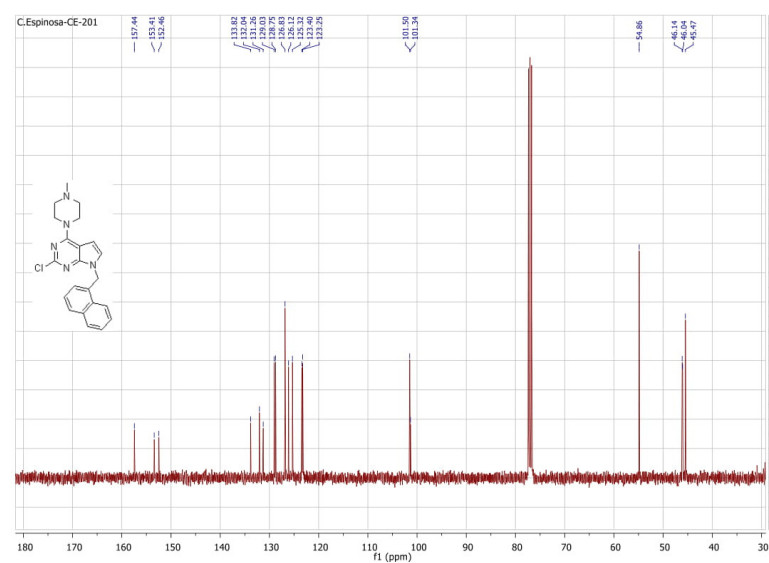


#### 4 New lead elements for histamine H3 receptor ligands in the pyrrolo[2,3-d]pyrimidine class

<sup>1</sup>H NMR for **3e**

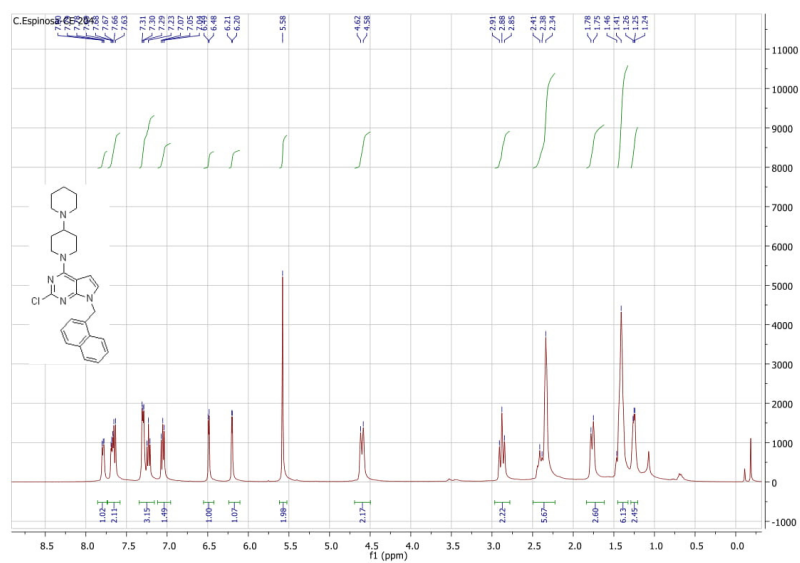


<sup>13</sup>C NMR for **3e**

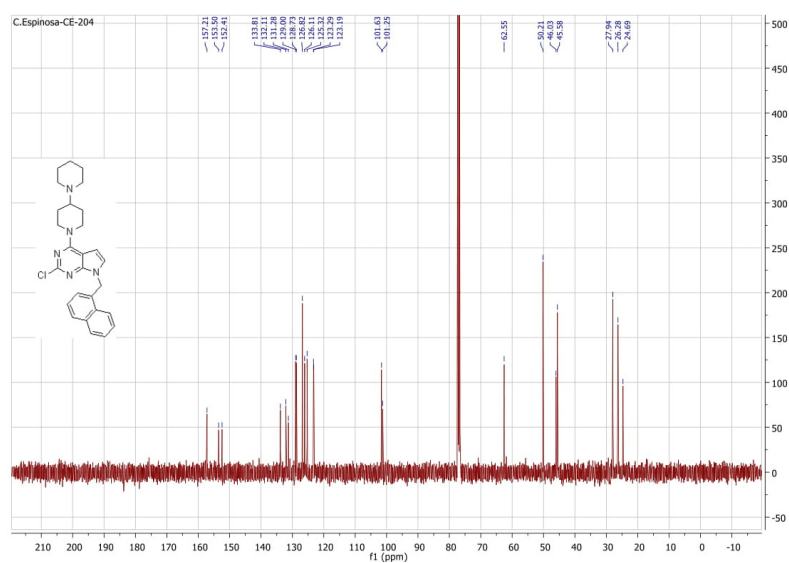


#### 4 New lead elements for histamine H3 receptor ligands in the pyrrolo[2,3-d]pyrimidine class

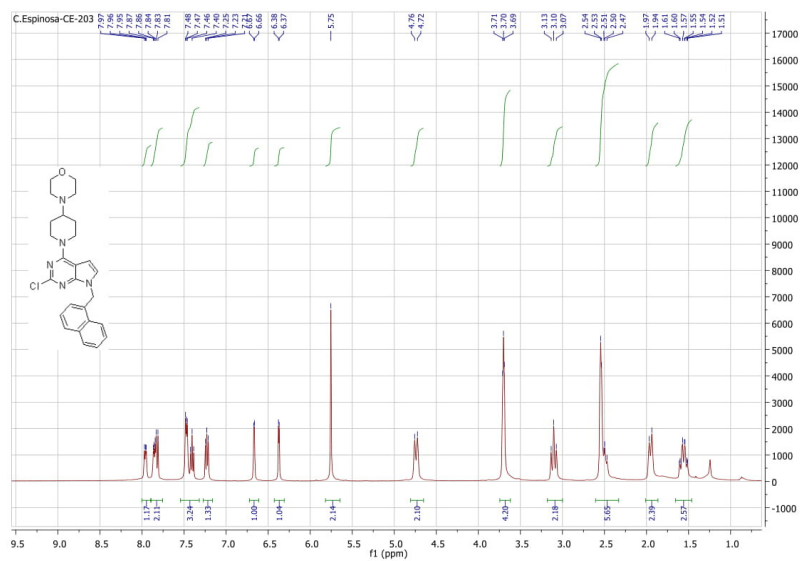
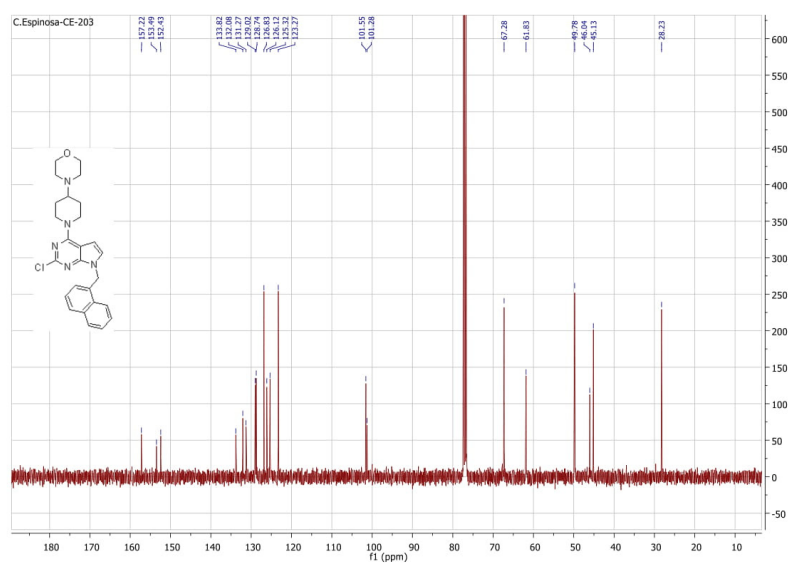
<sup>1</sup>H NMR for **3f**



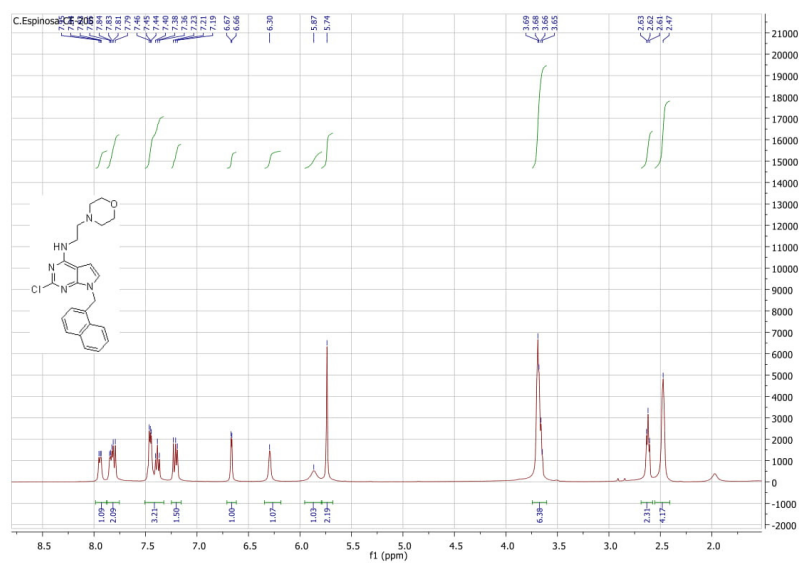
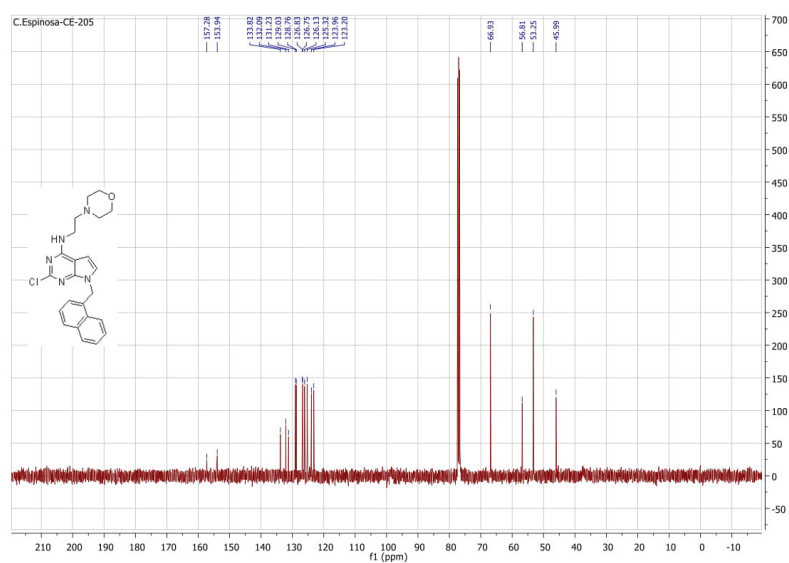
<sup>13</sup>C NMR for **3f**



#### 4 New lead elements for histamine H3 receptor ligands in the pyrrolo[2,3-d]pyrimidine class

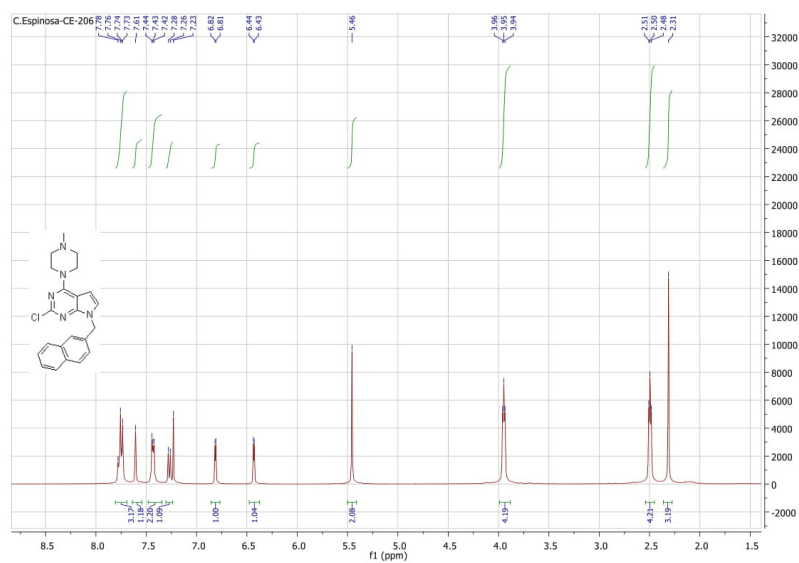
<sup>1</sup>H NMR for **3g** $^{13}\text{C}$  NMR for **3g**

#### 4 New lead elements for histamine H3 receptor ligands in the pyrrolo[2,3-d]pyrimidine class

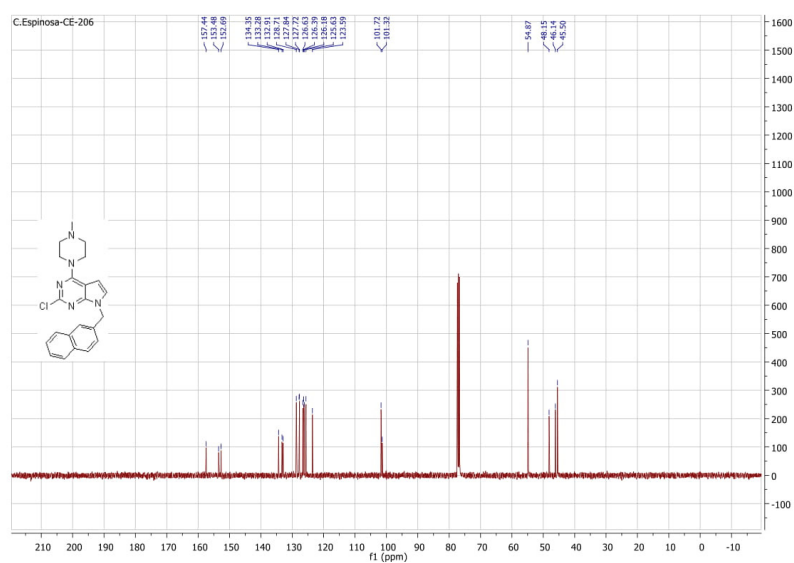
<sup>1</sup>H NMR for **3h**<sup>13</sup>C NMR for **3h**

#### 4 New lead elements for histamine H3 receptor ligands in the pyrrolo[2,3-d]pyrimidine class

<sup>1</sup>H NMR for **3i**



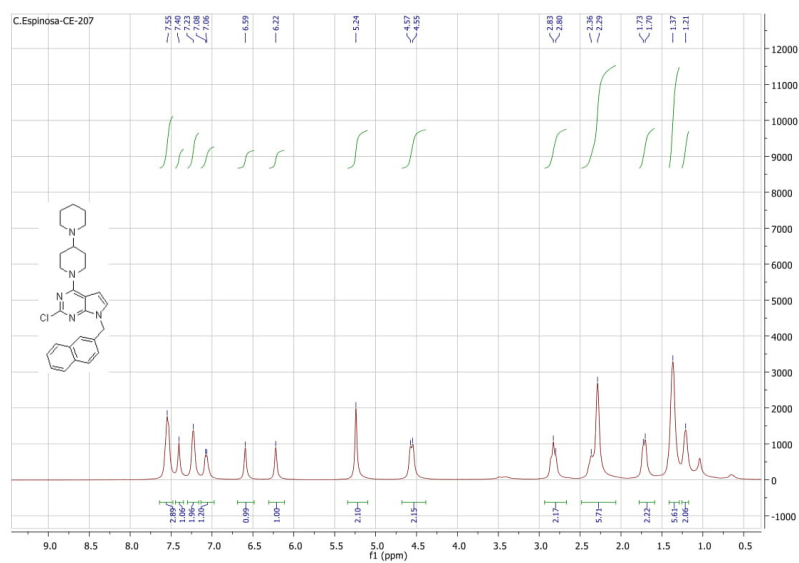
<sup>13</sup>C NMR for **3i**



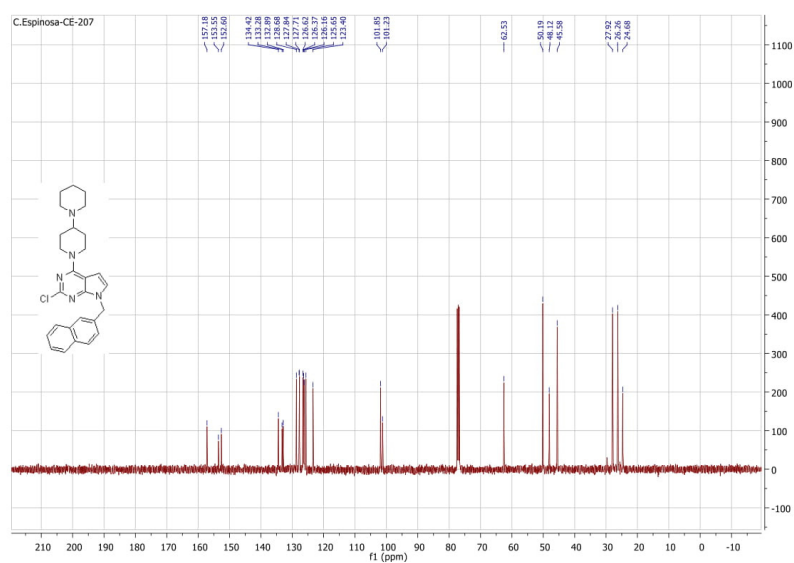


## 4 New lead elements for histamine H3 receptor ligands in the pyrrolo[2,3-d]pyrimidine class

<sup>1</sup>H NMR for **3j**

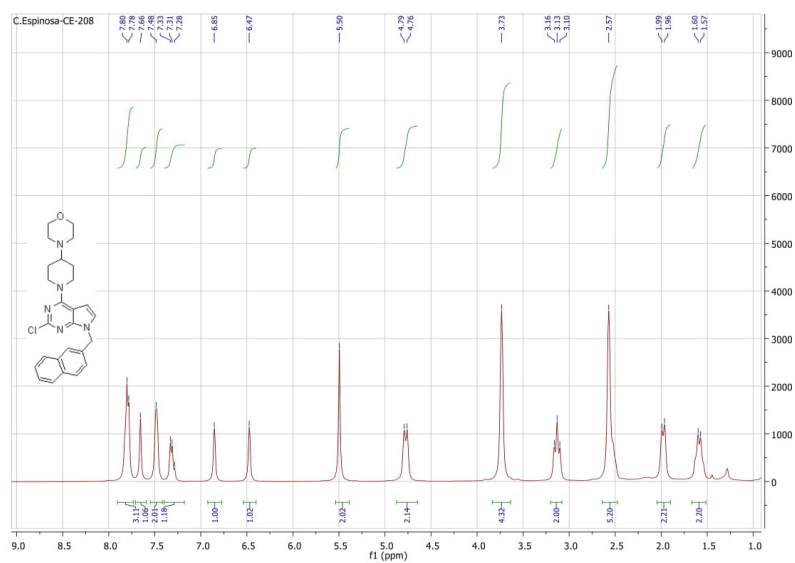


<sup>13</sup>C NMR for **3j**

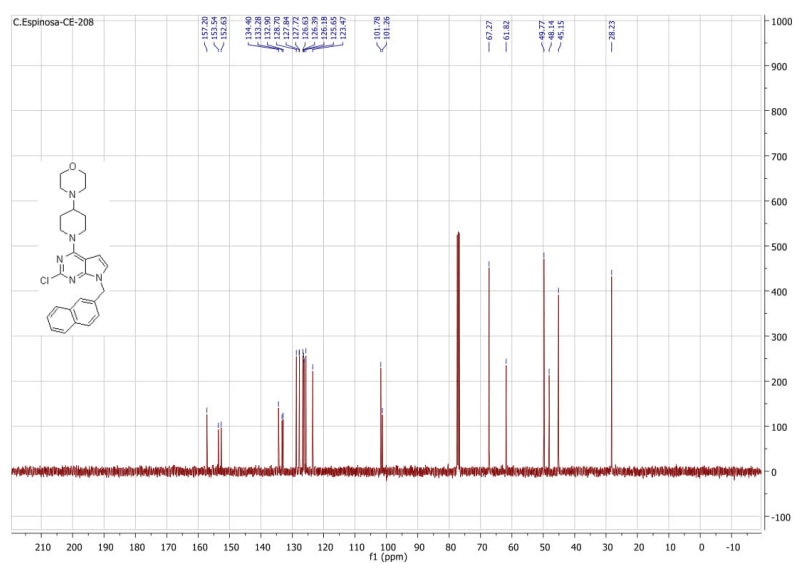


#### 4 New lead elements for histamine H3 receptor ligands in the pyrrolo[2,3-d]pyrimidine class

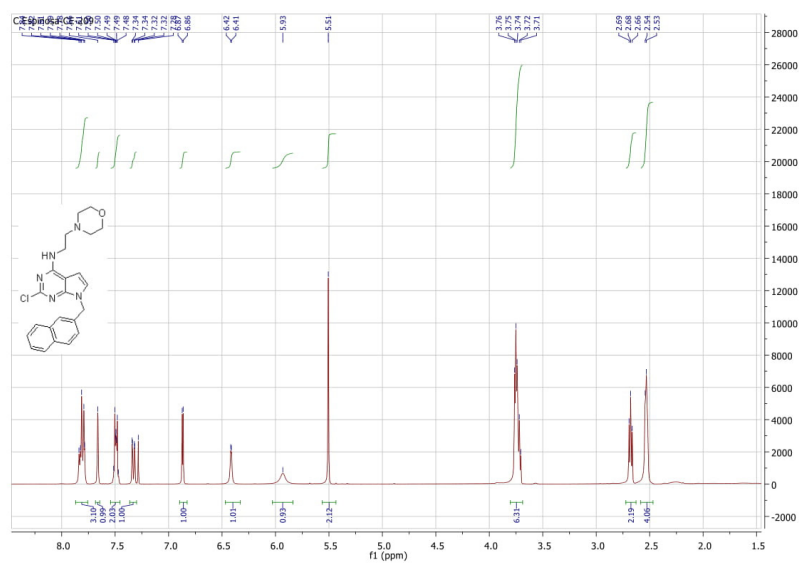
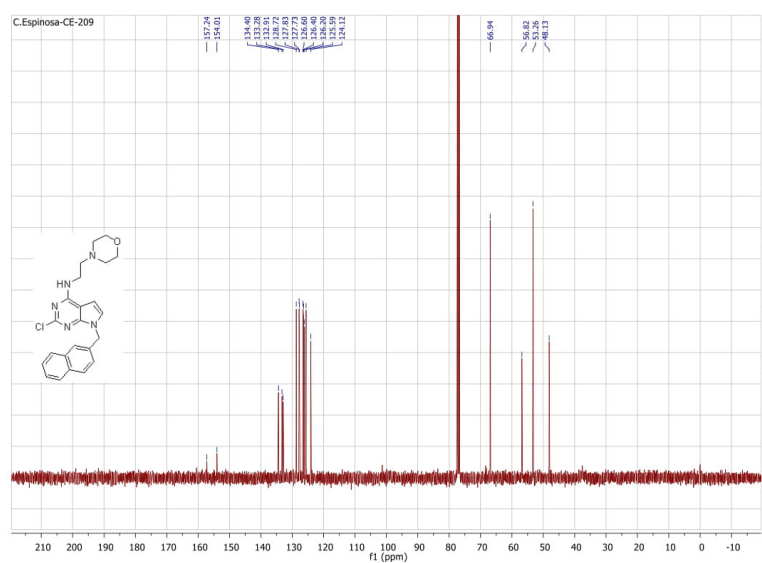
$^1\text{H}$  NMR for **3k**



$^{13}\text{C}$  NMR for **3k**



#### 4 New lead elements for histamine H3 receptor ligands in the pyrrolo[2,3-d]pyrimidine class

<sup>1</sup>H NMR for **3I**<sup>13</sup>C NMR for **3l**

### General structures

For the generation of models by homology in the different receptors, Modeller v9.15 software was used (András Fiser et al, 2003). For each receiver, 50 models were generated using standard parameters. It was further necessary to carry out a refinement of the receiver loops. Based on the internal score function (DopeScore) the best 3 models were selected for each receptor.

In the best selected models, a validation was carried out using the web servers ProSA (<https://www.came.sbg.ac.at/prosa.php>) and Molprobit (<http://molprobit.biochem.duke.edu/>), which perform a conformational and energetic evaluation of the structure, based on the results obtained, the selection of the final structure for each receiver was carried out.

### Ligand optimization

The ligands were built and optimized energetically by Spartan 8.0 software. A level of Hartree-Forck theory and a set of bases 6-31 \* were used.

### Molecular coupling

In the analysis of the interactions that take place between receptor-ligand, the molecular couplings realized between the receivers under study, the software AutoDock 4.0 was used. In the realization of the maps of the grid, a box of 60 x 60 x 60 points was used, with a spacing of 0.375 Å. For the rest of the parameters, the default conditions established by the program were used.

### Histamine H<sub>3</sub> receptor

For the generation of the human Histamine H<sub>3</sub> receptor model, it was used as template the model created for H<sub>1</sub>R. The amino acid sequence of the receptor Human histamine H<sub>3</sub> was obtained from the NCBI database (<https://www.ncbi.nlm.nih.gov/protein/AAH96840.1>). An alignment of these sequences was performed on the Multalin web server, of which a representative segment is observed in Figure 1, where it can be seen that these sequences have a very low amino acid identity, but the segments of greatest interest are preserved.

#### 4 New lead elements for histamine H3 receptor ligands in the pyrrolo[2,3-d]pyrimidine class

secuencia\_humano\_32/1-458 MPVVVLSITICLVTVGLLLVLYAVRSERKHTVGNLYIVSISVABLIVGAVVMPMNLYLMSKISLRPLGL  
P1,h3humano/1-360 VTAAFFMELVAFAIMLGALVILAFVVDKNRHRSSYFFLNLAISSEFFVGVISILYLPHTLF·EWDFGKEIDV

**Figure 1**

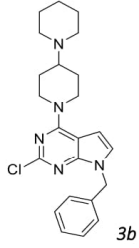
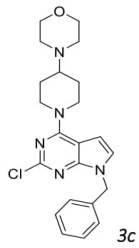
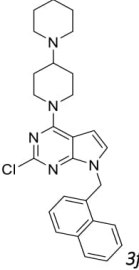
In the creation of the model, the same conditions described for the generation of the histamine H<sub>1</sub> receptor model were used. 50 possible models were generated and 3 better ones were selected, based on an energy criterion. Then, a validation of the selected models was carried out, values that can be observed in Table 1. In the results of the Ramachandran representation, 92.62% of favored rotamers were obtained as a result for the human H1 model.

**Table 2.** The *dope score* values of each selected model and the values delivered in the evaluation of these are represented by the *prosa* and *molprobit* web servers

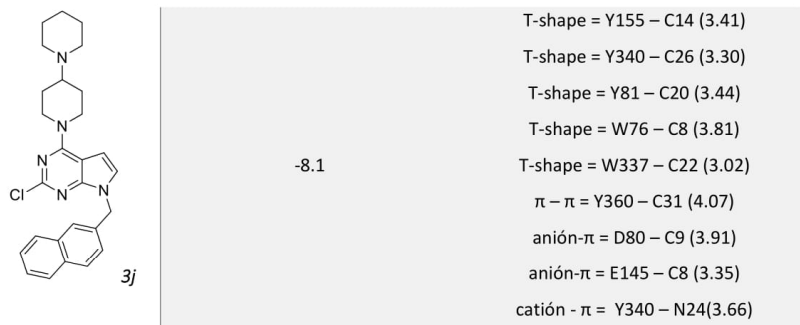
	<i>Dope Score</i>	<i>Prosa</i>	<i>Molprobit (%)</i>
<i>Modelo 44</i>	-41135	-3.89	91.09
<i>Modelo 46</i>	-41132	-3.48	92.62
<i>Modelo 50</i>	-41104	-3.53	92.11

The analysis of the receptor-ligand complex was carried out observing if the amino acids described in literature are preserved and the potential molecular interactions that occur in the binding cavity. Molecular coupling was performed to the structure created for the histamine H<sub>3</sub> receptor and the coordinates of amino acid Asp80 were used as a grid center, which has been described in literature that is close to the site where histamine binds. The ligands studied in the human histamine H<sub>3</sub> receptor interact in the binding site described in literature (Shimamura et al., 2011).

#### 4 New lead elements for histamine H3 receptor ligands in the pyrrolo[2,3-d]pyrimidine class

Compound	Interactions	
	Energy (Kcal/mol)	Interaction (distance Å)
 3b	-6.22	T-shape = F364 – C19 (3.48) T-shape = Y155 – C15 (3.32) T-shape = W337 – C22 (2.93) $\pi - \pi$ = Y81 – C20 (3.0) $\pi - \pi$ = Y340 – C23 (3.4) anion- $\pi$ = D80 – C9 (4.0)
 3c	-6.18	T-shape = W337 – C28 (4.52) T-shape = Y115 – C8 (3.25) T-shape = Y340 – C26 (4.15) T-shape = F364 – C22 (3.3) $\pi - \pi$ = Y81 – C26 (3.69) $\pi - \pi$ = Y360 – C16 (3.66) anión- $\pi$ = D80 – C20 (3.56) catión - $\pi$ = Y81 – N24(3.29 Å)
 3f	-8.63	T-shape = Y340 – C8 (4.35) T-shape = F364 – C6 (3.43) T-shape = F333 – C31 (3.20) $\pi - \pi$ = Y81 – C8 (3.26) $\pi - \pi$ = W337 – C16 (3.16) $\pi - \pi$ = F158 – C27 (4.02) anión- $\pi$ = E172 – C8 (4.0) anión- $\pi$ = D80 – C22 (4.5)

#### 4 New lead elements for histamine H3 receptor ligands in the pyrrolo[2,3-d]pyrimidine class



#### Ligand efficiency metrics <sup>1,2</sup>

Ligand	LLE	LELP
<b>3b</b>	2.2	13.91
<b>3c</b>	3.0	10.39
<b>3f</b>	1.5	18.77
<b>3j</b>	1.6	18.58

#### References

1. Nicholas A. Meanwell, Chem. Res. Toxicol., 2016, 29 (4), pp 564–616
2. Ákos Tarcsay, Kinga Nyíri, and György M. Keserű, J. Med. Chem., 2012, 55 (3), pp 1252-1260

## 5 Nature-inspired pyrrolo[2,3-d]pyrimidines targeting the histamine H<sub>3</sub> receptor

Frank A<sup>1</sup>, Meza-Arriagada F<sup>2</sup>, Salas CO<sup>3</sup>, Espinosa-Bustos C<sup>2</sup>, Stark H<sup>3</sup>, 2019.

<sup>1</sup>Institute of Pharmaceutical and Medicinal Chemistry, Heinrich Heine University Düsseldorf, Universitätsstr. 1, 40225 Düsseldorf, Germany.

<sup>2</sup>Departamento de Farmacia, Facultad de Química y de Farmacia, Pontificia Universidad Católica de Chile, Santiago 6094411, Chile.

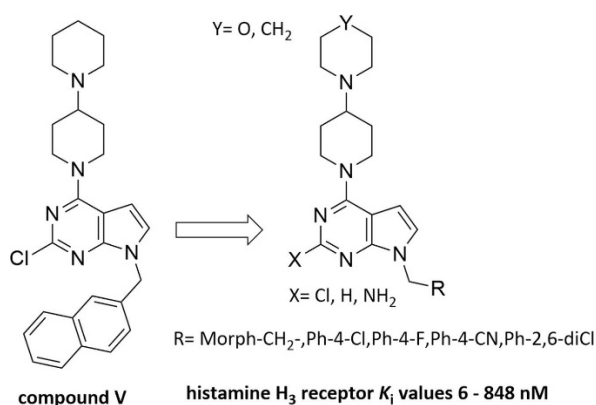
<sup>3</sup>Departamento de Química Orgánica, Facultad de Química y de Farmacia, Pontificia Universidad Católica de Chile, Santiago 6094411, Chile.

Published in: *Bioorganic & Medicinal Chemistry*, **27**: 3194-3200.

DOI: 10.1016/j.bmc.2019.05.042.

Research contribution: Pharmacological evaluation of compounds at the H<sub>3</sub> and H<sub>4</sub> receptor, interpretation of data and preparation of manuscript.

Graphical abstract:



Reprinted by permission from Elsevier. This article was published in *Bioorganic & Medicinal Chemistry*, 27, Annika Frank, Francisco Meza-Arriagada, Cristian O. Salas, Christian Espinosa-Bustos, Holger Stark, Nature-inspired pyrrolo[2,3-d]pyrimidines targeting the histamine H<sub>3</sub> receptor, 3194-3200, Copyright Elsevier Ltd. (2019).





## Nature-inspired pyrrolo[2,3-d]pyrimidines targeting the histamine H<sub>3</sub> receptor



Annika Frank<sup>a</sup>, Francisco Meza-Arriagada<sup>b</sup>, Cristian O. Salas<sup>c</sup>, Christian Espinosa-Bustos<sup>b,\*</sup>, Holger Stark<sup>a,\*</sup>

<sup>a</sup> Institute of Pharmaceutical and Medicinal Chemistry, Heinrich Heine University Düsseldorf, Universitätsstr. 1, 40225 Düsseldorf, Germany

<sup>b</sup> Departamento de Farmacia, Facultad de Química y de Farmacia, Pontificia Universidad Católica de Chile, Santiago 6094411, Chile

<sup>c</sup> Departamento de Química Orgánica, Facultad de Química y de Farmacia, Pontificia Universidad Católica de Chile, Santiago 6094411, Chile

### ARTICLE INFO

Dedicated to Prof. Peter Proksch on his 65<sup>th</sup> birthday

**Keywords:**  
Heterocycles  
Histamine  
G-protein coupled receptor  
Natural products  
H<sub>3</sub>R  
Microwave-assisted synthesis

### ABSTRACT

Inspired by marine compounds the derivatization of the natural pyrrolo[2,3-d]pyrimidine lead scaffold led to a series of novel compounds targeting the histamine H<sub>3</sub> receptor. The focus was set on improved binding towards the receptor and to establish an initial structure-activity relationship for this compound class based on the lead structure (**compound V**, K<sub>i</sub> value of 126 nM). As highest binding affinities were found with 1,4-bipiperidines as basic part of the ligands, further optimization was focused on 4-([1,4'-bipiperidin]-1'-yl)-pyrrolo[2,3-d]pyrimidines. Related pyrrolo[2,3-d]pyrimidines that were isolated from marine sponges like 4-amino-5-bromopyrrolo[2,3-d]pyrimidine (**compound III**), showed variations in halogenation pattern, though in a next step the impact of halogenation at 2-position was evaluated. The chloro variations did not improve the affinity compared to the dehalogenated compounds. However, the simultaneous introduction of lipophilic cores with electron-withdrawing substitution patterns in 7-position and dehalogenation at 2-position (**11b**, **12b**) resulted in compounds with significantly higher binding affinities (K<sub>i</sub> values of 7 nM and 6 nM, respectively) than the initial lead structure **compound V**. The presented structures allow for a reasonable structure-activity relationship of pyrrolo[2,3-d]pyrimidines as histamine H<sub>3</sub> receptor ligands and yielded novel lead structures within the natural compound library against this target.

### 1. Introduction

Natural products are a highly appreciated source for novel lead compounds, as they are pre-designed for biological activity by natural optimization and provide with large structural heterogeneity high hit rates in pharmacological screenings.<sup>1</sup> A remarkable amount of currently used therapeutics are natural compounds or are at least inspired by nature (e.g. antibiotic or cytostatic agents).<sup>2</sup> The combination of high hit rates and a given drug-likeness motivates researchers to re-investigate compounds, already applied for a certain application field, for the use in other areas as well. One of the most investigated drug targets to date, is the class of G-protein coupled receptors (GPCRs). Among these, the four subtypes of the histamine receptor represent a highly diverse target class as the different receptors are involved in allergy, gastric acid secretion, inflammation or even neurodegenerative diseases.<sup>3</sup> Recent research on the histamine H<sub>3</sub> receptor (H<sub>3</sub>R) emphasizes its crucial role in the central nervous system. The presynaptic H<sub>3</sub> autoreceptors modulate histamine release in the central nervous system

and due to its heterodimerization with non-histaminergic receptors also a variety of other neurotransmitters such as dopamine, acetylcholine or noradrenaline.<sup>4</sup> Owing to its involvement in the pathophysiology of Alzheimer's disease, attention deficit hyperactivity disorder and schizophrenia (amongst others), it became apparent that targeting the H<sub>3</sub>R may reduce the cognitive impairments of those diseases.<sup>5</sup> The search for agents targeting the receptor led to the investigation of two natural ligands, that were found as novel potential lead structures.<sup>4</sup> **Compound I** (Fig. 1, K<sub>i</sub> value of 30 nM) was isolated from the marine sponge *Aplysina* sp. and inspired the design of a variety of novel non-imidazole-based ligands.<sup>6</sup> Derivatization of the basic moiety and the spacer length of the bromotyrosine derivative led to the discovery of non-imidazole compounds like pitolisant (Fig. 2) that display high activity and optimized scaffolds towards the H<sub>3</sub>R. In a similar manner, various modifications were performed with the natural compound conessine<sup>7</sup> (**compound II**, Fig. 1) that was also found to be an H<sub>3</sub>R antagonist. One attempt aimed for rigidizing the alkaloid, while others attempted to aromatize and simplify the scaffold, resulting in H<sub>3</sub>R antagonists like

\* Corresponding authors.

E-mail addresses: [ccespino@uc.cl](mailto:ccespino@uc.cl) (C. Espinosa-Bustos), [stark@hhu.de](mailto:stark@hhu.de) (H. Stark).

<https://doi.org/10.1016/j.bmc.2019.05.042>

Received 15 March 2019; Received in revised form 5 April 2019; Accepted 28 May 2019

Available online 29 May 2019

0968-0896/ © 2019 Elsevier Ltd. All rights reserved.

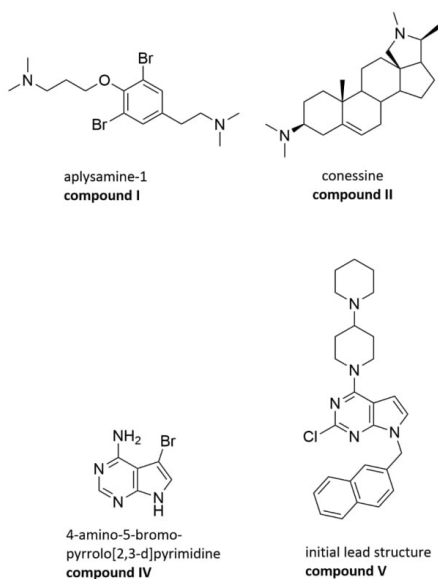


Fig. 1. Natural compounds targeting the H<sub>3</sub>R and inspired the presented drug design approach.

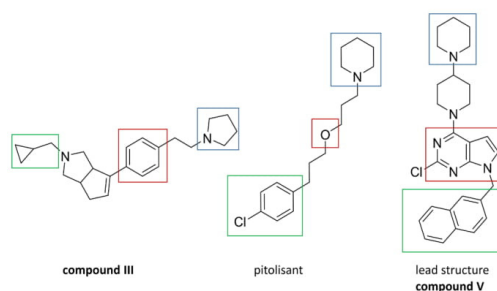


Fig. 2. General blueprint for H<sub>3</sub>R ligands and structures of pitolisant and the lead structure. Blue: basic amine, red: central core, green: arbitrary region.

**compound III** (Fig. 2), displaying affinities in the low nanomolar ranges.<sup>8</sup>

Although the compound library for targeting the H<sub>3</sub>R is increasing rapidly, to date, only one ligand passed clinical evaluation and entered the market. Pitolisant, an inverse H<sub>3</sub>R agonist has been approved for the treatment of narcolepsy by the EMA in 2016 and is currently undergoing clinical phase II and III studies for cognitive enhancement in patients with schizophrenia or Parkinson's disease.<sup>9,10</sup> The ligand adheres to the typical blueprint of H<sub>3</sub>R ligands (Fig. 2). It consists of a basic aliphatic amine moiety (blue), responsible for binding to the receptor, and a linker, most often an alkyl linker, connecting the amine to the central core (red). Through a second linker the core is connected to an arbitrary, lipophilic region (green), which aids in improving selectivity.<sup>11</sup> As shown with **compounds III** and pitolisant the derivatization of natural products can lead to novel compounds, adhering to this blueprint, with promising activities at the H<sub>3</sub>R. Though the drug research community at GPCRs is in constant search for novel scaffolds inspired by Mother Nature.

Pyrrolo[2,3-d]pyrimidines are a class of natural compounds that were found in several marine organisms, like sponges or algae. The brominated analogue **compound IV** (Fig. 1) for example, was isolated from *Echinodictyum* sp. and is a promising inhibitor of the adenosine kinase.<sup>12</sup> The compound class is known to provide promising results in anti-inflammatory and anti-infectious assays in various studies.<sup>13,14</sup> As the pathophysiology of neurodegenerative diseases involves inflammatory events too, multiple treatment strategies focus on the anti-inflammatory properties of novel substances.<sup>15</sup> H<sub>3</sub>R antagonists are reported to improve cognitive functions in neurodegenerative diseases,<sup>5</sup> though the synergistic effect of targeting the H<sub>3</sub>R and the known anti-inflammatory properties of pyrrolo[2,3-d]pyrimidines<sup>13</sup> may aid current drug development of neurological diseases. Though we recently conducted the combination of the natural pyrrolo[2,3-d]pyrimidines with the general pharmacophore of H<sub>3</sub>R ligands to expand possible application fields towards neurodegenerative diseases.<sup>16</sup> The novel ligands showed selectivity for the H<sub>3</sub>R compared to the H<sub>4</sub>R and displayed promising structure-activity relationships (SARs). Among the tested derivatives, a 1,4-bis(piperidine) warhead as the basic moiety of the molecule was superior to morpholines or piperazines regarding its affinity towards the H<sub>3</sub>R, with the most active compound (**compound V**, Fig. 1) displaying a K<sub>i</sub> value of 126 nM. Based on these results we went for a rationalized drug optimization approach to improve pharmacological activity of the novel scaffold. As morpholines are frequently used in the design of H<sub>3</sub>R ligands,<sup>17</sup> the first derivatization introduced morpholines as basic group (Y = O, Fig. 3) and into the lipophilic core at 7-position of the pyrrolo[2,3-d]pyrimidine (R, Fig. 3). A second focus was set on the impact of halogenation at 2-position (X, Fig. 3), as pyrrolo[2,3-d]pyrimidines isolated from marine organisms are typically halogenated, as seen with **compound IV**. To complete the SAR investigation R was derivatized by introducing varying lipophilic residues. All compounds were tested for their H<sub>3</sub>R binding affinities and screened for selectivity towards the H<sub>4</sub>R. The goal of this study was to optimize the existing pharmacophore of pyrrolo[2,3-d]pyrimidines and to increase H<sub>3</sub>R binding affinity compared to **compound V**. In doing so, the class of H<sub>3</sub>R ligands can be expanded by natural inspired compounds that may facilitate the jump from bench to bedside.

## 2. Material and methods

### 2.1. Materials

Melting points were determined on a Kofler Thermogate apparatus and were uncorrected. All reagents were purchased from Sigma-Aldrich, unless otherwise specified. The NMR spectra were recorded on NMR Bruker AV 400. Chemical shifts were given in parts per million relative to TMS [<sup>1</sup>H and <sup>13</sup>C, δ(SiMe<sub>4</sub>) = 0]. Most NMR assignments were supported by additional 2D experiments. HRMS-ESI-MS experiments were carried out using a Thermo Scientific Exactive Plus Orbitrap Spectrometer. Thin layer chromatography (TLC) was performed using Merck GF-254 type 60 silica gel. Column chromatography was carried out using Merck silica gel 60 (70–230 mesh). Radioligands [<sup>3</sup>H]N<sup>2</sup>-methylhistamine and [<sup>3</sup>H]histamine were purchased at PerkinElmer.

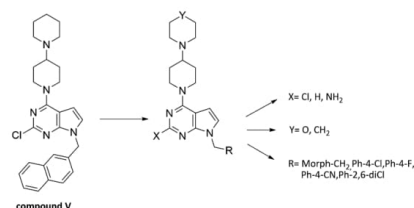
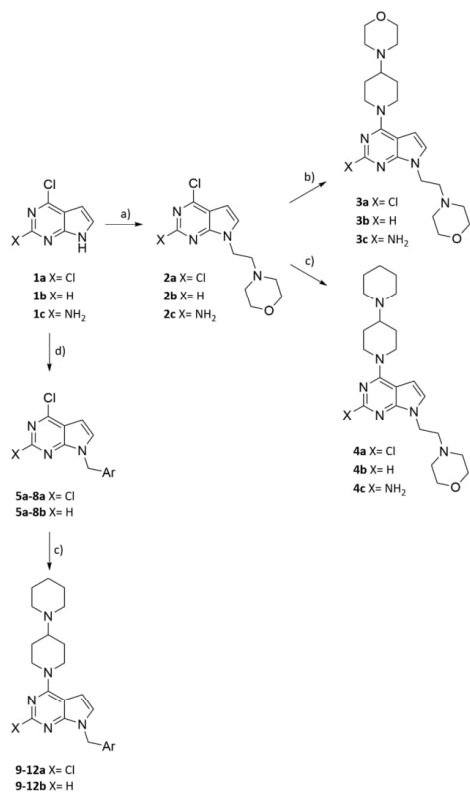


Fig. 3. Possible derivatization strategies of the initial lead structure.

## 5 Nature-inspired pyrrolo[2,3-d]pyrimidines targeting the histamine H3 receptor

A. Frank, et al.

Bioorganic & Medicinal Chemistry 27 (2019) 3194–3200



**Scheme 1.** Reagents and conditions. a) 2-(Chloroethyl)morpholine,  $K_2CO_3$ , MeCN, reflux, 6 h. b) 4-(Piperidin-4-yl)morpholine, EtOH,  $NEt_3$ , 80 °C, mw, 15 min. c) Bipiperidine, EtOH,  $NEt_3$ , 80 °C, mw, 15 min. d) Benzyl halides,  $K_2CO_3$ ,  $CH_3CN$ , reflux, 3 h.

HEK-293 cells stably expressing the human  $H_3$  receptor were kindly gifted by Prof. Dr. Jean-Charles Schwartz (Bioprojet, France). Sf9-hH<sub>4</sub>-Gα<sub>12</sub>-Gβ<sub>1</sub>γ<sub>2</sub> cells were a kind donation by Prof. Dr. Seifert.

### 2.2. Methods

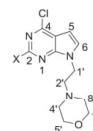
#### 2.2.1. Chemical part

For the synthesis of pyrrolo[2,3-d]pyrimidin-7-yl-ethylmorpholine derivatives **3a-c** and **4a-c**, a simple synthetic strategy was used (Scheme 1). Pyrrolo[2,3-d]pyrimidines **1a-c** (1 eq.), 2-chloroethylmorpholine (2 eq.) and potassium carbonate (3 eq.) were mixed in acetonitrile and the reaction mixture was stirred at 90 °C for 6 h, obtaining the corresponding **2a-c** derivatives. Subsequently, the target compounds were obtained through a microwave-assisted aromatic nucleophilic substitution reaction. The bipiperidine and morpholino-piperidine scaffolds were incorporated in the 4-position of the heterocycle using triethylamine and ethanol as the solvent.

The derivatives **9a-12a** and **9b-12b** were synthesized from the pyrrolopyrimidines **1a-b** according to Scheme 1. In a first synthetic step, an *N*-alkylation reaction was performed using various benzyl halides in acetonitrile under reflux conditions and then mediated by microwave-assisted conditions the bipiperidine fragment was added.

#### 2.2.2. Chemistry

**2.2.2.1. General synthetic procedure to obtain 4-(2-(4-chloro-7H-pyrrolo[2,3-d]pyrimidin-7-yl)ethyl)morpholine derivatives 2a-c.** A mixture of the corresponding pyrrolopyrimidine (1.0 mmol), 4-(2-chloroethyl)morpholine (2.0 mmol) and potassium carbonate (3.0 mmol) in acetonitrile (5 mL) was stirred for 6 h, then the mixture was filtered and evaporated under vacuum. The products were separated by flash chromatography on silica gel eluting with methanol/methylene chloride 1:20.

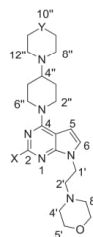


**2.2.2.1.1. 4-(2-(2,4-Dichloro-7H-pyrrolo[2,3-d]pyrimidin-7-yl)ethyl)morpholine 2a.** Light brown solid, yield 76%, Mp 79–80 °C.  $^1H$  NMR (400 MHz,  $CDCl_3$ )  $\delta$  6.91 (d,  $J$  = 3.6 Hz, 1H, H6), 6.33 (d,  $J$  = 3.6 Hz, 1H, H5), 4.13 (t,  $J$  = 6.5 Hz, 2H, 2 × H1'), 3.67–3.57 (m, 4H, 2 × H5' and 2 × H7'), 2.67 (t,  $J$  = 6.5 Hz, 2H, 2 × H2'), 2.53–2.43 (m, 4H, 2 × H4' and 2 × H8').  $^{13}C$  NMR (101 MHz,  $CDCl_3$ )  $\delta$  158.42, 153.41, 152.52, 126.24, 110.66, 99.49, 66.94 (2C), 57.94, 53.66 (2C), 41.67.

**2.2.2.1.2. 4-(2-(4-Chloro-7H-pyrrolo[2,3-d]pyrimidin-7-yl)ethyl)morpholine 2b.** Brown solid, yield 77%, Mp 126–128 °C.  $^1H$  NMR (400 MHz,  $CDCl_3$ )  $\delta$  8.57 (s, 1H, H2), 7.32 (d,  $J$  = 3.6 Hz, 1H, H6), 6.54 (d,  $J$  = 3.6 Hz, 1H, H5), 4.34 (t,  $J$  = 6.3 Hz, 2H, 2 × H1'), 3.65–3.56 (m, 4H, 2 × H5' and 2 × H7'), 2.72 (t,  $J$  = 6.3 Hz, 2H, 2 × H2'), 2.51–2.39 (m, 4H, 2 × H4' and 2 × H8').  $^{13}C$  NMR (101 MHz,  $CDCl_3$ )  $\delta$  162.48, 151.96, 151.03, 150.43, 129.73, 117.42, 99.25, 66.88 (2C), 58.04, 53.57 (2C), 42.02.

**2.2.2.1.3. 4-Chloro-7-(2-morpholinoethyl)-7H-pyrrolo[2,3-d]pyrimidin-2-amine 2c.** White solid, yield 75%, Mp 133–135 °C.  $^1H$  NMR (400 MHz,  $CDCl_3$ )  $\delta$  6.91 (d,  $J$  = 3.6 Hz, 1H, H6), 6.33 (d,  $J$  = 3.6 Hz, 1H, H5), 5.04 (s, 2H, NH<sub>2</sub>), 4.13 (t,  $J$  = 6.5 Hz, 2H, 2 × H1'), 3.69–3.50 (m, 4H, 2 × H5' and 2 × H7'), 2.67 (t,  $J$  = 6.5 Hz, 2H, 2 × H2'), 2.51–2.40 (m, 4H, 2 × H4' and 2 × H8').  $^{13}C$  NMR (101 MHz,  $CDCl_3$ )  $\delta$  158.45, 153.41, 152.51, 126.23, 110.63, 99.48, 66.94, 57.94, 53.66, 41.67.

**2.2.2.2. General synthetic procedure to obtain 4-(2-(4-([1,4'-Bipiperidin]-1'-yl)-7H-pyrrolo[2,3-d]pyrimidin-7-yl)ethyl)morpholine derivatives 3a-c and 4a-c.** Compounds **2a-c** and (1.0 mmol), 4-piperidinopiperidine or 4-(piperidin-4-yl)morpholine (3.0 mmol), triethylamine (4.5 mmol) and ethanol (5 mL) were added to a microwave reaction flask and the reaction mixture was irradiated for 15 min at 80 °C. Then the solvent was evaporated under vacuum and the crude product was purified by column chromatography on silica gel using chloroform/methanol (10:1) mixture.



**2.2.2.2.1. 4-(2-(2-Chloro-4-(4-morpholinopiperidin-1-yl)-7H-pyrrolo[2,3-d]pyrimidin-7-yl)ethyl)morpholine 3a.** Brown oil, yield 95%.  $^1H$  NMR (400 MHz,  $CDCl_3$ )  $\delta$  6.96 (d,  $J$  = 3.6 Hz, 1H, H6), 6.40 (d,  $J$  = 3.7 Hz, 1H, H5), 4.72 (d,  $J$  = 13.3 Hz, 2H, H2' and H6'), 4.21 (t,  $J$  = 6.3 Hz, 2H, 2 × H1'), 3.71–3.67 (m, 4H, 2 × H9' and 2 × H11'),

3196



## 5 Nature-inspired pyrrolo[2,3-d]pyrimidines targeting the histamine H3 receptor

A. Frank, et al.

Bioorganic & Medicinal Chemistry 27 (2019) 3194–3200

3.66–3.62 (m, 4H, 2 × H5' and 2 × H7'), 3.14–3.00 (m, 2H, H2'' and H6''), 2.68 (t,  $J = 6.3$  Hz, 2H, 2 × H2'), 2.56–2.52 (m, 4H, 2 × H8'' and 2 × H12''), 2.51–2.43 (m, 5H, 2 × H4', 2 × H8' and H4''), 1.95 (d,  $J = 12.8$  Hz, 2H, H3'' and H5''), 1.54 (ddd,  $J = 15.9, 12.5, 4.1$  Hz, 2H, H3'' and H5'').  $^{13}\text{C}$  NMR (101 MHz,  $\text{CDCl}_3$ )  $\delta$  157.13, 153.17, 152.35, 124.13, 101.24, 100.92, 67.25 (2C), 66.98 (2C), 61.88, 58.19, 53.65 (2C), 49.78 (2C), 45.13 (2C), 41.68, 28.24 (2C). HRMS  $m/z$  435.2270 [ $\text{M} + \text{H}^+$ ] (calcd. for  $\text{C}_{21}\text{H}_{31}\text{ClN}_6\text{O}_2$ , 435.2201).

2.2.2.2.2. 4-(1-(7-(2-Morpholinoethyl)-7H-pyrrolo[2,3-d]pyrimidin-4-yl)piperidin-4-yl)morpholine **3b**. Light brown solid, yield 65%, Mp 114–115 °C.  $^1\text{H}$  NMR (400 MHz,  $\text{CDCl}_3$ )  $\delta$  8.29 (s, 1H, H2), 6.99 (d,  $J = 3.6$  Hz, 1H, H6), 6.43 (d,  $J = 3.6$  Hz, 1H, H5), 4.75 (d,  $J = 13.3$  Hz, 2H, H2'' and H6''), 4.27 (t,  $J = 6.5$  Hz, 2H, 2 × H1'), 3.71–3.66 (m, 4H, 2 × H9'' and 2 × H11''), 3.66–3.61 (m, 4H, 2 × H5' and 2 × H7'), 3.12–3.01 (m, 2H, H2'' and H6''), 2.71 (t,  $J = 6.5$  Hz, 2H, 2 × H2'), 2.57–2.52 (m, 4H, 2 × H8'' and 2 × H12''), 2.52–2.43 (m, 5H, 2 × H4', 2 × H8' and H4''), 1.94 (d,  $J = 11.4$  Hz, 2H, H3'' and H5''), 1.55 (ddd,  $J = 24.1, 12.3, 4.1$  Hz, 2H, H3'' and H5'').  $^{13}\text{C}$  NMR (101 MHz,  $\text{CDCl}_3$ )  $\delta$  156.87, 151.19, 151.14, 123.87, 103.08, 100.59, 67.29 (2C), 66.98 (2C), 62.16, 58.22, 53.68 (2C), 49.78 (2C), 45.24 (2C), 41.80, 28.29 (2C). HRMS  $m/z$  401.2660 [ $\text{M} + \text{H}^+$ ] (calcd. for  $\text{C}_{21}\text{H}_{32}\text{N}_6\text{O}_2$ , 401.2599).

2.2.2.2.3. 7-(2-Morpholinoethyl)-4-(4-morpholinopiperidin-1-yl)-7H-pyrrolo[2,3-d]pyrimidin-2-amine **3c**. Light brown solid, yield 22%, Mp 153–155 °C.  $^1\text{H}$  NMR (400 MHz,  $\text{CDCl}_3$ )  $\delta$  6.70 (d,  $J = 3.6$  Hz, 1H, H6), 6.29 (d,  $J = 3.6$  Hz, 1H, H5), 4.70 (d,  $J = 13.2$  Hz, 2H, H2'' and H6''), 4.52 (s, 2H,  $\text{NH}_2$ ), 4.11 (t,  $J = 6.7$  Hz, 2H, 2 × H1'), 3.71–3.65 (m, 8H, 2 × H5', 2 × H7', 2 × H9'' and 2 × H11''), 2.97 (t,  $J = 12.0$  Hz, 2H, H2'' and H6''), 2.67 (t,  $J = 6.7$  Hz, 2H, 2 × H2'), 2.56–2.49 (m, 4H, 2 × H8'' and 2 × H12''), 2.48–2.41 (m, 5H, 2 × H4', 2 × H8' and H4''), 1.89 (d,  $J = 11.7$  Hz, 2H, H3'' and H5''), 1.51 (ddd,  $J = 24.2, 12.2, 3.9$  Hz, 2H, H3'' and H5'').  $^{13}\text{C}$  NMR (101 MHz,  $\text{CDCl}_3$ )  $\delta$  158.72, 157.62, 153.62, 121.03, 100.97, 97.13, 67.30 (2C), 66.98 (2C), 62.29, 58.13, 53.71 (2C), 49.74 (2C), 45.06 (2C), 41.46, 28.23 (2C). HRMS  $m/z$  416.2768 [ $\text{M} + \text{H}^+$ ] (calcd. for  $\text{C}_{21}\text{H}_{33}\text{N}_7\text{O}_2$ , 416.2708).

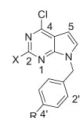
2.2.2.2.4. 4-(2-(4-([1,4'-Bipiperidin]-1'-yl)-2-chloro-7H-pyrrolo[2,3-d]pyrimidin-7-yl)ethyl)morpholine **4a**. Yellow oil, yield 87%.  $^1\text{H}$  NMR (400 MHz,  $\text{CDCl}_3$ )  $\delta$  6.96 (d,  $J = 3.6$  Hz, 1H, H6), 6.40 (d,  $J = 3.7$  Hz, 1H, H5), 4.76 (d,  $J = 13.3$  Hz, 2H, H2'' and H6''), 4.21 (t,  $J = 6.3$  Hz, 2H, 2 × H1'), 3.65–3.61 (m, 4H, 2 × H5' and 2 × H7'), 3.08–2.98 (m, 2H, H2'' and H6''), 2.67 (t,  $J = 6.3$  Hz, 2H, 2 × H2'), 2.64–2.58 (m, 1H, H4''), 2.57–2.51 (m, 4H, 2 × H8'' and 2 × H12''), 2.48–2.43 (m, 4H, 2 × H4', 2 × H8'), 1.96 (d,  $J = 12.0$  Hz, 2H, H9'' and H11''), 1.65–1.52 (m, 6H, 2 × H3'', 2 × H5'', H9'' and H11''), 1.46–1.38 (m, 2H, 2 × H10'').  $^{13}\text{C}$  NMR (101 MHz,  $\text{CDCl}_3$ )  $\delta$  157.09, 153.16, 152.34, 124.11, 101.22, 100.95, 66.98 (2C), 62.67, 58.19, 53.65 (2C), 50.17 (2C), 45.51 (2C), 41.68, 27.79 (2C), 26.00 (2C), 24.52. HRMS  $m/z$  433.2477 [ $\text{M} + \text{H}^+$ ] (calcd. for  $\text{C}_{22}\text{H}_{33}\text{ClN}_6\text{O}$ , 433.2418).

2.2.2.2.5. 4-(2-(4-([1,4'-Bipiperidin]-1'-yl)-7H-pyrrolo[2,3-d]pyrimidin-7-yl)ethyl)morpholine **4b**. Brown solid, yield 72%, Mp 110–112 °C.  $^1\text{H}$  NMR (400 MHz,  $\text{CDCl}_3$ )  $\delta$  8.31 (s, 1H, H2), 7.02 (d,  $J = 3.6$  Hz, 1H, H6), 6.44 (d,  $J = 3.6$  Hz, 1H, H5), 4.84 (d,  $J = 13.3$  Hz, 2H, 2 × H2''), 4.29 (t,  $J = 6.5$  Hz, 2H, 2 × H1'), 3.71–3.60 (m, 4H, 2 × H5' and 2 × H7'), 3.06 (t,  $J = 12.4$  Hz, 2H, H2'' and H6''), 2.84 (t,  $J = 10.9$  Hz, 1H, H4''), 2.76–2.61 (m, 6H, 2 × H2', 2 × H8'' and 2 × H12''), 2.52–2.46 (m, 4H, 2 × H4', 2 × H8'), 2.09 (d,  $J = 11.9$  Hz, 2H, H9'' and H11''), 1.81–1.60 (m, 6H, 2 × H3'', 2 × H5'', H9'' and H11''), 1.49 (br, 2H, 2 × H10'').  $^{13}\text{C}$  NMR (101 MHz,  $\text{CDCl}_3$ )  $\delta$  156.72, 151.22, 151.06, 124.08, 103.10, 100.48, 66.97 (2C), 63.31, 58.20, 53.67 (2C), 50.05 (2C), 45.35 (2C), 41.80, 27.33 (2C), 25.17 (2C), 24.01. HRMS  $m/z$  399.2867 [ $\text{M} + \text{H}^+$ ] (calcd. for  $\text{C}_{22}\text{H}_{34}\text{N}_6\text{O}$ , 399.2811).

2.2.2.2.6. 4-([1,4'-Bipiperidin]-1'-yl)-7-(2-morpholinoethyl)-7H-pyrrolo[2,3-d]pyrimidin-2-amine **4c**. White solid, yield 39%, Mp 146–148 °C.  $^1\text{H}$  NMR (400 MHz,  $\text{CDCl}_3$ )  $\delta$  6.68 (d,  $J = 3.6$  Hz, 1H, H6), 6.27 (d,  $J = 3.6$  Hz, 1H, H5), 4.73 (d,  $J = 13.3$  Hz, 2H, H2'' and

H6''), 4.57 (s, 2H,  $\text{NH}_2$ ), 4.09 (t,  $J = 6.7$  Hz, 2H, 2 × H1'), 3.68–3.61 (m, 4H, 2 × H5' and 2 × H7'), 2.92 (t,  $J = 12.1$  Hz, 2H, 2 × H2'), 2.71–2.61 (m, 3H, H2'', H4'' and H6''), 2.60–2.54 (m, 4H, 2 × H8'' and 2 × H12''), 2.48–2.43 (m, 4H, 2 × H4', 2 × H8'), 1.94 (d,  $J = 12.0$  Hz, 2H, H9'' and H11''), 1.68–1.50 (m, 6H, 2 × H3'', 2 × H5'', H9'' and H11''), 1.50–1.33 (m, 2H, 2 × H10'').  $^{13}\text{C}$  NMR (101 MHz,  $\text{CDCl}_3$ )  $\delta$  158.72, 157.52, 153.55, 121.09, 100.96, 97.10, 66.95 (2C), 63.20, 58.09, 53.69 (2C), 50.06 (2C), 45.30 (2C), 41.51, 27.53 (2C), 25.62 (2C), 24.31. HRMS  $m/z$  414.2976 [ $\text{M} + \text{H}^+$ ] (calcd. for  $\text{C}_{22}\text{H}_{35}\text{N}_7\text{O}$ , 414.2914).

2.2.2.3. General synthetic procedure to obtain *N*-benzyl-pyrrolo[2,3-d]pyrimidine derivatives **5a–8a** and **5b–8b**. A mixture of 4-chloro-7H-pyrrolo[2,3-d]pyrimidine or 2,4-dichloro-7H-pyrrolo[2,3-d]pyrimidine (1.0 mmol), the respective benzyl halide (1.2 mmol) and potassium carbonate (3.0 mmol) in acetonitrile (5 mL) was stirred for 3 h, then the mixture was filtered and evaporated under vacuum. The products were separated by flash chromatography on silica gel eluting with methylene chloride.



2.2.2.3.1. 2,4-Dichloro-7-(4-chlorobenzyl)-7H-pyrrolo[2,3-d]pyrimidine **5a**. White solid, yield 72%, Mp 129–131 °C.  $^1\text{H}$  NMR (400 MHz,  $\text{CDCl}_3$ )  $\delta$  7.24 (d,  $J = 8.4$  Hz, 2H, H3' and H5'), 7.12–7.07 (m, 3H, H6, H2' and H6'), 6.55 (d,  $J = 3.6$  Hz, 1H, H5), 5.31 (s, 2H,  $\text{N-CH}_2$ ).  $^{13}\text{C}$  NMR (101 MHz,  $\text{CDCl}_3$ )  $\delta$  152.84, 152.21, 152.11, 134.41, 134.18, 129.40, 129.24 (2C), 129.15 (2C), 116.30, 100.73, 47.93. HRMS  $m/z$  311.9857 [ $\text{M} + \text{H}^+$ ] (calcd. for  $\text{C}_{13}\text{H}_8\text{Cl}_3\text{N}_3$ , 311.9814).

2.2.2.3.2. 2,4-Dichloro-7-(4-fluorobenzyl)-7H-pyrrolo[2,3-d]pyrimidine **6a**. White solid, yield 67%, Mp 96–98 °C.  $^1\text{H}$  NMR (400 MHz,  $\text{CDCl}_3$ )  $\delta$  7.43 (dd,  $J = 8.4, 5.3$  Hz, 2H, H3' and H5'), 7.37 (d,  $J = 3.6$  Hz, 1H, H6), 7.23 (t,  $J = 8.6$  Hz, 2H, H2' and H6'), 6.81 (d,  $J = 3.6$  Hz, 1H, H5), 5.58 (s, 2H,  $\text{N-CH}_2$ ).  $^{13}\text{C}$  NMR (101 MHz,  $\text{CDCl}_3$ )  $\delta$  162.65 (d,  $J_{\text{CF}} = 247.6$  Hz), 152.78, 152.14, 152.06, 131.53 (d,  $J_{\text{CF}} = 3.3$  Hz), 129.68 (d,  $J_{\text{CF}} = 8.3$  Hz, 2C), 129.41, 116.31, 116.01 (d,  $J_{\text{CF}} = 21.7$  Hz, 2C), 100.63, 47.91. HRMS  $m/z$  296.0152 [ $\text{M} + \text{H}^+$ ] (calcd. for  $\text{C}_{13}\text{H}_8\text{Cl}_2\text{FN}_3$ , 296.0111).

2.2.2.3.3. 4-((2,4-Dichloro-7H-pyrrolo[2,3-d]pyrimidin-7-yl)methyl)benzonitrile **7a**. White solid, yield 56%. Mp 175–177 °C.  $^1\text{H}$  NMR (400 MHz,  $\text{CDCl}_3$ )  $\delta$  7.54 (d,  $J = 8.2$  Hz, 2H, H3' and H5'), 7.22 (d,  $J = 8.1$  Hz, 2H, H2' and H6'), 7.13 (d,  $J = 3.6$  Hz, 1H, H6), 6.58 (d,  $J = 3.6$  Hz, 1H, H5), 5.41 (s, 2H,  $\text{N-CH}_2$ ).  $^{13}\text{C}$  NMR (101 MHz,  $\text{CDCl}_3$ )  $\delta$  153.04, 152.37, 152.18, 140.98, 132.82 (2C), 129.46, 128.15 (2C), 118.22, 116.31, 112.36, 101.14, 48.08. HRMS  $m/z$  303.0199 [ $\text{M} + \text{H}^+$ ] (calcd. for  $\text{C}_{14}\text{H}_8\text{Cl}_2\text{N}_4$ , 303.0155).

2.2.2.3.4. 2,4-Dichloro-7-(2,6-dichlorobenzyl)-7H-pyrrolo[2,3-d]pyrimidine **8a**. White solid, yield 64%, Mp 140–142 °C.  $^1\text{H}$  NMR (400 MHz,  $\text{CDCl}_3$ )  $\delta$  7.24 (d,  $J = 8.0$  Hz, 2H, H3' and H5'), 7.14 (dd,  $J = 8.7, 7.3$  Hz, 1H, H4'), 6.83 (d,  $J = 3.7$  Hz, 1H, H6), 6.38 (d,  $J = 3.7$  Hz, 1H, H5), 5.52 (s, 2H,  $\text{N-CH}_2$ ).  $^{13}\text{C}$  NMR (101 MHz,  $\text{CDCl}_3$ )  $\delta$  152.56, 152.10, 151.94, 136.90, 130.93 (2C), 130.70, 128.90 (2C), 128.45, 116.18, 100.44, 43.67. HRMS  $m/z$  345.9467 [ $\text{M} + \text{H}^+$ ] (calcd. for  $\text{C}_{13}\text{H}_7\text{Cl}_4\text{N}_3$ , 345.9421).

2.2.2.3.5. 4-Chloro-7-(4-chlorobenzyl)-7H-pyrrolo[2,3-d]pyrimidine **5b**. White solid, yield 46%, Mp 144–145 °C.  $^1\text{H}$  NMR (400 MHz,  $\text{CDCl}_3$ )  $\delta$  8.73 (s, 1H, H2), 7.38–7.33 (m, 2H, H3' and H5'), 7.26 (d,  $J = 3.6$  Hz, 1H, H6), 7.22 (d,  $J = 7.6$  Hz, 2H, H2' and H6'), 6.70 (d,  $J = 3.6$  Hz, 1H, H5), 5.49 (s, 2H,  $\text{N-CH}_2$ ).  $^{13}\text{C}$  NMR (101 MHz,  $\text{CDCl}_3$ )  $\delta$  152.37, 151.14, 151.00, 134.78, 134.19, 129.16 (2C), 128.98 (2C), 128.83, 117.51, 100.26, 47.84. HRMS  $m/z$  278.0246 [ $\text{M} + \text{H}^+$ ] (calcd. for  $\text{C}_{13}\text{H}_9\text{Cl}_2\text{N}_3$ , 278.0210).

3197

## 5 Nature-inspired pyrrolo[2,3-d]pyrimidines targeting the histamine H3 receptor

A. Frank, et al.

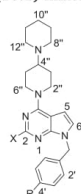
Bioorganic & Medicinal Chemistry 27 (2019) 3194–3200

**2.2.2.3.6. 4-Chloro-7-(4-fluorobenzyl)-7H-pyrrolo[2,3-d]pyrimidine 6b.** White solid, yield 56%, Mp 103–105 °C. <sup>1</sup>H NMR (400 MHz, CDCl<sub>3</sub>) δ 8.69 (s, 1H, H2), 7.27–7.22 (m, 3H, H6, H3' and H5'), 7.07–7.00 (m, 2H, H2' and H6'), 6.65 (d, *J* = 3.6 Hz, 1H, H5), 5.45 (s, 2H, N-CH<sub>2</sub>). <sup>13</sup>C NMR (101 MHz, CDCl<sub>3</sub>) δ 162.53 (d, *J*<sub>CF</sub> = 247.2 Hz), 152.28, 151.08, 150.92, 132.11 (d, *J*<sub>CF</sub> = 3.3 Hz), 129.46 (d, *J*<sub>CF</sub> = 8.3 Hz, 2C), 128.84, 117.50, 115.89 (d, *J*<sub>CF</sub> = 21.7 Hz, 2C), 100.13, 47.80. HRMS *m/z* 262.0542 [M + H<sup>+</sup>] (calcd. for C<sub>13</sub>H<sub>9</sub>ClFN<sub>3</sub>, 262.0507).

**2.2.2.3.7. 4-((4-Chloro-7H-pyrrolo[2,3-d]pyrimidin-7-yl)methyl)benzonitrile 7b.** White solid, yield 59%, Mp 157–159 °C. <sup>1</sup>H NMR (400 MHz, CDCl<sub>3</sub>) δ 8.59 (s, 1H, H2), 7.55 (d, *J* = 8.2 Hz, 2H, H3' and H5'), 7.22 (d, *J* = 8.1 Hz, 2H, H2' and H6'), 7.16 (d, *J* = 3.6 Hz, 1H, H6), 6.61 (d, *J* = 3.6 Hz, 1H, H5), 5.46 (s, 2H, N-CH<sub>2</sub>). <sup>13</sup>C NMR (101 MHz, CDCl<sub>3</sub>) δ 152.60, 151.18 (2C), 141.55, 132.77 (2C), 128.80, 127.99 (2C), 118.28, 117.53, 112.23, 100.69, 48.04. HRMS *m/z* 269.0589 [M + H<sup>+</sup>] (calcd. for C<sub>14</sub>H<sub>9</sub>ClN<sub>4</sub>, 269.0552).

**2.2.2.3.8. 4-Chloro-7-(2,6-dichlorobenzyl)-7H-pyrrolo[2,3-d]pyrimidine 8b.** White solid, yield 51%, Mp 151–153 °C. <sup>1</sup>H NMR (400 MHz, CDCl<sub>3</sub>) δ 8.59 (s, 1H, H2), 7.24 (d, *J* = 8.1 Hz, 2H, H3' and H5'), 7.18–7.06 (m, 1H, H4'), 6.87 (d, *J* = 3.7 Hz, 1H, H6), 6.40 (d, *J* = 3.7 Hz, 1H, H5), 5.59 (s, 2H, N-CH<sub>2</sub>). <sup>13</sup>C NMR (101 MHz, CDCl<sub>3</sub>) δ 152.09, 151.15, 150.76 (2C), 136.89, 131.25, 130.71, 128.85 (2C), 127.81, 117.32, 100.02, 43.42. HRMS *m/z* 311.9857 [M + H<sup>+</sup>] (calcd. for C<sub>13</sub>H<sub>8</sub>Cl<sub>3</sub>N<sub>3</sub>, 311.9815).

**2.2.2.4. General synthetic procedure to obtain substituted pyrrolo[2,3-d]pyrimidines 9a–12a and 9b–12b.** The *N*-benzyl-pyrrolo[2,3-d]pyrimidine **5a–8a** or **5b–8b** (1.0 mmol), 4-piperidinopiperidine (3.0 mmol), triethylamine (4.5 mmol) and ethanol (5 mL) were added to a microwave reaction flask and the reaction mixture was irradiated for 15 min at 80 °C. Then the solvent was evaporated under vacuum and the crude product was purified by column chromatographic on silica gel using chloroform/methanol (10:1) mixture.



**2.2.2.4.1. 4-((1,4'-Bipiperidin-1'-yl)-2-chloro-7-(4-chlorobenzyl)-7H-pyrrolo[2,3-d]pyrimidine 9a.** White solid, yield 53%, Mp 97–99 °C. <sup>1</sup>H NMR (400 MHz, CDCl<sub>3</sub>) δ 7.24 (d, *J* = 7.9 Hz, 2H, H3' and H5'), 7.09 (d, *J* = 8.2 Hz, 2H, H2' and H6'), 6.77 (d, *J* = 3.5 Hz, 1H, H6), 6.43 (d, *J* = 3.6 Hz, 1H, H5), 5.26 (s, 2H, CH<sub>2</sub>), 4.78 (d, *J* = 13.2 Hz, 2H, H2' and H6'), 3.05 (t, *J* = 12.5 Hz, 2H, H2' and H6'), 2.72 (t, *J* = 11.3 Hz, 1H, H4'), 2.60 (br, 4H, 2 × H8' and 2 × H12'), 2.02 (d, *J* = 12.1 Hz, 2H, H9' and H11'), 1.73–1.53 (m, 6H, 2 × H3'', 2 × H5'', H9'' and H11''), 1.45 (d, *J* = 4.6 Hz, 2H, 2 × H10''). <sup>13</sup>C NMR (101 MHz, CDCl<sub>3</sub>) δ 157.09, 153.56, 152.54, 135.47, 133.76, 129.05 (2C), 128.94 (2C), 123.28, 101.91, 101.22, 62.80, 50.14 (2C), 47.34, 45.41 (2C), 27.56 (2C), 25.62 (2C), 24.27. HRMS *m/z* 444.1716 [M + H<sup>+</sup>] (calcd. for C<sub>23</sub>H<sub>28</sub>Cl<sub>2</sub>N<sub>5</sub>, 444.1657).

**2.2.2.4.2. 4-((1,4'-Bipiperidin-1'-yl)-2-chloro-7-(4-fluorobenzyl)-7H-pyrrolo[2,3-d]pyrimidine 10a.** White solid, yield 57%, Mp 129–130 °C. <sup>1</sup>H NMR (400 MHz, CDCl<sub>3</sub>) δ 7.17 (dd, *J* = 8.3, 5.4 Hz, 2H, H3' and H5'), 6.98 (t, *J* = 8.6 Hz, 2H, H2' and H6'), 6.79 (d, *J* = 3.6 Hz, 1H, H6), 6.44 (d, *J* = 3.7 Hz, 1H, H5), 5.28 (s, 2H, CH<sub>2</sub>), 4.79 (d, *J* = 13.3 Hz, 2H, H2' and H6'), 3.06 (t, *J* = 12.1 Hz, 2H, H2' and H6'), 2.73–2.64 (m, 1H, H4'), 2.61–2.53 (m, 4H, 2 × H8' and 2 × H12'), 2.00 (d, *J* = 12.2 Hz, 2H, H9' and H11'), 1.70–1.55 (m, 6H, 2 × H3'', 2 × H5'', H9'' and H11''), 1.50–1.37 (m, 2H, 2 × H10''). <sup>13</sup>C NMR (101 MHz, CDCl<sub>3</sub>) δ 162.37 (d, *J*<sub>CF</sub> = 246.5 Hz), 157.11,

153.53, 152.48, 132.77 (d, *J*<sub>CF</sub> = 3.3 Hz), 129.47 (d, *J*<sub>CF</sub> = 8.2 Hz, 2C), 123.22, 115.65 (d, *J*<sub>CF</sub> = 21.6 Hz, 2C), 101.85, 101.21, 62.70, 50.16 (2C), 47.29, 45.47 (2C), 27.70 (2C), 25.86 (2C), 24.42. <sup>19</sup>F NMR (376 MHz, CDCl<sub>3</sub>) δ −114.37. HRMS *m/z* 428.2012 [M + H<sup>+</sup>] (calcd. for C<sub>23</sub>H<sub>27</sub>ClFN<sub>5</sub>, 428.1961).

**2.2.2.4.3. 4-((1,4'-Bipiperidin-1'-yl)-2-chloro-7H-pyrrolo[2,3-d]pyrimidin-7-yl)methyl)benzonitrile 11a.** White solid, yield 77%, Mp 158–160 °C. <sup>1</sup>H NMR (400 MHz, CDCl<sub>3</sub>) δ 7.56 (d, *J* = 8.2 Hz, 2H, H3' and H5'), 7.22 (d, *J* = 8.1 Hz, 2H, H2' and H6'), 6.82 (d, *J* = 3.7 Hz, 1H, H6), 6.49 (d, *J* = 3.7 Hz, 1H, H5), 5.37 (s, 2H, CH<sub>2</sub>), 4.79 (d, *J* = 13.3 Hz, 2H, H2' and H6'), 3.08 (t, *J* = 12.0 Hz, 2H, H2' and H6'), 2.77–2.66 (m, 1H, H4'), 2.66–2.53 (m, 4H, 2 × H8' and 2 × H12'), 2.03 (d, *J* = 12.1 Hz, 2H, H9' and H11'), 1.72–1.61 (m, 6H, 2 × H3'', 2 × H5'', H9'' and H11''), 1.46 (d, *J* = 5.0 Hz, 2H, 2 × H10''). <sup>13</sup>C NMR (101 MHz, CDCl<sub>3</sub>) δ 157.08, 153.71, 152.59, 142.41, 132.56 (2C), 127.97 (2C), 123.22, 118.50, 111.71, 102.38, 101.18, 62.66, 50.16 (2C), 47.51, 45.41 (2C), 27.65 (2C), 25.71 (2C), 24.31. HRMS *m/z* 435.2058 [M + H<sup>+</sup>] (calcd. for C<sub>24</sub>H<sub>27</sub>ClN<sub>6</sub>, 435.1999).

**2.2.2.4.4. 4-((1,4'-Bipiperidin-1'-yl)-2-chloro-7-(2,6-dichlorobenzyl)-7H-pyrrolo[2,3-d]pyrimidine 12a.** White solid, yield 65%, Mp 94–95 °C. <sup>1</sup>H NMR (400 MHz, CDCl<sub>3</sub>) δ 7.24 (d, *J* = 8.0 Hz, 2H, H3' and H5'), 7.15–7.11 (m, 1H, H4'), 6.42 (d, *J* = 3.7 Hz, 1H, H6), 6.23 (d, *J* = 3.7 Hz, 1H, H5), 5.46 (s, 2H, CH<sub>2</sub>), 4.66 (d, *J* = 13.3 Hz, 2H, H2' and H6'), 2.92 (t, *J* = 12.1 Hz, 2H, H2' and H6'), 2.58 (t, *J* = 10.9 Hz, 1H, H4'), 2.47 (br, 4H, 2 × H8' and 2 × H12'), 1.88 (d, *J* = 12.2 Hz, 2H, H9' and H11'), 1.63–1.43 (m, 6H, 2 × H3'', 2 × H5'', H9'' and H11''), 1.36–1.22 (m, 2H, 2 × H10''). <sup>13</sup>C NMR (101 MHz, CDCl<sub>3</sub>) δ 157.06, 153.31, 152.52 (2C), 137.04, 131.58, 130.44, 128.72 (2C), 121.99, 101.48, 101.20, 62.82, 50.12 (2C), 45.42, 43.39 (2C), 27.56 (2C), 25.69 (2C), 24.32. HRMS *m/z* 478.1327 [M + H<sup>+</sup>] (calcd. for C<sub>23</sub>H<sub>26</sub>Cl<sub>3</sub>N<sub>5</sub>, 478.1265).

**2.2.2.4.5. 4-((1,4'-Bipiperidin-1'-yl)-7-(4-chlorobenzyl)-7H-pyrrolo[2,3-d]pyrimidine 9b.** Brown solid, yield 47%, Mp 103–104 °C. <sup>1</sup>H NMR (400 MHz, CDCl<sub>3</sub>) δ 8.45 (s, 1H, H2), 7.36 (d, *J* = 8.1 Hz, 2H, H3' and H5'), 7.22 (d, *J* = 8.0 Hz, 2H, H2' and H6'), 7.00 (d, *J* = 3.1 Hz, 1H, H6), 6.60 (d, *J* = 3.2 Hz, 1H, H5), 5.45 (s, 2H, CH<sub>2</sub>), 4.97 (d, *J* = 13.0 Hz, 2H, H2' and H6'), 3.19 (t, *J* = 12.5 Hz, 2H, H2' and H6'), 3.00 (t, *J* = 11.1 Hz, 1H, H4'), 2.83 (br, 4H, 2 × H8' and 2 × H12'), 2.22 (d, *J* = 11.6 Hz, 2H, H9' and H11'), 1.94–1.77 (m, 6H, 2 × H3'', 2 × H5'', H9'' and H11''), 1.61 (s, 2H, 2 × H10''). <sup>13</sup>C NMR (101 MHz, CDCl<sub>3</sub>) δ 156.74, 151.44 (2C), 135.87, 133.56, 128.88 (2C), 128.79 (2C), 123.38, 103.05, 101.41, 63.28, 50.02 (2C), 47.30, 45.30 (2C), 27.23 (2C), 25.01 (2C), 23.90. HRMS *m/z* 410.2106 [M + H<sup>+</sup>] (calcd. for C<sub>23</sub>H<sub>28</sub>ClN<sub>5</sub>, 410.2048).

**2.2.2.4.6. 4-((1,4'-Bipiperidin-1'-yl)-7-(4-fluorobenzyl)-7H-pyrrolo[2,3-d]pyrimidine 10b.** Brown solid, yield 58%, Mp 118–120 °C. <sup>1</sup>H NMR (400 MHz, CDCl<sub>3</sub>) δ 8.61 (s, 1H, H2), 7.42 (dd, *J* = 8.2, 5.5 Hz, 2H, H3' and H5'), 7.23 (t, *J* = 8.6 Hz, 2H, H2' and H6'), 7.15 (d, *J* = 3.6 Hz, 1H, H6), 6.74 (d, *J* = 3.6 Hz, 1H, H5), 5.60 (s, 2H, CH<sub>2</sub>), 5.11 (d, *J* = 13.3 Hz, 2H, H2' and H6'), 3.33 (t, *J* = 12.2 Hz, 2H, H2' and H6'), 3.07 (t, *J* = 11.5 Hz, 1H, H4'), 2.93 (br, 4H, 2 × H8' and 2 × H12'), 2.34 (d, *J* = 12.0 Hz, 2H, H9' and H11'), 2.06–1.84 (m, 6H, 2 × H3'', 2 × H5'', H9'' and H11''), 1.75 (d, *J* = 4.9 Hz, 2H, 2 × H10''). <sup>13</sup>C NMR (101 MHz, CDCl<sub>3</sub>) δ 162.30 (d, *J*<sub>CF</sub> = 246.1 Hz), 156.79, 151.46, 151.42, 133.16 (d, *J*<sub>CF</sub> = 3.2 Hz), 129.19 (d, *J*<sub>CF</sub> = 8.2 Hz, 2C), 123.27, 115.61 (d, *J*<sub>CF</sub> = 21.6 Hz, 2C), 103.05, 101.36, 63.20, 50.08 (2C), 47.24, 45.40 (2C), 27.43 (2C), 25.34 (2C), 24.11. <sup>19</sup>F NMR (376 MHz, CDCl<sub>3</sub>) δ −114.67. HRMS *m/z* 394.2402 [M + H<sup>+</sup>] (calcd. for C<sub>23</sub>H<sub>28</sub>FN<sub>5</sub>, 394.2346).

**2.2.2.4.7. 4-((1,4'-Bipiperidin-1'-yl)-7H-pyrrolo[2,3-d]pyrimidin-7-yl)methyl)benzonitrile 11b.** Brown solid, yield 52%, Mp 101–103 °C. <sup>1</sup>H NMR (400 MHz, CDCl<sub>3</sub>) δ 8.32 (s, 1H, H2), 7.57 (d, *J* = 8.1 Hz, 2H, H3' and H5'), 7.22 (d, *J* = 8.0 Hz, 2H, H2' and H6'), 6.90 (d, *J* = 3.5 Hz, 1H, H6), 6.53 (d, *J* = 3.5 Hz, 1H, H5), 5.43 (s, 2H, CH<sub>2</sub>), 4.84 (d, *J* = 13.2 Hz, 2H, H2' and H6'), 3.08 (t, *J* = 12.4 Hz, 2H, H2' and H6'), 2.77 (t, *J* = 11.3 Hz, 1H, H4'), 2.68–2.57 (br, 4H,

3198

## 5 Nature-inspired pyrrolo[2,3-d]pyrimidines targeting the histamine H<sub>3</sub> receptor

A. Frank, et al.

Bioorganic & Medicinal Chemistry 27 (2019) 3194–3200

2 × H<sub>8</sub>" and 2 × H<sub>12</sub>" ), 2.06 (d, *J* = 11.9 Hz, 2H, H<sub>9</sub>" and H<sub>11</sub>" ), 1.77–1.56 (m, 6H, 2 × H<sub>3</sub>" , 2 × H<sub>5</sub>" , H<sub>9</sub>" and H<sub>11</sub>" ), 1.47 (s, 2H, 2 × H<sub>10</sub>" ). <sup>13</sup>C NMR (101 MHz, CDCl<sub>3</sub>) δ 156.83, 151.69, 151.52, 142.84, 132.56 (2C), 127.77 (2C), 123.15, 118.55, 111.61, 102.99, 101.94, 63.05, 50.14 (2C), 47.53, 45.43 (2C), 27.59 (2C), 25.54 (2C), 24.23. HRMS *m/z* 401.2448 [M + H<sup>+</sup>] (calcd. for C<sub>24</sub>H<sub>28</sub>N<sub>6</sub>, 401.2392).

2.2.2.4.8. 4-([1,4'-Bipiperidin]-1'-yl)-7-(2,6-dichlorobenzyl)-7H-pyrrolo[2,3-d]pyrimidine **12b**. White solid, yield 51%, Mp 122–124 °C. <sup>1</sup>H NMR (400 MHz, CDCl<sub>3</sub>) δ 8.27 (s, 1H, H<sub>2</sub>), 7.24 (d, *J* = 8.0 Hz, 2H, H<sub>3</sub>' and H<sub>5</sub>'), 7.12 (t, *J* = 8.0 Hz, 1H, H<sub>4</sub>'), 6.52 (d, *J* = 3.6 Hz, 1H, H<sub>6</sub>), 6.25 (d, *J* = 3.7 Hz, 1H, H<sub>5</sub>), 5.52 (s, 2H, CH<sub>2</sub>), 4.73 (d, *J* = 13.4 Hz, 2H, H<sub>2</sub>" and H<sub>6</sub>" ), 3.01–2.77 (m, 3H, H<sub>2</sub>" , H<sub>6</sub>" and H<sub>4</sub>" ), 2.67 (br, 4H, 2 × H<sub>8</sub>" and 2 × H<sub>12</sub>" ), 2.04 (d, *J* = 11.7 Hz, 2H, H<sub>9</sub>" and H<sub>11</sub>" ), 1.72 (br, 4H, 2 × H<sub>3</sub>" and 2 × H<sub>5</sub>" ), 1.57 (qd, *J* = 12.1, 3.6 Hz, 2H), 1.40 (s, 2H, 2 × H<sub>10</sub>" ). <sup>13</sup>C NMR (101 MHz, CDCl<sub>3</sub>) δ 156.63, 151.51, 151.17 (2C), 136.98, 131.93, 130.36, 128.72 (2C), 122.18, 103.01, 100.97, 63.65, 49.93 (2C), 45.14 (2C), 43.10, 26.83 (2C), 24.41 (2C), 23.54. HRMS *m/z* 444.1716 [M + H<sup>+</sup>] (calcd. for C<sub>23</sub>H<sub>27</sub>Cl<sub>2</sub>N<sub>5</sub>, 444.1655).

### 2.2.3. Pharmacological part

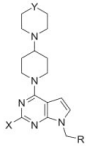
2.2.3.1. Radioligand displacement assays at the H<sub>3</sub>R. Radioligand displacement assays at the human histamine H<sub>3</sub>R were performed as published previously.<sup>18</sup> Briefly, membrane preparations of HEK-293 cells stably expressing the human histamine H<sub>3</sub>R (20 µg/well) were incubated with the compound and [<sup>3</sup>H]N<sup>m</sup>-methylhistamine (2 nM) in 200 µL of binding buffer (10 mM MgCl<sub>2</sub>, 100 mM NaCl and 75 mM Tris/HCl, pH 7.4) for 90 min. Compounds were tested in duplicates with 11 concentrations in at least three independent experiments. Data was analyzed with GraphPad Prism 7, using non-linear least squares fit and equation "one site competition" (representative Figures given in the SI). K<sub>i</sub> values were calculated according to the Cheng-Prusoff equation.<sup>19</sup> Values are reported as means with the 95% confidence interval. All statistical operations were performed on the pK<sub>i</sub> values and converted afterwards to mean K<sub>i</sub> values and the 95% confidence interval. Differences are considered significant if 95% confidence intervals are not overlapping.

2.2.3.2. Radioligand displacement assays at the H<sub>4</sub>R. H<sub>4</sub>R radioligand displacement assays were performed as described previously.<sup>20</sup> Briefly, Sf9 cell membrane preparations, expressing the human histamine H<sub>4</sub>R (40 µg/well), were co-incubated with the compound and [<sup>3</sup>H]histamine (10 nM) in 200 µL for 60 min. Compounds were tested in duplicates with at least five concentrations in two independent experiments. Data was analyzed with GraphPad Prism 7.

### 3. Results and discussion

The first synthesized set (compounds **3a–3c** and **4a–4c**) consisted of compounds bearing a morpholine group instead of the lipophilic core (**R**) that was connected to the pyrrolo[2,3-d]pyrimidine via an ethyl linker. All compounds displayed marked affinity at the H<sub>3</sub>R without H<sub>4</sub>R affinity (K<sub>i</sub> value > 10 µM). The general introduction of the morpholine group instead of a lipophilic core improved binding affinity slightly, when compared to compound **V** (K<sub>i</sub> value 126 nM), with K<sub>i</sub> values below 50 nM for derivatives **4a** and **4b**, although results were not significant. By comparing binding affinities of series **3** to **4** (Table 1) the pharmacodynamic superiority of 1,4-bipiperidine moieties (series **4**) as basic warhead (Y = CH<sub>2</sub>), compared to 4-(piperidin-4-yl)morpholines (series **3**), was once more verified.<sup>16</sup> The exchange towards the 1,4-bipiperidine resulted in a significant increase of binding affinity. Derivatization at position 2 (X) gave no significant difference between chlorinated compounds or the unsubstituted central core but revealed a pronounced loss of affinity for the aminated compounds (**3c**, **4c**). Due to these findings, only compounds **4a** and **4b** were further derivatized. In compounds **9a–12a** the 4-([1,4'-bipiperidin]-1'-yl)-2-chloro-7H-

**Table 1**  
Affinities at the H<sub>3</sub>R of compounds **3a–3c**, **4a–4c**, **9a–12a** and **9b–12b**.



Compound	Substitution pattern			K <sub>i</sub> (nM) <sup>a</sup> [95% CI nM]
	X	Y	R	
<b>3a</b>	Cl	O	Morph-CH <sub>2</sub> <sup>b</sup>	317 [135;743]
<b>3b</b>	H	O	Morph-CH <sub>2</sub>	374 [162;865]
<b>3c</b>	NH <sub>2</sub>	O	Morph-CH <sub>2</sub>	848 [386;1866]
<b>4a</b>	Cl	CH <sub>2</sub>	Morph-CH <sub>2</sub>	22 [11;45]
<b>4b</b>	H	CH <sub>2</sub>	Morph-CH <sub>2</sub>	31 [16;62]
<b>4c</b>	NH <sub>2</sub>	CH <sub>2</sub>	Morph-CH <sub>2</sub>	121 [49;301]
<b>9a</b>	Cl	CH <sub>2</sub>	Ph-4-Cl <sup>c</sup>	42 [14;127]
<b>9b</b>	H	CH <sub>2</sub>	Ph-4-Cl	26 [15;46]
<b>10a</b>	Cl	CH <sub>2</sub>	Ph-4-F <sup>d</sup>	30 [11;81]
<b>10b</b>	H	CH <sub>2</sub>	Ph-4-F	35 [10;120]
<b>11a</b>	Cl	CH <sub>2</sub>	Ph-4-CN <sup>e</sup>	18 [5;66]
<b>11b</b>	H	CH <sub>2</sub>	Ph-4-CN	7 [4;11]
<b>12a</b>	Cl	CH <sub>2</sub>	Ph-2,6-diCl <sup>f</sup>	54 [25;116]
<b>12b</b>	H	CH <sub>2</sub>	Ph-2,6-diCl	6 [2;19]

<sup>a</sup> K<sub>i</sub> values were measured at the human histamine H<sub>3</sub>R. Membrane preparations of HEK-293T cells expressing the H<sub>3</sub>R (20 µg/well) were incubated with the compound of interest and [<sup>3</sup>H]N<sup>m</sup>-methylhistamine (2 nM) in 200 µL for 90 min.

<sup>b</sup> Morph-CH<sub>2</sub>, morpholinomethyl.

<sup>c</sup> Ph-4-Cl, 4-chlorophenyl.

<sup>d</sup> Ph-4-F, 4-fluorophenyl.

<sup>e</sup> Ph-4-CN, 4-cyanophenyl.

<sup>f</sup> Ph-2,6-diCl, 2,6-dichlorophenyl.

pyrrolo[2,3-d]pyrimidine moiety was connected to differently substituted benzyl moieties. Inspired by the substitution pattern of pitolisant, the first ligand displayed a 4-chlorophenyl residue, which was exchanged by several other electron-withdrawing substituted benzyl derivatives. The compounds showed high affinity at the H<sub>3</sub>R, without affinity at the H<sub>4</sub>R (K<sub>i</sub> value > 10 µM) and no significant changes in affinity, based on the derivatization pattern of the benzyl (Table 1).

For the compounds **9b–12b** without chlorination on the heterocyclic moiety affinity at the H<sub>3</sub>R increased by increasing electron-withdrawing properties of the aromatic core (Table 1), while no compound showed considerable affinity at the H<sub>4</sub>R (K<sub>i</sub> values > 10 µM). For compound **11b** the increase of binding affinity at the H<sub>3</sub>R was significant when compared to those of **4b** (morpholinomethyl as **R**) or **9b**, the compound with the weakest electron-withdrawing properties. Furthermore, compound **12b** is the only compound where dechlorination led to a significant increase of binding affinity compared to the chlorinated compound (**12a**). When compared to compound **V** the introduction of a 4-cyanobenzyl moiety (**11b**) or a 2,6-dichlorobenzyl

(12b) increased affinity significantly with  $K_i$  values of 7 and 6 nM, respectively. Although functional studies were not performed on the scaffold of pyrrolo[2,3-d]pyrimidines, the evidence of many non-imidazole ligands being H<sub>3</sub>R antagonist or inverse agonists (aplysamine-1, conessine and pitolisant<sup>6,7,11</sup>) could rationalize an *in vivo* evaluation of these novel compounds as H<sub>3</sub>R antagonists/inverse agonists.

Based on the **lead structure** the presented compounds allow for an initial structure-activity relationship evaluation for the class of pyrrolo[2,3-d]pyrimidine as novel H<sub>3</sub>R scaffolds.

The 1,4-bipiperidine motif in position 4 seems to be crucial for high affinity towards the H<sub>3</sub>R (compare **series 3** and **4**). The introduction of a 2-morpholinoethyl instead of a 2-naphthylmethyl moiety in position 7 (**compounds 3a-3c, 4a-4c**) improved binding affinity not significantly compared to **compound V**. The introduction of an amine group at position 2 leads to a loss in affinity (**series c**, significant for **4a** to **4c**). For a given structure, with or without chloro substitution in 2-position did not result in any significant affinity changes (compare **3a** to **3b, 4a** to **4b**, etc.), except for the most active **compound 12b**. The introduction of substituted benzyl moieties at 7-position did not further increase binding affinity, if chlorinated at 2-position (**compounds 9a-12a**) and derivatization pattern of the benzyl did not influence affinity. For compounds without chloro or amino substitution at 2-position of the heterocycle (**9b-12b**) affinity was increased by increasing electron-withdrawing abilities of the substitution pattern, with the most active compounds (**11b** and **12b**) displaying significantly higher affinities than that of **compound V**.

#### 4. Conclusion

Within this study we were able to synthesize 14 novel pyrrolo[2,3-d]pyrimidines that adhere to the general pharmacophore of H<sub>3</sub>R ligands. The 1,4-bipiperidine motif as basic centre has proven itself highly effective for designing H<sub>3</sub>R ligands with superior binding affinity. The arbitrary, lipophilic region was best modulated by benzyl residues with electron-withdrawing groups. *In vivo* evaluation of these nature inspired synthetic pyrrolo[2,3-d]pyrimidines will be highly interesting, as the potential anti-inflammatory properties of this class may have synergistic effects with the human H<sub>3</sub>R modulation<sup>21</sup> on cognitive

impairments in neurodegenerative diseases. By that approach drug development of CNS disorders may be complemented by a new class of active agents and natural compounds have once more proven their versatility within the drug research and development community.

#### Acknowledgements

Support by the DFG with GRK2158, INST 208/664-1 and by FONDECYT project N° 11180292 is greatly acknowledged.

#### Appendix A. Supplementary data

Supplementary data to this article can be found online at <https://doi.org/10.1016/j.bmc.2019.05.042>.

#### References

- Breinbauer R, Vetter IR, Waldmann H. *Angew Chem Int Ed*. 2002;41:2878–2890.
- Newman DJ, Cragg GM. *J Nat Prod*. 2016;79:629–661.
- Parsons ME, Ganellin CR. *Br J Pharmacol*. 2006;147:127–135.
- Sander K, Kottke T, Stark H. *Biol Pharm Bull*. 2008;31:2163–2181.
- Vohora D, Bhowmik M. *Front Syst Neurosci*. 2012;6. <https://doi.org/10.3389/fnsys.2012.00072>.
- Swanson DM, Wilson SJ, Boggs JD, et al. *Bioorg Med Chem Lett*. 2006;16:897–900.
- Zhao C, Sun M, Bennani YL, et al. *J Med Chem*. 2008;51:5423–5430.
- Santora VJ, Covell JA, Hayashi R, et al. *Bioorg Med Chem Lett*. 2008;18:1490–1494.
- Inocente C, Arnulf I, Bastuji H, et al. *Clin Neuropharmacol*. 2012;35:203–212.
- Knier B, Mitra MT, Logishetty K, Chaudhuri KR. *CNS Drugs*. 2011;25:203–212.
- Wingen K, Stark H. *Drug Discovery Today: Technol*. 2013;10:e483–e489.
- Kazlauskas R, Murphy PT, Wells R, Jamieson DD. *Aust J Chem*. 1983;36:165–170.
- Mohamed MS, Kamel R, Fatahalla SS. *Eur J Med Chem*. 2010;45:2994–3004.
- Hilmy KMH, Khalifa MMA, Hawata MAA, Keshk RMA, El-Torgman AA. *Eur J Med Chem*. 2010;45:5243–5250.
- McGeer PL, McGeer EG. *Brain Res Rev*. 1995;21:195–218.
- Espinosa-Bustos C, Frank A, Arancibia-Opazo S, Salas CO, Fierro A, Stark H. *Bioorg Med Chem Lett*. 2018;28:2890–2893.
- Dvorak CA, Apodaca R, Barbier AJ, et al. *J Med Chem*. 2005;48:2229–2238.
- Sander K, Kottke T, Weizel L, Stark H. *Chem Pharm Bull*. 2010;58:1353–1361.
- Yung-Chi C, Prusoff WH. *Biochem Pharmacol*. 1973;22:3099–3108.
- Sadek B, Schreeb A, Schwed JS, Weizel L, Stark H. *Drug Des Dev Ther*. 2014;8:1499–1513.
- Hancock AA, Bennani YL, Bush EN, et al. *Eur J Pharmacol*. 2004;487:183–197.

## Supporting Information

### Nature-Inspired Pyrrolo[2,3-*d*]pyrimidines Targeting the Histamine H<sub>3</sub> Receptor

Annika Frank<sup>a</sup>, Francisco Meza-Arriagada<sup>b</sup>, Cristian O. Salas<sup>c</sup>,  
Christian Espinosa-Bustos<sup>b\*</sup>, Holger Stark<sup>a\*</sup>

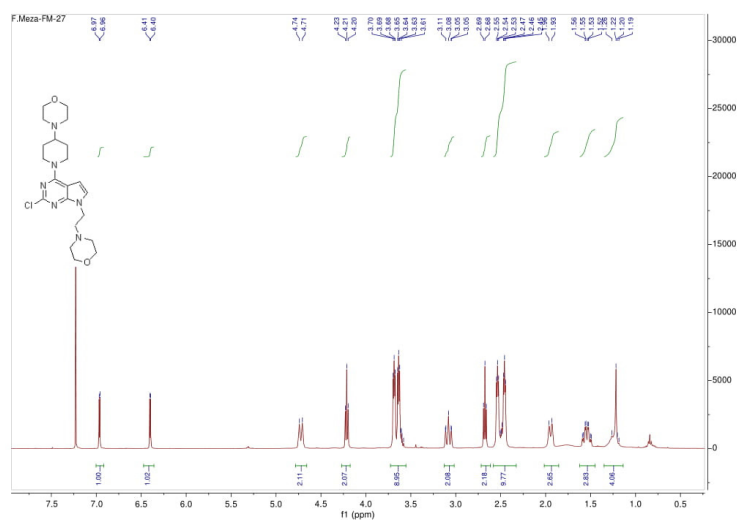
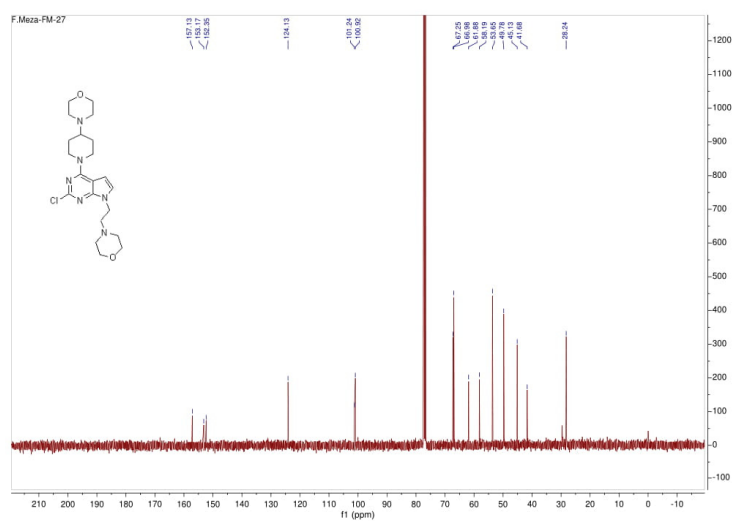
<sup>a</sup>Institute of Pharmaceutical and Medicinal Chemistry, Heinrich Heine University Düsseldorf,  
Universitätsstr. 1, 40225 Düsseldorf, Germany; E-mail: stark@hhu.de

<sup>b</sup>Departamento de Farmacia, Facultad de Química y de Farmacia, Pontificia Universidad Católica de  
Chile, Santiago 6094411, Chile; E-mail: ccespino@uc.cl

<sup>c</sup>Departamento de Química Orgánica, Facultad de Química y de Farmacia, Pontificia Universidad  
Católica de Chile, Santiago 6094411, Chile

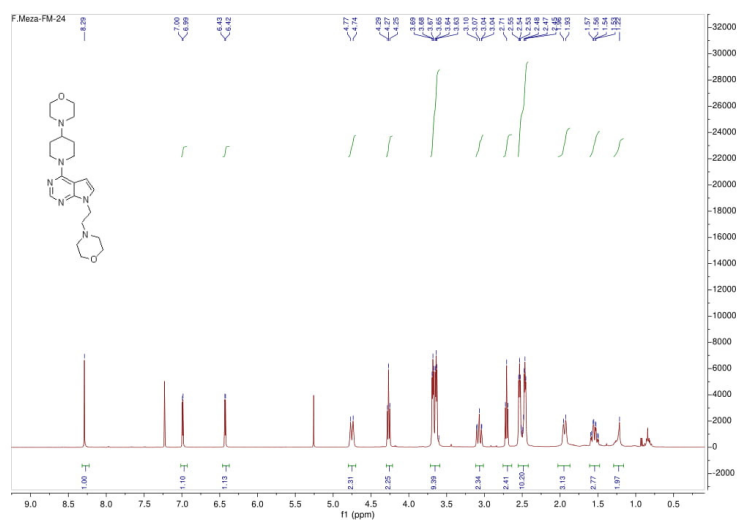


## 5 Nature-inspired pyrrolo[2,3-d]pyrimidines targeting the histamine H3 receptor

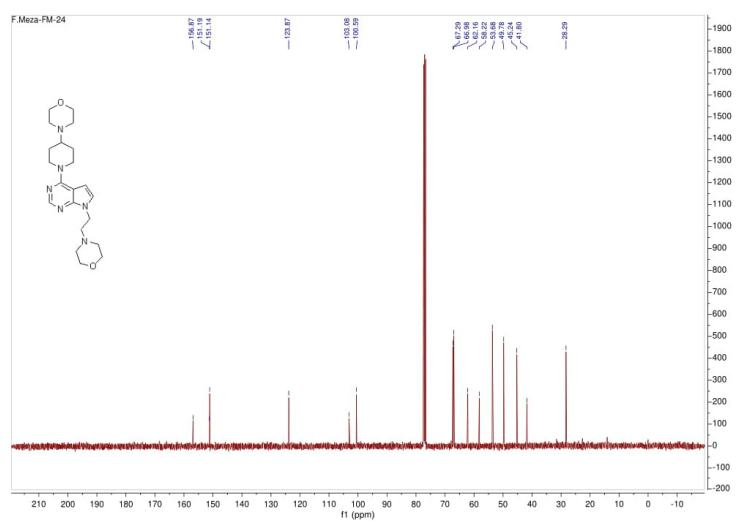
<sup>1</sup>H NMR for compound **3a**<sup>13</sup>C NMR for compound **3a**

## 5 Nature-inspired pyrrolo[2,3-d]pyrimidines targeting the histamine H3 receptor

<sup>1</sup>H NMR for compound **3b**

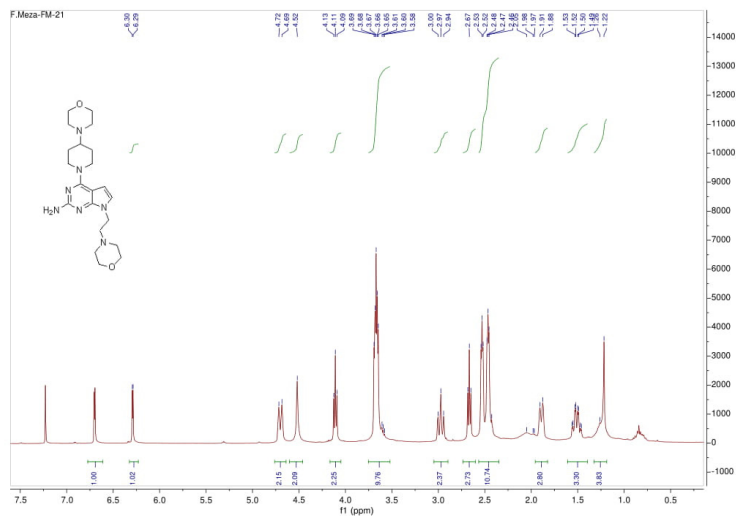


<sup>13</sup>C NMR for compound **3b**

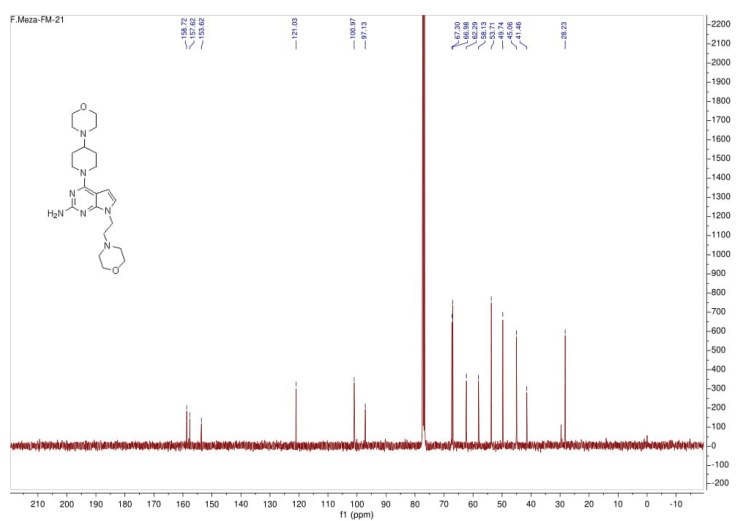


## 5 Nature-inspired pyrrolo[2,3-d]pyrimidines targeting the histamine H3 receptor

<sup>1</sup>H NMR for compound **3c**

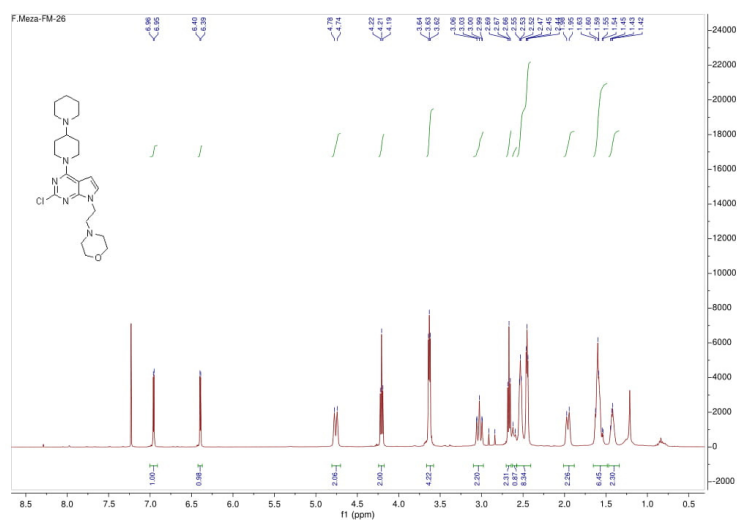


<sup>13</sup>C NMR for compound **3c**

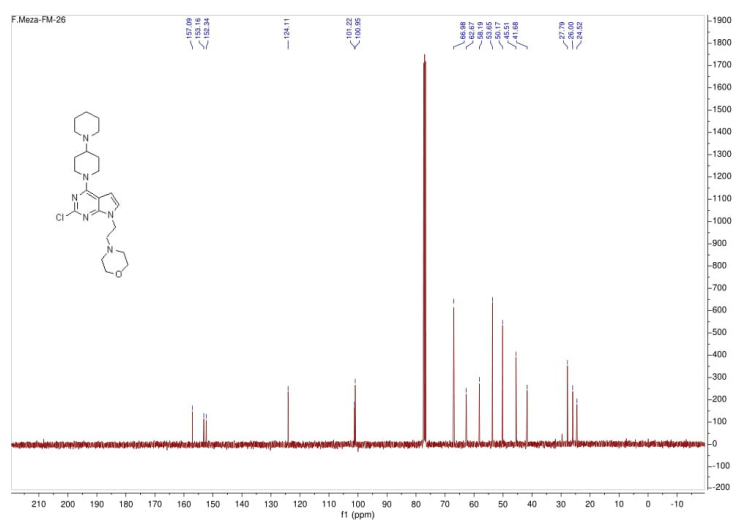


## 5 Nature-inspired pyrrolo[2,3-d]pyrimidines targeting the histamine H3 receptor

<sup>1</sup>H NMR for compound **4a**

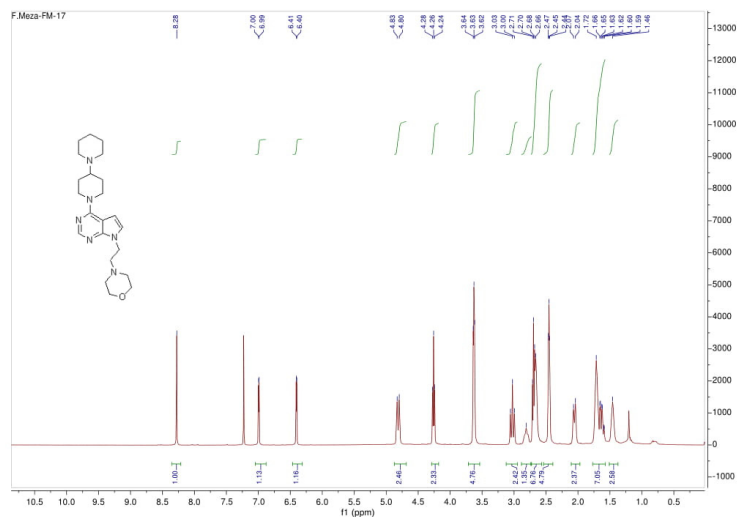


<sup>13</sup>C NMR for compound **4a**

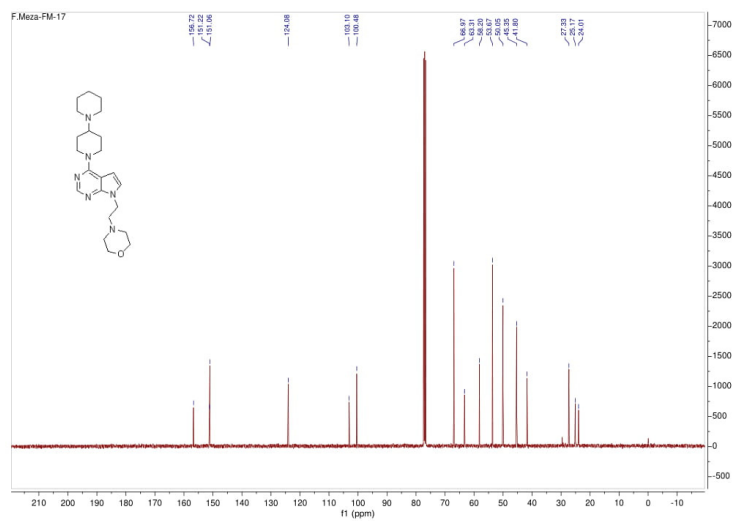


## 5 Nature-inspired pyrrolo[2,3-d]pyrimidines targeting the histamine H3 receptor

<sup>1</sup>H NMR for compound **4b**

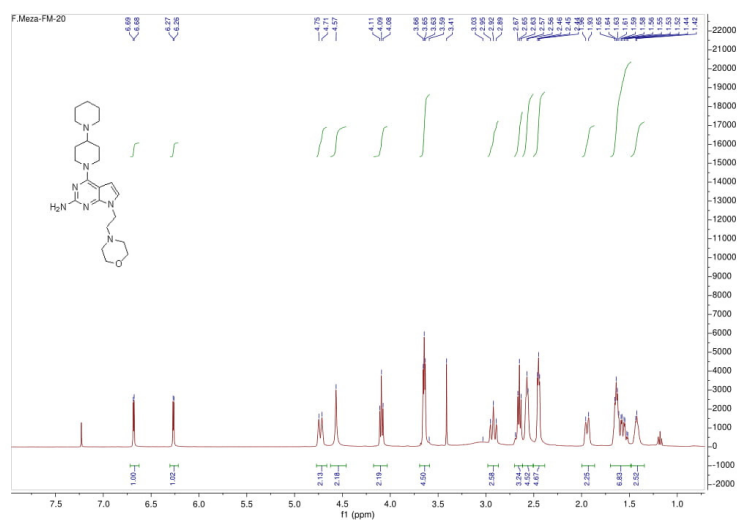


<sup>13</sup>C NMR for compound **4b**

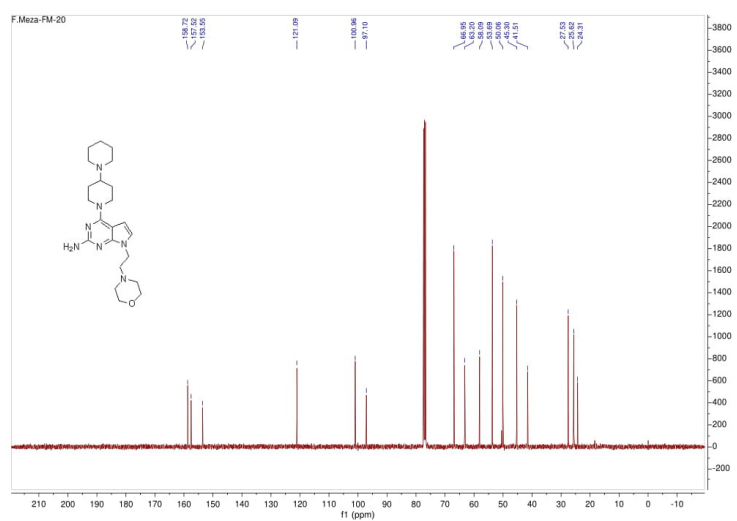


## 5 Nature-inspired pyrrolo[2,3-d]pyrimidines targeting the histamine H3 receptor

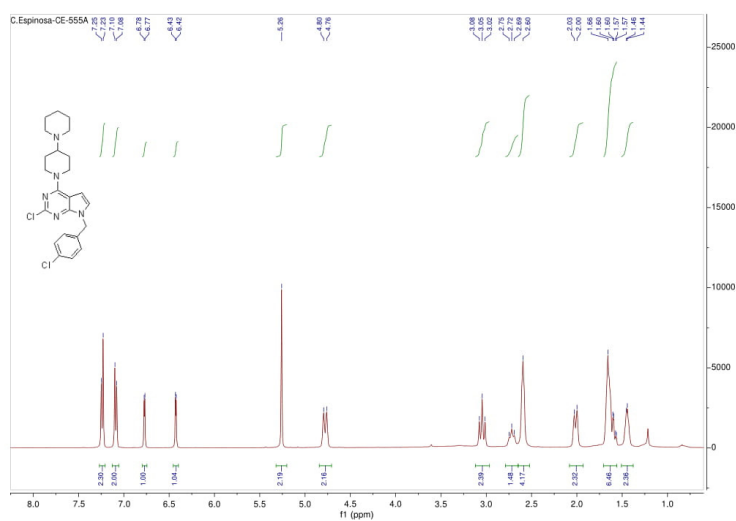
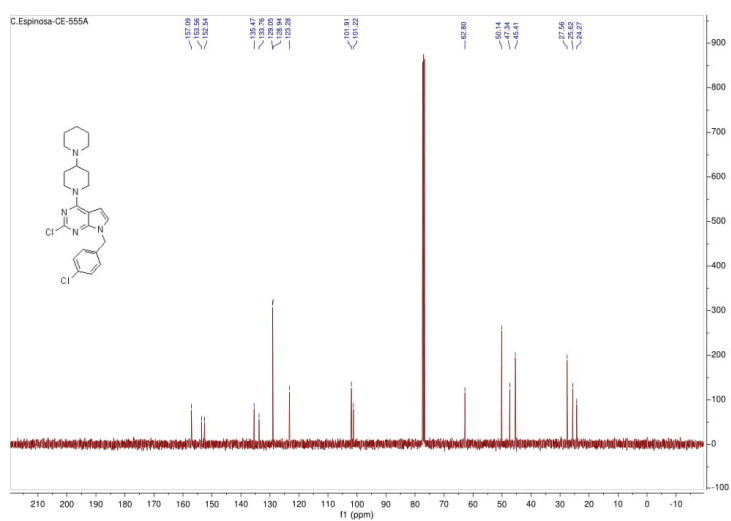
<sup>1</sup>H NMR for compound **4c**



<sup>13</sup>C NMR for compound **4c**



## 5 Nature-inspired pyrrolo[2,3-d]pyrimidines targeting the histamine H3 receptor

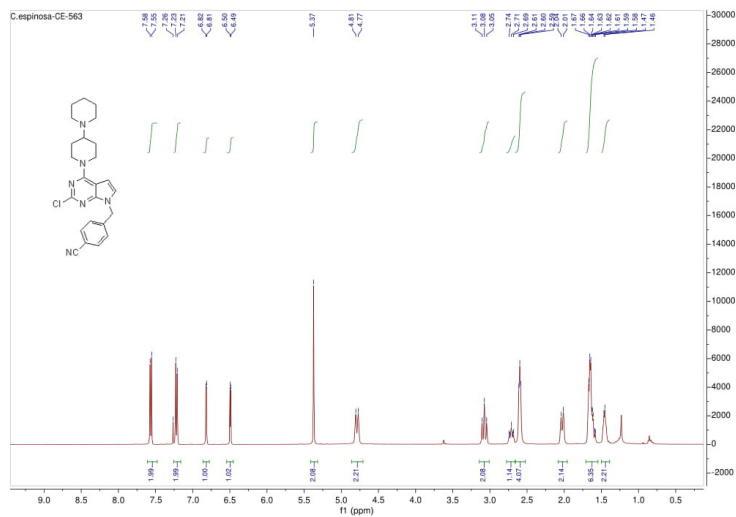
<sup>1</sup>H NMR for compound **9a**<sup>13</sup>C NMR for compound **9a**



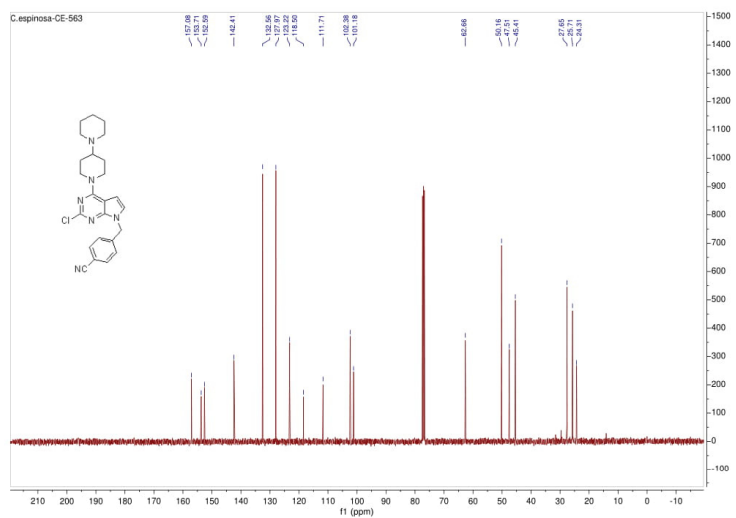


## 5 Nature-inspired pyrrolo[2,3-d]pyrimidines targeting the histamine H3 receptor

<sup>1</sup>H NMR for compound **11a**

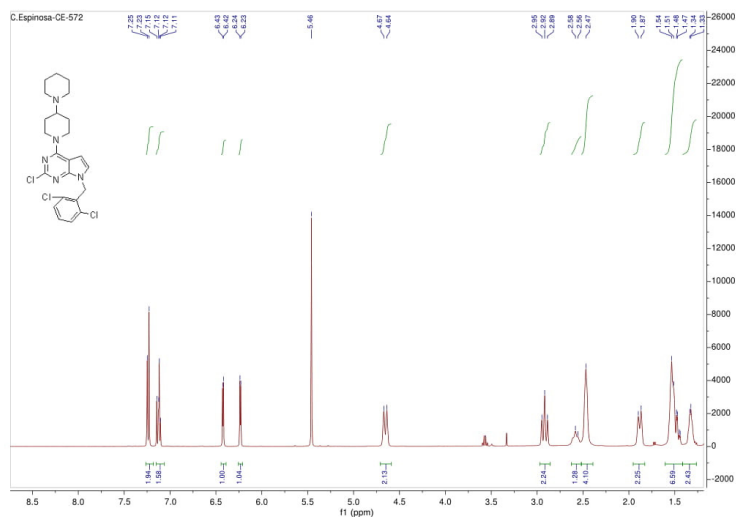


<sup>13</sup>C NMR for compound **11a**

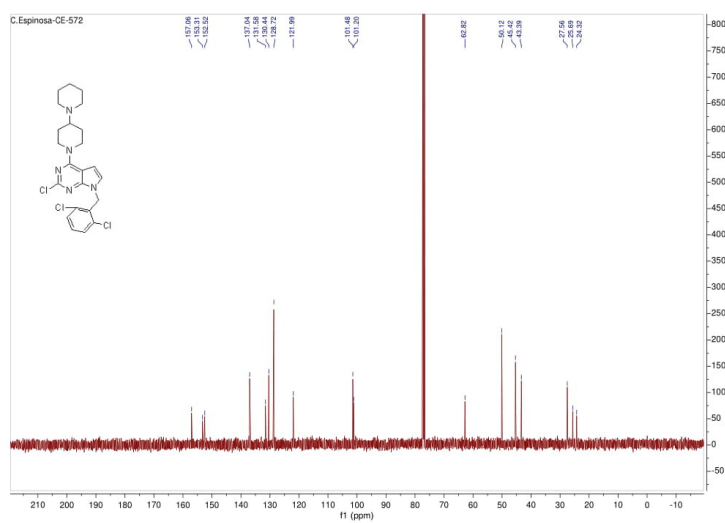


## 5 Nature-inspired pyrrolo[2,3-d]pyrimidines targeting the histamine H3 receptor

<sup>1</sup>H NMR for compound **12a**

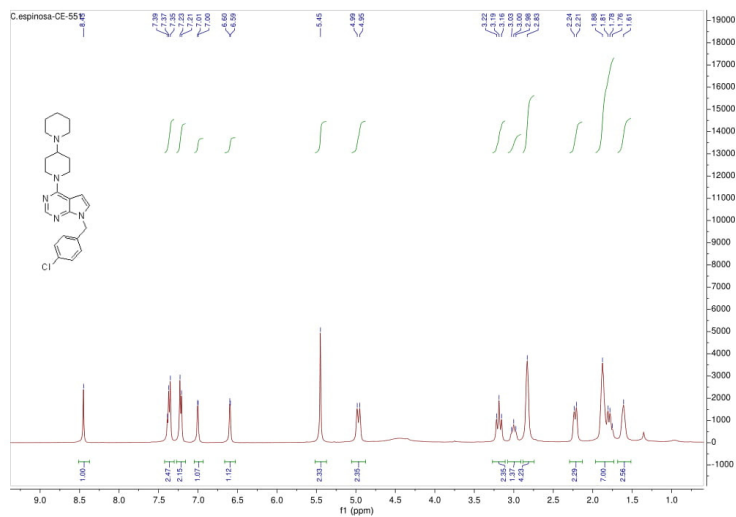


<sup>13</sup>C NMR for compound **12a**

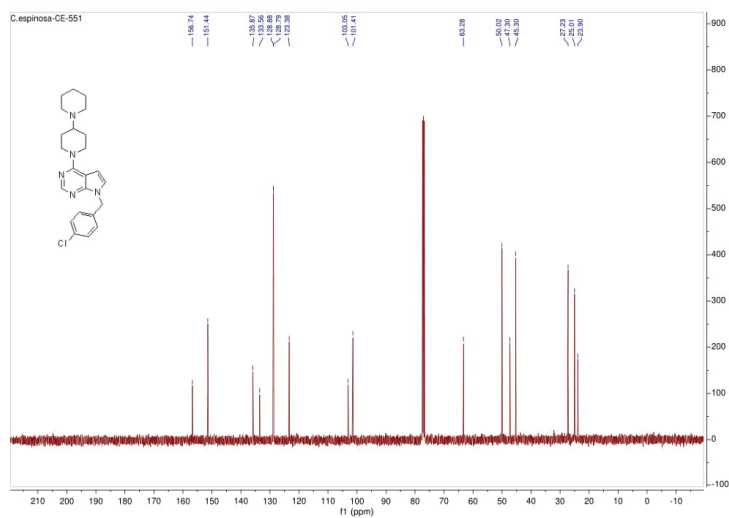


## 5 Nature-inspired pyrrolo[2,3-d]pyrimidines targeting the histamine H3 receptor

<sup>1</sup>H NMR for compound **9b**

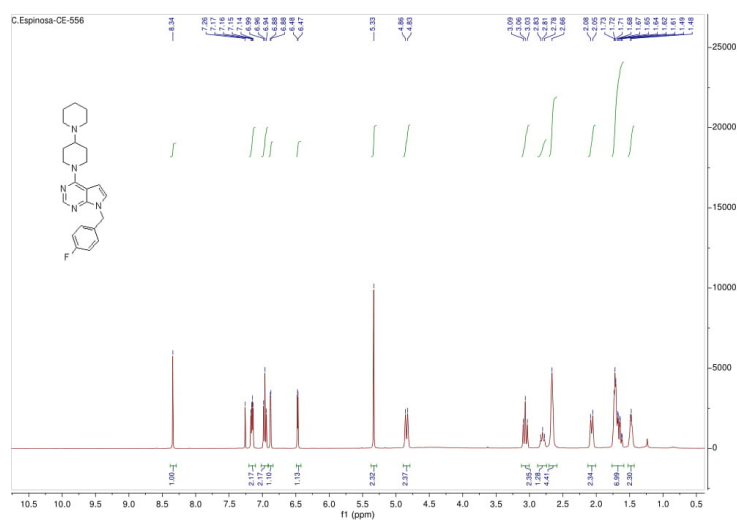


<sup>13</sup>C NMR for compound **9b**

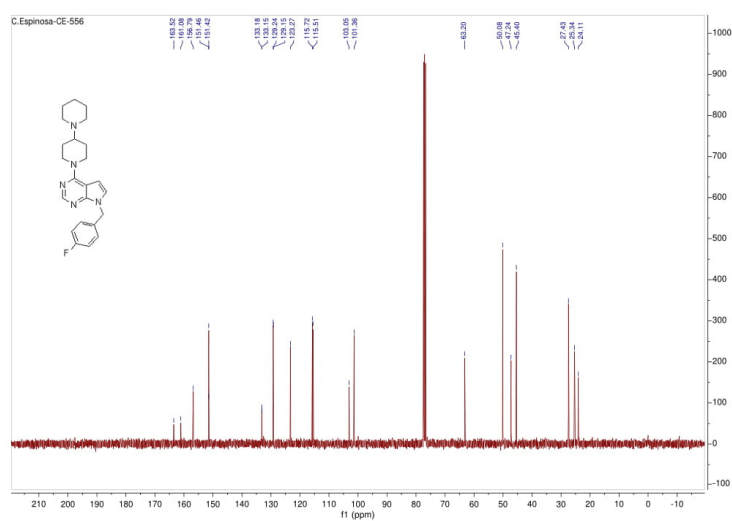


## 5 Nature-inspired pyrrolo[2,3-d]pyrimidines targeting the histamine H3 receptor

$^1\text{H}$  NMR for compound **10b**

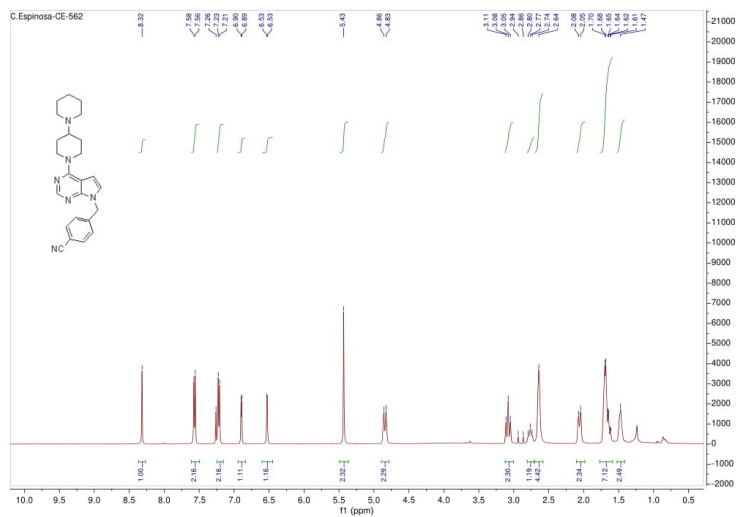


$^{13}\text{C}$  NMR for compound **10b**

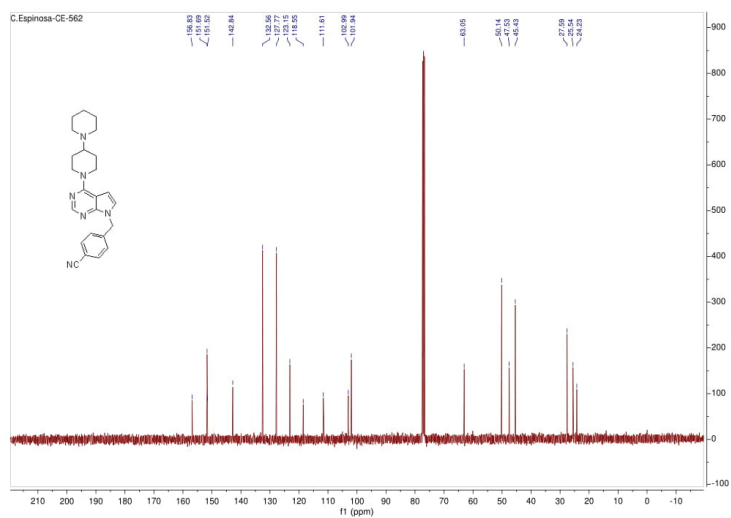


## 5 Nature-inspired pyrrolo[2,3-d]pyrimidines targeting the histamine H3 receptor

$^1\text{H}$  NMR for compound **11b**

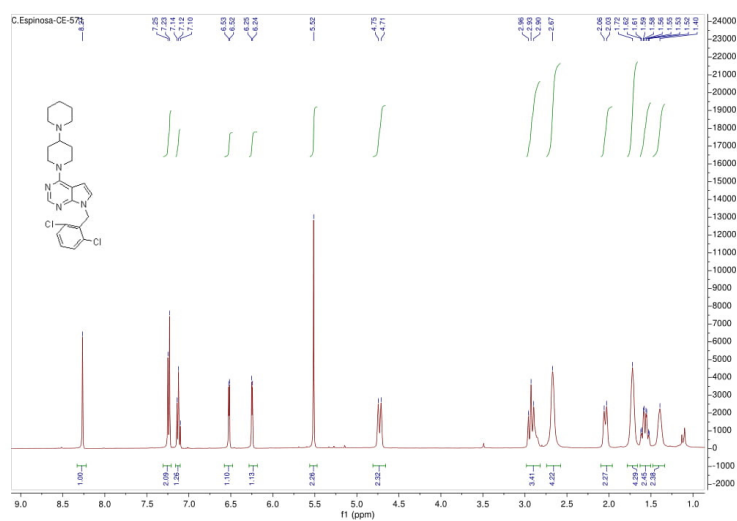


$^{13}\text{C}$  NMR for compound **11b**

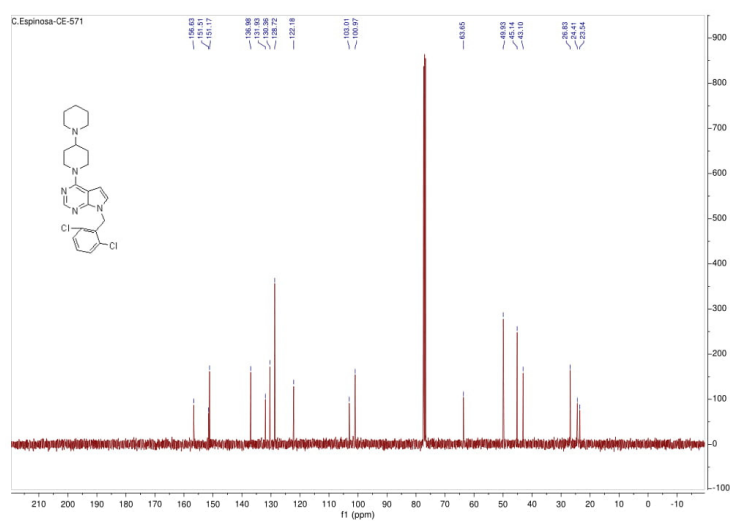


## 5 Nature-inspired pyrrolo[2,3-d]pyrimidines targeting the histamine H3 receptor

$^1\text{H}$  NMR for compound **12b**



$^{13}\text{C}$  NMR for compound **12b**



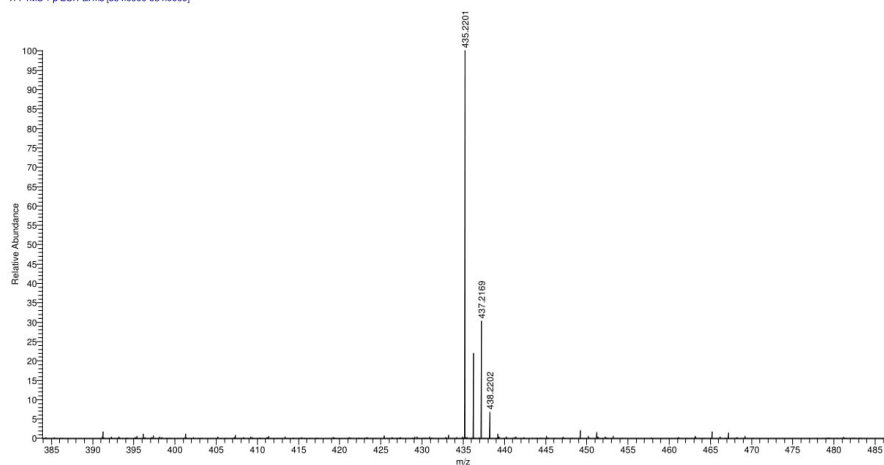
## 5 Nature-inspired pyrrolo[2,3-d]pyrimidines targeting the histamine H3 receptor

### HRMS for compound **3a**

D:\Tunes\2019\Febrero\28.02.19\3A

02/28/19 13:27:00

3A #10 RT: 0.09 AV: 1 NL: 1.74E8  
T: FTMS + p ESI Full ms [334.0000-534.0000]

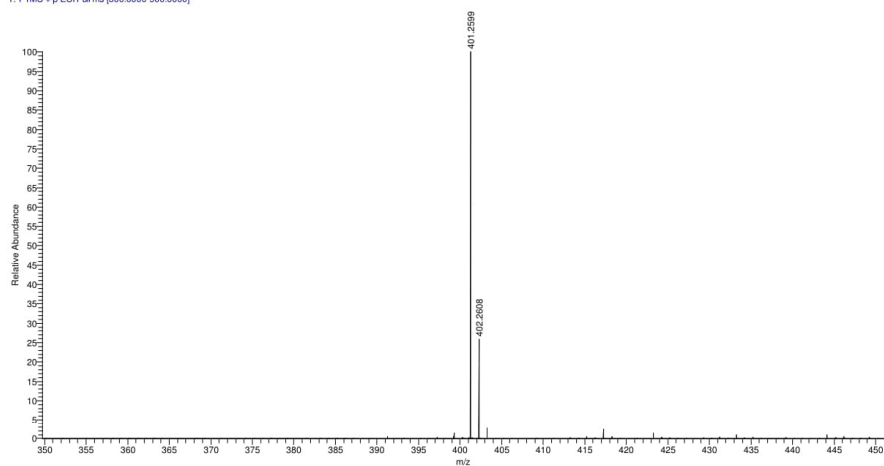


### HRMS for compound **3b**

D:\Tunes\2019\Febrero\28.02.19\3B

02/28/19 13:36:47

3B #15 RT: 0.13 AV: 1 NL: 4.95E8  
T: FTMS + p ESI Full ms [300.0000-500.0000]



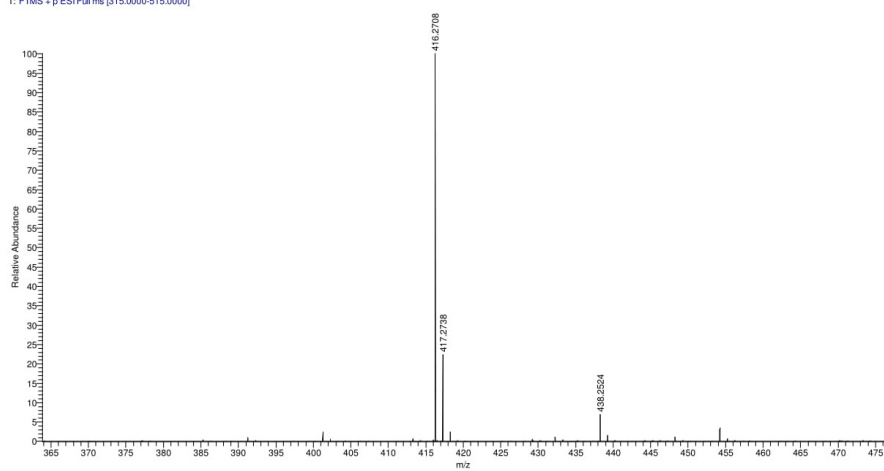
## 5 Nature-inspired pyrrolo[2,3-d]pyrimidines targeting the histamine H3 receptor

### HRMS for compound **3c**

D:\Tunes\2019\Febrero\28.02.19\3C

02/28/19 13:43:54

3C #19 RT: 0.17 AV: 1 NL: 2.19E8  
T: FTMS + p ESI Full ms [315.0000-515.0000]

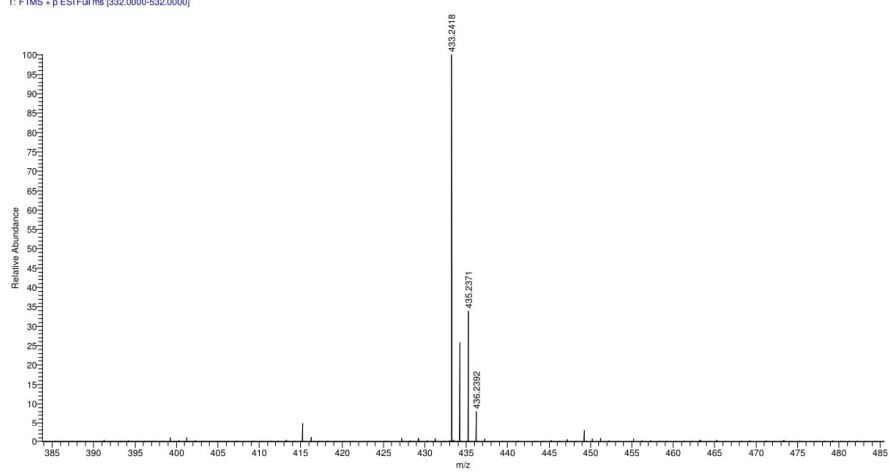


### HRMS for compound **4a**

D:\Tunes\2019\Febrero\28.02.19\4A

02/28/19 13:49:03

4A #14 RT: 0.12 AV: 1 NL: 2.66E8  
T: FTMS + p ESI Full ms [332.0000-532.0000]





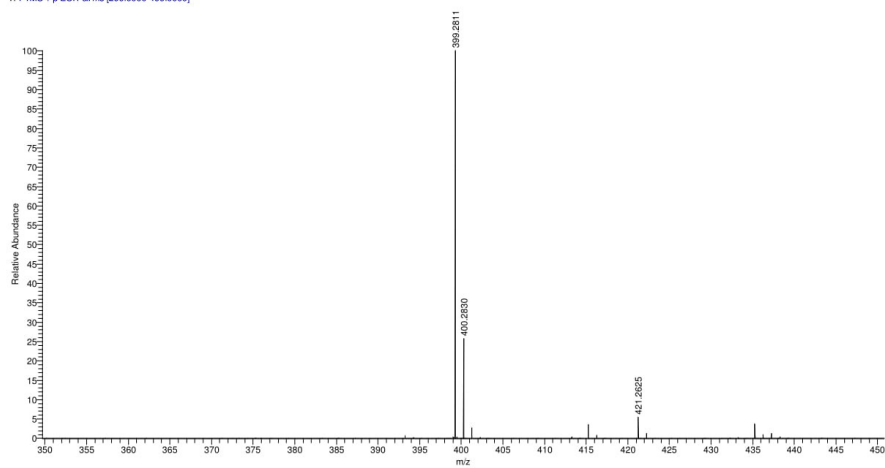
## 5 Nature-inspired pyrrolo[2,3-d]pyrimidines targeting the histamine H3 receptor

### HRMS for compound **4b**

D:\Tunes\2019\Febrero\28.02.19\4B

02/28/19 13:57:42

4B #12 RT: 0.10 AV: 1 NL: 7.05E9  
T: FTMS + p ESI Full ms [299.0000-499.0000]

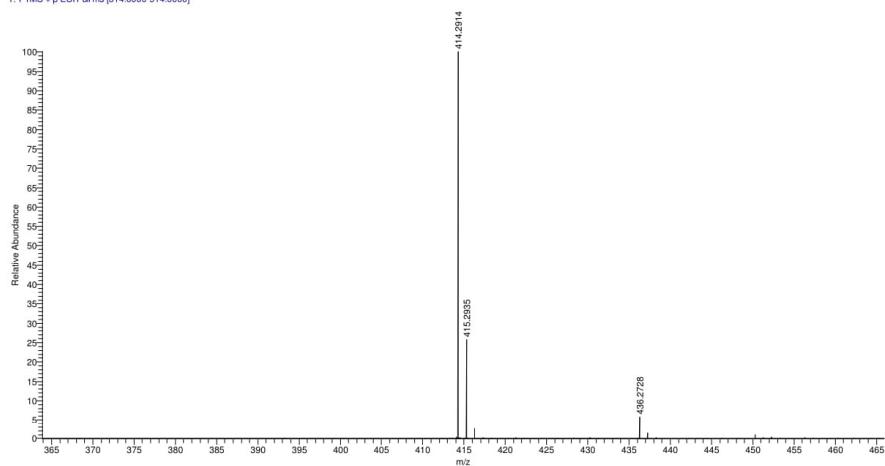


### HRMS for compound **4c**

D:\Tunes\2019\Febrero\28.02.19\4C

02/28/19 14:03:07

4C #14 RT: 0.12 AV: 1 NL: 6.33E9  
T: FTMS + p ESI Full ms [314.0000-514.0000]



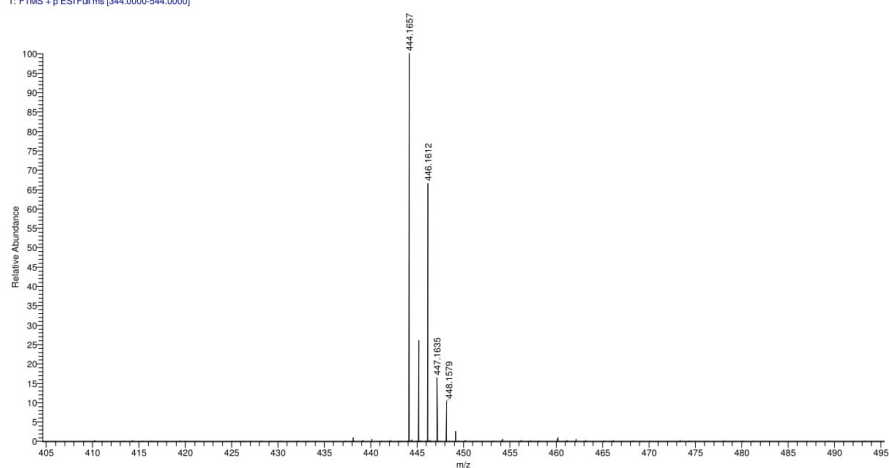
## 5 Nature-inspired pyrrolo[2,3-d]pyrimidines targeting the histamine H3 receptor

### HRMS for compound **9a**

D:\Tunes\2019\Febrero\28.02.19\9A

02/28/19 16:03:38

9A #20 RT: 0.17 AV: 1 NL: 1.70E9  
T: FTMS + p ESI Full ms [344.0000-544.0000]

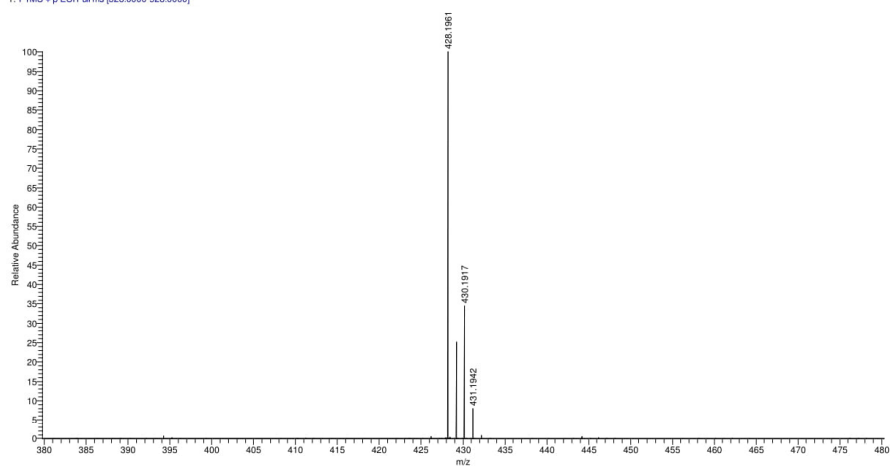


### HRMS for compound **10a**

D:\Tunes\2019\Febrero\28.02.19\10A

02/28/19 16:09:54

10A #24 RT: 0.21 AV: 1 NL: 1.98E9  
T: FTMS + p ESI Full ms [328.0000-528.0000]



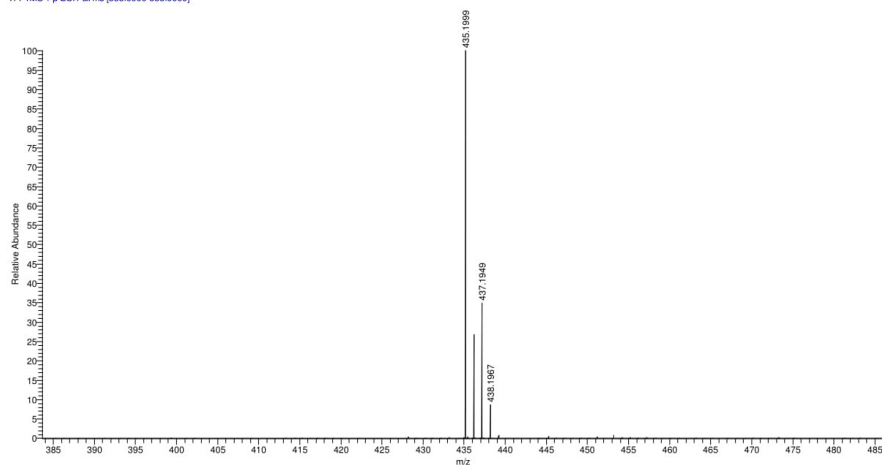
## 5 Nature-inspired pyrrolo[2,3-d]pyrimidines targeting the histamine H3 receptor

### HRMS for compound **11a**

D:\Tunes\2019\Febrero\28.02.19\11A

02/28/19 16:16:40

11A #12 RT: 0.10 AV: 1 NL: 1.45E9  
T: FTMS + p ESI Full ms [335.0000-535.0000]

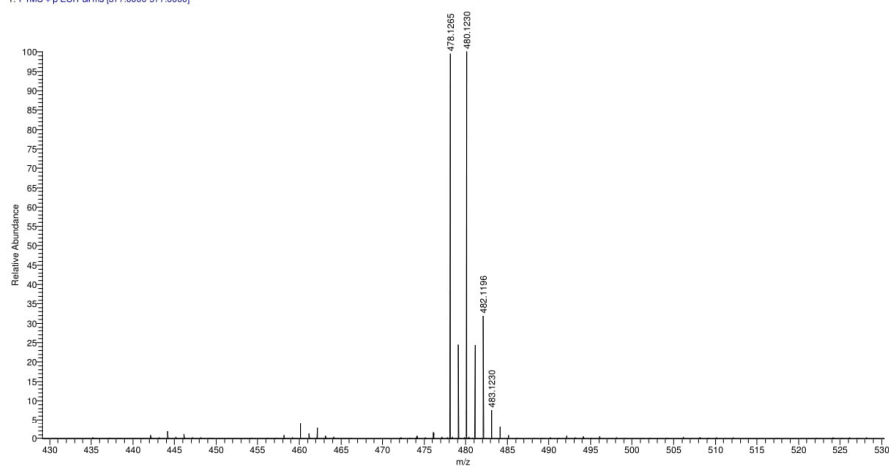


### HRMS for compound **12a**

D:\Tunes\2019\Febrero\28.02.19\12A

02/28/19 16:21:05

12A #24 RT: 0.21 AV: 1 NL: 3.19E9  
T: FTMS + p ESI Full ms [377.0000-577.0000]



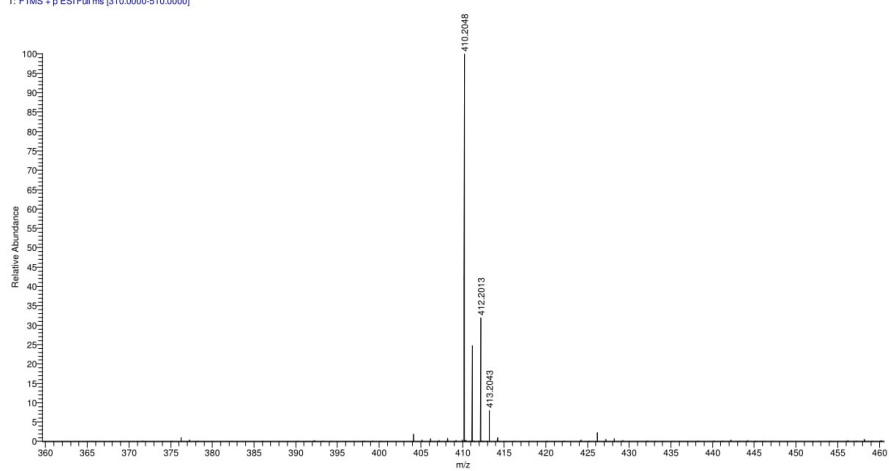
## 5 Nature-inspired pyrrolo[2,3-d]pyrimidines targeting the histamine H3 receptor

### HRMS for compound **9b**

D:\Tunes\2019\Febrero\28.02.19\9B

02/28/19 16:31:31

9B #15 RT: 0.13 AV: 1 NL: 5.53E9  
T: FTMS + p ESI Full ms [310.0000-510.0000]

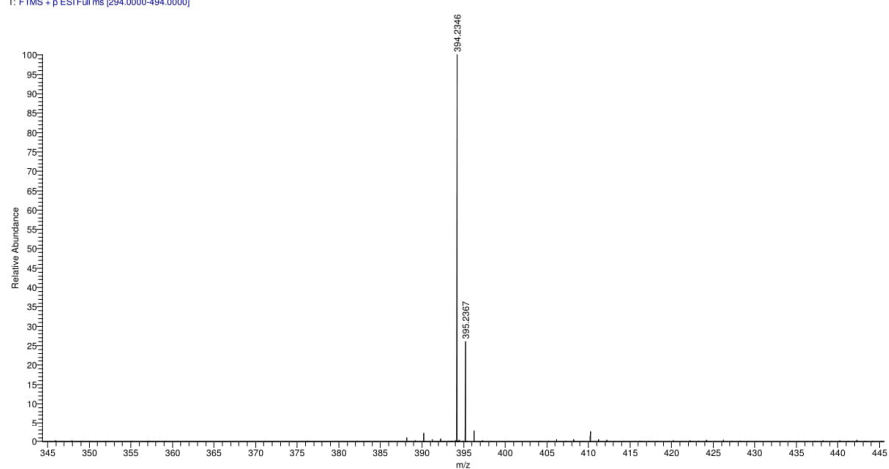


### HRMS for compound **10b**

D:\Tunes\2019\Febrero\28.02.19\10B

02/28/19 16:37:28

10B #20 RT: 0.17 AV: 1 NL: 3.38E9  
T: FTMS + p ESI Full ms [294.0000-494.0000]



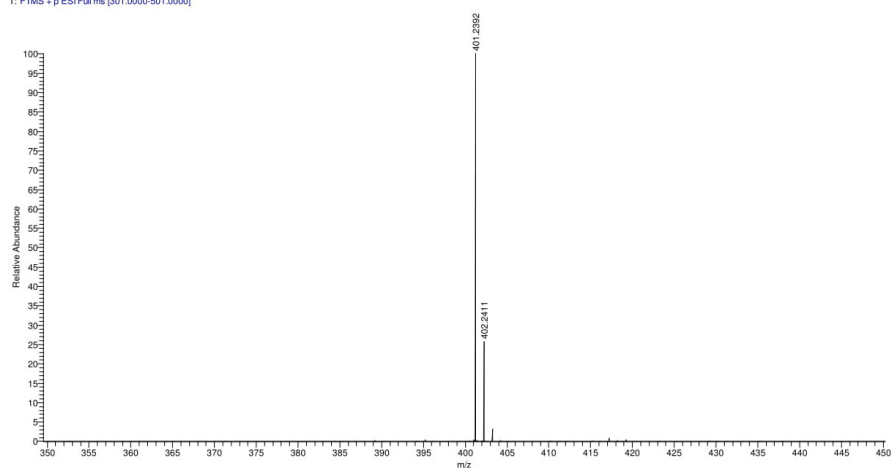
## 5 Nature-inspired pyrrolo[2,3-d]pyrimidines targeting the histamine H3 receptor

### HRMS for compound **11b**

D:\Tunes\2019\Febrero\28.02.19\11B

02/28/19 16:41:02

11B #15 RT: 0.13 AV: 1 NL: 6.71E9  
T: FTMS + p ESI Full ms [301.0000-501.0000]

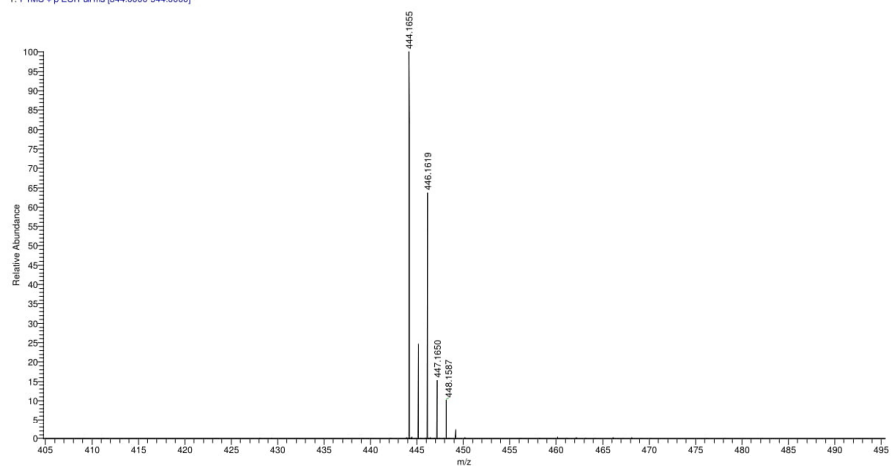


### HRMS for compound **12b**

D:\Tunes\2019\Febrero\28.02.19\12B

02/28/19 16:45:05

12B #16 RT: 0.14 AV: 1 NL: 5.42E9  
T: FTMS + p ESI Full ms [344.0000-544.0000]



## 6 Studies on anticonvulsant effects of novel histamine H<sub>3</sub>R antagonists in electrically and chemically induced seizures in rats

Alachkar A<sup>1</sup>, Łażewska D<sup>2</sup>, Latacz G<sup>2</sup>, Frank A<sup>3</sup>, Siwek A<sup>4</sup>, Lubelska A<sup>2</sup>, Honkisz-Orzechowska E<sup>2</sup>, Handzlik J<sup>2</sup>, Stark H<sup>3</sup>, Kieć-Kononowicz K<sup>2</sup>, Sadek B<sup>1</sup>, **2018**.

<sup>1</sup>Department of Pharmacology & Therapeutics, College of Medicine & Health Sciences, United Arab Emirates University, P.O. Box 17666, Al Ain, UAE.

<sup>2</sup>Department of Technology and Biotechnology of Drugs, Faculty of Pharmacy, Jagiellonian University Medical College, 9 Medyczna Street, 30-688 Kraków, Poland.

<sup>3</sup>Institute of Pharmaceutical and Medicinal Chemistry, Heinrich Heine University Düsseldorf, Universitaetsstr. 1, 40225 Düsseldorf, Germany.

<sup>4</sup>Department of Pharmacobiology, Faculty of Pharmacy, Jagiellonian University Medical College, 9 Medyczna Street, 30-688 Kraków, Poland.

Published in: *International Journal of Molecular Sciences*, **19**: 3386.

DOI: 10.3390/ijms19113386.

Research contribution: Statistical evaluation of *in vitro* compound data at the H<sub>3</sub> and H<sub>4</sub> receptor, interpretation of data and partial preparation of manuscript.

Reprinted by permission from the authors. Alaa Alachkar, Dorota Łażewska, Gniewomir Latacz, Annika Frank, Agata Siwek, Annamaria Lubelska, Ewelina Honkisz-Orzechowska, Jadwiga Handzlik, Holger Stark, Katarzyna Kieć-Kononowicz, Bassem Sadek, *International Journal of Molecular Sciences*, Studies on anticonvulsant effects of novel histamine H<sub>3</sub>R antagonists in electrically and chemically induced seizures in rats, 2018, 19: 3368, DOI: 10.3390/ijms19113386. Copyright © 2018 by the authors.



Article

## Studies on Anticonvulsant Effects of Novel Histamine H3R Antagonists in Electrically and Chemically Induced Seizures in Rats

Alaa Alachkar <sup>1</sup>, Dorota Łażewska <sup>2</sup> , Gniewomir Latacz <sup>2</sup> , Annika Frank <sup>3</sup> , Agata Siwek <sup>4</sup>,  
Annamaria Lubelska <sup>2</sup>, Ewelina Honkisz-Orzechowska <sup>2</sup>, Jadwiga Handzlik <sup>2</sup>, Holger Stark <sup>3</sup> ,  
Katarzyna Kieć-Kononowicz <sup>2,†</sup> and Bassem Sadek <sup>1,\*,†</sup>

<sup>1</sup> Department of Pharmacology & Therapeutics, College of Medicine & Health Sciences, United Arab Emirates University, P.O. Box 17666, Al Ain, UAE; 201590025@uaeu.ac.ae

<sup>2</sup> Department of Technology and Biotechnology of Drugs, Faculty of Pharmacy, Jagiellonian University Medical College, 9 Medyczna Street, 30-688 Kraków, Poland; dlażewska@cm-uj.krakow.pl (D.Ł.); glatacz@cm-uj.krakow.pl (G.L.); annamaria@outlook.com (A.L.); ewelina.honkisz@uj.edu.pl (E.H.-O.); jhandz@interia.pl (J.H.); mfonono@cyf-kr.edu.pl (K.K.-K.)

<sup>3</sup> Institute of Pharmaceutical and Medicinal Chemistry, Heinrich Heine University Düsseldorf, Universitätsstr. 1, 40225 Düsseldorf, Germany; a.frank@hhu.de (A.F.); stark@hhu.de (H.S.)

<sup>4</sup> Department of Pharmacobiology, Faculty of Pharmacy, Jagiellonian University Medical College, 9 Medyczna Street, 30-688 Kraków, Poland; agat.siwiek@uj.edu.pl

\* Correspondence: bassem.sadek@uaeu.ac.ae; Tel.: +971-3-7137-512, Fax: +971-3-7672-033

† These authors have contributed equally to this work.

Received: 9 October 2018; Accepted: 26 October 2018; Published: 29 October 2018



**Abstract:** A newly developed series of non-imidazole histamine H3 receptor (H3R) antagonists (**1–16**) was evaluated *in vivo* for anticonvulsant effects in three different seizure models in Wistar rats. Among the novel H3R antagonists examined, H3R antagonist **4** shortened the duration of tonic hind limb extension (THLE) in a dose-dependent fashion in the maximal electroshock (MES)-induced seizure and offered full protection against pentylenetetrazole (PTZ)-induced generalized tonic-clonic seizure (GTCS), following acute systemic administration (2.5, 5, 10, and 15 mg/kg, *i.p.*). However, only H3R antagonist **13**, without appreciable protective effects in MES- and PTZ-induced seizure, fully protected animals in the strychnine (STR)-induced GTCS following acute systemic pretreatment (10 mg/kg, *i.p.*). Moreover, the protective effect observed with H3R antagonist **4** in MES-induced seizure was completely abolished when animals were co-administered with the H3R agonist (R)- $\alpha$ -methylhistamine (RAMH, 10 mg/kg, *i.p.*). However, RAMH failed to abolish the full protection provided by the H3R antagonist **4** in PTZ-induced seizure and H3R antagonist **13** in STR-induced seizure. Furthermore, *in vitro* antiproliferative effects or possible metabolic interactions could not be observed for compound **4**. Additionally, the predictive *in silico*, as well as *in vitro*, metabolic stability for the most promising H3R antagonist **4** was assessed. The obtained results show prospective effects of non-imidazole H3R antagonists as innovative antiepileptic drugs (AEDs) for potential single use against epilepsy.

**Keywords:** histamine H3 receptors; antagonists; anticonvulsant; maximal electroshock; pentylenetetrazole; strychnine; antiproliferative action; metabolic stability

### 1. Introduction

Epilepsy is considered as a brain disease characterized by repeated seizures due to different complex causes including idiopathic (ion channel or protein defects), symptomatic stroke, head injury

## 6 Studies on anticonvulsant effects of novel histamine H3R antagonists in electrically and chemically induced seizures in rats

Int. J. Mol. Sci. 2018, 19, 3386

2 of 23

(tumors in the brain or central infectious diseases), metabolic disorders (e.g., imbalance of several electrolytes, uremia, and hyperglycemia), or genetic mutation of DNA sequences in genes responsible for encoding various ion channels or neurotransmitter receptors [1,2]. In addition, many patients diagnosed with epilepsy also show cognitive comorbid features, for example, deficiency in intellectual ability; impaired learning and memory; and behavioral neuropsychiatric disorders, such as depression, aggression, or problems in social relationships that intensify the costs for their healthcare [3]. Clinically obtainable antiepileptic drugs (AEDs) still have a large number of non-responders with the clinical drawback that around 30% of epileptic patients do not respond to current therapies [4,5]. More than fifteen new AEDs, including lamotrigine, levetiracetam, retigabine, and perampanel, were approved during the last twenty-five years [6]. However, numerous AEDs cause several unwanted adverse effects, with the most common ones being behavioral and cognitive deficiencies, weight gain, coordination problems, dizziness, and gait disturbance [6]. As long life drug treatment is indispensable, the search for new and more effective AEDs with improved safety profiles is an imperative therapeutic goal [5]. Therefore, there is still a high therapeutic need for new medical entities.

Preclinical and clinical studies indicated that several brain monoamines such as serotonin, dopamine, noradrenaline, histamine, or melatonin play a significant role in seizure activity [7,8]. Previous studies have investigated in the brain histamine's role in seizure pathophysiology [9,10]. Accordingly, histamine itself is considered as an endogenous anticonvulsant [9,11], while histamine H1 receptor (H1R) antagonists were found to prompt or promote seizures [12,13]. Furthermore, preclinical experiments in several rodents revealed that inhibition of *N*-methyltransferase, the histamine metabolizing enzyme in the central nervous system (CNS), using metoprine elevated the levels of brain histamine and, therefore, reduced seizure susceptibility [14–17]. On the other hand,  $\alpha$ -fluoromethylhistidine ( $\alpha$ -FMH, the histamine synthesizing enzyme in the CNS) escalated seizure activity in experimental animals as a result of inhibition of histidine decarboxylase (HDC), which minimized the biosynthesis of brain histamine [18].

Histamine acts by four distinct histamine receptor subtypes (H1R–H4R), which belong to class A of the G-protein coupled receptor family [19]. H1R and H2R are largely found in the CNS and periphery, H3Rs are abundant in the brain, while H4Rs are chiefly expressed in mast cells and leukocytes [20]. Activation of H1R and H2R stimulates slow excitatory postsynaptic potential, while H3Rs is coupled to  $G_i/G_o$ -proteins, which regulate the biosynthesis and release of brain histamine by acting as auto-receptors [19,21,22]. Moreover, H3Rs operating as hetero-receptors can also modulate the release of various other brain neurotransmitters in different brain regions, for example, acetylcholine, glutamate, gamma-aminobutyric acid (GABA), norepinephrine, serotonin, and dopamine [23].

Previous experimental observations from our research [24–30] and that of other research groups [18,31–34] signified the anticonvulsant activity of several histamine H3R antagonists, which could be connected to their antagonistic effects on histamine H3Rs. In different rodent models of seizure, both the imidazole-based H3R antagonist thioperamide [32,35,36] and non-imidazole-based H3R antagonists [26–29] reduced seizures or displayed full protective effects in the maximal electroshock (MES)- and pentylenetetrazole (PTZ)-induced seizure models. Pitolisant (PIT), which is the first H3R antagonist to reach the market (Wakix®; Bioprojet Pharma—as an orphan drug for the treatment of narcolepsy [37]), also presented effectiveness in different animal models of epilepsy [25,33,38], which could not be confirmed so far in clinical trials [34] (Table 1).

Based on the aforementioned preclinical and clinical results, the current study examined the anticonvulsant effects of newly developed *N*-alkyl-substituted (homo)piperidine ether derivatives (1–16) (Table 1). These novel H3R antagonists (1–16) were developed as structural modifications of PIT and comprise different cycloalkylamine functionalities in the basic part of target ligands, different alkyl chain lengths (five or six methylene groups), as well as variable positions of methyl at the basic piperidine ring (3-CH<sub>3</sub> or 4-CH<sub>3</sub>) (Table 1). First, their *in vitro* affinities on human histamine H3Rs (*h*H3Rs) were evaluated. Second, their anticonvulsant effects were examined in the MES-, PTZ-, and strychnine (STR)-induced seizures in male adult rats. The latter



## 6 Studies on anticonvulsant effects of novel histamine H3R antagonists in electrically and chemically induced seizures in rats

Int. J. Mol. Sci. 2018, 19, 3386

3 of 23

in vivo seizure test models were selected based on earlier preclinical observations, in which the anticonvulsant efficacy of numerous imidazole as well as non-imidazole H3R antagonists was established [39–41]. Third, the ability of the CNS penetrant H3R agonist (*R*)- $\alpha$ -methylhistamine (RAMH) to counteract the protection provided by the most promising H3R antagonists was considered. Fourth, the in vitro selectivity profile towards HRs subtypes for compounds with the most promising anticonvulsant effects was evaluated on human HRs expressed in different cell lines. Fifth, the absorption-distribution-metabolism-excretion-Toxicology (ADME-Tox) profile of the H3R antagonist with the most promising anticonvulsant efficacy was further assessed for antiproliferative activity, for metabolic stability, and for the potential of drug-drug interaction.

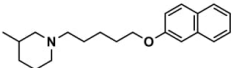
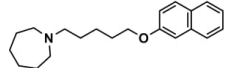
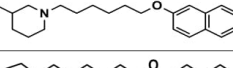
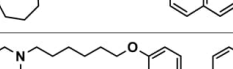
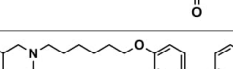
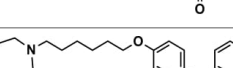
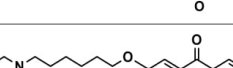
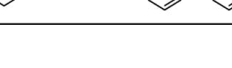
### 2. Material and Methods

#### 2.1. In Vitro Pharmacology

##### 2.1.1. Human Histamine H3 Receptor (hH3R) Binding Affinity for Tested Compounds 1–16

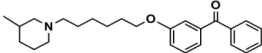
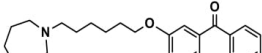
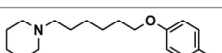
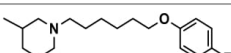
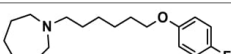


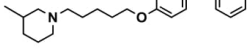
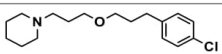
As described previously [28,42,43], the affinity for the human histamine H3R was tested utilizing radioligand displacement assays with [ $^3$ H] $N^{\alpha}$ -methylhistamine at membrane preparations from human embryonic kidney (HEK)-293 cells, stably expressing the receptor. Assays ran in triplicates with seven concentrations of the test compounds 1–16 (Table 1). The analysis of data was conducted by the software GraphPad Prism 7 (San Diego, CA, USA), using the “one-site competition” equation.  $K_i$  values were calculated from the 50 percent of inhibitory concentration (IC<sub>50</sub>) values according to the Cheng-Prusoff equation [44] (Table 1).

**Table 1.** In vitro human histamine H3 receptor (hH3R) affinities of ligands 1–16.

Ligand	Structure	In Vitro Affinity $K_i$ (hH <sub>3</sub> R) <sup>a</sup> in nM [CI]
1		42.3 <sup>b</sup> [18.3; 97.4]
2		57.3 <sup>b</sup> [47.2; 69.7]
3		55.9 <sup>b</sup> [44.8; 69.7]
4		69.3 <sup>b</sup> [59.2; 81.1]
5		41.1 [25.6; 66.2]
6		52.8 [31.4; 88.8]
7		40.5 [32.9; 50.0]
8		76.1 [53.5; 108.3]

## 6 Studies on anticonvulsant effects of novel histamine H<sub>3</sub>R antagonists in electrically and chemically induced seizures in rats

Table 1. Cont.

Ligand	Structure	In Vitro Affinity $K_i$ (hH <sub>3</sub> R) <sup>a</sup> in nM [CI]
9		110.2 [61.8; 196.4]
10		69.5 [44.4; 108.8]
11		115.2 [78.4; 169.5]
12		83.6 [65.8; 106.4]
13		137.2 [60.0; 313.9]
14		36.2 [10.0; 130.3]
15		40.2 [13.5; 119.4]
16		38.5 [10.5; 141.6]
Pitolisant (PIT)		11.69 <sup>c</sup>

<sup>a</sup> [<sup>3</sup>H]N<sup>α</sup>-Methylhistamine binding assay performed with cell membrane preparations of human embryonic kidney (HEK) cells stably expressing the human histamine H<sub>3</sub>R. CI—confidence interval; <sup>b</sup> data from Łazewska et al., 2018; <sup>c</sup> data from the literature [45].

### 2.1.2. Human Histamine H<sub>1</sub> Receptor (hH<sub>1</sub>R) Binding Affinity for Selected Compounds 4, 7 and 13

Radioligand binding was performed as previously described using membranes from CHO-K1 cells stably transfected with the human H<sub>1</sub> receptor (PerkinElmer, Waltham, MA, USA) [30,42]. Data were fitted to a one-site curve-fitting equation with Prism 6 (GraphPad Software, city, state, country) and  $K_i$  values were estimated from the Cheng–Prusoff equation [44].

### 2.1.3. Human Histamine H<sub>4</sub> Receptor (hH<sub>4</sub>R) Binding Affinity for Selected Compounds 4, 7 and 13

H<sub>4</sub>R radioligand displacement assays were performed with Sf9 cell membrane preparations, expressing the hH<sub>4</sub>R, as described previously [28,42,43]. Assays ran in triplicates with four appropriate concentrations of the test compound. Data were analyzed by GraphPad Prism 7, using the “one-site competition” equation.

## 2.2. In Vivo Pharmacology

### 2.2.1. Animals

Inbred male Wistar rats aged between six and eight weeks (body weight: 180–220 g, Central Animal Facility of the United Arab Emirates (UAE) University, Al Ain/ Abu Dhabi, United Arab

## 6 Studies on anticonvulsant effects of novel histamine H3R antagonists in electrically and chemically induced seizures in rats

Int. J. Mol. Sci. 2018, 19, 3386

5 of 23

Emirates) were used. Animals were kept in an air-conditioned animal facility room with controlled temperature ( $24 \pm 1$  °C) and humidity ( $55 \pm 15\%$ ) under a 12-h light/dark cycle. The animals were allowed free access to food and water. The experiments of the current study were carried out between 09:00 and 12:00, and all procedures were performed according to the guidelines of the European Communities Council Directive of 24 November 1986 (86/609/European Economic Community (EEC)) and were previously approved for epilepsy study by the College of Medicine and Health Sciences/United Arab Emirates University (Institutional Animal Ethics Committee, approval number; ERA\_2017\_5676).

### 2.2.2. Drugs

H3R agonist (*R*)- $\alpha$ -methylhistamine (RAMH, 10 mg/kg, i.p.), pentylentetrazole (PTZ, 60 mg/kg, i.p.), strychnine (STR, 3.5 mg/kg, i.p.), phenytoin (PHT), and valproic acid (VPA, 300 mg/kg, i.p.) were purchased from Sigma-Aldrich (St Louis, MI, USA). H3R antagonists: (1) 3-methyl-1-(5-(naphthalen-2-yloxy)pentyl)piperidine hydrogen oxalate [45]; (2) 1-(5-(naphthalen-2-yloxy)pentyl)azepane hydrogen oxalate [45]; (3) 3-methyl-1-(6-(naphthalen-2-yloxy)hexyl)piperidine hydrogen oxalate [45]; (4) 1-(6-(naphthalen-2-yloxy)hexyl)azepane hydrogen oxalate [45]. All other compounds are unpublished to best of our knowledge: (5) phenyl(4-(6-(piperidin-1-yl)hexyloxy)phenyl)methanone hydrogen oxalate; (6) 4-(6-(3-methylpiperidin-1-yl)hexyloxy)phenyl(phenyl)methanone hydrogen oxalate; (7) 4-(6-(azepan-1-yl)hexyloxy)phenyl(phenyl)methanone hydrogen oxalate; (8) phenyl(3-(6-(piperidin-1-yl)hexyloxy)phenyl)methanone hydrogen oxalate (unpublished); (9) 3-(6-(3-methylpiperidin-1-yl)hexyloxy)phenyl(phenyl)methanone hydrogen oxalate; (10) 3-(6-(azepan-1-yl)hexyloxy)phenyl(phenyl)methanone hydrogen oxalate; (11) 1-(6-(4-fluorophenoxy)hexyl)piperidine hydrogen oxalate; (12) 1-(6-(4-fluorophenoxy)hexyl)-3-methylpiperidine hydrogen oxalate; (13) 1-(6-(4-fluorophenoxy)hexyl)azepane hydrogen oxalate; (14) phenyl(4-(5-(piperidin-1-yl)pentyloxy)phenyl)methanone hydrogen oxalate; (15) 4-(5-(3-methylpiperidin-1-yl)pentyloxy)phenyl(phenyl)methanone hydrogen oxalate; and (16) 4-(5-(azepan-1-yl)pentyloxy)phenyl(phenyl)methanone hydrogen oxalate. These synthesized by us in the Department of Technology and Biotechnology of Drugs (Kraków, Poland) (Table 1) according to methods described previously [24,45]. For the *in vivo* anticonvulsant screening, test compounds 1–16, PHT, VPA, and RAMH were suspended in 1% aqueous solution of Tween 80 and administered intraperitoneally (i.p.) at a volume of 1 mL/kg 30–45 min before the test. Control animals (negative control) were given an appropriate amount of vehicle (1% aqueous solution of Tween 80; i.p.) 30–45 min before the test. Doses of all test compounds were expressed in terms of the free base. For each test compound, a group of six to seven animals was used for the anticonvulsant study (Table 1).

### 2.2.3. Maximal Electroshock (MES)-Induced Seizure

As previously described [30,46], the seizures were induced in rats with a 50 Hz alternating current of 120 mA intensity. The current was applied through ear electrodes for 1 s. Protection against the spread of MES-induced seizure was defined as the abolition of the tonic hind limb extension (THLE) component of the seizure [25,29,47]. For the first screening of protective effects of test compounds 1–16 in the MES-induced seizure model, the animals were divided into eighteen groups of seven rats ( $n = 7$ ) as follows; group (1) control group injected with vehicle (SAL), group (2) positive control group in which rats were injected with PHT at a dose of 10 mg/kg (this being the minimal dose of PHT that protected animals against the spread of MES-induced seizures without mortality), and groups (3)–(18) animals in the experimental groups were administered H3R antagonists 1–16 at a dose of 10 mg/kg. In another MES experiment in three separate groups of six rats ( $n = 6$ ), H3R antagonist 4 with the most promising protection in MES model was administered at doses of 2.5, 5, or 15 mg/kg, i.p. 30–45 min before the MES challenge. In an additional abrogative experiment, the most effective dose of H3R antagonist 4 was designated for further analysis in which a separate group of six rats

## 6 Studies on anticonvulsant effects of novel histamine H3R antagonists in electrically and chemically induced seizures in rats

Int. J. Mol. Sci. 2018, 19, 3386

6 of 23

( $n = 6$ ) was co-injected with the selected dose of H3R antagonist **4** (30–45 min prior to MES test) with RAMH (10 mg/kg, i.p., 15–20 min before MES challenge) (Figure 1, Table 2).

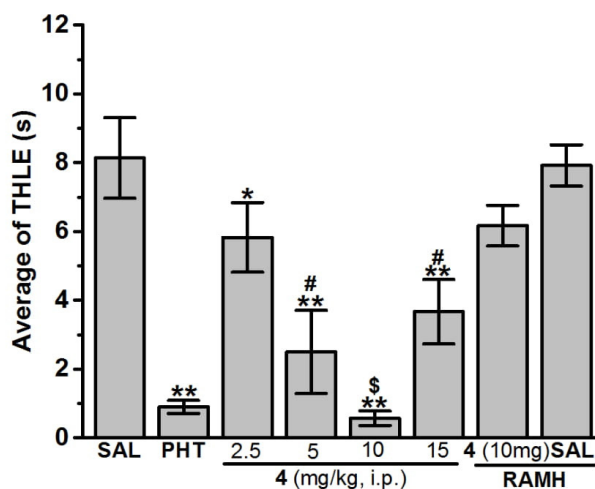


**Figure 1.** Dose-dependent protective effect of histamine H3 receptor (H3R) antagonist **4** and effect of (*R*)- $\alpha$ -methylhistamine (RAMH) pretreatment on the H3R antagonist **4** provided protection against maximal electroshock (MES)-induced convulsions. The figure shows the protection provided by standard antiepileptic drug (AED) phenytoin (PHT, 10 mg/kg, i.p.) and test compound **4** (2.5, 5, 10, and 15 mg/kg, i.p.) on the duration of tonic hind limb extension (THLE) induced in the MES model in rats. Each value represents mean  $\pm$  standard error of mean (SEM) ( $n = 6$ –7). \*  $p < 0.05$  vs. sal (saline)-treated group. \*\*  $p < 0.001$  vs. (saline)-treated group. #  $p < 0.05$  vs. (2.5 mg)-treated group. \$  $p < 0.05$  vs. (5 mg or 15 mg)-treated groups.

**Table 2.** Screening of in vivo anticonvulsant effects for H3R antagonists 1–16.

Ligand	Structure	MES <sup>a</sup> -Induced Seizure	PTZ <sup>b</sup> -Induced Seizure	STR <sup>c</sup> -Induced Seizure
1		–	–	–
2		–	–	–
3		++	–	–
4		++	++	–
5		++	–	–
6		+	–	–

## 6 Studies on anticonvulsant effects of novel histamine H3R antagonists in electrically and chemically induced seizures in rats

Table 2. Cont.

Ligand	Structure	MES <sup>a</sup> -Induced Seizure	PTZ <sup>b</sup> -Induced Seizure	STR <sup>c</sup> -Induced Seizure
7		+	++	–
8		+	–	–
9		–	–	–
10		–	–	–
11		–	++	–
12		–	+	–
13		–	+	+
14		+	+	–
15		–	+	–
16		–	–	–

<sup>a</sup> 50-Hz alternating current of 120 mA intensity applied through ear electrodes for a duration of 1 s, <sup>b</sup> 60 mg/kg, <sup>c</sup> 3.5 mg/kg. –, no protection (not significant from saline-treated group); +, moderate protective effect (tonic hind limb extension (THLE) duration in the range of 2–5 s, seizure score in the range of 2–4); ++, high protective effect (THLE duration <1, seizure score 0). MES—maximal electroshock; PTZ—pentylenetetrazole; STR—strychnine.

### 2.2.4. Chemically-Induced Seizures

In this study and according to previously used protocols, two chemical agents have been used to induce seizures, namely pentylenetetrazole (PTZ, 60 mg/kg, i.p.) and strychnine (STR, 3.5 mg/kg, i.p.) [27,47]. PTZ 60 mg/kg or STR 3.5 mg/kg were administered i.p. to all groups of seven rats ( $n = 7$ ), that is, animals pretreated with vehicle or test compounds 1–16. Vehicle, VPA (300 mg/kg, i.p.), [26,47–49] or test compounds 1–16 (10 mg/kg, i.p.) were systemically administered 30–45 min before PTZ (60 mg/kg, i.p.) or STR (3.5 mg/kg, i.p.) injection, and animals were directly observed for any signs of convulsion for a duration of 30 min. The observed scores as well as percent protection against generalized tonic-clonic seizure (GTCS) were graded and scaled according to the Racine scale (stage 0, no change in behavior; stage 1, stereotype mouthing, eye blinking, and/or mild facial clonus; stage 2, head nodding and/or severe facial clonus; stage 3, myoclonic jerk in forelimbs; stage 4, clonic convulsions in the forelimbs with rearing; stage 5, generalized clonic convulsions associated with loss of balance [50]) to evaluate the protection provided by the respective test compound against seizures. The animals were divided into eighteen groups of seven rats ( $n = 7$ ) and treated as follows.

(1) Control group injected with vehicle + PTZ (SAL group), (2) positive control group in which rats were injected with VPA (300 mg/kg) + PTZ (VPA group), and animals in the test groups (3)–(18)



## 6 Studies on anticonvulsant effects of novel histamine H3R antagonists in electrically and chemically induced seizures in rats

Int. J. Mol. Sci. 2018, 19, 3386

8 of 23

were systemically administered with test compounds **1–16** (10 mg/kg), respectively. An additional PTZ experiment was conducted using three different groups of seven rats ( $n = 7$ ), the H3R ligand with the most promising protection in PTZ model was administered at doses of 2.5, 5, or 15 mg/kg, i.p. 30–45 min before the PTZ challenge. In an additional abrogative PTZ experiment, the most effective dose of H3R antagonist **4** was selected for further analysis, namely in a separate group of seven rats ( $n = 7$ ), the selected dose of **4** was co-injected (30–45 min prior to PTZ test) together with RAMH (10 mg/kg, i.p., 15–20 min before PTZ challenge) (Figure 2, Table 2). The same experimental procedure was followed in the STR-induced seizure model applying the reference drug VPA, which was used at a dose of 300 mg/kg, i.p. (Figure 3, Table 2).

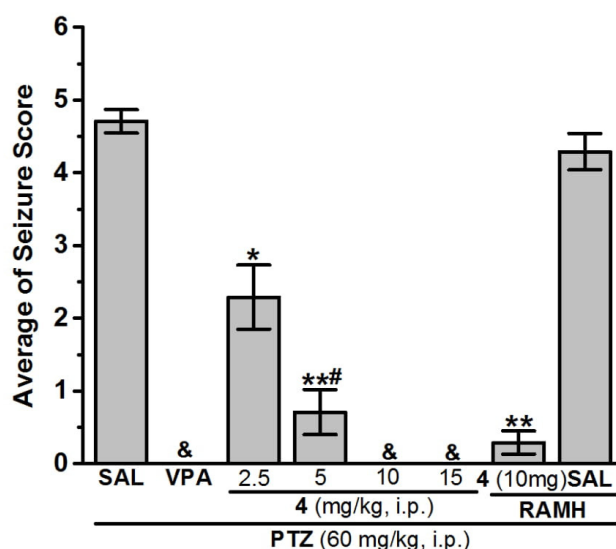


**Figure 2.** Anticonvulsant effect of H3R antagonist **4** pretreatment on pentylenetetrazole (PTZ)-induced convulsion in rats. Valproic acid (VPA, 300 mg/kg, i.p.) and test compound **4** (2.5, 5, 10, and 15 mg/kg, i.p.) were injected 30–45 min before PTZ (60 mg/kg, i.p.) treatments. Values are represented as the mean  $\pm$  SEM ( $n = 7$ ). \*  $p < 0.05$  vs. (saline)-treated group. \*\*  $p < 0.001$  vs. (saline)-treated group. #  $p < 0.05$  vs. (2.5 mg)-treated group. & Full protection.

### 2.2.5. Statistical Analysis

For statistical comparisons, the software package SPSS 25.0 (IBM Middle East, Dubai, UAE) was used. All data are expressed as the means  $\pm$  standard error of mean (SEM).  $K_i$  values at the H3R are given as means with the 95% confidence interval. Following normal distribution assessment, the anticonvulsant effects observed for H3R antagonists **1–16** in MES-, PTZ-, and STR-induced convulsion models were analyzed using one-way analysis of variance, followed by the *Bonferroni* post hoc test for multiple comparisons. The criterion for statistical significance was set at  $p < 0.05$ .

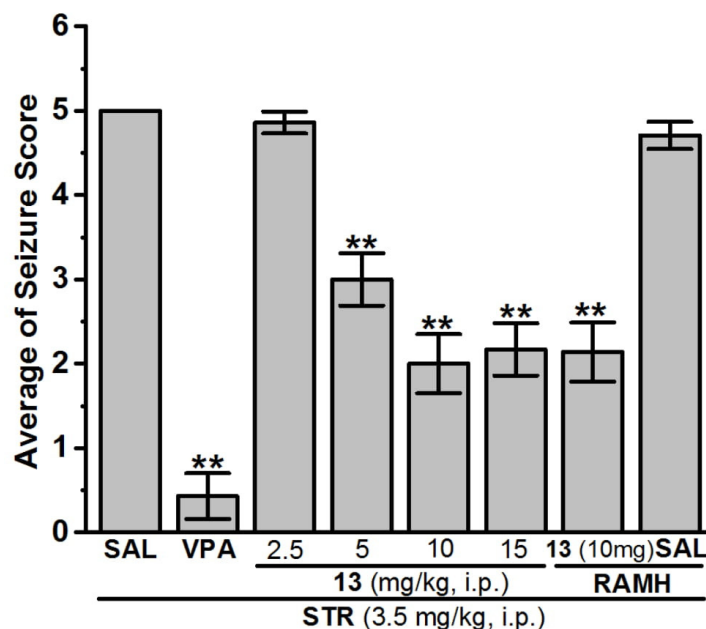


**Figure 3.** Anticonvulsant effect of H3R antagonist **13** pretreatment on strychnine (STR)-induced seizure in rats. Valproic acid (VPA, 300 mg/kg, i.p.) and test compound **13** (2.5, 5, 10, and 15 mg/kg, i.p.) were injected 30–45 min before STR (3.5 mg/kg, i.p.) treatments. Values are represented as the mean  $\pm$  SEM ( $n = 7$ ). \*\*  $p < 0.001$  vs. (saline)-treated group.

### 2.3. ADME-Tox Properties

#### 2.3.1. Antiproliferative Activity

Human embryonic kidney (HEK)-293 cell line (ATCC CRL-1573) was kindly donated by Prof. Dr. Christa Müller (Pharmaceutical Institute, Pharmaceutical Chemistry I, University of Bonn). Hepatoma HepG2 (ATCC HB-8065) cell line was kindly donated by the Department of Pharmacological Screening, Jagiellonian University Medical College. The cell cultures' growth conditions in presence of H3R antagonist **4** were applied as described before [46,51]. The cells' viability was assessed after 72 h of incubation with H3R antagonist and the following references: doxorubicin (Sigma-Aldrich) and carbonyl cyanide 3-chlorophenylhydrazone (CCCP) (Sigma-Aldrich). CellTiter 96<sup>®</sup> AQueous non-radioactive cell proliferation assay (MTS) was purchased from Promega<sup>®</sup> and added to each well in the volume of 20  $\mu$ L. The cells were then incubated for 2–5 h. The microplate reader EnSpire (PerkinElmer Ltd., Waltham, MA, USA) was used to measure the absorbance at 490 nm.

#### 2.3.2. Prediction of In Silico Metabolism

The in silico prediction for sites of metabolism of H3R antagonist **4** was performed by MetaSite 5.1.1 provided by Molecular Discovery Ltd. (Borehamwood, Hertfordshire, UK). The most probable sites of metabolism were predicted during this study by the liver computational model [52] (Figure 5).

#### 2.3.3. Metabolic Stability

Rat liver microsomes (RLMs) purchased from Sigma-Aldrich (St. Louis, MO, USA) were used for in vitro determination of compound **4**'s metabolic stability. The NADPH regeneration system

## 6 Studies on anticonvulsant effects of novel histamine H3R antagonists in electrically and chemically induced seizures in rats

*Int. J. Mol. Sci.* **2018**, *19*, 3386

10 of 23

was purchased from Promega (Madison, WI, USA). All experiments were performed as described before [26,45,46]. The reaction mixture was preincubated at 37 °C for 5 min, and then the reaction was started by adding 50 µL of NADPH regeneration system. The reaction was ended after 120 min by the addition of cold methanol (200 µL). The mixture was then centrifuged at 14,000 rpm for 15 min and the ultra-performance liquid chromatography–mass spectrometry (UPLC/MS) analysis of the supernatant was conducted. Ion fragment analyses were also performed for metabolic pathways' determination.

### 2.3.4. Metabolic Interactions

The metabolic interactions of H3R antagonist **4** were determined by the luminescent P450-Glo™ 3A4 and 2D6 assays purchased from Promega®. All enzymatic reactions were performed according to the manufacturer protocols and as previously described [26]. The references ketoconazole (KE, CYP3A4 inhibitor) and quinidine (QD, CYP2D6 inhibitor) were obtained from Sigma-Aldrich. The luminescence was measured with a microplate reader EnSpire (PerkinElmer). The final concentration of H3R antagonist **4** was in the range of 0.1–25 µM, whereas reference inhibitory effects ranged from 0.01 µM to 10 µM. The IC<sub>50</sub> values' calculations were performed by GraphPad Prism™ software (version 5.01, San Diego, CA, USA).

## 3. Results

### 3.1. Pharmacology

#### 3.1.1. In Vitro Affinities at hH1Rs, hH3Rs, and hH4Rs

The novel ligands **1–16** were tested for their H3R affinity by [<sup>3</sup>H]N<sup>α</sup>-methylhistamine displacement assays on membrane preparations of HEK-293 cells, stably expressing the hH3R (Table 1). Following assessment of in vivo anticonvulsant effects in MES-, PTZ-, and STR-induced seizure models for H3R antagonists **1–16**, only selected H3R antagonists (**4**, **7**, and **13**), with the most promising in vivo anticonvulsant effects, were further evaluated for their affinity at human histamine H1 (hH1R) and H4 (hH4R) receptors. The results show that test compounds **1–16** had an H3R affinity of 40–140 nM compared with the standard H3R antagonist PIT with an H3R affinity of 12 nM (Table 1). Selected test compounds with the most promising in vivo anticonvulsant effects, namely **4** (1273.0 nM for H1R, 69.3 nM for H3R, >10,000 nM for H4R), **7** (915 nM for H1R, 40.5 nM for H3R, >10,000 nM for H4R), and **13** (1338.0 nM for H1R, 137.2 nM for H3R, >10,000 nM for H4R), showed a selectivity profile toward H3Rs with at least 10-fold lower affinity at hH1- and H4Rs.

#### 3.1.2. In Vivo Seizure Models

With regard to the MES test, the current one used in the study produced seizures in 100% of animals without mortality. Likewise, the dose of PTZ and STR used in the present study formed seizures (score 4–5) in 100% of animals without mortality.

#### Anticonvulsant Screening of H3R Antagonists **1–16** in MES-Induced Seizure

The preliminary screening for anticonvulsant activities of acute systemic pretreatment with H3R ligands **1–16** on MES-induced seizures in rats was carried out and the observed results were compared with the protective effect of the reference antiepileptic drug PHT in MES-induced seizure in rats (Tables 2 and 3). The obtained results showed that acute systemic administration of PHT (10 mg/kg, i.p.) and H3R ligands **1–16** (10 mg/kg, i.p.) demonstrated a significant protection against MES-induced seizures as confirmed by one-way analysis of variance [ $F_{(17,108)} = 8.352$ ;  $p < 0.001$ ]. Among the H3R antagonists tested and following post hoc analyses, compound **4** at a dose of 10 mg/kg significantly exhibited the most promising protective effect in MES-induced seizure when compared with the saline-treated group with [ $F_{(1,12)} = 34.608$ ;  $p < 0.001$ ], and provided comparable protection to that of PHT with [ $F_{(1,12)} = 1.135$ ;  $p < 0.308$ ] (Tables 2 and 3, Figure 1). Moreover, the protection observed



## 6 Studies on anticonvulsant effects of novel histamine H3R antagonists in electrically and chemically induced seizures in rats

with H3R antagonist **4** at a dose of 10 mg/kg, i.p. was significantly higher than that found for H3R antagonists **3**, **5**, **6**, **7**, **8**, and **14** with [ $F_{(1,12)} = 5.882$ ;  $p < 0.05$ ], [ $F_{(1,12)} = 9.722$ ;  $p < 0.05$ ], [ $F_{(1,12)} = 8.20$ ;  $p < 0.05$ ], [ $F_{(1,12)} = 6.030$ ;  $p < 0.05$ ], [ $F_{(1,12)} = 11.377$ ;  $p < 0.05$ ], and [ $F_{(1,12)} = 7.108$ ;  $p < 0.05$ ], respectively (Table S1, Supplementary Material). On the other hand, the results show that animals pretreated with 2.5, 5, and 15 mg/kg of H3R antagonist **4** were protected to a significantly lesser extent against seizures when compared with the H3R antagonist **4** (10 mg)-treated group with [ $F_{(1,11)} = 6.087$ ;  $p < 0.05$ ] [ $F_{(1,11)} = 21.843$ ;  $p < 0.001$ ], and [ $F_{(1,11)} = 8.609$ ;  $p < 0.05$ ], respectively (Figure 1). Moreover, the abrogation of H3R antagonist **4**-provided protection was assessed by systemic co-administration with CNS penetrant histamine H3R agonist RAMH (10 mg/kg, i.p.). The results showed that co-injection with CNS penetrant histamine H3R agonist RAMH (10 mg/kg, i.p.) abrogated the H3R antagonist **4** (10 mg)-provided protection with [ $F_{(1,10)} = 0.711$ ;  $p = 0.419$ ] for the comparison of saline–saline vs. **4** + RAMH (Figure 2). Notably, RAMH when administered alone did not affect MES-induced seizures with [ $F_{(1,10)} = 0.359$ ;  $p = 0.563$ ] for saline–saline vs. saline–RAMH (Figure 1).

### Anticonvulsant Screening for H3R Antagonists 1–16 in PTZ-Induced Seizures

The protective effects of H3R antagonists **1–16** (10 mg/kg, i.p.) were assessed and compared with the protection obtained for the reference antiepileptic drug VPA in PTZ-induced seizures in rats (Tables 2 and 3). The results show that acute systemic pretreatment with VPA (300 mg/kg, i.p.) and H3R antagonists **1–16** delivered a significant protective action against PTZ-induced seizures as confirmed by applying one-way analysis of variance [ $F_{(17,108)} = 23.925$ ;  $p < 0.001$ ] (Tables 2 and 3). Pairwise comparison of the provided protective effects observed over 30 min revealed that H3R antagonists **4**, **7**, and **11** delivered full protective activities when compared with the saline-treated group (all  $p < 0.001$ ) (Tables 2 and 3). Similarly, VPA (300 mg/kg, i.p.) provided full protection when compared with saline-treated group with [ $F_{(1,12)} = 653.40$ ;  $p < 0.001$ ] (Tables 2 and 3). Moreover, analysis of variance revealed that full protection was provided after acute systemic administration with 10 or 15 mg/kg of H3R antagonist **4** (all  $p < 0.001$ ) (Figure 2, Tables 2 and 3). However, pretreatment with 2.5 or 5 mg/kg of H3R antagonist **4** provided significantly lower protection when compared with that provided with 10 or 15 mg/kg of the same compound (all  $p < 0.05$ ) (Figure 2, Tables 2 and 3). Furthermore, Figure 2 shows the reversal of H3R antagonist **4**-provided protection when co-injected with 10 mg/kg of histamine H3R agonist RAMH. The observed results showed that RAMH failed to reverse the H3R antagonist **4**-provided protection in PTZ-induced seizure model with [ $F_{(1,12)} = 2.40$ ;  $p = 0.147$ ] for **6**-treated group versus **4** + RAMH-treated group (Figure 2). Importantly, RAMH alone did not affect seizure score when compared with effects of the saline-treated group with  $p = 0.232$  (Figure 2, Tables 2 and 3).

## 6 Studies on anticonvulsant effects of novel histamine H3R antagonists in electrically and chemically induced seizures in rats

Int. J. Mol. Sci. 2018, 19, 3386

12 of 23

**Table 3.** Effects of H3R antagonists **4** and **13** on THLE duration, average score, and percentage of provided protection against generalized tonic-clonic seizure (GTCS) in MES-, PTZ-, and STR-induced convulsion models.

Group	MES <sup>a</sup> -Induced Seizure	Group	PTZ <sup>b</sup> -Induced Seizure		Group	STR <sup>c</sup> -Induced Seizure	
	Average THLE (s)		Average Seizure Score	% Protection against GTCS		Average Seizure Score	% Protection against GTCS
SAL	8.14 ± 1.17	SAL	4.71 ± 0.16	28.57	SAL	5	0
PHT (10 mg)	0.90 ± 0.19 **	VPA (300 mg)	0.00 ± 0.00	100	VPA (300 mg)	0	100
<b>4</b> (2.5 mg)	5.83 ± 1.01 *	<b>4</b> (2.5 mg)	2.29 ± 0.44 *	100	<b>4</b> (2.5 mg)	—	—
<b>4</b> (5 mg)	2.50 ± 1.21 **, <sup>#</sup>	<b>4</b> (5 mg)	0.71 ± 0.31 **, <sup>#</sup>	100	<b>4</b> (5 mg)	—	—
<b>4</b> (10 mg)	0.57 ± 0.21 **, <sup>5</sup>	<b>4</b> (10 mg)	0.00 ± 0.00 <sup>6</sup>	100	<b>4</b> (10 mg)	4.57 ± 0.19	28.57
<b>4</b> (15 mg)	3.67 ± 0.94 **, <sup>#</sup>	<b>4</b> (15 mg)	0.00 ± 0.00 <sup>6</sup>	100	<b>4</b> (15 mg)	—	—
<b>4</b> (10 mg) + RAMH	6.17 ± 0.59	<b>4</b> (10 mg) + RAMH	0.29 ± 0.16 **	100	<b>4</b> (10 mg) + RAMH	—	—
SAL + RAMH	7.92 ± 0.60	SAL + RAMH	4.29 ± 0.25	14.29	SAL + RAMH	—	—
<b>13</b> (2.5 mg)	—	<b>13</b> (2.5 mg)	—	—	<b>13</b> (2.5 mg)	4.86 ± 0.13	14.29
<b>13</b> (5 mg)	—	<b>13</b> (5 mg)	—	—	<b>13</b> (5 mg)	3.00 ± 0.31 **	85.71
<b>13</b> (10 mg)	6.43 ± 1.14	<b>13</b> (10 mg)	2.14 ± 0.47 *	85.71	<b>13</b> (10 mg)	2.00 ± 0.35 **	100
<b>13</b> (15 mg)	—	<b>13</b> (15 mg)	—	—	<b>13</b> (15 mg)	2.17 ± 0.31 **	100
<b>13</b> (10 mg) + RAMH	—	<b>13</b> (10 mg) + RAMH	—	—	<b>13</b> (10 mg) + RAMH	2.14 ± 0.35 **	100
SAL + RAMH	—	SAL + RAMH	—	—	SAL + RAMH	4.71 ± 0.16	28.57

<sup>a</sup> 50-Hz alternating current of 120 mA intensity applied through ear electrodes for a duration of 1 s; <sup>b</sup> 60 mg/kg; <sup>c</sup> 3.5 mg/kg. —: not determined. +: means that two compounds were co-administered to the tested animals. \*  $p < 0.05$  vs. (saline)-treated group. \*\*  $p < 0.001$  vs. (saline)-treated group. <sup>#</sup>  $p < 0.05$  vs. (2.5 mg)-treated group. <sup>5</sup>  $p < 0.05$  vs. (5 mg or 15 mg)-treated groups. <sup>6</sup> Full protection. SAL—saline; PHT—phenytoin; VPA—valproic acid; RAMH—(R)- $\alpha$ -methylhistamine.

## 6 Studies on anticonvulsant effects of novel histamine H3R antagonists in electrically and chemically induced seizures in rats

Int. J. Mol. Sci. 2018, 19, 3386

13 of 23

### Anticonvulsant Screening for H3R Antagonists 1–16 in STR-Induced Seizures

In STR-induced seizure in rats, H3R antagonist **4** with the most promising effect in MES- and PTZ-induced seizures failed to provide any appreciable protection in STR-induced seizure when compared with the saline-treated group after 30 min of observation time with [ $F_{(1,12)} = 4.50$ ;  $p = 0.055$ ] (Tables 2 and 3). However, H3R antagonist **13** without protection in MES-induced seizure and with weak protection in PTZ-induced seizure exhibited a moderate protective effect in STR-induced seizure when compared with the saline-treated group with [ $F_{(1,12)} = 63.00$ ;  $p < 0.001$ ] (Figure 3, Table 3). Notably, the reference antiepileptic drug VPA (VPA 300 mg/kg, i.p.) showed significant protection when compared with saline-treated group after 30 min observation time with [ $F_{(1,12)} = 236.308$ ;  $p < 0.001$ ] (Figure 3, Tables 2 and 3). Moreover, the results showed that acute systemic pretreatment with H3R antagonist **13** at a lower dose (2.5 mg/kg, i.p.) failed to exhibit protection against STR-induced seizures when compared with the saline-treated group with [ $F_{(1,12)} = 1.00$ ;  $p = 0.337$ ] (Figure 3, Tables 2 and 3). Furthermore, no significant differences in the protection provided by H3R antagonist **13** (10 mg/kg, i.p.) were observed when 5 or 15 mg/kg of the same compound was administered with [ $F_{(1,12)} = 2.842$ ;  $p = 0.118$ ] [ $F_{(1,12)} = 0.079$ ;  $p = 0.784$ ], respectively (Figure 3, Table 3).

### 3.2. ADME-Tox Properties

#### 3.2.1. Antiproliferative Assay

The effect of H3R antagonist **4** (0.1–100  $\mu\text{M}$ ) on proliferation of HEK-293 and *hepatoma* HepG2 cell lines was assessed and compared with the reference cytostatic drug doxorubicin (DX) and hepatotoxin carbonyl cyanide 3-chlorophenylhydrazone (CCCP) (Figure 4A,B). The results showed that H3R antagonist **4** significantly decreased proliferation of HepG2 cells only at the highest concentration used (100  $\mu\text{M}$ ), however, decline in proliferation of HEK-293 cells was achieved with two doses of the same compound, namely 10 and 100  $\mu\text{M}$  ( $p < 0.001$ ) (Figure 4A,B).

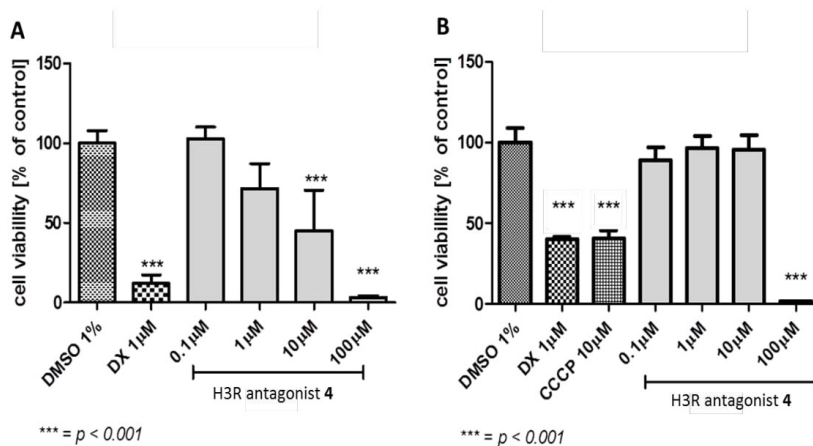


**Figure 4.** Antiproliferative effects of H3R antagonist **4**. (A) Antiproliferative effects of the reference drug doxorubicin (DX) and H3R antagonist **4** on HEK-293 cell line after 72 h of incubation. (B) Antiproliferative effects of the reference drug doxorubicin (DX), hepatotoxin carbonyl cyanide 3-chlorophenylhydrazone (CCCP), and H3R antagonist **4** on HepG2 cell line after 72 h of incubation. DMSO: dimethyl sulfoxide.

## 6 Studies on anticonvulsant effects of novel histamine H3R antagonists in electrically and chemically induced seizures in rats

*Int. J. Mol. Sci.* **2018**, *19*, 3386

14 of 23

### 3.2.2. In Silico Metabolic Stability

The computational procedure MetaSite.5.1.1 provided by Molecular Discovery Ltd. indicated the sixth position of naphthalene moiety as the most probable site of H3R antagonist **4** metabolism (blue circle marked; Figure 5). Moreover, the azepane moiety was also shown to be susceptible for metabolic biotransformations (the darker red color of the marked functional group indicates its higher probability of being involved in the metabolism pathway; Figure 5). The predicted in silico most probable metabolic routes included hydroxylation at the sixth position of naphthalene or azepane group followed by the compound's oxidative degradation of the aliphatic alkyl chain (data not shown).

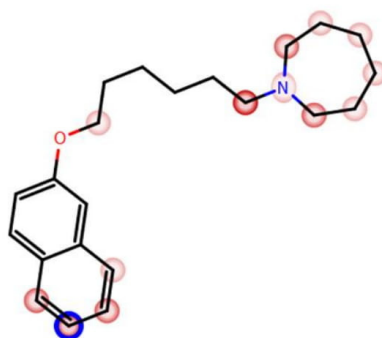


**Figure 5.** Potential sites of metabolism for H3R antagonist **4**. The blue circle marks the site involved in metabolism with the highest probability. Other potential sites are marked with red color; the darker the color, the higher the probability of involvement in the metabolism pathway (calculated with MetaSite [53]).

### 3.2.3. In Vitro Metabolic Stability

The UPLC analysis of the reaction mixture of H3R antagonist **4** incubated for 120 min with rat liver microsomes (RLMs) showed that ~18% of this compound was converted into four metabolites, namely M-I–M-IV (Figure 6A). The MS determination of the molecular mass of the main metabolite M-I (+32 units) and the comparison of the ion fragments analyses of H3R antagonist **4** and metabolite M-I suggests the double-hydroxylation at the 6-*n*-hexylazepane moiety as the main metabolic pathway (Figure 6B). Moreover, the hydroxylation reactions at the naphthalene moiety and at the aliphatic alkyl chain were also identified (metabolites M-II–M-IV, Figure 6C).

## 6 Studies on anticonvulsant effects of novel histamine H3R antagonists in electrically and chemically induced seizures in rats

Int. J. Mol. Sci. 2018, 19, 3386

15 of 23

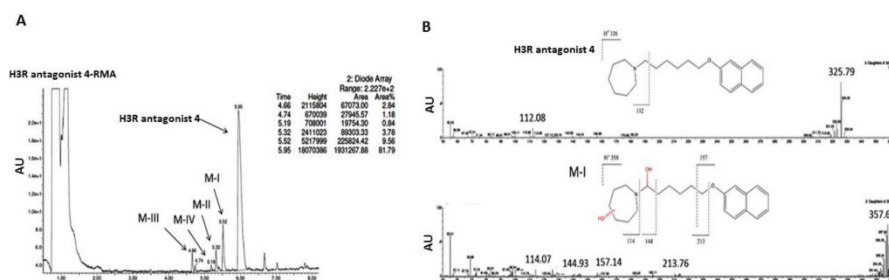
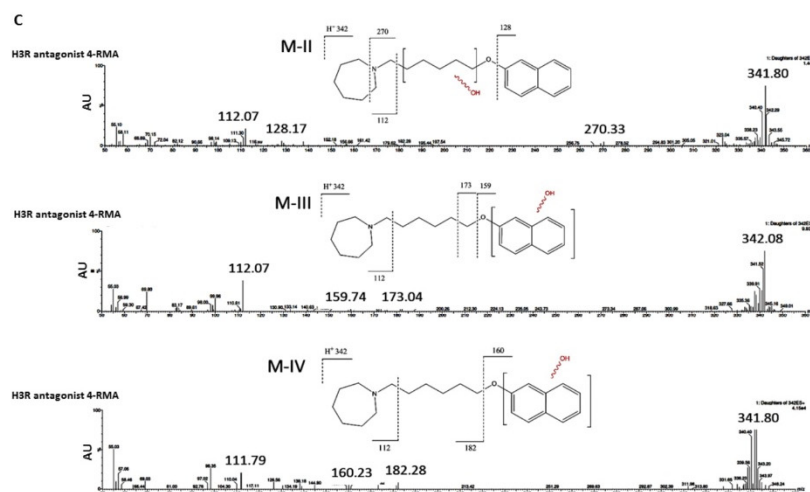


Figure 6. Cont.

Int. J. Mol. Sci. 2018, 19, 3386

16 of 23



**Figure 6.** The metabolic profile of H3R antagonist after incubation of H3R antagonist 4 with rat liver microsomes. The UPLC spectrum obtained two hours post incubation of H3R antagonist 6 with rat liver microsomes. (A) Around 20% of H3R antagonist 4 was metabolized. (B) Main metabolite M-I of H3R antagonist 4 with a double-hydroxylation identified as the main metabolic route. (C) The mass spectrometry (MS) fragmentation analysis of most probable hydroxylation sites MII–MIV with rat liver microsomes. Abbreviations: UPLC, ultra-performance liquid chromatography.

## 6 Studies on anticonvulsant effects of novel histamine H3R antagonists in electrically and chemically induced seizures in rats

Int. J. Mol. Sci. 2018, 19, 3386

17 of 23

### 3.2.4. Metabolic Interactions

The results observed in luminescent CYP3A4 P450-Glo™ assay showed no inhibitory effects of H3R antagonist 4 on CYP3A4 activity at examined concentrations of 0.1–25  $\mu$ M (Figure 7A). Moreover, the observed results in luminescent CYP2D6 P450-Glo™ assay revealed that the inhibitory effect of H3R antagonist 6 was detected with an  $IC_{50}$  value of 0.67  $\mu$ M (Figure 7B).

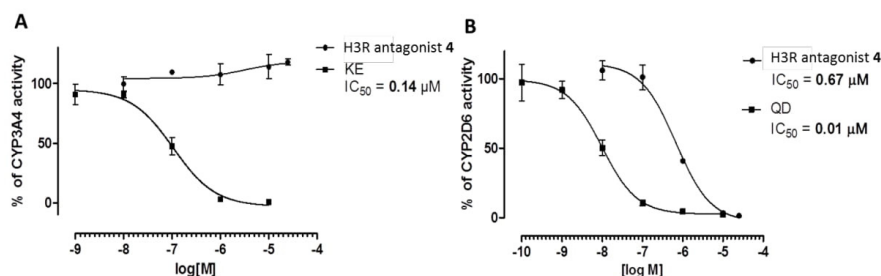


**Figure 7.** Effect of H3R antagonist 4 on CYP3A4 and CYP2D6 activity. (A) Effects of ketoconazole (KE) and H3R antagonist 4 on CYP3A4 activity. (B) Effect of quinidine (QD) and H3R antagonist 4 on CYP2D6 activity.

## 4. Discussion

### 4.1. In Vitro Histamine H3 Receptor Affinity of Test Compounds 1–16

All novel H3R antagonists were evaluated in the form of hydrogen oxalate salts in radioligand displacement assays. Tested H3R antagonists 1–16 displayed affinities at the human H3R in a nanomolar concentration range ( $K_i$ : 36–137 nM, Table 1). Compounds 13–15 displayed  $K_i$  values similar to that of pitolisant (12 nM, Table 1), while the 4-fluorophenyl derivatives were the least potent ones (11–13;  $K_i$ : 83.6–137.2 nM).

### 4.2. Selectivity of Selected H3R Antagonists towards Other Histamine Receptors (H1 and H4)

#### 4.2.1. Histamine H1 Receptor Affinity

As the two histamine receptors H1R and H3R play a pivotal role in the anticonvulsant activity of the central histamine [41], selected H3R antagonists (6, 9, and 15) were examined in a binding assay at the human histamine H1R and showed weak affinities ( $915 \leq K_i \leq 1338$  nM), being 10-fold lower than at the H3R.

#### 4.2.2. Histamine H4 Receptor Affinity

As H3R represents the highest degree of homology with H4R [19], the potential interaction with this receptor subtype for selected H3R antagonists (4, 7, and 13) was evaluated. The observed results showed that none of the tested H3R antagonists displayed affinity for hH4R ( $K_i > 10,000$  nM).

### 4.3. In Vivo Anticonvulsant Activity

The results demonstrated that H3R antagonist 4 exhibited the most promising protection against MES-induced seizures when animals were administered with 10 mg/kg i.p., and as compared with the saline-treated group of animals (Tables 2 and 3). However, lower doses (2.5 and 5 mg/kg, i.p.) and a higher dose (15 mg/kg, i.p.) failed to increase the (10 mg) H3R antagonist 4-provided protection (Figure 1, Table 3). Accordingly, the observed results show a dose-response relationship of the protection provided and the presence of a ceiling effect for H3R antagonist 4 in the MES-induced seizure model achieved with a dose of 10 mg/kg, i.p. (Figure 1, Table 3). Notably, the protective



## 6 Studies on anticonvulsant effects of novel histamine H3R antagonists in electrically and chemically induced seizures in rats

effect of H3R antagonist **4** (10 mg/kg, i.p.) was similar to that observed in the group treated with the reference antiepileptic drug PHT (10 mg/kg, i.p.), and was significantly higher than that observed for H3R ligands **3**, **5**, **6**, **7**, **8**, and **14** (Figure 1, Table 1). The latter observations are in agreement with recent preclinical outcomes that showed a dose-dependent anticonvulsant effect of several H3R antagonists tested in several animal models of seizures. Also, the present results are in line with earlier observations for the H3R antagonist PIT in a photosensitivity seizure model in adult patients, and in agreement with earlier observations for several H3R antagonists tested for their anticonvulsant potential in different animal models of seizures [25–30,33,40,54]. An additional test in the present study showed that the protection observed for H3R antagonist **4** was abolished when animals were co-administered with the CNS penetrant histamine H3R agonist RAMH (10 mg/kg i.p.) (Figure 1, Table 3), proposing that the provided protective effect of H3R antagonist **4** in the MES-induced seizure model involves, at least to some extent, H3R blockade provided by H3R antagonist **4**. Notably, these observations are consistent with the earlier preclinical results for numerous imidazole- and non-imidazole-based H3R antagonists [14,25–30,40,54].

H3Rs are auto-receptors presynaptically positioned on histaminergic neurons with an inhibitory effect on the biosynthesis and release of histamine [21]. Therefore, blocking H3Rs by selective H3R antagonists, such as H3R antagonist **4**, would escalate neuronal release of brain histamine, providing the protection in the MES-induced seizure in rats. The latter proposed mechanism underlying the anticonvulsant effect of H3R antagonist **4** is also in line with previous preclinical observations in animal seizure models in which high doses of several centrally acting H1R antagonists used as anti-allergic drugs promoted the development of convulsions of tested animals, indicating the involvement of H1R antagonism, and consequently, brain histaminergic neurotransmission in the seizure promotion. Noticeably, similar protective effects of imidazole-based and non-imidazole-based H3R antagonists were earlier described to be abolished either by H3R agonists or by centrally acting H1R antagonists, suggesting an interaction of the H3R antagonism-released histamine with postsynaptically located H1Rs on neurons [14,25–30,53,54].

In the PTZ-induced seizure mode, acute systemic administration of VPA (100 mg/kg, i.p.) as well as H3R antagonists **4**, **7**, and **11** (10 mg/kg, i.p.) showed full protection (Figure 2, Table 3). Furthermore, the anticonvulsant effects observed for H3R antagonist **4** at lower doses (2.5 and 5 mg/kg, i.p.) or a higher dose (15 mg/kg, i.p.) showed a dose-dependent protection in the PTZ-induced seizure model (Figure 2, Table 3). However, the protective effect of H3R antagonist **4** (10 mg/kg, i.p.) was not reversed when rats were pretreated with RAMH (10 mg/kg, i.p.) before PTZ challenge, suggesting that the protection observed for H3R antagonist **4** in PTZ-induced seizure is not facilitated through modulation of central histaminergic neurotransmission (Figure 2, Table 3). The latter observation may be explained with the differences in the triggers or the mechanisms and types of seizures each model represents (MES is considered as a model of generalized tonic-clonic seizures, whereas PTZ (60 mg/kg, i.p.) induces generalized myoclonic and/or tonic-clonic seizures) [11,53–55]. The failure of RAMH to reverse the protections provided by H3R antagonist **4** might be explained with its capability to reduce the suppression of glutamatergic and GABAergic synaptic transmission through blockade of H3 heteroreceptor function in CNS, necessitating additional future investigations of whether H3R antagonist **4** modulated the release of inhibitory neurotransmitters, for example, GABA [56].

In the STR-induced seizure model, the results showed that acute systemic administration of H3R antagonists **4**, **7**, and **11** (10 mg/kg, i.p.) failed to exhibit appreciable protection during 30 min of the time observation, whereas H3R antagonist **13** with moderate protection in PTZ and without any considerable protection in MES demonstrated reasonable protection following 30 min during the time observation (Figure 3, Table 3). Moreover, the lower doses (2.5 and 5 mg/kg, i.p.) as well as the higher dose (15 mg/kg, i.p.) of H3R antagonist **13** failed to exhibit a dose-dependent protection against STR-induced seizure in rats (Figure 3, Table 3). In resemblance to the observations in PTZ-induced seizure, an additional experiment showed that the H3R antagonist **13**-provided moderate protection in STR-induced seizure was not reversed when animals were co-injected with

## 6 Studies on anticonvulsant effects of novel histamine H3R antagonists in electrically and chemically induced seizures in rats

*Int. J. Mol. Sci.* **2018**, *19*, 3386

19 of 23

10 mg/kg i.p. of the CNS penetrant histamine H3R agonist RAMH 30–45 min before STR challenge (Figure 3, Table 3). These findings in STR-induced seizure further comprehend the present results for the protective effects of the H3R antagonist 4 in PTZ-induced seizure model, as both models are considered as chemically-induced seizure models. The latter observations for H3R antagonists 1–16 in the STR-induced seizure model show that the moderate protection provided with H3R antagonist 13 in STR model is also not facilitated through central histaminergic neurotransmission. Notably, STR is an established competitive antagonist of the inhibitory amino acid glycine. Therefore, the inability of H3R antagonist 13 to afford a dose-dependent protection against STR-induced seizure model advocates little or no modulation effect of H3R antagonist 13 on the glycine receptors, because the mechanisms underlying STR-induced seizures are supposed to be attributed to its blocking activity on glycine receptors in the brain as well as in the spinal cord [56]. Notably, most marketed AEDs were not effective in all conducted convulsion models during preclinical drug development. Accordingly, carbamazepine, oxcarbazepine and PHT were found to be, and are still, highly effective in MES-induced model in rodents, however, they failed to protect against convulsions in rodents induced by PTZ, STR, or picrotoxin [57,58]. On the contrary, ethosuximide and tiagabine, which show high protection in chemically-induced convulsion models in rodents, lack protection in the MES-induced model when used at nontoxic doses [58]. Nonetheless, the diversity in preclinical activities detected for numerous AEDs was translated into the clinical utility of PHT, carbamazepine, and oxcarbazepine, but not ethosuximide or tiagabine, in patients diagnosed with generalized tonic-clonic convulsions.

### 4.4. ADME-Tox Properties

The most promising H3R antagonist 4 was selected to evaluate its ADME-Tox properties, which included the determination of the in vitro safety profile by applying eukaryotic cell lines, the in silico and in vitro determination of the metabolic stability and main metabolic routes, and the in vitro assessment of potential drug-drug interactions by bioluminescent enzymatic assays.

In order to determine the potential toxicity, the standard colorimetric MTS test was used. This test allowed one to follow up the influence of H3R antagonist 4 on the human embryonic kidney (HEK-293) and *hepatoma* HepG2 cell lines' proliferation. The antiproliferative activity of H3R antagonist 4 differed between both used cell lines. HEK-293 cells were more susceptible for antiproliferative activity as revealed in the statistically significant decrease of HEK-293 cell line viability ( $p < 0.001$ ), which was observed at concentrations of 10 and 100  $\mu\text{M}$ , whereas in the HepG2 cell line, the antiproliferative effect was achieved only at a concentration of 100  $\mu\text{M}$  (Figure 4A,B). However, the obtained results for HEK-293 indicated a satisfying safety profile of H3R antagonist 4 in comparison with the reference DX, which significantly decreased HEK-293 viability at a much lower concentration (1  $\mu\text{M}$ ) (Figure 4A). Moreover, no significant hepatotoxic effect was observed for H3R antagonist 4, as the reference drug CCCP decreased HepG2 viability at 10  $\mu\text{M}$ , whereas H3R antagonist 4 only did so at 100  $\mu\text{M}$  (Figure 4B).

In further in vitro metabolic stability studies, the results observed for H3R antagonist 4 applying RLMS revealed good metabolic stability of H3R antagonist 4, as only ~18% of the substrate was metabolized and converted into four different metabolites after 120 min of incubation at 37 °C (Figure 6). Moreover, the in silico data and the MS fragmentation analyses showed one hydroxylation on the azepane moiety and another hydroxylation on the hexyl chain, followed by oxidative degradation of the alkyl chain as the main metabolic routes of H3R antagonist 4 (Figure 5).

Furthermore, H3R antagonist 4 did not affect CYP3A4, whereas CYP2D6 was inhibited in a more pronounced manner. However, this effect was observed with a 67-fold higher  $\text{IC}_{50}$  ( $\text{IC}_{50} = 0.67 \mu\text{M}$ ) as compared with the reference drug QD with a calculated  $\text{IC}_{50}$  value of 0.01  $\mu\text{M}$  (Figure 7).

## 5. Conclusions

The tested series of H3R antagonists showed in vitro affinity at the hH3R in the nanomolar range. The most promising H3R antagonist 4 having the 1-(6-(naphthalen-2-yloxy)hexyl)azepane



## 6 Studies on anticonvulsant effects of novel histamine H3R antagonists in electrically and chemically induced seizures in rats

Int. J. Mol. Sci. 2018, 19, 3386

20 of 23

pharmacophore exhibited an affinity for hH3R ( $K_i = 69.3$  nM). The in vivo anticonvulsant results revealed that H3R antagonist **4** exhibited most promising protection following acute systemic administration in MES- and PTZ-induced seizure models in rats. Moreover, the protection observed for H3R antagonist **4** in the MES-induced seizure model was fully reversed when rats were pretreated with the CNS-penetrant H3R agonist RAMH. However, RAMH failed to abrogate the protective effects observed for H3R antagonist in PTZ- or STR-induced seizure models, indicating that histaminergic pathways appear to be involved in the provided anticonvulsant efficacy of H3R antagonist **4** in only the MES-induced seizure model, but additional pharmacological properties of the compounds or their metabolites cannot be fully excluded. Moreover, ADME-Tox parameters' screening revealed satisfying low cytotoxicity, good metabolic stability, as well as no inhibition of CYP3A4 activity and moderate inhibition of CYP2D6 activity. Therefore, the overall experimental observations provide promising potential for the novel H3R antagonist **4** to be used as a potential template for further drug design and synthesis in the search for potent and active in vivo H3R antagonists, for example, as AED drugs with a high safety profile. Nonetheless, a battery of additional seizure models with different species is still required to further corroborate the current results observed for H3R antagonist **4**, and to strengthen the translational value of its potential applicability in the therapeutic management of epilepsy.

**Supplementary Materials:** Supplementary Materials can be found at <http://www.mdpi.com/1422-0067/19/11/3386/s1>.

**Author Contributions:** B.S. was responsible for the study concept, design, acquisition, and analysis of animal data. A.A. conducted in vivo seizure experiments. G.L., A.L., J.H., and E.H.-O. were responsible for determination of antiproliferative activity, evaluation of in silico and in vitro metabolic stability, and drug-drug interaction probability of the obtained compounds. A.S. was responsible for carrying out tests of novel ligands for human histamine H1 receptors. A.F. and H.S. were responsible for affinity evaluation of novel ligands at the human histamine H3 and H4 receptors. K.K.-K. and D.L. were responsible for the design, synthesis, and analysis of all novel H3R antagonists. B.S. drafted the manuscript. K.K.-K., D.L., A.F., and H.S. provided critical revision for the manuscript. All authors critically reviewed content and approved final version for publication.

**Funding:** Bassem Sadek was supported by intramural funds from the College of Medicine and Health Sciences and the Office of Graduate Studies and Research, UAE University. The authors acknowledge the partial support of National Science Center granted on the basis of decision number DEC-2016/23/B/NZ7/02327 (D.L.) and the Jagiellonian University grant K/ZDS/007121 (K.K.-K.). Support was kindly provided by the EU COST Action CA15135 (D.L., H.S. and K.K.-K.), as well by DFG INST 208/664-1 FUGG (H.S.).

**Conflicts of Interest:** The authors declare no conflict of interest.

### References

1. Baulac, M.; de Boer, H.; Elger, C.; Glynn, M.; Kalviainen, R.; Little, A.; Mifsud, J.; Perucca, E.; Pitkanen, A.; Ryvlin, P. Epilepsy priorities in Europe: A report of the ILAE-IBE Epilepsy Advocacy Europe Task Force. *Epilepsia* **2015**, *56*, 1687–1695. [[CrossRef](#)] [[PubMed](#)]
2. Kobow, K.; Blumcke, I. Epigenetics in epilepsy. *Neurosci. Lett.* **2018**, *667*, 40–46. [[CrossRef](#)] [[PubMed](#)]
3. Lin, J.J.; Mula, M.; Hermann, B.P. Uncovering the neurobehavioural comorbidities of epilepsy over the lifespan. *Lancet* **2012**, *380*, 1180–1192. [[CrossRef](#)]
4. Schmidt, D. The clinical impact of new antiepileptic drugs after a decade of use in epilepsy. *Epilepsy Res.* **2002**, *50*, 21–32. [[CrossRef](#)]
5. Franco, V.; French, J.A.; Perucca, E. Challenges in the clinical development of new antiepileptic drugs. *Pharmacol. Res.* **2016**, *103*, 95–104. [[CrossRef](#)] [[PubMed](#)]
6. Burakgazi, E.; French, J.A. Treatment of epilepsy in adults. *Epileptic Disord.* **2016**, *18*, 228–239. [[PubMed](#)]
7. Di Giovanni, G.; Svob Strac, D.; Sole, M.; Unzeta, M.; Tipton, K.F.; Muck-Seler, D.; Bolea, I.; Della Corte, L.; Nikolac Perkovic, M.; Pivac, N.; et al. Monoaminergic and Histaminergic Strategies and Treatments in Brain Diseases. *Front. Neurosci.* **2016**, *10*, 541. [[CrossRef](#)] [[PubMed](#)]
8. Svob Strac, D.; Pivac, N.; Smolders, I.J.; Fogel, W.A.; De Deurwaerdere, P.; Di Giovanni, G. Monoaminergic Mechanisms in Epilepsy May Offer Innovative Therapeutic Opportunity for Monoaminergic Multi-Target Drugs. *Front. Neurosci.* **2016**, *10*, 492. [[CrossRef](#)] [[PubMed](#)]

## 6 Studies on anticonvulsant effects of novel histamine H3R antagonists in electrically and chemically induced seizures in rats

Int. J. Mol. Sci. 2018, 19, 3386

21 of 23

9. Kamei, C. Involvement of central histamine in amygdaloid kindled seizures in rats. *Behav. Brain Res.* **2001**, *124*, 243–250. [\[CrossRef\]](#)
10. Kamei, C.; Ishizawa, K.; Kakinoki, H.; Fukunaga, M. Histaminergic mechanisms in amygdaloid-kindled seizures in rats. *Epilepsy Res.* **1998**, *30*, 187–194. [\[CrossRef\]](#)
11. Vohora, D.; Pal, S.N.; Pillai, K.K. Histamine and selective H3-receptor ligands: A possible role in the mechanism and management of epilepsy. *Pharmacol. Biochem. Behav.* **2001**, *68*, 735–741. [\[CrossRef\]](#)
12. Miyata, I.; Saegusa, H.; Sakurai, M. Seizure-modifying potential of histamine H1 antagonists: A clinical observation. *Pediatr. Int.* **2011**, *53*, 706–708. [\[CrossRef\]](#) [\[PubMed\]](#)
13. Ago, J.; Ishikawa, T.; Matsumoto, N.; Ashequr Rahman, M.; Kamei, C. Mechanism of imipramine-induced seizures in amygdala-kindled rats. *Epilepsy Res.* **2006**, *72*, 1–9. [\[CrossRef\]](#) [\[PubMed\]](#)
14. Kakinoki, H.; Ishizawa, K.; Fukunaga, M.; Fujii, Y.; Kamei, C. The effects of histamine H3-receptor antagonists on amygdaloid kindled seizures in rats. *Brain Res. Bull.* **1998**, *46*, 461–465. [\[CrossRef\]](#)
15. Yawata, I.; Tanaka, K.; Nakagawa, Y.; Watanabe, Y.; Murashima, Y.L.; Nakano, K. Role of histaminergic neurons in development of epileptic seizures in EL mice. *Brain Res. Mol. Brain Res.* **2004**, *132*, 13–17. [\[CrossRef\]](#) [\[PubMed\]](#)
16. Onodera, K.; Yamatodani, A.; Watanabe, T. Effects of alpha-fluoromethylhistidine on locomotor activity, brain histamine and catecholamine contents in rats. *Methods Find Exp. Clin. Pharmacol.* **1992**, *14*, 97–105. [\[PubMed\]](#)
17. Tuomisto, L.; Tacke, U. Is histamine an anticonvulsive inhibitory transmitter? *Neuropharmacology* **1986**, *25*, 955–958. [\[CrossRef\]](#)
18. Zhang, L.S.; Chen, Z.; Huang, Y.W.; Hu, W.W.; Wei, E.Q.; Yanai, K. Effects of endogenous histamine on seizure development of pentylentetrazole-induced kindling in rats. *Pharmacology* **2003**, *69*, 27–32. [\[CrossRef\]](#) [\[PubMed\]](#)
19. Panula, P.; Chazot, P.L.; Cowart, M.; Gutzmer, R.; Leurs, R.; Liu, W.L.; Stark, H.; Thurmond, R.L.; Haas, H.L. International Union of Basic and Clinical Pharmacology. XCVIII. Histamine Receptors. *Pharmacol. Rev.* **2015**, *67*, 601–655. [\[CrossRef\]](#) [\[PubMed\]](#)
20. Schneider, E.H.; Seifert, R. The histamine H-receptor and the central and peripheral nervous system: A critical analysis of the literature. *Neuropharmacology* **2015**, *106*, 116–128. [\[CrossRef\]](#) [\[PubMed\]](#)
21. Arrang, J.M.; Garbarg, M.; Schwartz, J.C. Auto-inhibition of brain histamine release mediated by a novel class (H3) of histamine receptor. *Nature* **1983**, *302*, 832–837. [\[CrossRef\]](#) [\[PubMed\]](#)
22. Arrang, J.M.; Garbarg, M.; Schwartz, J.C. Autoinhibition of histamine synthesis mediated by presynaptic H3-receptors. *Neuroscience* **1987**, *23*, 149–157. [\[CrossRef\]](#)
23. Brown, R.E.; Stevens, D.R.; Haas, H.L. The physiology of brain histamine. *Prog. Neurobiol.* **2001**, *63*, 637–672. [\[CrossRef\]](#)
24. Kuder, K.; Lazewska, D.; Latacz, G.; Schwed, J.S.; Karcz, T.; Stark, H.; Karolak-Wojciechowska, J.; Kiec-Kononowicz, K. Chlorophenoxy aminoalkyl derivatives as histamine H(3)R ligands and antiseizure agents. *Bioorg. Med. Chem.* **2016**, *24*, 53–72. [\[CrossRef\]](#) [\[PubMed\]](#)
25. Sadek, B.; Kuder, K.; Subramanian, D.; Shafiullah, M.; Stark, H.; Lazewska, D.; Adem, A.; Kiec-Kononowicz, K. Anticonvulsive effect of nonimidazole histamine H3 receptor antagonists. *Behav. Pharmacol.* **2014**, *25*, 245–252. [\[CrossRef\]](#) [\[PubMed\]](#)
26. Sadek, B.; Saad, A.; Latacz, G.; Kuder, K.; Olejarz, A.; Karcz, T.; Stark, H.; Kiec-Kononowicz, K. Non-imidazole-based histamine H3 receptor antagonists with anticonvulsant activity in different seizure models in male adult rats. *Drug Des. Dev. Ther.* **2016**, *10*, 3879–3898. [\[CrossRef\]](#) [\[PubMed\]](#)
27. Sadek, B.; Saad, A.; Schwed, J.S.; Weizel, L.; Walter, M.; Stark, H. Anticonvulsant effects of isomeric nonimidazole histamine H3 receptor antagonists. *Drug Des. Dev. Ther.* **2016**, *10*, 3633–3651. [\[CrossRef\]](#) [\[PubMed\]](#)
28. Sadek, B.; Saad, A.; Subramanian, D.; Shafiullah, M.; Lazewska, D.; Kiec-Kononowicz, K. Anticonvulsant and procognitive properties of the non-imidazole histamine H3 receptor antagonist DL77 in male adult rats. *Neuropharmacology* **2016**, *106*, 46–55. [\[CrossRef\]](#) [\[PubMed\]](#)
29. Sadek, B.; Schwed, J.S.; Subramanian, D.; Weizel, L.; Walter, M.; Adem, A.; Stark, H. Non-imidazole histamine H3 receptor ligands incorporating antiepileptic moieties. *Eur. J. Med. Chem.* **2014**, *77*, 269–279. [\[CrossRef\]](#) [\[PubMed\]](#)

## 6 Studies on anticonvulsant effects of novel histamine H3R antagonists in electrically and chemically induced seizures in rats

Int. J. Mol. Sci. **2018**, *19*, 3386

22 of 23

30. Sadek, B.; Shehab, S.; Wiecek, M.; Subramanian, D.; Shafiullah, M.; Kiec-Kononowicz, K.; Adem, A. Anticonvulsant properties of histamine H3 receptor ligands belonging to N-substituted carbamates of imidazopropanol. *Bioorg. Med. Chem. Lett.* **2013**, *23*, 4886–4891. [[CrossRef](#)] [[PubMed](#)]
31. Zhang, L.; Chen, Z.; Ren, K.; Leurs, R.; Chen, J.; Zhang, W.; Ye, B.; Wei, E.; Timmerman, H. Effects of clobenpropit on pentylenetetrazole-kindled seizures in rats. *Eur. J. Pharmacol.* **2003**, *482*, 169–175. [[CrossRef](#)] [[PubMed](#)]
32. Zhang, L.S.; Chen, J.F.; Chen, G.F.; Hu, X.Y.; Ding, M.P. Effects of thioperamide on seizure development and memory impairment induced by pentylenetetrazole-kindling epilepsy in rats. *Chin. Med. J.* **2013**, *126*, 95–100. [[PubMed](#)]
33. Kasteleijn-Nolst Trenite, D.; Parain, D.; Genton, P.; Masnou, P.; Schwartz, J.C.; Hirsch, E. Efficacy of the histamine 3 receptor (H3R) antagonist pitolisant (formerly known as tiprolisant; BF2.649) in epilepsy: Dose-dependent effects in the human photosensitivity model. *Epilepsy Behav.* **2013**, *28*, 66–70. [[CrossRef](#)] [[PubMed](#)]
34. Collart Dutilleul, P.; Ryvlin, P.; Kahane, P.; Vercueil, L.; Semah, F.; Biraben, A.; Schwartz, J.C.; De Seze, J.; Hirsch, E.; Collongues, N. Exploratory Phase II Trial to Evaluate the Safety and the Antiepileptic Effect of Pitolisant (BF2.649) in Refractory Partial Seizures, Given as Adjunctive Treatment During 3 Months. *Clin. Neuropharmacol.* **2016**, *39*, 188–193. [[CrossRef](#)] [[PubMed](#)]
35. Arrang, J.M.; Garbarg, M.; Lancelot, J.C.; Lecomte, J.M.; Pollard, H.; Robba, M.; Schunack, W.; Schwartz, J.C. Highly potent and selective ligands for histamine H3-receptors. *Nature* **1987**, *327*, 117–123. [[CrossRef](#)] [[PubMed](#)]
36. Ligneau, X.; Morisset, S.; Tardivel-Lacombe, J.; Gbahou, F.; Ganellin, C.R.; Stark, H.; Schunack, W.; Schwartz, J.C.; Arrang, J.M. Distinct pharmacology of rat and human histamine H(3) receptors: Role of two amino acids in the third transmembrane domain. *Br. J. Pharmacol.* **2000**, *131*, 1247–1250. [[CrossRef](#)] [[PubMed](#)]
37. Kollb-Sielecka, M.; Demolis, P.; Emmerich, J.; Markey, G.; Salmonson, T.; Haas, M. The European Medicines Agency review of pitolisant for treatment of narcolepsy: Summary of the scientific assessment by the Committee for Medicinal Products for Human Use. *Sleep Med.* **2017**, *33*, 125–129. [[CrossRef](#)] [[PubMed](#)]
38. Ligneau, X.; Perrin, D.; Landais, L.; Camelin, J.C.; Calmels, T.P.; Berrebi-Bertrand, I.; Lecomte, J.M.; Parmentier, R.; Anacleto, C.; Lin, J.S.; et al. BF2.649 [1-[3-[3-(4-Chlorophenyl)propoxy]propyl]piperidine, hydrochloride], a nonimidazole inverse agonist/antagonist at the human histamine H3 receptor: Preclinical pharmacology. *J. Pharmacol. Exp. Ther.* **2007**, *320*, 365–375. [[CrossRef](#)] [[PubMed](#)]
39. Sadek, B.; Stark, H. Cherry-picked ligands at histamine receptor subtypes. *Neuropharmacology* **2015**, *106*, 56–73. [[CrossRef](#)] [[PubMed](#)]
40. Sadek, B.; Saad, A.; Sadeq, A.; Jalal, F.; Stark, H. Histamine H3 receptor as a potential target for cognitive symptoms in neuropsychiatric diseases. *Behav. Brain Res.* **2016**, *312*, 415–430. [[CrossRef](#)] [[PubMed](#)]
41. Bhowmik, M.; Khanam, R.; Vohora, D. Histamine H3 receptor antagonists in relation to epilepsy and neurodegeneration: A systemic consideration of recent progress and perspectives. *Br. J. Pharmacol.* **2012**, *167*, 1398–1414. [[CrossRef](#)] [[PubMed](#)]
42. Sander, K.; Kottke, T.; Weizel, L.; Stark, H. Kojic acid derivatives as histamine H(3) receptor ligands. *Chem. Pharm. Bull.* **2010**, *58*, 1353–1361. [[CrossRef](#)] [[PubMed](#)]
43. Sadek, B.; Schreeb, A.; Schwed, J.S.; Weizel, L.; Stark, H. Drug-likeness approach of 2-aminopyrimidines as histamine H3 receptor ligands. *Drug Des. Dev. Ther.* **2014**, *8*, 1499–1513. [[CrossRef](#)] [[PubMed](#)]
44. Cheng, Y.; Prusoff, W.H. Relationship between the inhibition constant (K1) and the concentration of inhibitor which causes 50 per cent inhibition (I50) of an enzymatic reaction. *Biochem. Pharmacol.* **1973**, *22*, 3099–3108. [[PubMed](#)]
45. Lazewska, D.; Kaleta, M.; Hagenow, S.; Mogilski, S.; Latacz, G.; Karcz, T.; Lubelska, A.; Honkisz, E.; Handzlik, J.; Reiner, D.; et al. Novel naphthyloxy derivatives—Potent histamine H3 receptor ligands. Synthesis and pharmacological evaluation. *Bioorg. Med. Chem.* **2018**, *26*, 2573–2585. [[CrossRef](#)] [[PubMed](#)]
46. Alachkar, A.; Latacz, G.; Siwek, A.; Lubelska, A.; Honkisz, E.; Grybos, A.; Lazewska, D.; Handzlik, J.; Stark, H.; Kiec-Kononowicz, K.; et al. Anticonvulsant evaluation of novel non-imidazole histamine H3R antagonists in different convulsion models in rats. *Pharmacol. Biochem. Behav.* **2018**, *170*, 14–24. [[CrossRef](#)] [[PubMed](#)]



## 6 Studies on anticonvulsant effects of novel histamine H3R antagonists in electrically and chemically induced seizures in rats

Int. J. Mol. Sci. 2018, 19, 3386

23 of 23

47. Sadek, B.; Khanian, S.S.; Ashoor, A.; Prytkova, T.; Ghattas, M.A.; Atatreh, N.; Nurulain, S.M.; Yang, K.H.; Howarth, F.C.; Oz, M. Effects of antihistamines on the function of human  $\alpha 7$ -nicotinic acetylcholine receptors. *Eur. J. Pharmacol.* **2014**, *746*, 308–316. [[CrossRef](#)] [[PubMed](#)]
48. Loscher, W. Critical review of current animal models of seizures and epilepsy used in the discovery and development of new antiepileptic drugs. *Seizure* **2011**, *20*, 359–368. [[CrossRef](#)] [[PubMed](#)]
49. Serdiuk, S.E.; Gmiro, V.E. Phenylephrine potentiates antidepressive and eliminates sedative action of amitriptyline in rats. *Russ Fiziol. Zh Im I M Sechenova* **2014**, *100*, 18–26. [[PubMed](#)]
50. Racine, R.J. Modification of seizure activity by electrical stimulation. II. Motor seizure. *Electroencephalogr. Clin. Neurophysiol.* **1972**, *32*, 281–294. [[CrossRef](#)]
51. Sadek, B.; Oz, M.; Nurulain, S.M.; Jayaprakash, P.; Latacz, G.; Kiec-Kononowicz, K.; Szymanska, E. Phenylalanine derivatives with modulating effects on human  $\alpha 1$ -glycine receptors and anticonvulsant activity in strychnine-induced seizure model in male adult rats. *Epilepsy Res.* **2017**, *138*, 124–131. [[CrossRef](#)] [[PubMed](#)]
52. Cruciani, G.; Carosati, E.; De Boeck, B.; Ethirajulu, K.; Mackie, C.; Howe, T.; Vianello, R. MetaSite: Understanding metabolism in human cytochromes from the perspective of the chemist. *J. Med. Chem.* **2005**, *48*, 6970–6979. [[CrossRef](#)] [[PubMed](#)]
53. Loscher, W.; Honack, D.; Fassbender, C.P.; Nolting, B. The role of technical, biological and pharmacological factors in the laboratory evaluation of anticonvulsant drugs. III. Pentylene-tetrazole seizure models. *Epilepsy Res.* **1991**, *8*, 171–189. [[CrossRef](#)]
54. Vohora, D.; Pal, S.N.; Pillai, K.K. Thioperamide, a selective histamine H3 receptor antagonist, protects against PTZ-induced seizures in mice. *Life Sci.* **2000**, *66*, PL297–PL301. [[CrossRef](#)]
55. Sowemimo, A.A.; Adio, O.; Fagayinbo, S. Anticonvulsant activity of the methanolic extract of *Justicia extensa* T. Anders. *J. Ethnopharmacol.* **2011**, *138*, 697–699. [[CrossRef](#)] [[PubMed](#)]
56. Takei, H.; Yamamoto, K.; Bae, Y.C.; Shirakawa, T.; Kobayashi, M. Histamine H3 Heteroreceptors Suppress Glutamatergic and GABAergic Synaptic Transmission in the Rat Insular Cortex. *Front Neural Circuits.* **2017**, *9*, 85. [[CrossRef](#)] [[PubMed](#)]
57. Swinyard, E.A.; Sofia, R.D.; Kupferberg, H.J. Comparative anticonvulsant activity and neurotoxicity of felbamate and four prototype antiepileptic drugs in mice and rats. *Epilepsia* **1986**, *27*, 27–34. [[CrossRef](#)] [[PubMed](#)]
58. White, H.S. Comparative anticonvulsant and mechanistic profile of the established and newer antiepileptic drugs. *Epilepsia* **1999**, *40*, S2–S10. [[CrossRef](#)] [[PubMed](#)]



© 2018 by the authors. Licensee MDPI, Basel, Switzerland. This article is an open access article distributed under the terms and conditions of the Creative Commons Attribution (CC BY) license (<http://creativecommons.org/licenses/by/4.0/>).

**Supplementary Material**

**Studies on anticonvulsant effects of novel histamine H3R antagonists in electrically and chemically induced seizures in rats**

Alaa Alachkar<sup>1</sup>, Dorota Łażewska<sup>2</sup>, Gniewomir Latacz<sup>2</sup>, Annika Frank<sup>3</sup>, Agata Siwek<sup>4</sup>, Annamaria Lubelska<sup>2</sup>, Ewelina Honkisz-Orzechowska<sup>2</sup>, Jadwiga Handzlik<sup>2</sup>, Holger Stark<sup>3</sup>, Katarzyna Kieć-Kononowicz<sup>2†</sup>, Bassem Sadek<sup>1,\*†</sup>

<sup>†</sup>These authors have contributed equally to this work.

<sup>1</sup>Department of Pharmacology & Therapeutics, College of Medicine & Health Sciences, United Arab Emirates University, P.O. Box 17666 Al Ain, United Arab Emirates.

<sup>2</sup>Department of Technology and Biotechnology of Drugs, Faculty of Pharmacy, Jagiellonian University Medical College, 9 Medyczna Street, 30-688 Kraków, Poland.

<sup>3</sup>Institute of Pharmaceutical and Medicinal Chemistry, Heinrich Heine University Düsseldorf, Universitätsstr. 1, 40225 Duesseldorf, Germany.

<sup>4</sup>Department of Pharmacobiology, Faculty of Pharmacy, Jagiellonian University Medical College, 9 Medyczna Street, 30-688 Kraków, Poland.

\* Corresponding address: bassem.sadek@uaeu.ac.ae; Tel + 971 3 7137 512; Fax + 971 3 7672 033

## 6 Studies on anticonvulsant effects of novel histamine H3R antagonists in electrically and chemically induced seizures in rats

Table. Anticonvulsant effects of H3R antagonists 1-16 in MES-, PTZ-, and STR-induced seizures.

Group	MES <sup>a</sup> -induced seizure	Group	PTZ <sup>b</sup> -induced seizure		Group	STR <sup>c</sup> -induced seizure	
	Average THLE (s)		Average seizure score	% Protection against GTCS		Average seizure score	% Protection against GTCS
SAL	8.14±1.17	SAL	4.71±0.16	28.57	SAL	5.00±0.00	NP
PHT (10 mg)	0.90±0.19 <sup>**</sup>	VPA (300 mg)	0.00±0.00 <sup>**</sup>	100	VPA (300 mg)	0.43±0.27 <sup>**</sup>	100
1 <sup>d</sup>	6.43±1.14	1 <sup>d</sup>	4.00±0.35	57.14	1 <sup>d</sup>	4.43±0.27	42.86
2 <sup>d</sup>	7.86±0.84	2 <sup>d</sup>	4.43±0.27	42.86	2 <sup>d</sup>	4.57±0.19	28.57
3 <sup>d</sup>	1.29±0.17 <sup>**</sup>	3 <sup>d</sup>	4.29±0.17	71.43	3 <sup>d</sup>	4.29±0.39	42.86
4 <sup>d</sup>	0.57±0.21 <sup>**</sup>	4 <sup>d</sup>	0.00±0.00 <sup>**</sup>	100	4 <sup>d</sup>	4.57±0.19	28.57
5 <sup>d</sup>	1.71±0.26 <sup>**</sup>	5 <sup>d</sup>	4.43±0.34	28.57	5 <sup>d</sup>	4.57±0.19	42.86
6 <sup>d</sup>	3.00±0.75 <sup>*</sup>	6 <sup>d</sup>	4.14±0.24	71.43	6 <sup>d</sup>	4.43±0.27	42.86
7 <sup>d</sup>	2.00±0.49 <sup>**</sup>	7 <sup>d</sup>	0.00±0.00 <sup>**</sup>	100	7 <sup>d</sup>	4.86±0.13	14.29
8 <sup>d</sup>	5.71±1.39 <sup>*</sup>	8 <sup>d</sup>	4.29±0.33	57.14	8 <sup>d</sup>	4.43±0.19	42.86
9 <sup>d</sup>	8.29±1.57	9 <sup>d</sup>	4.57±0.27	28.57	9 <sup>d</sup>	4.57±0.19	42.86
10 <sup>d</sup>	6.43±0.75	10 <sup>d</sup>	4.43±0.19	57.14	10 <sup>d</sup>	4.71±0.17	28.57
11 <sup>d</sup>	8.14±0.62	11 <sup>d</sup>	0.00±0.00 <sup>**</sup>	100	11 <sup>d</sup>	4.29±0.33	42.86
12 <sup>d</sup>	7.86±0.51	12 <sup>d</sup>	2.86±0.62 <sup>*</sup>	71.43	12 <sup>d</sup>	4.43±0.27	42.86
13 <sup>d</sup>	6.43±1.14	13 <sup>d</sup>	2.14±0.47 <sup>*</sup>	85.71	13 <sup>d</sup>	2.00±0.35 <sup>**</sup>	100
14 <sup>d</sup>	3.14±0.59 <sup>*</sup>	14 <sup>d</sup>	3.71±0.56 <sup>*</sup>	42.86	14 <sup>d</sup>	4.57±0.19	28.57
15 <sup>d</sup>	7.14±0.74	15 <sup>d</sup>	3.86±0.51 <sup>*</sup>	57.14	15 <sup>d</sup>	4.00±0.40	57.14
16 <sup>d</sup>	6.57±1.22	16 <sup>d</sup>	4.00±0.53	42.86	16 <sup>d</sup>	4.43±0.27	42.86
4 <sup>e</sup>	5.83±1.01 <sup>†*</sup>	4 <sup>e</sup>	2.29±0.44 <sup>†*</sup>	100	13 <sup>e</sup>	4.86±0.13	14.29
4 <sup>f</sup>	2.50±1.21 <sup>**†</sup>	4 <sup>f</sup>	0.71±0.31 <sup>**†</sup>	100	13 <sup>f</sup>	3.00±0.31 <sup>**</sup>	85.71
4 <sup>g</sup>	3.67±0.94 <sup>**†</sup>	4 <sup>g</sup>	0.00±0.00 <sup>**†</sup>	100	13 <sup>g</sup>	2.17±0.31 <sup>**</sup>	100
4 <sup>h</sup> +RAMH <sup>d</sup>	6.17±0.59	4 <sup>h</sup> +RAMH <sup>d</sup>	0.29±0.16 <sup>**</sup>	100	13 <sup>h</sup> +RAMH <sup>d</sup>	2.14±0.35	100
SAL+RAMH <sup>d</sup>	7.92±0.6	SAL+RAMH <sup>d</sup>	4.29±0.25 <sup>*</sup>	14.29	SAL+RAMH <sup>d</sup>	4.71±0.16	28.57

<sup>a</sup>50-Hz alternating current of 120 mA intensity applied through ear electrodes for a duration of 1 s <sup>b</sup>60 mg/kg, <sup>c</sup>3.5 mg/kg, <sup>d</sup>10 mg/kg, <sup>e</sup>2.5 mg/kg, <sup>f</sup>5 mg/kg, <sup>g</sup>15 mg/kg, and H3R antagonists 1-16 (10 mg/kg, i.p.) were injected 30-45 min before MES, PTZ (60 mg/kg, i.p.) or STR (3.5 mg/kg, i.p.) challenge. The table shows the protective effects of phenytoin (PHT, 10 mg/kg, i.p.), VPA (300 mg/kg, i.p.) and H3R antagonists 1-16 (10 mg/kg, i.p.) on the duration of tonic hind limb extension (THLE) induced in the maximal electroshock

2

(MES) model in rats. Protective effects in PTZ- and STR-induced convulsion model are expressed as score of seizures for 30 min observation time after PTZ or STR injection, and percentage generalized tonic-clonic seizures (GTCS) was observed. Dose-dependent effect of H3R antagonist 4 (2.5, 5, 10, and 15 mg/kg, i.p.) on duration of THLE induced in MES-model in rats. Dose-dependent effect of H3R antagonist 13 (2.5, 5, 10, and 15 mg/kg, i.p.) on seizure score as well as percentage of GTCS in STR-model in rats. Effect of RAMH (10 mg/kg, i.p.) pretreatment on the protection provided by H3R antagonist 4 (10 mg/kg, i.p.) against MES- and PTZ-induced seizures. Effect of RAMH (10 mg/kg, i.p.) pretreatment on the protection provided by H3R antagonist 13 (10 mg/kg, i.p.) against STR-induced seizures. Each value represents mean ± SEM (n=6-7). <sup>\*</sup>P< 0.05 vs. (saline)-treated group. <sup>\*\*</sup>P< 0.001 vs. (saline)-treated group. <sup>†</sup>P< 0.05 vs. (5 mg)-treated group.

3

## 7 Talipexole variations as novel bitopic dopamine D<sub>2</sub> and D<sub>3</sub> receptor ligands

Stank L<sup>1</sup>, Frank A<sup>1</sup>, Hagenow S<sup>1</sup>, Stark H<sup>1</sup>, **2019**.

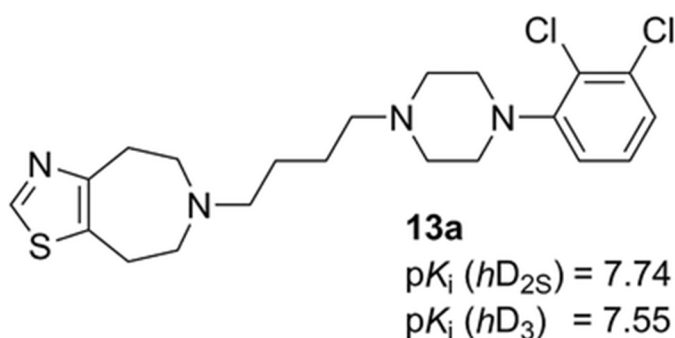
<sup>1</sup>Institute of Pharmaceutical and Medicinal Chemistry, Heinrich Heine University Düsseldorf, Universitaetsstr. 1, 40225  
Duesseldorf, Germany

Published in: *MedChemComm*; epub, ahead of print.

DOI: 10.1039/C9MD00379G.

Research contribution: Pharmacological evaluation of compounds at the D<sub>2</sub> and D<sub>3</sub> receptor, interpretation of data and partial preparation of manuscript.

Graphical abstract:



Reproduced from Stank et al. (Lars Stank, Annika Frank, Stefanie Hagenow, Holger Stark, *MedChemComm*, 2019, DOI: 10.1039/C9MD00379G, Talipexole variations as novel bitopic dopamine D<sub>2</sub> and D<sub>3</sub> receptor ligands) with permission from The Royal Society of Chemistry.



Cite this: DOI: 10.1039/c9md00379g

Received 24th July 2019,  
Accepted 12th August 2019

DOI: 10.1039/c9md00379g

rsc.li/medchemcomm

Talipexole variations as novel bitopic dopamine D<sub>2</sub> and D<sub>3</sub> receptor ligands

Lars Stank, Annika Frank, Stefanie Hagenow and Holger Stark \*

We linked 2-aminothiazoloazepane scaffolds with phenylpiperazine pharmacophores to generate bitopic dopamine receptor ligands. Highest D<sub>2</sub>R/D<sub>3</sub>R binding affinities up to pK<sub>i</sub> values of 7.74 were observed for compounds containing a 1-(2,3-dichlorophenyl)piperazinoyl moiety, maintaining affinity with deaminated 5,6,7,8-tetrahydro-4H-thiazoloazepine derivatives.

Targeting dopamine receptors in neuropsychiatric diseases like Parkinson's disease (PD) has become a common strategy.<sup>1</sup> Although numerous drugs are applied, few overcome the challenges presented by the receptor's particularities. Dopamine receptors are divided into two families according to their G-protein coupling and signalling pathways: D<sub>1</sub>-like receptors (D<sub>1</sub> and D<sub>5</sub> receptor subtypes) activate, while D<sub>2</sub>-like receptors (D<sub>2</sub>, D<sub>3</sub> and D<sub>4</sub> receptor subtypes) inhibit adenylyl cyclase. In particular, dopamine D<sub>2</sub> and D<sub>3</sub> receptors (D<sub>2</sub>R/D<sub>3</sub>R) are highly investigated for their specific receptor properties and treatment opportunities for PD or schizophrenia. Recent research puts emphasis on the development of bitopic ligands bearing two pharmacophores to target the orthosteric binding pocket (OBP) and the secondary allosteric binding pocket (SBP) found within the receptors.<sup>2,3</sup> The SBP is not as highly conserved as the OBP in the D<sub>2</sub>R and D<sub>3</sub>R. Hence, bitopic ligands provide higher subtype selectivity or modified pharmacodynamic properties such as functional selectivity or kinetic interaction with additional binding regions.<sup>4</sup> For the design of bitopic ligands at the D<sub>2</sub>R and D<sub>3</sub>R, various scaffolds are described to yield satisfactory binding affinities.<sup>2,5,6</sup> They usually contain at least one basic centre to allow for interaction with the highly conserved aspartate residue in the OBP. Among these promising scaffolds are (2-methoxyphenyl)piperazines and (2,3-dichlorophenyl)piperazines as shown in compounds D-210 and D-219 (Fig. 1). In these compounds, dopamine's catechol moiety is replaced by a bioisosteric aminothiazole that was found to bind to the D<sub>2</sub>R and D<sub>3</sub>R in nanomolar concentration ranges when coupled to arylpiperazines.<sup>7,8</sup> The aminothiazole derivative talipexole (Fig. 1 and Table 1) was developed as a dopamine D<sub>2</sub>R/D<sub>3</sub>R agonist for symptomatic treatment of PD and is approved by the Japanese Pharmaceuticals and Medical Devices

Agency (PMDA). Talipexole features incorporation of its basic amine into a ring system, thereby lacking stereo-selectivity of compounds D-210 and D-219. Reducing stereochemistry in molecules is beneficial for drug development as it facilitates synthesis and purification and simplifies clinical development. Thus, talipexole derivatives were coupled to arylpiperazines or other motifs *via* different alkyl linkers, to achieve bitopic ligands containing two basic centres without stereo-chemical properties. The second motif did include classic scaffolds like (2,3-dichlorophenyl)piperazine or (2-methoxyphenyl)piperazine, but also unusual motifs to generate more versatile bitopic compounds. The objective was to modify their binding selectivity compared to talipexole. Additionally, the influence of amination or deamination of these aminothiazoles was evaluated to explore bioisosteric exchange of catechols.

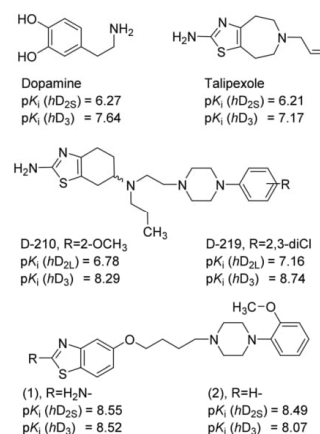


Fig. 1 Structures and pK<sub>i</sub> values of dopamine,<sup>8</sup> talipexole<sup>9</sup> and bitopic D<sub>2</sub>/D<sub>3</sub> receptor ligands.<sup>7,8</sup>

Institute of Pharmaceutical and Medicinal Chemistry, Heinrich Heine University Düsseldorf, Universitätsstr. 1, 40225 Düsseldorf, Germany.  
E-mail: stark@hhu.de



# 7 Talipexole variations as novel bitopic dopamine D<sub>2S</sub> and D<sub>3</sub> receptor ligands

View Article Online

Research Article

MedChemComm

**Table 1** *In vitro* binding affinities at human dopamine D<sub>2S</sub> and D<sub>3</sub> receptors of bitopic talipexole derivatives

Compound	R <sup>1</sup>	n	R <sup>2</sup>	<i>h</i> D <sub>2S</sub> p <i>K<sub>i</sub></i> $\bar{x}$ ( $\pm$ S.E.M.)	<i>h</i> D <sub>3</sub> p <i>K<sub>i</sub></i> $\bar{x}$ ( $\pm$ S.E.M.)
Talipexole	H <sub>2</sub> N-	1		6.21 <sup>9</sup> ( $\pm$ 0.02)	7.17 <sup>9</sup> ( $\pm$ 0.03)
12a	H <sub>2</sub> N-	4		7.65 ( $\pm$ 0.09)	7.59 ( $\pm$ 0.11)
12b	H <sub>2</sub> N-	4		5.56 ( $\pm$ 0.07)	5.42 ( $\pm$ 0.11)
13a	H-	4		7.74 ( $\pm$ 0.05)	7.55 ( $\pm$ 0.09)
13b	H-	4		5.60 ( $\pm$ 0.09)	5.51 ( $\pm$ 0.15)
13c	H-	2		4.38 ( $\pm$ 0.01)	4.91 ( $\pm$ 0.21)
13d	H-	2		6.82 ( $\pm$ 0.15)	6.62 ( $\pm$ 0.05)
13e	H-	3		7.19 ( $\pm$ 0.10)	6.78 ( $\pm$ 0.13)
13f	H-	4		7.07 ( $\pm$ 0.07)	6.51 ( $\pm$ 0.19)
13g	H-	4		5.20 ( $\pm$ 0.27)	5.42 ( $\pm$ 0.18)
13h	H-	4		5.26 ( $\pm$ 0.20)	6.35 ( $\pm$ 0.17)
14				6.75 ( $\pm$ 0.21)	6.59 ( $\pm$ 0.12)

p*K<sub>i</sub>* values are derived by incubating membrane preparations from CHO-K1 cells, stably expressing the human D<sub>2S</sub>R (25  $\mu$ g per well) or D<sub>3</sub>R (20  $\mu$ g per well) with the compound and [<sup>3</sup>H]spiperone (0.2 nM) for 120 min at RT. Data represent the mean ( $\bar{x}$ )  $\pm$  standard error of mean (S.E.M.) of at least three independent experiments (two for compounds 13c–13e and 12b), each performed in triplicates with seven appropriate concentrations or in duplicates with eleven concentrations.

The three 5,6,7,8-tetrahydro-4*H*-scaffolds 2-aminothiazolo[4,5-*d*]azepine **6**, thiazolo[4,5-*d*]azepine **8** and thiazolo[5,4-*c*]azepine **9** were prepared according to Scheme 1. Carboxybenzyl (Cbz)-protected piperidone underwent ring expansion by means of freshly synthesized ethyl diazoacetate **2** and a Lewis acid to form the azepanone derivative **3**. Cleavage of the  $\beta$ -keto ester with a strong base produced **4**. The  $\alpha$ -keto position of **4** was brominated and subsequently converted with thiourea in a Hantzsch thiazole synthesis, yielding **5**, a mixture of two 2-aminothiazole isomers. Due to their similar physicochemical properties, the resulting isomers were not separated, but instead were used without further purification in the next steps. They were either directly deprotected using strong acid (**6**) or deaminated with isopentyl nitrite in THF, followed by deprotection (**8** and **9**). Secondary amines **6**,

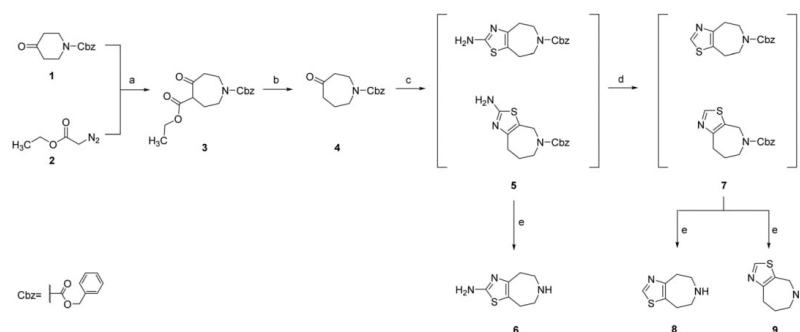
**8** and **9** were each isolated by column chromatography after the deprotection step. The regioisomer of **6** was neither isolated nor used for further synthesis. Alcohols **10a–g** were converted to the respective aldehydes **11a–g** by Swern oxidation (Scheme 2). **11g** was obtained by deprotection of *N*-(4,4-diethoxybutyl)adamantane-1-carboxamide. Aldehydes **11a–h** were used without further purification for reductive amination of either thiazoloazepane **6**, **8** or **9** to form target compounds **12–14**. Compounds were investigated for their binding affinities (Table 1) by [<sup>3</sup>H]spiperone displacement studies in binding buffer (120 mM NaCl, 5 mM KCl, 1 mM CaCl<sub>2</sub>, 1 mM MgCl<sub>2</sub>, 50 mM Tris) using crude membrane extracts prepared from stably transfected CHO-K1 cells, overexpressing human D<sub>2S</sub> and D<sub>3</sub> receptors as described previously.<sup>7</sup> CHO-K1 cells (American Type Culture Collection,

## 7 Talipexole variations as novel bitopic dopamine D2 and D3 receptor ligands

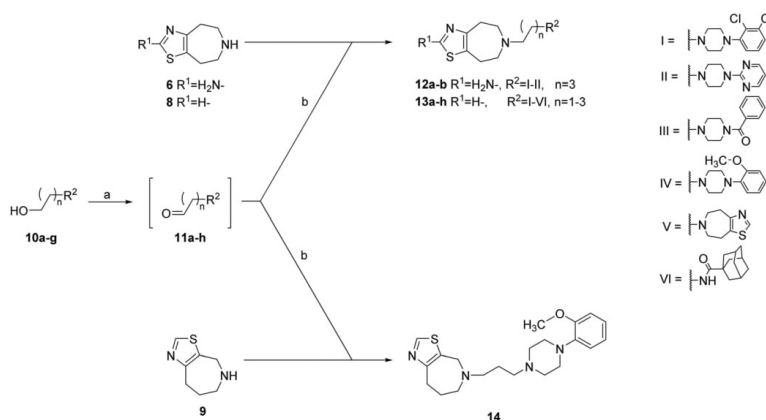
MedChemComm

View Article Online

Research Article



**Scheme 1** Synthesis of thiazoloazepanes. Reagents and conditions: (a) boron trifluoride diethyl etherate, Et<sub>2</sub>O, -78 °C, 1 h; (b) KOH, EtOH/H<sub>2</sub>O, reflux, 2.5 h; (c) Br<sub>2</sub>, CHCl<sub>3</sub>, rt, until completion, followed by thiourea, EtOH, rt to reflux, 2 h; (d) isopentyl nitrite, THF, reflux, 2 h; (e) 6 N HCl, iPrOH, reflux, 10 h.



**Scheme 2** Coupling of thiazoloazepanes to arylpiperazines. Reagents and conditions: (a) oxalyl chloride, dimethyl sulfoxide, Et<sub>3</sub>N, DCM, -50 °C, 0.5 h; (b) Na(OAc)<sub>3</sub>BH, 1,2-dichloroethane, rt, overnight.

Rockville, MD; CCL 61) were transfected using pAXhd2 and pSVD<sub>3</sub> plasmids, respectively. CHO-K1 cells for D<sub>3</sub>R transfection were deficient in dihydrofolate reductase. The final constructs of stably transfected CHO-K1 cell lines for D<sub>2s</sub>R and D<sub>3</sub>R were kindly donated by Prof. Dr. Shine (Australia) and Prof. Dr. Sokoloff (France), respectively.

Among bitopic talipexole derivatives, highest affinities at the D<sub>2</sub>R and the D<sub>3</sub>R were found for compounds containing a 1-(2,3-dichloro)piperazine moiety (12a and 13a). Compared to talipexole,<sup>9</sup> 12a and 13a showed improved D<sub>2</sub>R/D<sub>3</sub>R affinity, while minor D<sub>3</sub>R preference is abolished in these bitopic ligands. In contrast, tetrathydrobenzothiazoles D-210 and D-219 (Fig. 1) showed a D<sub>3</sub>R preference.<sup>8</sup> Interestingly, a slight D<sub>3</sub>R preference was found for adamantane-1-carboxamide (13h). A pair of 2-aminothiazoles and their deaminated analogues (12a & 13a, 12b & 13b) were synthesized in order to evaluate the impact of the aromatic amino group

on D<sub>2</sub>R/D<sub>3</sub>R affinity. Since the deamination was performed without loss of affinity, the deaminated core motif was chosen as our preferred pharmacophore for the design of further bitopic dopamine receptor ligands. It has to be noted that deamination of compound 13f could contribute to these findings, but was not performed in this small series. Variation of the alkyl linker lengths between the two pharmacophores of deaminated 1-(2-methoxyphenyl)piperazine-coupled talipexole derivatives showed minor influences on D<sub>2</sub>R/D<sub>3</sub>R affinity with a slight tendency for D<sub>2</sub>R preference with prolonged linker lengths (13f & 13e > 13d). These findings are in good accordance with bitopic (de)aminated benzothiazoles (compounds 1 and 2, Fig. 1) coupled to analogous arylpiperazine motifs.<sup>7</sup> In contrast to this, a small series of structurally related tetrathydrobenzothiazoles, *e.g.*, D-210 and D-219 (Fig. 1), achieved D<sub>3</sub>R preference, showing negligible affinity differences for two and four carbon linkers.<sup>8,10</sup> The influence of the highly

flexible alkyl lengths on dopamine receptor subtype selectivity remains controversial,<sup>3</sup> but appears to be less crucial for (de)aminated thiazoles. However, it would have been interesting to perform these alterations with compounds 12a and 12b, but within this small series they were not conducted. The necessity of the 2-amino moiety for thiazoles as catechol bioisosteres is also still disputed. In most cases, the amino function was preserved due to initial assumptions of its pivotal importance or completely replaced by different bioisosteric heterocycles.<sup>11,12</sup> However, the importance and arrangement of hydrogen-bond donors and acceptors of heterocyclic catechol bioisosteres is not fully understood. While aromatic planar systems provide  $\pi$ -stacking interactions with aromatic amino acids in the binding pocket, endo/exocyclic hydrogen-bond donor properties (e.g. hydroxyl and amino groups) are hypothesized to be compensable either by hydrophobic interactions or water-mediated ligand-receptor interactions.<sup>12,13</sup> Thus, potent and selective heterocyclic ligands, lacking hydrogen donor functions or even non-aromatic, but conjugated bitopic enyne-type ligands are described.<sup>14–16</sup> Modification on hydrogen-bond donor and acceptor capacities, i.e. deamination of 2-aminothiazole, provides alterations of physicochemical properties, being determining factors for drug-likeness and for bioavailability of drug candidates. Accordingly, deaminated thiazoles, providing only proton acceptor properties, may be novel suitable catechol bioisosteres to fit the D<sub>2</sub>R/D<sub>3</sub>R binding pocket. However, the homobivalent compound 13g showed only marginal affinity at both dopamine receptors. This demonstrates the more dominant impact on receptor binding by the arylpiperazine pharmacophore rather than the thiazolozepane moiety of the presented bitopic ligands. Repositioning of the azepane nitrogen led to the decrease of D<sub>2</sub>R affinity (13e vs. 14). Although some of the compounds could improve on binding affinity compared to talipexole, they lacked the desired selectivity. Nonetheless, they provide valuable insights into the SAR of bioisosteric exchange with aminothiazoles. *In silico* evaluation of these compounds could yield a structural rationale for their lack of selectivity and provide optimization proposals for further derivatization of the 5,6,7,8-tetrahydro-4H-thiazolozepine motif.<sup>17</sup>

## Conclusions

With advantages over the tetrathydrobenzothiazoles (D-210 and D-219),<sup>8</sup> synthesized talipexole derivatives are achiral, do not require stereo-selective synthesis with further characterization of enantiomers, and therefore may be more favourable for drug development. With this small series of bitopic talipexole derivatives, it could be shown that deamination of bitopic thiazole-type ligands is well tolerated by D<sub>2</sub>Rs/D<sub>3</sub>Rs. By increasing the library of bitopic ligands, further exploration regarding the possibilities of this targeting approach is facilitated and 1-(2,3-dichloro)piperazines, connected *via* a flexible alkyl linker, are proven valuable pharmacophores for increasing dopamine receptor affinity within bitopic compounds. Synthesis of deaminated thiazoles for adjusting

physicochemical properties provides suitable scaffolds for bitopic dopamine D<sub>2</sub>R/D<sub>3</sub>R ligands, awaiting prospective modification for lead optimization to further improve affinity and modulate subtype selectivity.

## Conflicts of interest

There are no conflicts to declare.

## Acknowledgements

AF and HS are kindly funded by the GRK2158, HS was also supported by the EU COST Actions CA15135 and CA18133. The CHO-K1 cell lines for D<sub>2</sub>R and D<sub>3</sub>R were kindly donated by Prof. Shine (Australia) and Prof. Sokoloff (France), respectively.

## Notes and references

- W. Poewe, K. Seppi, C. Tanner, G. M. Halliday, P. Brundin, J. Volkmann, A. E. Schrag and A. E. Lang, *Nat. Rev. Dis. Primers*, 2017, 3, 17013, DOI: 10.1038/nrdp.2017.13.
- A. H. Newman, T. Beuming, A. K. Banala, P. Donthamsetti, K. Pongetti, A. LaBounty, B. Levy, J. Cao, M. Michino, R. R. Luedtke, J. Javitch and L. J. Shi, *J. Med. Chem.*, 2012, 55, 6689–6699.
- S. Kassel, J. S. Schwed and H. Stark, *Eur. Neuropsychopharmacol.*, 2015, 25, 1480–1499.
- P. Fronik, B. I. Gaiser and D. Sejer Pedersen, *J. Med. Chem.*, 2017, 60, 4126–4134.
- S. N. Mistry, J. Shonberg, C. J. Draper-Joyce, C. Klein Herenbrink, M. Michino, L. Shi, A. Christopoulos, B. Capuano, P. J. Scammells and J. R. Lane, *J. Med. Chem.*, 2015, 58, 6819–6843.
- B. Ghosh, T. Antonio, M. E. A. Reith and A. K. Dutta, *J. Med. Chem.*, 2010, 53, 2114–2125.
- M. Schübler, B. Sadek, T. Kottke, L. Weizel and H. Stark, *Front. Chem.*, 2017, 5, 1–19.
- S. Biswas, S. Hazeldine, B. Ghosh, I. Parrington, E. Kuzhikandathil, M. E. A. Reith and A. K. Dutta, *J. Med. Chem.*, 2008, 51, 3005–3019.
- A. Newman-Tancredi, D. Cussac, V. A. L. Erie, J. Nicolas and F. R. Ed, *J. Pharmacol. Exp. Ther.*, 2002, 303, 805–814.
- G. Modi, T. Antonio, M. Reith and A. K. Dutta, *Med. Chem.*, 2014, 57, 1557–1572.
- J. Maillard, P. Delaunay, M. Langlois, B. Portevin, J. Legeai and C. Manuel, *Eur. J. Med. Chem.*, 1984, 19, 451–456.
- F. Boeckler and P. Gmeiner, *Pharmacol. Ther.*, 2006, 112, 281–333.
- F. Boeckler and P. Gmeiner, *Biochim. Biophys. Acta*, 2007, 1768, 871–887.
- M. Dörfler, N. Tschammer, K. Hamperl, H. Hübner and P. Gmeiner, *J. Med. Chem.*, 2008, 51, 6829–6838.
- J. Elsner, F. Boeckler, F. W. Heinemann, H. Hübner and P. Gmeiner, *J. Med. Chem.*, 2005, 48, 5771–5779.
- C. Hiller, R. C. Kling, F. W. Heinemann, K. Meyer, H. Hübner and P. Gmeiner, *J. Med. Chem.*, 2013, 56, 5130–5141.
- M. Michino, T. Beuming, P. Donthamsetti, A. Hauck Newman, J. A. Javitch and L. Shi, *Pharmacol. Rev.*, 2015, 67, 198–213.

## 8 Prior activation of 5-HT<sub>7</sub> receptors modulates the conditioned place preference with methylphenidate

Carbone C<sup>1</sup>, Lo Russo SLM<sup>1</sup>, Lacivita E<sup>2</sup>, Frank A<sup>3</sup>, Alleva E<sup>1</sup>, Stark H<sup>3</sup>, Saso L<sup>4</sup>, Leopoldo M<sup>2,5</sup>, Adriani W<sup>1</sup>, **2019**.

<sup>1</sup>Center for Behavioral Sciences and Mental Health, Istituto Superiore di Sanità, Rome, Italy

<sup>2</sup>Dipartimento di Farmacia—Scienze del Farmaco, Università degli Studi di Bari, Bari, Italy

<sup>3</sup>Institute of Pharmaceutical and Medicinal Chemistry, Heinrich Heine University Düsseldorf, Düsseldorf, Germany

<sup>4</sup>Department of Physiology and Pharmacology “V. Erspamer”, Sapienza University, Rome, Italy

<sup>5</sup>BIOFORDRUG s.r.l., Università degli Studi di Bari, Bari, Italy

Published in: *Frontiers in Behavioral Neuroscience*, **13**: 208.

DOI: 10.3389/fnbeh.2019.00208.

Research contribution: Pharmacological affinity evaluation of compounds at the D<sub>1</sub>, D<sub>2</sub>, D<sub>3</sub> and D<sub>5</sub> receptor, interpretation of data and partial preparation of manuscript.

Reprinted by permission from the authors. Cristiana Carbone, Sara Lucia Maria Lo Russo, Enza Lacivita, Annika Frank, Enrico Alleva, Holger Stark, Luciano Saso, Marcello Leopoldo, Walter Adriani, *Frontiers in Behavioral Neuroscience*, Prior activation of 5-HT<sub>7</sub> receptors modulates the conditioned place preference with methylphenidate, 2019, 13: 208, DOI: 10.3389/fnbeh.2019.00208.





## Prior Activation of 5-HT7 Receptors Modulates the Conditioned Place Preference With Methylphenidate

Cristiana Carbone<sup>1</sup>, Sara Lucia Maria Lo Russo<sup>1</sup>, Enza Lacivita<sup>2</sup>, Annika Frank<sup>3</sup>, Enrico Alleva<sup>1</sup>, Holger Stark<sup>3</sup>, Luciano Saso<sup>4</sup>, Marcello Leopoldo<sup>2,5</sup> and Walter Adriani<sup>1\*</sup>

<sup>1</sup>Center for Behavioral Sciences and Mental Health, Istituto Superiore di Sanità, Rome, Italy, <sup>2</sup>Dipartimento di Farmacia—Scienze del Farmaco, Università degli Studi di Bari, Bari, Italy, <sup>3</sup>Institute of Pharmaceutical and Medicinal Chemistry, Heinrich Heine University Düsseldorf, Düsseldorf, Germany, <sup>4</sup>Department of Physiology and Pharmacology "V. Erspamer", Sapienza University, Rome, Italy, <sup>5</sup>BIOFORDRUG s.r.l., Università degli Studi di Bari, Bari, Italy

### OPEN ACCESS

#### Edited by:

Liana Fattore,  
Italian National Research Council  
(CNR), Italy

#### Reviewed by:

Alfredo Meneses,  
Center for Research and Advanced  
Studies (CINVESTAV), Mexico  
Frank Scott Hall,  
University of Toledo, United States  
Agnieszka Nikiforuk,  
Polish Academy of Sciences, Poland

#### \*Correspondence:

Walter Adriani  
walter.adriani@iss.it

#### Specialty section:

This article was submitted to  
Motivation and Reward, a section of  
the journal *Frontiers in Behavioral  
Neuroscience*

**Received:** 20 September 2018

**Accepted:** 29 August 2019

**Published:** 18 September 2019

#### Citation:

Carbone C, Lo Russo SLM,  
Lacivita E, Frank A, Alleva E, Stark H,  
Saso L, Leopoldo M and Adriani W  
(2019) Prior Activation of 5-HT7  
Receptors Modulates the  
Conditioned Place Preference With  
Methylphenidate.  
*Front. Behav. Neurosci.* 13:208.  
doi: 10.3389/fnbeh.2019.00208

The serotonin receptor subtype 7 (5-HT7R) is clearly involved in behavioral functions such as learning/memory, mood regulation and circadian rhythm. Recent discoveries proposed modulatory physiological roles for serotonergic systems in reward-guided behavior. However, the interplay between serotonin (5-HT) and dopamine (DA) in reward-related behavioral adaptations needs to be further assessed. TP-22 is a recently developed arylpiperazine-based 5-HT7R agonist, which is also showing high affinity and selectivity towards D1 receptors. Here, we report that TP-22 displays D1 receptor antagonist activity. Moreover, we describe the first *in vivo* tests with TP-22: first, a pilot experiment (assessing dosage and timing of action) identified the 0.25 mg/kg i.v. dosage for locomotor stimulation of rats. Then, a conditioned place preference (CPP) test with the DA-releasing psychostimulant drug, methylphenidate (MPH), involved three rat groups: prior i.v. administration of TP-22 (0.25 mg/kg), or vehicle (VEH), 90 min before MPH (5 mg/kg), was intended for modulation of conditioning to the white chamber (saline associated to the black chamber); control group (SAL) was conditioned with saline in both chambers. Prior TP-22 further increased the stimulant effect of MPH on locomotor activity. During the place-conditioning test, drug-free activity of TP-22+MPH subjects remained steadily elevated, while VEH+MPH subjects showed a decline. Finally, after a priming injection of TP-22 in MPH-free conditions, rats showed a high preference for the MPH-associated white chamber, which conversely had vanished in VEH-primed MPH-conditioned subjects. Overall, the interaction between MPH and pre-treatment with TP-22 seems to improve both locomotor stimulation and the conditioning of motivational drives to environmental cues. Together with recent studies, a main modulatory role of 5-HT7R for the processing of rewards can be suggested. In the present study, TP-22 proved to be a useful psychoactive tool to better elucidate the role of 5-HT7R and its interplay with DA in reward-related behavior.

**Keywords:** reward processing, behavioral adaptation, context evaluation, 5-HT, DA, memory consolidation, synaptic plasticity

## 8 Prior activation of 5-HT7 receptors modulates the conditioned place preference with methylphenidate

Carbone et al.

5-HT7R Activation in Modulating Reward

### INTRODUCTION

The neurotransmitter serotonin (5-hydroxy-tryptamine, 5-HT) is responsible for multiple physiological functions, including modulation of behavioral flexibility, cognition and memory processing, whereas its dysregulation has been often identified in many psychiatric disorders (Branchi, 2011; Sachs et al., 2015) as well as in addictive behavior (Müller and Homberg, 2014). Serotonergic drugs are widely used for therapy or abused as recreational drugs. Nevertheless, 5-HT multiple physiological roles are still under investigation and studies have often provided conflicting results, probably depending on different functioning of its many receptor subtypes. Among these subtypes, the serotonin 7 receptor (5-HT7R) was the last to be discovered, in 1993 (Bard et al., 1993). 5-HT7R is positively coupled to adenylate cyclase (AC) through activation of Gs, resulting in an intracellular increase of cAMP (Lovenberg et al., 1993; Ruat et al., 1993), and can also couple with G12, thus modulating neuronal morphology and increasing the neural network construction through activation of MMP-9 and Cdc42 (Bijata et al., 2017). 5-HT7R is broadly expressed in the central nervous system (CNS), with high concentrations in raphe, limbic areas, putamen and caudate nuclei, as well as in cortical regions (Leopoldo et al., 2011). 5-HT7R's wide distribution in the CNS reflects its involvement in many functions (thermoregulation, circadian rhythm, sleep, learning, and memory). A dysregulation of 5-HT7Rs has been related to many neuropathological processes as well as to cognitive and mood dysfunctions, including anxiety, schizophrenia and depression (Kvachnina et al., 2005; Hedlund, 2009; Nikiforuk, 2015).

Assessing the exact implication of 5-HT7R in brain physiologic and pathologic mechanisms is complex because of the interaction between 5-HT7 and 5-HT1A receptors (Eriksson et al., 2012). These two receptor subtypes are localized in the same brain areas and exert opposite effects on the intracellular levels of cAMP. Unfortunately, most of the available ligands show a similar affinity for both receptors. Besides, 5-HT7 and 5-HT1A receptors can form both homo- and hetero-dimers (Renner et al., 2012). Functionally, the 5-HT7/5-HT1A hetero-dimerization decreases 5-HT1A receptor activity without affecting 5-HT7R-mediated signaling. In addition, hetero-dimerization is involved in the initiation of the serotonin-mediated 5-HT1A receptor internalization. A great advancement in this research area has been obtained with the identification of selective 5-HT7R antagonists and, more recently, of agonists.

Among these, the brain penetrant selective agonist LP-211 showed to be a suitable tool to elucidate the multiple functions of 5-HT7R *in vivo* (Romano et al., 2014). In previous studies, we investigated the modulatory effects of LP-211 on learning and memory processing, resulting in alterations of behavioral parameters (Beaudet et al., 2017; Carbone et al., 2018). In particular, activation of 5-HT7Rs, through LP-211 administration in rats, seems to favor exploration by enhancing visual consolidation and improving the ability to discriminate a familiar environment. Furthermore, LP-211 seems to strengthen the consolidation of emotional components of memory. These results suggest the potential use of LP-211 in the treatment of

diseases that imply cognitive as well as emotional impairments, including depressive-like behavior (Zhang et al., 2015).

However, the activation of 5-HT7R alone gave contrasting results in several studies concerning the modulatory effect of this receptor on the depressive as well as the anxious-like behavior (Balcer et al., 2019; Maxwell et al., 2019). Indeed, while some research suggests that the blockade of the 5-HT7R is responsible for an antidepressant and anxiolytic effect (Lax et al., 2018), others prove that these same effects are unexpectedly also mediated by the activation of this receptor (Zhang et al., 2015). A possible explanation of this apparent inconsistency may rely on the synergistic role of both the serotonergic and the dopaminergic systems in modulating cognitive as well as emotional functions. Indeed, the exact direction of the serotonergic effects of drugs seems to depend on the simultaneous activation (or not) of the dopaminergic system. As just an example, the chronic administration of the selective serotonin reuptake inhibitor (SSRI) fluoxetine selectively upregulates dopamine (DA) D1-like receptors in the hippocampus of mice (Kobayashi et al., 2012); recent findings demonstrate that D1 receptors act as a pivotal mediator of the antidepressant action of this compound (Shuto et al., 2018). We underline therefore that, when studying the possible effects of a 5-HT7R-targeting drug, it is essential to also monitor for a modulatory dopaminergic intervention. Conversely, a modulatory serotonergic intervention can well be suggested, and addressed, for the well-known rewarding effects of psychostimulants.

In the present study, we tested the novel 5-HT7R agonist, TP-22, an arylpiperazine derivative structurally related to LP-211, the more thoroughly investigated agonist. TP-22 exhibited 5-HT7R agonist properties (Table 1) and improved *in vitro* metabolic stability as compared to LP-211 (half-life = 45 min and 15 min, respectively; Lacivita et al., 2016). TP-22 was able to stimulate neurite outgrowth in neuronal primary cultures in shorter time and at a lower concentration than LP-211, showing a comparable *in vivo* bio-distribution profile (brain  $C_{max}$  515 ng/mL and 540 ng/mL, respectively; Lacivita et al., 2016; Modica et al., 2018). Starting from the evidence that the administration of methylphenidate (MPH) causes an upregulation of 5-HT7Rs (Adriani et al., 2006; Leo et al., 2009), and in light of the several findings that propose a physiological role for 5-HT in reward guided behavior (Broderick and Phelix, 1997; Luo et al., 2016; Fischer and Ullsperger, 2017), we formulated the hypothesis that a previous administration of a 5-HT7 agonist could have modulatory effects on the well-known rewarding and stimulant MPH effects.

Therefore, we presently performed a conditioned place preference test (CPP), a common behavioral test for the associative rewarding effects of drugs in rodents. It is well known

**TABLE 1 |** Binding affinity profiles (data taken from Lacivita et al., 2016).

Compound	K <sub>i</sub> (nM)				
	5-HT7	5-HT1A	5-HT6	D2	Alfa-1
TP-22	25.5	771	614	522	6.6
LP-211	15	379	1,571	242	22.6



## 8 Prior activation of 5-HT7 receptors modulates the conditioned place preference with methylphenidate

Carbone et al.

5-HT7R Activation in Modulating Reward

that psychostimulant vs. rewarding action can be dissected into D1-like vs. D2-like components (Stewart and Vezina, 1989). As such, we investigated here whether TP-22 also showed affinity towards either D1/D5 or D2/D3 dopaminergic receptors. Our goal was to further assess the role of the 5-HT7R in modulating the reinforcement process, presently triggered by MPH (Cummins et al., 2013). Ultimately, we sought to better understand the interplay between 5-HT and DA in reward-related behavioral adaptations.

### MATERIALS AND METHODS

All experimental procedures have been approved by the ISS animal welfare survey board on behalf of the Italian Ministry of Health (formal license 937/2018-PR, to WA, veterinary surveillance by G. Panzini). Procedures were carried out in close agreement with the directive of the European Community Council (2010/63/EEC) and with the Italian Law guidelines. All efforts have made to minimize animal suffering and to reduce the number of animal used, according to the 3Rs principle.

#### Experiment 1: The Multidose Pilot

##### Subjects, Rearing and Testing Conditions

Experimental subjects were 15 adult male (Wistar-Han) rats, born on April 2017 from the colony in our facility (>120 days old; average weight 420 g). Animals were placed at weaning in triplets within Plexiglas cages (33 × 13 × 14 cm), in an air-conditioned room (T 21° ± 1°C, relative humidity 60 ± 10%) with a 12 h dark-light cycle (lights turned on at 8.00 PM). Water and food (Altromin-R, A. Rieper S.p.A., Vandoies, Italy) were available *ad libitum*. The experiments were conducted inside the facility animal room to minimize the impact of transport to a novel testing room.

##### Locomotor Activity With TP-22

To assess the dose-related pharmacological effect of TP-22 on rats' locomotor activity, we assigned animals to receive more than one injection following a Latin square design, to complete four dosage groups:

1. Control subjects, injected with vehicle (2% DMSO in saline solution, 200 µl/kg i.v.)
2. D25 subjects, injected with a dose of 0.25 mg/kg TP-22 i.v.
3. D12 subjects, injected with a dose of 0.12 mg/kg TP-22 i.v.
4. D06 subjects, injected with a dose of 0.06 mg/kg TP-22 i.v.

The home-cages were carefully placed on a cart, the three homemate animals were weighed, injected and gently placed individually in new home-cage-like Plexiglas cages with clean sawdust, which were immediately positioned in a recording rack. The experiment was designed so that each homemate out of a triplet was randomly assigned to receive more than one of the four planned doses (vehicle, 0.25 mg/kg, 0.12 mg/kg, 0.06 mg/kg) on separate days in a counterbalanced order. Intravenous (i.v.) injection was selected as a route of administration of TP-22 since it causes a rapid onset of action, bypassing the first-pass gastro-intestinal and hepatic metabolism. Furthermore, through i.v. administration, the possible visceral side effects (due to the

presence of 5-HT receptors in the gastro-intestinal tract) have been avoided. After injection, the rats were monitored for a total of 24 h, of which only the first 4 h after injection were analyzed.

##### Experimental Apparatus

A recording rack was used to continuously monitor for locomotion. The ActiScope system<sup>®</sup> is an automatic device, with small passive infrared sensors placed over the top of each home-cage (ActiScope; TechnoSmart, Rome, Italy)<sup>1</sup>. Locomotor activity cycle was measured as number of infrared interruptions caused by the movement of the rat (i.e., the infrared source) under the sensor (counts taken at 20 Hz, i.e., up to 20 counts per second). Data were recorded by a computer with dedicated software. Scores were automatically divided into 10-min intervals and then further grouped three by three to obtain 30-min bins. The access of authorized personnel to the animal room was not restricted and followed the routine schedule.

#### Experiment 2: Conditioned Place Preference With MPH and TP-22

##### Subjects, Rearing and Testing Conditions

Experimental subjects were 18 adult male (Wistar-Han) rats born on April 2017 from the colony in our facility (>240 days old; average weight 560 g). Animals were placed at weaning in triplets within Plexiglas cages (33 × 13 × 14 cm), in an air-conditioned room (T 21° ± 1°C, relative humidity 60 ± 10%) with a 12 h dark-light cycle (lights turned on at 8.00 PM). Water and food (Altromin-R, A. Rieper S.p.A., Vandoies, Italy) were available *ad libitum*. The experiments were conducted inside the facility animal room to minimize the impact of transport to a novel testing room.

##### Experimental Apparatus

The experimental apparatus used for the CPP test is a Black/White Box (BWB; Adriani et al., 2012), i.e., a Plexiglas box with smooth walls and floor (70 × 30 × 35 cm) composed of two environments separated by a central gray wall placed at a distance of about 35 cm from end walls. The walls on the longer sides are gray whereas those on the short margins can be distinguished by black or white color. To make the two environments more recognizable, we added additional visual cues: three horizontal white stripes to the black wall and three vertical black stripes to the white wall. On the central gray wall there is a door with an easily removable panel (partition), allowing the experimental subjects to pass (or not) from one compartment chamber to the other, when required.

On both longer sides of the box, there are two aluminum bars equipped with eight photocells connected by cables to a computer. The software in use is *Cage controller 1.27 for Dark Light for Rat and Mouse*<sup>®</sup> (PRS, Rome, Italy)<sup>2</sup>, that allows to score for each subject:

1. Motor activity (beam interruptions per second) in either chamber

<sup>1</sup>www.newbehavior.com

<sup>2</sup>www.prsitalia.it

## 8 Prior activation of 5-HT7 receptors modulates the conditioned place preference with methylphenidate

Carbone et al.

5-HT7R Activation in Modulating Reward

2. Time spent in each chamber (both forepaws and hindpaws in a same chamber)
3. Transitions (number of times a subject crosses the door between the two chambers)

Data were divided into 300 s intervals (bins).

### Experimental protocol

This test was carried out under dim light and required nine not consecutive days divided into four steps (Figures 2–4):

- **Day 1, initial preference test.** The spontaneous place preference of experimental subjects was tested in drug-free conditions. They were initially placed in the black chamber (chosen as starting room) and central door was open during the whole test (15 min). The triplet of rats residing in each home cage was tested at the same time.
- **Days 2–7, drug conditioning.** On odd days all 18 subjects were injected with saline solution only and, after injection, immediately placed in the black chamber. The central door was closed and animals were forced to remain in the black chamber for the duration of the session (25 min) in order to associate the lack of any pharmacological effect with this environment. On even days subjects were injected with only saline, 2% DMSO+MPH or TP-22+MPH according to groups described below and, after the last injection, immediately placed in the white chamber. The central door was closed so that animals were forced to stay in the white side during all the 25-min session, in order to associate the pharmacological effects with this environment. This procedure was repeated three times, alternating saline day and drugs days.
- **Day 8, post-conditioning preference test.** The post-conditioning place preference of experimental subjects was tested in drug-free conditions. This session was conducted in exactly the same way as the initial preference test (see above). Rats were placed in the black chamber as starting room and allowed to freely access and explore both environments.
- **Day 9, post-conditioning preference test with priming.** To test the acute effect of a TP-22 pre-treatment on the place preference, after a week only the MPH conditioned subjects were tested again. The rats were injected respectively with either DMSO 2% or TP-22 and, 1 h and a half after, they were placed in the black start room for the 15-min free-choice task, in MPH-free conditions.

### Conditioned CPP Drug Conditioning, Place Preference With MPH and TP-22 Modulation: Drug Conditioning

Home-cages were carefully placed one by one on a cart adjacent to the three experimental apparatuses. Rats residing in triplets within each home-cage were treated and tested at the same time. Animals were individually injected with intravenous infusions (200  $\mu$ l/kg): TP-22 at a dose of 0.25 mg/kg or vehicle, MPH (5 mg/kg), or saline solution 0.9%. Tests were conducted during the dark cycle between 9:30 AM and 14:30 PM. In this experiment, a pre-treatment with TP-22 was administered for

assessing its modulatory effects on the place conditioning with MPH and resulting preference. To study modulation by TP-22, subjects received one administration of TP-22 (or vehicle) 1 h and a half before MPH and the start of the white-chamber session. Three experimental groups were therefore formed (see Table 2):

1. Control subjects ( $N = 6$ ), injected with saline solution 0.9% immediately before the start of the session in white chamber (SAL).
2. Subjects pre-injected with vehicle (DMSO at 2% in saline,  $N = 6$ ) 1 h and a half before, then with MPH dissolved in saline solution immediately before the start of the session in white chamber (VEH+MPH).
3. Subjects pre-injected with TP-22 dissolved in vehicle (DMSO at 2% in saline,  $N = 6$ ) 1 h and a half before, then with MPH dissolved in saline solution immediately before the start of the session in white chamber (TP-22+MPH).

Timing and dose of TP-22 were selected based on the previous pilot experiment (Experiment 1), in which TP-22 showed its maximum effect on locomotor activity after 1 h 30 min at the dose of 0.25 mg/kg.

After exposure to the session in the white chamber, each subject was gently replaced in his own home-cage. On alternate days, the same subjects were exposed to the black chamber following saline injection (“biased” CPP).

### Radioligand Displacement Assays at the Human Dopamine D2 and D3 Receptors

Cell culture and membrane preparations were performed with slight modifications to Sokoloff et al. (1992). Briefly, CHO cells containing the D2-short receptor were cultured in DMEM F12 (supplemented with 10% FBS, and 1% penicillin/streptomycin). CHO cells transfected with D3 receptor were cultured in DMEM containing 1% glutamine and 10% FBS. After reaching confluence, the cells were collected in PBS buffer and centrifuged (3,000  $\times$  g, 10 min, 4°C). The pellet was resuspended in binding buffer (1 mM MgCl<sub>2</sub>, 1 mM CaCl<sub>2</sub>, 5 mM KCl, 120 mM NaCl and

TABLE 2 | Experimental groups.

SALINE GROUP	VEH+MPH GROUP	TP-22+MPH GROUP
Initial place preference test in drug free conditions.	Initial place preference test in drug free conditions.	Initial place preference test in drug free conditions.
Drug conditioning: saline in both black (3x) and white (3x) chambers.	Drug conditioning: saline in black chamber (3x), previous VEH then MPH in white chamber (3x).	Drug conditioning: saline in black chamber (3x), previous TP-22 then MPH in white chamber (3x).
Post conditioning preference test in drug free conditions.	Post conditioning preference test in drug free conditions.	Post conditioning preference test in drug free conditions.
	1 Week after	
	Post conditioning preference test in MPH free conditions with priming (VEH).	Post conditioning preference test in MPH free conditions with priming (TP-22).



## 8 Prior activation of 5-HT7 receptors modulates the conditioned place preference with methylphenidate

Carbone et al.

5-HT7R Activation in Modulating Reward

50 mM Tris, pH 7.4), disrupted and centrifuged at  $23,000 \times g$  for 30 min ( $4^{\circ}\text{C}$ ). The resulting pellet was stored in binding buffer at  $-80^{\circ}\text{C}$  for further use.

Radioligand displacement assays were performed as reported previously (Frank et al., 2018). Briefly, membrane preparations described above were co-incubated with [ $^3\text{H}$ ]spiperone (0.2 nM) and the test ligand. Non-specific binding was measured with haloperidol (10  $\mu\text{M}$ ). Concentrations required to inhibit 50% of radioligand specific radioligand binding ( $\text{IC}_{50}$ ) were determined by using six to nine different concentrations (0.01 nM–10  $\mu\text{M}$ ) of the drug studied in two or three experiments with samples in duplicate/triplicates. Apparent inhibition constant ( $K_i$ ) values were determined by non-linear least-squares fitting and equation “one site competition” using Prism 7<sup>®</sup> (GraphPad Software Inc., San Diego, CA, USA). All statistical operations were performed on the  $\text{pK}_i$  values and converted afterward to mean  $K_i$  values and the 95% confidence interval.

### Radioligand Displacement Assays at the Human Dopamine D1 and D5 Receptors

CHO cells stably expressing the human DA D1 and/or D5 receptor were washed and collected with PBS buffer. Membrane preparations were obtained as described previously (Bautista-Aguilera et al., 2017). Membrane preparations (20 and 10  $\mu\text{g}/\text{well}$  in a final volume of 0.2 ml binding buffer for D1R and D5R, respectively) were incubated for 120 min with [ $^3\text{H}$ ]-SCH23390 (0.3 nM) and the test ligand. Nonspecific binding was measured with fluphenazin (100  $\mu\text{M}$ ). Concentrations required to inhibit 50% of radioligand specific binding ( $\text{IC}_{50}$ ) were determined by using 6–9 appropriate concentrations of the drug studied in two or three experiments with samples in duplicate/triplicates. Apparent inhibition constant ( $K_i$ ) values were determined by non-linear least-squares fitting and equation “one site competition” using Prism 7<sup>®</sup> (GraphPad Software Inc., San Diego, CA, USA). All statistical operations were performed on the  $\text{pK}_i$  values and converted afterward to mean  $K_i$  values and the 95% confidence interval.

### Dopamine D1 Receptor Gs-Mediated cAMP Accumulation Assay

The agonist and antagonist properties of TP-22 against the human D1 receptor were evaluated in functional assays performed at Eurofins<sup>3</sup> using CHO cells expressing D1 and according to previously reported protocols (Zhou et al., 1990). To assess the agonist properties, TP-22 was tested using eight different concentrations in two experiments with samples in duplicate. Cellular agonist effect was calculated as % of control response to the reference agonist DA ( $\text{EC}_{50} = 24$  nM). To assess the antagonist properties, cells were stimulated with DA (125 nM) and the effect of TP-22 on cAMP production was assessed using eight different concentrations in two experiments with samples in duplicate. The antagonist effect was calculated as % inhibition of reference agonist response. The standard

D1R antagonist SCH 23390 was tested as reference compound ( $\text{IC}_{50} = 2.9$  nM,  $K_b = 0.45$  nM).

## Statistics

### Behavioral Data

#### Experiment 1

Data were analyzed using StatView II<sup>®</sup> (Abacus Concepts, CA, USA) and were processed by analysis of variance (ANOVA). Analysis was carried out by a split-plot  $4 \times 8$  model (average  $n = 10/11$  per group) with two independent variables: treatment (four levels: VEH, D25, D12, D06), and time (eight levels: 30-min bins from 4 h of registration).

#### Experiment 2

Data (displayed as mean  $\pm$  SEM) were analyzed using StatView II<sup>®</sup> (Abacus Concepts, CA, USA) and were processed by ANOVA. For test and priming (days 8 and 9), analysis was carried out by a split-plot  $3 \times 3 \times 2$  model with three independent variables: treatment (three levels: SALINE, VEH+MPH and TP-22+MPH), time (3 levels: 05, 10, 15 min bins), and side (two levels: black side and white side). The dependent variable was calculated as final preference day minus initial preference day. Drug conditioning design implied the same independent variables with addition of a two-level day (first vs. last) factor.

Level of significance was set at  $P < 0.05$ ; significant trends at  $0.10 < P < 0.05$  were also considered whenever effects were then confirmed by *post hoc* analysis. Multiple *post hoc* comparisons were run by Tukey HSD test, which is protected against the false positives and may be used even on non-significant ANOVA effects. Sample size was calculated before starting the experiment: from values of  $P = 0.05$  and power of 0.80 with expected increases of 30% in all variables, the appropriate groups should have  $N = 6$  each. Two experimental subjects showed an overtly abnormal behavior including lack of interest in environmental exploration and extreme inactivity during the entire duration of the experiment. After performing an interquartile range test, they were identified as outliers and excluded from the analysis.

### Dopamine D1 Receptor Gs-Mediated cAMP Accumulation Assay

The effect on cAMP accumulation of TP-22 was determined as a percent of control agonist response or inverse agonist response and as a percent inhibition of control agonist response. The  $\text{EC}_{50}$  values (concentration producing a half-maximal response) and  $\text{IC}_{50}$  values (concentration causing a half-maximal inhibition of the control agonist response) were determined by non-linear regression analysis of the concentration-response curves generated with mean replicate values using Hill equation curve fitting. Analysis was performed using custom software developed at Cerep (Hill software) and validated by comparison with data generated by the commercial software SigmaPlot<sup>®</sup> (SPSS Inc., USA). For the antagonists, the apparent dissociation constants ( $K_b$ ) were calculated using the modified Cheng–Prusoff equation.

<sup>3</sup>www.eurofins.com

## 8 Prior activation of 5-HT7 receptors modulates the conditioned place preference with methylphenidate

Carbone et al.

5-HT7R Activation in Modulating Reward

### RESULTS

#### Experiment 1: The Multidose Pilot

##### Locomotor Activity

Dose-related pharmacological effect on locomotor activity, after treatment with TP-22, showed a significant trend ( $F_{(3,38)} = 2.612$ ,  $P = 0.0653$ ), confirmed by *post hoc*s (see below), whereas interaction between time and treatment did not show significance ( $F_{(21,266)} = 0.769$ ,  $P = 0.7570$ ). *Post hoc* analysis, performed with the Tukey HSD test, displayed a significant difference in dose response between D25 (0.25 mg/kg) and vehicle ( $P < 0.05$ ) especially for the time-point of 120 min after the injection. D12 (0.12 mg/kg) and D06 (0.06 mg/kg) did not seem to differ from the vehicle control (Tukey threshold = 128.5;  $df = 38$ ;  $k = 3$ ; **Figure 1**).

#### Experiment 2: Conditioned Place Preference With MPH and TP-22

##### Drug Conditioning Days

We recorded and analyzed activity rates for all three groups during the first and last drug conditioning sessions. Regarding

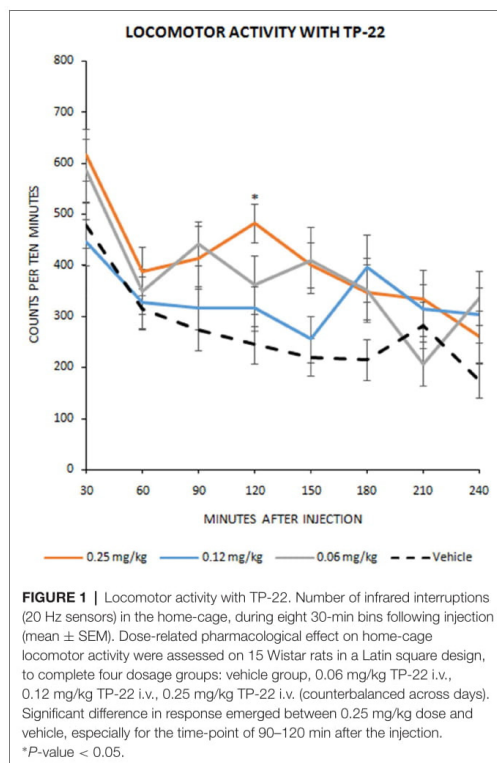
the treatment, overall analysis displayed a significantly increased locomotor activity ( $p < 0.05$ ) in both TP-22+MPH and VEH+MPH subjects compared to control subjects (saline solution; Treatment:  $F_{(2,13)} = 16.076$ ,  $P = 0.0003$ ). There was also a significant locomotor activity increase in rats who received TP-22 compared to rats receiving vehicle 1 h and a half before the MPH injection (VEH+MPH subjects; data not shown).

It should be noted that locomotor activity was increased only in the white side (drug associated), as expected. Indeed, both TP-22+MPH and VEH+MPH subjects showed in this chamber an enhanced activity ( $P < 0.01$ ) compared to the black (and saline-associated) one (Side\*Treatment:  $F_{(2,13)} = 31.439$ ,  $P < 0.0001$ ). Hence, for both these groups locomotor activity appeared higher on the days of drug administration (white chamber) compared to those of saline administration (black chamber), whereas control subjects did not show any difference. Moreover, on days with drug administration, locomotor activity of TP-22+MPH subjects was significantly increased ( $P < 0.01$ ) compared both to VEH+MPH subjects and control group. Activity of VEH+MPH group was also significantly enhanced compared to control group ( $P < 0.01$ ). On the contrary, on days with black-side saline administration, locomotor activities of all the three groups appeared superimposable (data not shown).

For both TP-22+MPH and VEH+MPH groups analysis displayed a significantly enhanced locomotor activity during the last conditioning session compared to the first one ( $P < 0.01$ ) only in the white side (associated with drug administration), denoting a presumable sensitization to the drug effect: of course, there were no such differences for control group in both sides of the apparatus (Side\*Day\*Treatment:  $F_{(2,13)} = 11.367$ ,  $P = 0.0014$ ). Notably, TP-22+MPH subjects showed a significantly higher locomotor activity than VEH+MPH ones, in particular during the last conditioning session ( $P < 0.01$ ; **Figure 2A**). After last drug administration (white side) TP-22+MPH subjects showed a significantly increased locomotor activity specifically between minutes 05 and 10 ( $P < 0.05$ ), whereas MPH subjects displayed a constant activity for the entire duration of the conditioning session (white side: Time\*Treatment  $F_{(8,52)} = 5.687$ ,  $P < 0.0001$ ). On the contrary, control group showed a clear and significant decrease in locomotor activity between minutes 05 and 10, as expected ( $P < 0.05$ ; **Figure 2B**).

##### Post-conditioning Preference Test

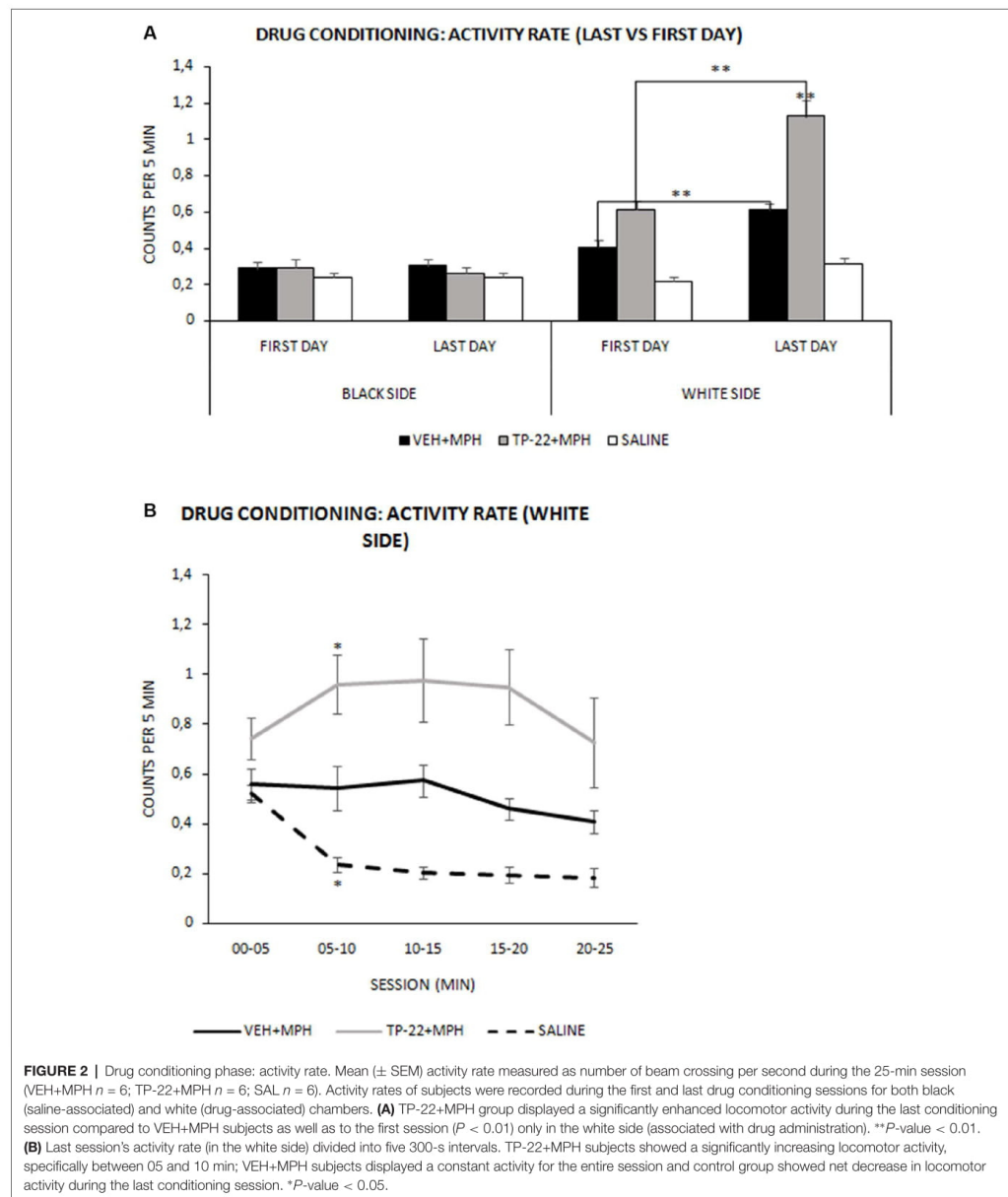
We recorded and analyzed time spent in each chamber, activity rate and transitions for all three groups during the post-conditioning preference test, in drug-free conditions. Time spent in the white side after drug conditioning did not seem significantly different from the initial preference test and analysis did not show any significant difference between the three experimental groups except for a slight preference for the white side displayed by the VEH+MPH in the first 05 min (Time\*Treatment:  $F_{(4,26)} = 0.356$ ,  $P = 0.8374$ ; **Figure 3B**). Nevertheless, activity rate and transitions showed an interesting profile. The difference in VEH+MPH locomotor activity between the post-conditioning



## 8 Prior activation of 5-HT7 receptors modulates the conditioned place preference with methylphenidate

Carbone et al.

5-HT7R Activation in Modulating Reward



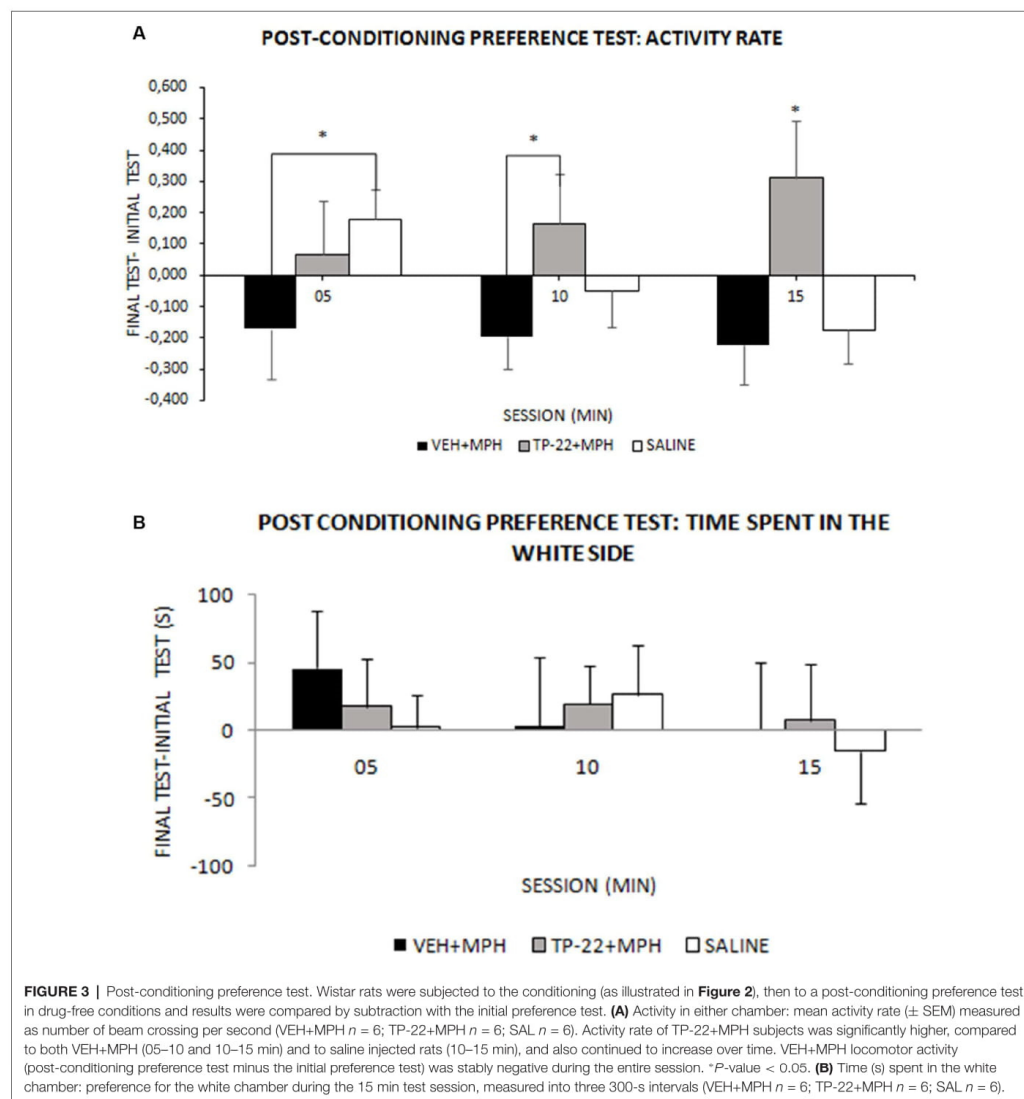
preference test and the initial preference test was negative during the entire session, whereas activity rate of TP-22+MPH subjects was positive and significantly higher compared to

both VEH+MPH (05–10 and 10–15 min,  $P < 0.05$ ) and to saline-injected rats (10–15 min,  $P < 0.05$ ); locomotor activity of TP-22+MPH rats also continued to increase over

## 8 Prior activation of 5-HT7 receptors modulates the conditioned place preference with methylphenidate

Carbone et al.

5-HT7R Activation in Modulating Reward



time (Time\*Treatment:  $F_{(4,26)} = 2.663$ ,  $P = 0.0550$ ), an effect particularly evident in the white side (Side\*Time\*Treatment:  $F_{(4,26)} = 3.190$ ,  $P = 0.0294$ ; **Figure 3A**). Locomotor activity of saline-injected subjects gradually diminished over time, as expected.

Even transitions between the two environments were gradually decreasing for saline-injected subjects as well as for

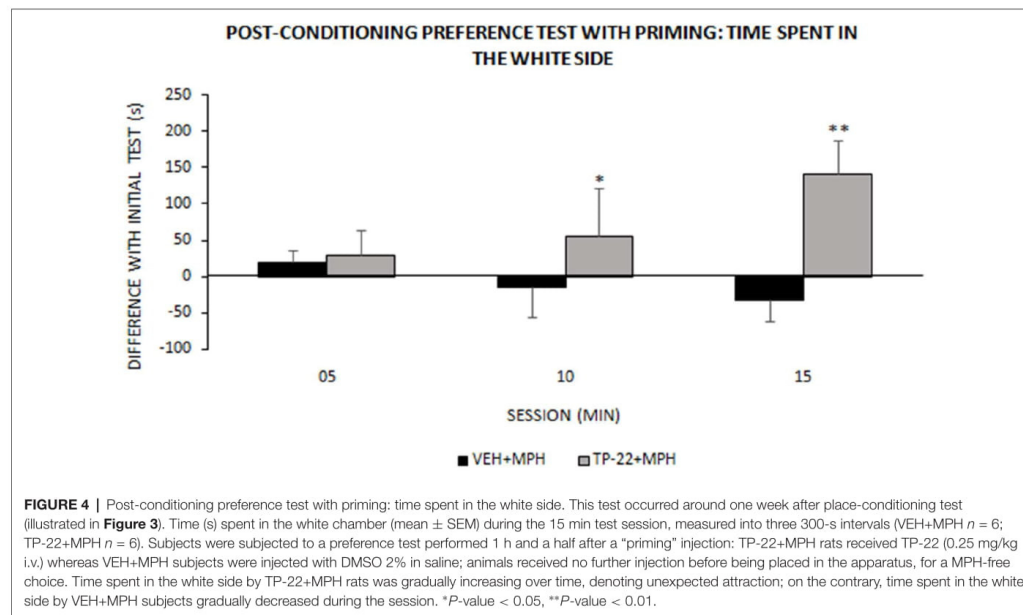
VEH+MPH rats, whereas TP-22+MPH subjects crossed the door dividing the two environments with increasing frequency over time (Time\*Treatment:  $F_{(4,26)} = 2.841$ ,  $P = 0.0445$ ). *Post hoc* analysis displayed a significant difference between TP-22+MPH and VEH+MPH group in the time interval between 05 and 10 min, whereas there were no differences between both these groups and saline controls ( $P < 0.05$ ; data not shown).



## 8 Prior activation of 5-HT7 receptors modulates the conditioned place preference with methylphenidate

Carbone et al.

5-HT7R Activation in Modulating Reward



### Post-conditioning Preference Test With Priming

We recorded and analyzed time spent in each chamber, activity rate and transitions for TP-22+MPH and VEH+MPH group in a preference test performed 1 h and a half after a “priming” injection: the latter was TP-22 for TP-22+MPH subjects and DMSO 2% for VEH+MPH group. The difference in time spent in the white side between the “primed” preference test and the initial preference test was the dependent variable: it was positive for TP-22+MPH subjects whereas VEH+MPH ones spent less time in the white side compared to the initial preference test (Treatment:  $F_{(1,8)} = 4.883$ ,  $P = 0.0581$ ).

Furthermore, time spent in the white side by TP-22+MPH rats was gradually increasing over time whereas VEH+MPH subjects gradually decreased the time spent in the white side during the session. There was indeed a significant trend for Time\*Treatment ( $P = 0.0963$ ) and *post hoc* analysis showed that time spent in the white side by TP-22+MPH subjects during the time interval between 05 and 15 min was significantly higher compared to VEH+MPH group ( $P < 0.05$ ), in particular during the last 5-min ( $P < 0.01$ ; **Figure 4**). Regarding activity rate, there were no significant differences between the two groups. There were no significant differences in transitions too.

### Affinity at Dopamine D1, D2, D3 and D5 Receptors

The radioligand displacement assays indicated that TP-22 interacted differently with DA receptor subtypes. In fact, the compound displayed considerable affinities at human DA D1

( $K_i = 3.93$  nM) and D5 ( $K_i = 16.9$  nM) receptors, whereas it showed much lower affinities at human DA D2 ( $K_i = 1127$  nM) and D3 ( $K_i = 1512$  nM) receptors (**Table 3**).

### Functional Activity at Dopamine D1 Receptor

The evaluation of the DA D1 receptor Gs-mediated cAMP accumulation indicated that TP-22 behaved as an antagonist. In fact, TP-22 alone was not able to induce cAMP accumulation showing less than 25% effect at the highest validated testing concentration. In the same assay, the standard agonist DA showed  $EC_{50}$  value of 24 nM. Instead, TP-22 behaved as a competitive antagonist at D1 receptor being able to dose-dependently antagonize the agonist response with low and sub-micromolar potency ( $IC_{50} = 0.97$  nM;  $K_b = 0.16$  nM).

### DISCUSSION

MPH, commonly prescribed for the treatment of Attention-Deficit/Hyperactivity Disorder (ADHD), is a psychostimulant drug whose mechanism of action is indirect DA agonism: MPH inhibits the DA transporter protein, increasing the DA concentration in the synaptic cleft (Volkow et al., 2002). Its psychostimulant vs. rewarding action can be dissected into D1-like vs. D2-like components (Stewart and Vezina, 1989). In the present study, we found that prior administration of the selective 5-HT7R agonist/D1-like receptor antagonist TP-22, at a dose of 0.25 mg/kg i.v., increased the stimulant effect of

## 8 Prior activation of 5-HT7 receptors modulates the conditioned place preference with methylphenidate

Carbone et al.

5-HT7R Activation in Modulating Reward

**TABLE 3 |** Dopamine receptor subtypes affinities as measured by radioligand binding experiments.

$K_i$ (nM) [95% CI] (nM) $\pm$ SEM			
D1 receptor	D2 receptor	D3 receptor	D5 receptor
3.93 [1.11; 14.0] 3.93 $\pm$ 0.7	1,127 [605; 2,098] 1,127 $\pm$ 130	1,512 [1,092; 2,093] 1,512 $\pm$ 92	16.9 [10.8; 26.7] 16.9 $\pm$ 2.1

Data is expressed as means with the corresponding 95% confidence interval.

MPH on locomotor activity during the subsequent acute and subchronic administration. Furthermore, after the conditioning phase, 3 days after the last drug administration, the activity of TP-22+MPH injected subjects remained steadily elevated, whereas the MPH-only injected subjects showed a sharp decline in activity compared to the saline vehicle controls. Finally, after a priming injection of TP-22 in MPH-free conditions, rats showed a higher preference for the MPH-associated white chamber than the vehicle-primed subjects. Overall, compared to the administration of MPH alone, the interaction between MPH and prior TP-22 seems to improve the conditioning of motivational drives to environmental cues, suggesting a main modulatory role of 5-HT7R in processing of rewarding power of psychostimulants.

In the first experiment, we characterized a range of TP-22 dosages by means of a recording rack, and found that the 0.25 mg/kg dose was the most effective in altering locomotor activity: the observed increase, although marginally significant in the ANOVA, was however fully significant by Tukey *post hoc* analysis. The maximum effect was reached an hour and a half after acute drug administration.

Subsequently, we performed a CPP test with MPH and its modulation by TP-22 at the selected dose. An initial preference test was run in order to assess the spontaneous locomotion and place preference in drug-free conditions. During the drug conditioning phase, we found that the activity rate of TP-22 pre-injected rats resulted significantly higher than both other groups, suggesting a potentiation when compared to the MPH-only injected subjects.

A possible explanation of this excitatory effect may be an enhanced drug-induced stimulation. In other words, we may propose enhanced post-synaptic effects, due to prior activation of 5-HT7R, related to (even unchanged) DA release by MPH. As a matter of fact, different studies have demonstrated that 5-HT-releasing drugs, such as 3,4-methylenedioxymethamphetamine (MDMA), are experienced as inducing a more positive mood by humans, even compared to high doses of amphetamine (Camí et al., 2000; Tancer and Johanson, 2003; Carhart-Harris et al., 2015). On the other hand, selective 5-HT releasers that spare DA are not experienced as pleasurable by humans (Tancer and Johanson, 2003). Furthermore, the 5-HT7R selective antagonist, SB-269970, significantly attenuated amphetamine-induced hyperactivity in mice and rats (Galici et al., 2008; Waters et al., 2012).

Another relevant feature of TP-22 is that the affinity for D2 and D3 DA receptors (Tables 1, 3) is far lower than that for 5-HT7R and D1-like receptors. A few considerations shall

be put forward. First, we presently found that TP-22 has great affinity to D1 receptors at which it acts as an antagonist. According to previous literature, D1 antagonists usually inhibit the MPH effect on locomotor activity (Claussen et al., 2015). Therefore, hyperlocomotion induced by TP-22 cannot rely on its D1 antagonism and is likely due to its action onto 5-HT7R. However, the dosage of TP-22 producing a peak of locomotion in the multidose pilot (Experiment 1) was quite low, so that the engagement of DA system through direct interaction of TP-22 with such D1 DA receptors might be questioned. In any case, potentiation of MPH stimulation was not caused by an additive and direct D1 receptor activation after TP-22 acute administration. Such notions may confirm a modulatory role of 5-HT7R, recruited by TP-22, on the stimulant effect elicited by DA-releasing drugs such as MPH.

In the third step, we examined place preference in drug-free conditions again. MPH-subjects spent slightly more time in the white (drug-associated) chamber during the first 5-min. However, interesting results emerged concerning locomotor activity. Regardless of conditioning effect, MPH-subjects had a clear-cut decline in activity when exposed in drug-free to the environment. This was, probably, due to conditioned inhibitory effects on DA neuronal activity: this resembles the well-known “down” elicited by psychostimulants like MPH (Shi et al., 2000; Dela Peña et al., 2018). Indeed, MPH, as well as other amphetamine-like psychostimulants, may inhibit DA neuron firing by increasing extracellular DA and by activating DA D2 autoreceptors and long-loop feedback pathways. On the contrary, activity and transitions of TP-22+MPH injected subjects remained steadily elevated and continued to increase over time during the post-conditioning test, particularly in the white side. These results may suggest a long-lasting enhancement of brain reward activity, due to 5-HT7R action of TP-22. As an additional possibility, the likely occupancy and incomplete blockade of D1 receptors, by TP-22 subchronic exposure, may well prevent the aforementioned DA depletion. Contrarily than VEH+MPH rats, and similarly to a “rebound” phenomenon, a receptor upregulation may have occurred in TP-22+MPH rats, leading to a further increase in locomotor activity during the post-conditioning test session. On the same reasoning, D1 antagonism possibly showed by TP-22 may be partly responsible for the enhanced sensitization to the MPH stimulant effects, displayed by the TP-22 pretreated subjects during the conditioning days (subchronic administration).

The fourth step was a place preference test with priming: this was to assess the eliciting effect of a TP-22 pre-injection. Notably, the TP-22 pre-injected subjects displayed a clear and increasing preference toward the white environment, compared to the vehicle-primed subjects. The latter, conversely, showed a slight preference for the black chamber, denoting that their slight preference for MPH-associated chamber had already vanished. A higher expectation for reward, elicited by just approaching the white chamber, seems to be the behavioral driving force of TP-22-primed subjects.

LP-211, as well as other 5-HT7R agonists, showed in several studies to modulate the construction of neural networks, hence improving the long-term memory (Meneses et al., 2015;



## 8 Prior activation of 5-HT7 receptors modulates the conditioned place preference with methylphenidate

Carbone et al.

5-HT7R Activation in Modulating Reward

Shahidi et al., 2018). TP-22 is able to stimulate neurite outgrowth in neuronal primary cultures in a shorter time and at a lower concentration than LP-211 (Lacivita et al., 2016). Overall, as already highlighted for LP-211, our results suggest that TP-22 may enhance the consolidation of emotional components of memory, causing a stronger association to develop between the environment and the MPH-driven hedonic experience. Alternatively, or in parallel, TP-22 may potentiate the consolidation of visual components (Carbone et al., 2018); hence, the MPH-associated white chamber could be better recalled. The encoding of novel visuo-spatial information also involves activation of DA D1/D5 receptors, as demonstrated in several studies performed on rats (see Lemon and Manahan-Vaughan, 2006, 2012; Hagen and Manahan-Vaughan, 2016).

Nevertheless, the D1-like receptor antagonism, possibly shown by TP-22, seems to exclude a direct involvement of dopaminergic pathways. According to previous literature, D1/D5 antagonists usually inhibit the acquisition of drug-related incentive memories, in particular for cocaine CPP memories (Kramar et al., 2014); on the other hand, D1 receptor antagonism reduces compulsive-like reward seeking and restores behavioral flexibility (Barker et al., 2013); as such, TP-22 priming injection is unlikely to trigger an overt seeking for MPH effects. In this line, activation of 5-HT neurons promotes patience to wait for future reward (Miyazaki et al., 2012, 2014; Liu et al., 2014). The theory assumes that activation of 5-HT neurons increases the subjective confidence of reward delivery (Li et al., 2016; Miyazaki et al., 2018). Therefore, after repeated TP-22/MPH pairings established a CPP, an acute 5-HT7R activation alone (as witnessed by our “priming” test) seems to trigger a hedonic attraction for the white MPH-conditioned chamber, in that it potentiates the expectation of experiencing again a reward therein. Since TP-22 priming injection *per se* did not massively affect locomotor activity nor transitions, it is confirmed that TP-22 alone is only a weak stimulant; conversely, in the TP-22+MPH group during the pairing phase, the stimulation was nearly double compared to MPH alone: effects on these parameters become likely additive.

### Implications for Serotonergic Modulation of Reward

Several theories have been proposed to explain the implication of 5-HT neurons in behavioral modulation, i.e., the “punishment” theory (Soubrié, 1986; Dayan and Huys, 2009); the “behavioral inhibition theory” (Miyazaki et al., 2011, 2012); the “mood” theory (Daw et al., 2002; Savitz et al., 2009). Many authors have reported modulatory effects on reward processing by manipulating central 5-HT levels (Roiser et al., 2006; Tanaka et al., 2007; Seymour et al., 2012) while others have proved that the serotonergic system is implied both in punishment and reward processing (Palmiter et al., 2012; Worbe et al., 2016; Scholl et al., 2017). Recent physiological, neuropathological, and optogenetic studies suggest an interpretation that seems to reconcile the different and controversial results so far achieved (Fischer and Ullsperger, 2017). The origin of most of the forebrain serotonergic innervation is the dorsal raphe nucleus (DRN), which is functionally interconnected with the ventral tegmental area (VTA). Recently, novel cell-type specific tracing

techniques allowed to describe more precisely the structural connectivity between DRN and VTA. It was found that DRN projects to VTA mainly *via* glutamatergic, but additionally via 5-HT co-releasing neurons (McDevitt et al., 2014; Qi et al., 2014). Tonic stimulation of 5-HT neurons in the DRN produces a weak reinforcing effect (Liu et al., 2014; Fonseca et al., 2015). Therefore, while DA neurons are critical for driving motivation (i.e., wanting), 5-HT neurons of DRN may play a major role in other aspects of rewards, such as consolidation of positive emotion and predictions *via* context evaluation. Hence, DA and 5-HT could provide a combined reward signal, whereas its dissociation (i.e., 5-HT in absence or reduction of DA) may encode punishment (see Fischer and Ullsperger, 2017).

Some recent studies can shed light on the persistent state of excitement showed by TP-22+MPH animals. Several animal and human studies demonstrate that 5-HT not only transfers information on short timescales but also acts over protracted timescales of days and weeks (Cohen et al., 2015; Luo et al., 2016; Scholl et al., 2017) leading to changes in plasticity, as also proven through 5-HT7R activation (Jitsuki et al., 2011; Bijata et al., 2017), and in particular by administration of TP-22 (Lacivita et al., 2016). Hence, the previous activation of 5-HT7R combined with the subsequent administration of MPH may have changed the perception of the white environment. TP-22 was enhancing the possible consolidation of information about the net benefit of the current context (white chamber; Luo et al., 2016).

We have been studying such interaction during a decade. Evidences, emerged from our previous studies, suggested an interplay between DA neurotransmission and 5-HT7R (Adriani et al., 2006; Leo et al., 2009). Indeed, MPH administration to adolescent rats, besides a reduction of basal behavioral impulsivity, produced a marked and persistent increment of 5-HT7R expression, denoting that MPH-induced effects could have been mediated, at least in part, by 5-HT7R modulation. Our present findings suggest that MPH, combined with activation of 5-HT7R and possibly with D1/D5 antagonism (besides additive modulatory effect on DA-induced arousal), could be strongly involved in drug conditioning mechanisms, switching the MPH-free preference by rats to the previously reward-associated environment.

### CONCLUSION

Further investigation is needed to thoroughly assess the role of 5-HT7Rs in punishment/reward-guided learning, nevertheless, the present outcomes suggest a direct involvement of 5-HT7R in modulating reward features, such as conditioned locomotion and priming of drug seeking. Beyond present results, activation of 5-HT7R combined with the D1/D5 modulation may lead to an improvement in behavioral flexibility, therefore to a better adaptation to adverse situations (Ruocco et al., 2014).

The great potential of targeting together the 5-HT7R and D1R is noticeable: a putative application may be to trigger the confidence for rewarding experiences in the presence of salient environmental cues. Preclinical studies may be useful for achieving an in-depth understanding of the molecular pathways involved. This, in turn, will favor the possible future treatment

# 8 Prior activation of 5-HT7 receptors modulates the conditioned place preference with methylphenidate

Carbone et al.

5-HT7R Activation in Modulating Reward

of diseases involving a dysregulation of the 5-HT system, such as depression, ADHD, schizophrenia, as well as alcohol and drug addiction (Hauser et al., 2015; Lax et al., 2018).

## ETHICS STATEMENT

All experimental procedures have been approved by the ISS animal welfare survey board on behalf of the Italian Ministry of Health (formal license 937/2018-PR, delivered to WA, veterinary surveillance by G. Panzini). Procedures were carried out in close agreement with the directive of the European Community Council (2010/63/EEC) and with the Italian law guidelines. We minimized animals' suffering and used as few animals as possible, according to the principle of the 3Rs.

## AUTHOR CONTRIBUTIONS

CC and WA conceived the study. CC and SLR realized the behavioral experiments. EL and ML provided essential tools (the drug). AF and HS realized the affinity radioligand assays.

LS provided funding for these experiments. CC with ML and WA wrote a first draft of the manuscript. LS, EA, and HS critically commented on the manuscript. All authors have approved the final version.

## FUNDING

The financial support from Ministero degli Affari Esteri e della Cooperazione Internazionale (MAECI, Italy), Progetto Grande Rilevanza Italia-Polonia 2013–2015, and from the FRAXA Research Foundation (USA) is gratefully acknowledged (to ML). Support by the DFG INST 208/664-1, GRK2158 as well as by the COST Actions CA15135 and CA18133 is also acknowledged (to HS).

## ACKNOWLEDGMENTS

We thank Stella Falsini, for help with all management issues, and Luigia Cancemi, for animal care and welfare.

## REFERENCES

- Adriani, W., Leo, D., Greco, D., Rea, M., di Porzio, U., Laviola, G., et al. (2006). Methylphenidate administration to adolescent rats determines plastic changes on reward-related behavior and striatal gene expression. *Neuropsychopharmacology* 31, 1946–1956. doi: 10.1038/sj.npp.1300962
- Adriani, W., Travaglini, D., Lacivita, E., Saso, L., Leopoldo, M., and Laviola, G. (2012). Modulatory effects of two novel agonists for serotonin receptor 7 on emotion, motivation and circadian rhythm profiles in mice. *Neuropharmacology* 62, 833–842. doi: 10.1016/j.neuropharm.2011.09.012
- Balcer, O. M., Seager, M. A., Gleason, S. D., Li, X., Rasmussen, K., Maxwell, J. K., et al. (2019). Evaluation of 5-HT<sub>7</sub> receptor antagonism for the treatment of anxiety, depression and schizophrenia through the use of receptor-deficient mice. *Behav. Brain Res.* 360, 270–278. doi: 10.1016/j.bbr.2018.12.019
- Bard, J. A., Zgombick, J., Adham, N., Vaysse, P., Branchek, T. A., and Weinshank, R. L. (1993). Cloning of a novel human serotonin receptor (5-HT<sub>7</sub>) positively linked to adenylate cyclase. *J. Biol. Chem.* 268, 23422–23426.
- Barker, J. M., Torregrossa, M. M., and Taylor, J. R. (2013). Bidirectional modulation of infralimbic dopamine D1 and D2 receptor activity regulates flexible reward seeking. *Front. Neurosci.* 7:126. doi: 10.3389/fnins.2013.00126
- Beaudet, G., Paizanis, E., Zoratto, F., Lacivita, E., Leopoldo, M., Freret, T., et al. (2017). LP-211, a selective 5-HT<sub>7</sub> receptor agonist, increases novelty-preference and promotes risk-prone behavior in rats. *Synapse* 71:e21995. doi: 10.1002/syn.21995
- Bijata, M., Labus, J., Guseva, D., Stawarski, M., Butzlaff, M., Dzwonek, J., et al. (2017). Synaptic remodeling depends on signaling between serotonin receptors and the extracellular matrix. *Cell Rep.* 19, 1767–1782. doi: 10.1016/j.celrep.2017.05.023
- Branchi, I. (2011). The double edged sword of neural plasticity: increasing serotonin levels leads to both greater vulnerability to depression and improved capacity to recover. *Psychoneuroendocrinology* 36, 339–351. doi: 10.1016/j.psyneuen.2010.08.011
- Broderick, P. A., and Phelix, C. F. (1997). I. Serotonin (5-HT) within dopamine reward circuits signals open-field behavior. II. Basis for 5-HT–DA interaction in cocaine dysfunctional behavior. *Neurosci. Biobehav. Rev.* 21, 227–260. doi: 10.1016/s0149-7634(96)00048-6
- Bautista-Aguilera, O. M., Hagenow, S., Palomino-Antolin, A., Farré-Alins, V., Ismaili, L., Joffrin, P.-L., et al. (2017). Multitarget-Directed Ligands Combining Cholinesterase and Monoamine Oxidase Inhibition with Histamine H3R Antagonism for Neuro-degenerative Diseases. *Angew. Chem. Int. Ed.* 56, 12765–12769.
- Cami, J., Farré, M., Mas, M., Roset, P. N., Poudevida, S., Mas, A., et al. (2000). Human pharmacology of 3,4-methylenedioxymeth-amphetamine ("ecstasy"): psychomotor performance and subjective effects. *J. Clin. Psychopharmacol.* 20, 455–466. doi: 10.1097/00004714-200008000-00010
- Carbone, C., Adinolfi, A., Cinque, S., Lacivita, E., Alleve, E., Leopoldo, M., et al. (2018). Activation of 5-HT<sub>7</sub> receptor by administration of its selective agonist, LP-211, modifies explorative-curiosity behavior in rats in two paradigms which differ in visuospatial parameters. *CNS Neurosci. Ther.* 24, 712–720. doi: 10.1111/cns.12812
- Carhart-Harris, R. L., Murphy, K., Leech, R., Erritzoe, D., Wall, M. B., Ferguson, B., et al. (2015). The effects of acutely administered 3,4-methylenedioxymethamphetamine on spontaneous brain function in healthy volunteers measured with arterial spin labeling and blood oxygen level-dependent resting state functional connectivity. *Biol. Psychiatry* 78, 554–562. doi: 10.1016/j.biopsych.2013.12.015
- Claussen, C. M., Witte, L. J., and Dafny, N. (2015). Single exposure of dopamine D1 antagonist prevents and D2 antagonist attenuates methylphenidate effect. *J. Exp. Pharmacol.* 7, 1–9. doi: 10.2147/jep.s75300
- Cohen, J. Y., Amoroso, M. W., and Uchida, N. (2015). Serotonergic neurons signal reward and punishment on multiple timescales. *Elife* 4:e06346. doi: 10.7554/elife.06346
- Cummins, E. D., Griffin, S. B., Burgess, K. C., Peterson, D. J., Watson, B. D., Buendia, M. A., et al. (2013). Methylphenidate place conditioning in adolescent rats: an analysis of sex differences and the dopamine transporter. *Behav. Brain Res.* 257, 215–223. doi: 10.1016/j.bbr.2013.09.036
- Daw, N. D., Kakade, S., and Dayan, P. (2002). Opponent interactions between serotonin and dopamine. *Neural Netw.* 15, 603–616. doi: 10.1016/s0893-6080(02)00052-7
- Dayan, P., and Huys, Q. J. (2009). Serotonin in affective control. *Annu. Rev. Neurosci.* 32, 95–126. doi: 10.1146/annurev.neuro.051508.135607
- Dela Peña, I. C., Shen, G., and Shi, W. X. (2018). Methylphenidate significantly alters the functional coupling between the prefrontal cortex and dopamine neurons in the ventral tegmental area. *Neuropharmacology* 131, 431–439. doi: 10.1016/j.neuropharm.2018.01.015
- Eriksson, T. M., Holst, S., Stan, T. L., Hager, T., Sjögren, B., Ögren, S. Ö., et al. (2012). 5-HT<sub>1A</sub> and 5-HT<sub>7</sub> receptor crosstalk in the regulation of emotional memory: implications for effects of selective serotonin reuptake inhibitors. *Neuropharmacology* 63, 1150–1160. doi: 10.1016/j.neuropharm.2012.06.061



# 8 Prior activation of 5-HT7 receptors modulates the conditioned place preference with methylphenidate

Carbone et al.

5-HT7R Activation in Modulating Reward

- Fischer, A. G., and Ullsperger, M. (2017). An update on the role of serotonin and its interplay with dopamine for reward. *Front. Hum. Neurosci.* 11:484. doi: 10.3389/fnhum.2017.00484
- Fonseca, M. S., Murakami, M., and Mainen, Z. F. (2015). Activation of dorsal raphe serotonergic neurons promotes waiting but is not reinforcing. *Curr. Biol.* 25, 306–315. doi: 10.1016/j.cub.2014.12.002
- Frank, A., Kiss, D. J., Keseru, G. M., and Stark, H. (2018). Binding kinetics of cariprazine and aripiprazole at the dopamine D3 receptor. *Sci. Rep.* 8:12509. doi: 10.1038/s41598-018-30794-y
- Galici, R., Boggs, J. D., Miller, K. L., Bonaventure, P., and Atack, J. R. (2008). Effects of SB-269970, a 5-HT<sub>7</sub> receptor antagonist, in mouse models predictive of antipsychotic-like activity. *Behav. Pharmacol.* 19, 153–159. doi: 10.1097/fbp.0b013e3282f62d8c
- Hagena, H., and Manahan-Vaughan, D. (2016). Dopamine D1/D5, but not D2/D3, receptor dependency of synaptic plasticity at hippocampal mossy fiber synapses that is enabled by patterned afferent stimulation, or spatial learning. *Front. Synaptic Neurosci.* 8:31. doi: 10.3389/fnsyn.2016.00031
- Hauser, S. R., Hedlund, P. B., Roberts, A. J., Sari, Y., Bell, R. L., and Engleman, E. A. (2015). The 5-HT<sub>7</sub> receptor as a potential target for treating drug and alcohol abuse. *Front. Neurosci.* 8:448. doi: 10.3389/fnins.2014.00448
- Hedlund, P. B. (2009). The 5-HT receptor and disorders of the nervous system: an overview. *Psychopharmacology* 206, 345–354. doi: 10.1007/s00213-009-1626-0
- Jitsuki, S., Takemoto, K., Kawasaki, T., Tada, H., Takahashi, A., Becamel, C., et al. (2011). Serotonin mediates cross-modal reorganization of cortical circuits. *Neuron* 69, 78–792. doi: 10.1016/j.neuron.2011.01.016
- Kobayashi, K., Haneda, E., Higuchi, M., Suhara, T., and Suzuki, H. (2012). Chronic fluoxetine selectively upregulates dopamine D<sub>1</sub>-like receptors in the hippocampus. *Neuropsychopharmacology* 37, 1500–1508. doi: 10.1038/npp.2011.335
- Kramar, C. P., Barbano, M. F., and Medina, J. H. (2014). Dopamine D1/D5 receptors in the dorsal hippocampus are required for the acquisition and expression of a single trial cocaine-associated memory. *Neurobiol. Learn. Mem.* 116, 172–180. doi: 10.1016/j.nlm.2014.10.004
- Kvachina, E., Liu, G., Dityatev, A., Renner, U., Dumuis, A., Richter, D. W., et al. (2005). 5-HT<sub>7</sub> receptor is coupled to G $\alpha$  subunits of heterotrimeric G12-protein to regulate gene transcription and neuronal morphology. *J. Neurosci.* 25, 7821–7830. doi: 10.1523/JNEUROSCI.1790-05.2005
- Lacivita, E., Podlowska, S., Speranza, L., Niso, M., Satala, G., Perrone, R., et al. (2016). Structural modifications of the serotonin 5-HT<sub>7</sub> receptor agonist N-(4-cyanophenylmethyl)-4-(2-biphenyl)-1-piperazinehexanamide (LP-211) to improve *in vitro* microsomal stability: a case study. *Eur. J. Med. Chem.* 120, 363–379. doi: 10.1016/j.ejmech.2016.05.005
- Lax, N. C., Parker, S. J., Hilton, E. J., Seliman, Y., Tidgewell, K. J., and Kolber, B. J. (2018). Cyanobacterial extract with serotonin receptor subtype 7 (5-HT<sub>7</sub> R) affinity modulates depression and anxiety-like behavior in mice. *Synapse* 72:e22059. doi: 10.1002/syn.22059
- Lemon, N., and Manahan-Vaughan, D. (2006). Dopamine D1/D5 receptors gate the acquisition of novel information through hippocampal long-term potentiation and long-term depression. *J. Neurosci.* 26, 7723–7729. doi: 10.1523/JNEUROSCI.1454-06.2006
- Lemon, N., and Manahan-Vaughan, D. (2012). Dopamine D1/D5 receptors contribute to de novo hippocampal LTD mediated by novel spatial exploration or locus coeruleus activity. *Cereb. Cortex* 22, 2131–2138. doi: 10.1093/cercor/bhr297
- Leo, D., Adriani, W., Cavaliere, C., Cirillo, G., Marco, E. M., Romano, E., et al. (2009). Methylphenidate to adolescent rats drives enduring changes of accumbal Htr7 expression: implications for impulsive behavior and neuronal morphology. *Genes Brain Behav.* 8, 356–368. doi: 10.1111/j.1601-183x.2009.00486.x
- Leopoldo, M., Lacivita, E., Berardi, F., Perrone, R., and Hedlund, P. B. (2011). Serotonin 5-HT<sub>7</sub> receptor agents: structure-activity relationship and potential therapeutic applications in central nervous system disorders. *Pharmacol. Ther.* 129, 120–148. doi: 10.1016/j.pharmthera.2010.08.013
- Li, Y., Zhong, W., Wang, D., Feng, Q., Liu, Z., Zhou, J., et al. (2016). Serotonin neurons in the dorsal raphe nucleus encode reward signals. *Nat. Commun.* 7:10503. doi: 10.1038/ncomms10503
- Liu, Z., Zhou, J., Li, Y., Hu, F., Lu, Y., Ma, M., et al. (2014). Dorsal raphe neurons signal reward through 5-HT and glutamate. *Neuron* 81, 1360–1374. doi: 10.1016/j.neuron.2014.02.010
- Lovenberg, T. W., Baron, B. M., de Lecea, L., Miller, J. D., Prosser, R. A., Rea, M. A., et al. (1993). A novel adenylyl cyclase-activating serotonin receptor (5-HT<sub>7</sub>) implicated in the regulation of mammalian circadian rhythms. *Neuron* 11, 449–458. doi: 10.1016/0896-6273(93)90149-1
- Luo, M., Li, Y., and Zhong, W. (2016). Do dorsal raphe 5-HT neurons encode “beneficialness”? *Neurobiol. Learn. Mem.* 135, 40–49. doi: 10.1016/j.nlm.2016.08.008
- Maxwell, J., Gleason, S. D., Falcone, J., Svensson, K., Balcer, O. M., Li, X., et al. (2019). Effects of 5-HT<sub>7</sub> receptor antagonists on behaviors of mice that detect drugs used in the treatment of anxiety, depression, or schizophrenia. *Behav. Brain Res.* 359, 467–473. doi: 10.1016/j.bbr.2018.11.019
- McDevitt, R. A., Tiran-Cappello, A., Shen, H., Balderas, I., Britt, J. P., Marino, R. A. M., et al. (2014). Serotonergic versus nonserotonergic dorsal raphe projection neurons: differential participation in reward circuitry. *Cell Rep.* 8, 1857–1869. doi: 10.1016/j.celrep.2014.08.037
- Meneses, A., Perez-Garcia, G., Liy-Salmeron, G., Ponce-López, T., Lacivita, E., and Leopoldo, M. (2015). 5-HT<sub>7</sub> receptor activation: precognitive and anti-amnesic effects. *Psychopharmacology* 232, 595–603. doi: 10.1007/s00213-014-3693-0
- Miyazaki, K. W., Miyazaki, K., and Doya, K. (2012). Activation of dorsal raphe serotonin neurons is necessary for waiting for delayed rewards. *J. Neurosci.* 32, 10451–10457. doi: 10.1523/JNEUROSCI.0915-12.2012
- Miyazaki, K. W., Miyazaki, K., Tanaka, K. F., Yamanaka, A., Takahashi, A., Tabuchi, S., et al. (2014). Optogenetic activation of dorsal raphe serotonin neurons enhances patience for future rewards. *Curr. Biol.* 24, 2033–2040. doi: 10.1016/j.cub.2014.07.041
- Miyazaki, K., Miyazaki, K. W., and Doya, K. (2011). Activation of dorsal raphe serotonin neurons underlies waiting for delayed rewards. *J. Neurosci.* 31, 469–479. doi: 10.1523/JNEUROSCI.3714-10.2011
- Miyazaki, K., Miyazaki, K. W., Yamanaka, A., Tokuda, T., Tanaka, K. F., and Doya, K. (2018). Reward probability and timing uncertainty alter the effect of dorsal raphe serotonin neurons on patience. *Nat. Commun.* 9:2048. doi: 10.1038/s41467-018-04496-y
- Modica, M. N., Lacivita, E., Intagliata, S., Salerno, L., Romeo, G., Pittalà, V., et al. (2018). Structure-activity relationships and therapeutic potentials of 5-HT<sub>7</sub> receptor ligands: an update. *J. Med. Chem.* 61, 8475–8503. doi: 10.1021/acs.jmedchem.7b01898
- Müller, C. P., and Homberg, J. R. (2014). The role of serotonin in drug use and addiction. *Behav. Brain Res.* 277, 146–192. doi: 10.1016/j.bbr.2014.04.007
- Nikiforuk, A. (2015). Targeting the serotonin 5-HT<sub>7</sub> receptor in the search for treatments for CNS disorders: rationale and progress to date. *CNS Drugs* 29, 265–275. doi: 10.1007/s40263-015-0236-0
- Palmiter, S., Clair, A.-H., Mallet, L., and Pessiglione, M. (2012). Similar improvement of reward and punishment learning by serotonin reuptake inhibitors in obsessive-compulsive disorder. *Biol. Psychiatry* 72, 244–250. doi: 10.1016/j.biopsych.2011.12.028
- Qi, J., Zhang, S., Wang, H.-L., Wang, H., de Jesus Aceves Buendia, J., Hoffman, A. F., et al. (2014). A glutamatergic reward input from the dorsal raphe to ventral tegmental area dopamine neurons. *Nat. Commun.* 5:5390. doi: 10.1038/ncomms6390
- Renner, U., Zeug, A., Woehler, A., Niebert, M., Dityatev, A., Dityateva, G., et al. (2012). Heterodimerization of serotonin receptors 5-HT<sub>1A</sub> and 5-HT<sub>7</sub> differentially regulates receptor signalling and trafficking. *J. Cell Sci.* 125, 2486–2499. doi: 10.1242/jcs.101337
- Roiser, J. P., Blackwell, A. D., Cools, R., Clark, L., Rubinsztein, D. C., Robbins, T. W., et al. (2006). Serotonin transporter polymorphism mediates vulnerability to loss of incentive motivation following acute tryptophan depletion. *Neuropsychopharmacology* 31, 2264–2272. doi: 10.1038/sj.npp.1301084
- Romano, E., Ruocco, L. A., Nativio, P., Lacivita, E., Ajmone-Cat, M. A., Boatto, G., et al. (2014). Modulatory effects following subchronic stimulation of brain 5-HT<sub>7</sub>-R system in mice and rats. *Rev. Neurosci.* 25, 383–400. doi: 10.1515/revneuro-2014-0007
- Ruat, M., Traifort, E., Leurs, R., Tardivel-Lacombe, J., Diaz, J., Arrang, J. M., et al. (1993). Molecular cloning, characterization, and localization of a high-affinity

## 8 Prior activation of 5-HT7 receptors modulates the conditioned place preference with methylphenidate

Carbone et al.

5-HT7R Activation in Modulating Reward

- serotonin receptor (5-HT<sub>7</sub>) activating cAMP formation. *Proc. Natl. Acad. Sci. U S A* 90, 8547–8551. doi: 10.1073/pnas.90.18.8547
- Ruocco, L. A., Romano, E., Treno, C., Lacivita, E., Arra, C., Gironi-Carnevale, U. A., et al. (2014). Emotional and risk seeking behavior after prepubertal subchronic or adult acute stimulation of 5-HT<sub>7</sub>-Rs in Naples High Excitability rats. *Synapse* 68, 159–167. doi: 10.1002/syn.21724
- Sachs, B. D., Ni, J. R., and Caron, M. G. (2015). Brain 5-HT deficiency increases stress vulnerability and impairs antidepressant responses following psychosocial stress. *Proc. Natl. Acad. Sci. U S A* 112, 2557–2562. doi: 10.1073/pnas.1416866112
- Savitz, J., Lucki, I., and Drevets, W. C. (2009). 5-HT<sub>1A</sub> receptor function in major depressive disorder. *Prog. Neurobiol.* 88, 17–31. doi: 10.1016/j.pneurobio.2009.01.009
- Scholl, J., Kolling, N., Nelissen, N., Browning, M., Rushworth, M. F. S., and Harmer, C. J. (2017). Beyond negative valence: 2-week administration of a serotonergic antidepressant enhances both reward and effort learning signals. *PLoS Biol.* 15:e2000756. doi: 10.1371/journal.pbio.2000756
- Seymour, B., Daw, N. D., Roiser, J. P., Dayan, P., and Dolan, R. (2012). Serotonin selectively modulates reward value in human decision-making. *J. Neurosci.* 32, 5833–5842. doi: 10.1523/JNEUROSCI.0053-12.2012
- Shahidi, S., Asl, S. S., Komaki, A., and Hashemi-Firouzi, N. (2018). The effect of chronic stimulation of serotonin receptor type 7 on recognition, passive avoidance memory, hippocampal long-term potentiation, and neuronal apoptosis in the amyloid  $\beta$  protein treated rat. *Psychopharmacology* 235, 1513–1525. doi: 10.1007/s00213-018-4862-3
- Shi, W. X., Pun, C. L., Zhang, X. X., Jones, M. D., and Bunney, B. S. (2000). Dual effects of D-amphetamine on dopamine neurons mediated by dopamine and nondopamine receptors. *J. Neurosci.* 20, 3504–3511. doi: 10.1523/JNEUROSCI.20-09-03504.2000
- Shuto, T., Kuroiwa, M., Sotogaku, N., Kawahara, Y., Oh, Y. S., Jang, J. H., et al. (2018). Obligatory roles of dopamine D1 receptors in the dentate gyrus in antidepressant actions of a selective serotonin reuptake inhibitor, fluoxetine. *Mol. Psychiatry* doi: 10.1038/s41380-018-0316-x[Epub ahead of print].
- Sokoloff, P., Andrieux, M., Besançon, R., Pilon, C., Martres, M. P., Giros, B., et al. (1992). Pharmacology of human dopamine D3 receptor expressed in a mammalian cell line: comparison with D2 receptor. *Eur. J. Pharmacol.* 225, 331–337. doi: 10.1016/0922-4106(92)90107-7
- Soubrié, P. (1986). Reconciling the role of central serotonin neurons in human and animal behavior. *Behav. Brain Sci.* 9, 319–335. doi: 10.1017/s0140525x00022871
- Stewart, J., and Vezina, P. (1989). Microinjections of SCH-23390 into the ventral tegmental area and substantia nigra pars reticulata attenuate the development of sensitization to the locomotor activating effects of systemic amphetamine. *Brain Res.* 495, 401–406. doi: 10.1016/0006-8993(89)90236-9
- Tanaka, S. C., Schweighofer, N., Asahi, S., Shishida, K., Okamoto, Y., Yamawaki, S., et al. (2007). Serotonin differentially regulates short- and long-term prediction of rewards in the ventral and dorsal striatum. *PLoS One* 2:e1333. doi: 10.1371/journal.pone.0001333
- Tancer, M., and Johanson, C. E. (2003). Reinforcing, subjective, and physiological effects of MDMA in humans: a comparison with d-amphetamine and mCPP. *Drug Alcohol Depend.* 72, 33–44. doi: 10.1016/s0376-8716(03)00172-8
- Volkow, N. D., Fowler, J. S., Wang, G., Ding, Y., and Gatley, S. J. (2002). Mechanism of action of methylphenidate: insights from PET imaging studies. *J. Atten. Disord.* 6, S31–S43. doi: 10.1177/070674370200601s05
- Waters, K. A., Stean, T. O., Hammond, B., Virley, D. J., Upton, N., Kew, J. N., et al. (2012). Effects of the selective 5-HT<sub>7</sub> receptor antagonist SB-269970 in animal models of psychosis and cognition. *Behav. Brain Res.* 228, 211–218. doi: 10.1016/j.bbr.2011.12.009
- Worbe, Y., Palminteri, S., Savulich, G., Daw, N. D., Fernandez-Egea, E., Robbins, T. W., et al. (2016). Valence-dependent influence of serotonin depletion on model-based choice strategy. *Mol. Psychiatry* 21, 624–629. doi: 10.1038/mp.2015.46
- Zhang, Q. J., Du, C. X., Tan, H. H., Zhang, L., Li, L. B., Zhang, J., et al. (2015). Activation and blockade of serotonin<sub>7</sub> receptors in the prefrontal cortex regulate depressive-like behaviors in a 6-hydroxydopamine-induced Parkinson's disease rat model. *Neuroscience* 311, 45–55. doi: 10.1016/j.neuroscience.2015.10.016
- Zhou, Q. Y., Grandy, D. K., Thambi, L., Kushner, J. A., Van Tol, H. H., Cone, R., et al. (1990). Cloning and expression of human and rat D1 dopamine receptors. *Nature* 347, 76–80. doi: 10.1038/347076a0

**Conflict of Interest Statement:** The authors declare that the research was conducted in the absence of any commercial or financial relationships that could be construed as a potential conflict of interest.

Copyright © 2019 Carbone, Lo Russo, Lacivita, Frank, Alleva, Stark, Saso, Leopoldo and Adriani. This is an open-access article distributed under the terms of the Creative Commons Attribution License (CC BY). The use, distribution or reproduction in other forums is permitted, provided the original author(s) and the copyright owner(s) are credited and that the original publication in this journal is cited, in accordance with accepted academic practice. No use, distribution or reproduction is permitted which does not comply with these terms.

## 9 Binding kinetics of cariprazine and aripiprazole at the dopamine D<sub>3</sub> receptor

Frank A<sup>1</sup>, Kiss DJ<sup>2,3</sup>, Keserű GM<sup>2</sup>, Stark H<sup>1</sup>, **2018**.

<sup>1</sup>Institute of Pharmaceutical and Medicinal Chemistry, Heinrich Heine University Düsseldorf, Duesseldorf, Germany.

<sup>2</sup>Medicinal Chemistry Research Group, Research Centre for Natural Sciences, Hungarian Academy of Sciences, Budapest, Hungary.

<sup>3</sup>ELTE Eötvös Loránd University, Doctoral School of Chemistry, Budapest, Hungary.

Published in: *Scientific Reports* **8**, 12509.

DOI:10.1038/s41598-018-30794-y.

Research contribution: Development and evaluation of a novel residence time assay at the D<sub>2</sub> and D<sub>3</sub> receptor, pharmacological evaluation of compounds at the D<sub>2</sub> and D<sub>3</sub> receptor and for  $\beta$ -arrestin recruitment at the D<sub>3</sub> receptor, interpretation of data and preparation of manuscript.

Reprinted by permission from the authors. This article was published in Scientific Reports, 8, Annika Frank, Dóra J. Kiss, György M. Keserű, Holger Stark, Binding kinetics of cariprazine and aripiprazole at the dopamine D<sub>3</sub> receptor, 12509, DOI:10.1038/s41598-018-30794-y. Copyright Springer Nature (2018).

## SCIENTIFIC REPORTS

OPEN

Binding kinetics of cariprazine and aripiprazole at the dopamine D<sub>3</sub> receptor

Received: 17 May 2018

Accepted: 3 August 2018

Published online: 21 August 2018

Annika Frank<sup>1</sup>, Dóra J. Kiss<sup>2,3</sup>, György M. Keserű<sup>2</sup> & Holger Stark<sup>1</sup> 

The dissociation behaviours of aripiprazole and cariprazine at the human D<sub>2</sub> and D<sub>3</sub> receptor are evaluated. A potential correlation between kinetics and *in vivo* profiles, especially cariprazine's action on negative symptoms in schizophrenia, is investigated. The binding kinetics of four ligands were indirectly evaluated. After the receptor preparations were pre-incubated with the unlabelled ligands, the dissociation was initiated with an excess of [<sup>3</sup>H]spiperone. Slow dissociation kinetics characterizes aripiprazole and cariprazine at the D<sub>2</sub> receptor. At the D<sub>3</sub> receptor, aripiprazole exhibits a slow monophasic dissociation, while cariprazine displays a rapid biphasic behaviour. Functional  $\beta$ -arrestin assays and molecular dynamics simulations at the D<sub>3</sub> receptor confirm a biphasic binding behaviour of cariprazine. This may influence its *in vivo* action, as the partial agonist could react rapidly to variations in the dopamine levels of schizophrenic patients and the ligand will not quantitatively dissociate from the receptor in one single step. With these findings novel agents may be developed that display rapid, biphasic dissociation from the D<sub>3</sub>R to further investigate this effect on *in vivo* profiles.

Schizophrenia is a group of neurological diseases characterized by specific symptom complexes. Positive symptoms, which are exaggerated in schizophrenic patients, include hallucinations or delusions. Negative symptoms (e.g. depression or anhedonia) represent the impairment of healthy cognitive behaviour. The origin of the symptoms is not clarified, but a neurotransmitter dysregulation in different parts of the brain is likely. Hyperactive dopamine transmission and increased D<sub>2</sub> receptor (D<sub>2</sub>R) activation may cause positive symptoms. Hypoactive dopamine transmission and hence less D<sub>1</sub> receptor activation in the prefrontal areas may be responsible for negative symptoms<sup>1</sup>. D<sub>3</sub> receptors (D<sub>3</sub>Rs) seem to contribute to the origin of negative symptoms<sup>2</sup>. To date schizophrenia is treated only symptomatically. Typical first generation antipsychotic drugs reduce the positive symptoms but display severe and therapy limiting adverse drug effects (ADE) like extrapyramidal motoric symptoms (EPMS). The second generation, also known as atypical antipsychotic drugs reduce these adverse effects, while remain highly effective against positive symptoms. Aripiprazole, an atypical antipsychotic agent, exhibits good efficacy on the positive symptomatic of schizophrenia and a rather beneficial ADE profile. However it is not able to treat the negative symptoms of the disease sufficiently. Cariprazine, a novel antipsychotic agent<sup>3,4</sup>, entered the US market in 2016 and obtained European Medicines Agency (EMA) approval in May 2017. Unlike most other antipsychotics it is effective against negative symptoms in clinical trials<sup>5</sup>, although the mechanism of this action remains elusive.

Distinct residence times (RTs) are discussed to influence drug profiles *in vivo*<sup>6</sup>, although proof of this hypothesis remains pending. As the RT ( $1/k_{off}$ ) determines the duration of receptor occupancy it may influence signalling pathways or ADE<sup>7,8</sup>. Several studies address the RTs of antipsychotic drugs at the D<sub>2</sub>R and the correlation to efficacy or ADE<sup>9</sup>, however, to date such approaches have not been made for the D<sub>3</sub>R. A recent review highlighted the relevance of conformational receptor states and biased signalling at G-protein coupled receptors (GPCRs)<sup>10</sup>. With increasing insights into the crystal structure and signal transduction of GPCRs, it becomes more important to evaluate pharmacological characteristics of novel agents. We hypothesize that cariprazine's dissociation behaviour elucidates possible mechanisms for its action on negative symptoms in schizophrenia. Its profile is compared to the partial agonist aripiprazole, the antagonist spiperone and the agonist rotigotine. In doing so, the

<sup>1</sup>Institute of Pharmaceutical and Medicinal Chemistry, Heinrich Heine University Düsseldorf, Duesseldorf, Germany. <sup>2</sup>Medicinal Chemistry Research Group, Research Centre for Natural Sciences, Hungarian Academy of Sciences, Budapest, Hungary. <sup>3</sup>ELTE Eötvös Loránd University, Doctoral School of Chemistry, Budapest, Hungary. Correspondence and requests for materials should be addressed to G.M.K. (email: [keseru.gyorgy@ttk.mta.hu](mailto:keseru.gyorgy@ttk.mta.hu)) or H.S. (email: [stark@hhu.de](mailto:stark@hhu.de))



Drug	$k_{\text{off}}$ [ $\text{min}^{-1}$ ] $\pm$ s.d. (n)	$\text{pK}_i \pm$ s.d. ( $K_i$ [nM]) (n)
Aripiprazole	$0.026 \pm 0.001$ [3]	$8.95 \pm 0.06$ (1.1) [3]
Cariprazine	$0.041 \pm 0.002$ [3]	$8.80 \pm 0.12$ (1.6) [3]
Rotigotine	$0.113 \pm 0.029$ [3]	$7.73 \pm 0.10$ (18.5) [4]
Spiperone	$0.028 \pm 0.018$ [3]	$10.01 \pm 0.29$ (0.1) [4]

**Table 1.**  $\text{D}_2\text{R}$   $k_{\text{off}}$  and equilibrium dissociation constants ( $\pm$  s.d.) of the unlabelled ligands.  $\text{pK}_i$  are determined by radioligand displacement assays.  $\text{D}_2\text{R}$  membrane preparations were incubated with [ $^3\text{H}$ ]spiperone and the compound.  $k_{\text{off}}$  are determined by radioligand dilution assays.  $\text{D}_2\text{R}$  membrane preparations were pre-incubated with the compound. Afterwards dissociation was initiated with an excess of [ $^3\text{H}$ ]spiperone. Results are means  $\pm$  s.d. at least performed with  $n = 3$  independent experiments at room temperature.

Drug	Monophasic fit	Biphasic fit		$\text{pK}_i \pm$ s.d. ( $K_i$ [nM]) (n)
	$k_{\text{off}}$ [ $\text{min}^{-1}$ ] $\pm$ s.d. (n)	$k_{\text{off1}}$ [ $\text{min}^{-1}$ ] $\pm$ s.d. (n)	$k_{\text{off2}}$ [ $\text{min}^{-1}$ ] $\pm$ s.d. (n)	
Aripiprazole	$0.05 \pm 0.02$ [3]	$0.03 \pm 0.02$ [3]	$0.15 \pm 0.08$ [3]	$8.13 \pm 0.19$ (7.3) [5]
Cariprazine	$0.16 \pm 0.04$ [9]	$0.03 \pm 0.01$ [8]	$0.63 \pm 0.38$ [8]	$9.24 \pm 0.18$ (0.6) [6]
Rotigotine	$0.07 \pm 0.02$ [4]	$0.04 \pm 0.02$ [3]	$0.18 \pm 0.01$ [3]	$8.44 \pm 0.26$ (3.7) [3]
Spiperone	$0.05 \pm 0.02$ [3]	$0.02 \pm 0.01$ [2]	$0.47 \pm 0.35$ [2]	$8.96 \pm 0.28$ (1.1) [4]

**Table 2.**  $\text{D}_3\text{R}$   $k_{\text{off}}$  and equilibrium dissociation constants ( $\pm$  s.d.) of the unlabelled ligands.  $\text{pK}_i$  are determined by radioligand displacement assays.  $\text{D}_3\text{R}$  membrane preparations were incubated with [ $^3\text{H}$ ]spiperone and the compound.  $k_{\text{off}}$  are determined by radioligand dilution assays.  $\text{D}_3\text{R}$  membrane preparations were pre-incubated with the compound. Afterwards dissociation was initiated with an excess of [ $^3\text{H}$ ]spiperone. Results are means  $\pm$  s.d. at least performed with  $n = 3$  independent experiments at room temperature.  $k_{\text{off}}$  displays the  $k_{\text{off}}$  derived by the monophasic fit, while  $k_{\text{off1}}$  and  $k_{\text{off2}}$  are the two  $k_{\text{off}}$  derived by the biphasic fit.

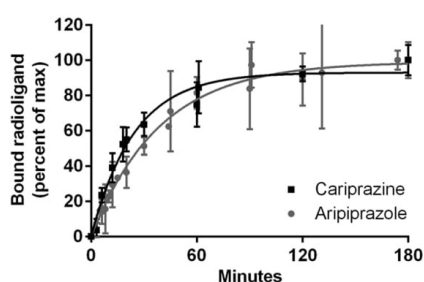


**Figure 1.** Dissociation of aripiprazole and cariprazine from the  $\text{D}_2\text{R}$ , determined by dilution assays. After pre-incubating  $\text{D}_2\text{R}$  membrane preparations with the compounds, dissociation was initiated with an excess of [ $^3\text{H}$ ]spiperone. Figure displays normalized values globally fitted for all experiments ( $n = 3$ , triplicates) given as mean with s.d.

understanding of ligand binding to the  $\text{D}_3\text{R}$  could be improved and drug development might benefit from clinically optimized drugs, focused on specific symptoms.

## Results

**[ $^3\text{H}$ ]spiperone kinetic experiments.** Dissociation rate constants ( $k_{\text{off}}$ ) of [ $^3\text{H}$ ]spiperone are  $0.013 \text{ min}^{-1}$  ( $\pm 0.003 \text{ min}^{-1}$ ) at the  $\text{D}_2\text{R}$  and  $0.033 \text{ min}^{-1}$  ( $\pm 0.019 \text{ min}^{-1}$ ) at the  $\text{D}_3\text{R}$ . The  $k_{\text{off}}$  of unlabelled spiperone in the indirect assay matches the  $k_{\text{off}}$  of [ $^3\text{H}$ ]spiperone at both receptors (Tables 1 and 2), supporting the applicability of the dilution method.

**$\text{D}_2\text{R}$  kinetic experiments.** Aripiprazole and cariprazine share similar RTs at the  $\text{D}_2\text{R}$  with 38 min for aripiprazole and slightly faster (24 min) for cariprazine (Table 1, Fig. 1). These results are in accordance to those of Klein Herenbrink, who found only slight differences at the  $\text{D}_2\text{R}$ . The  $k_{\text{off}}$  of aripiprazole is concordant with studies performed on rat<sup>8,11</sup> and human receptors<sup>12,13</sup> and the slow dissociation of spiperone<sup>7,14–16</sup> is also corroborated. References, predicting a fast  $k_{\text{off}}$  of aripiprazole from the  $\text{D}_1\text{R}$ <sup>7,17</sup> and a slow  $k_{\text{off}}$  for rotigotine<sup>18</sup>, are not confirmed. The measured RTs at the  $\text{D}_2\text{R}$  correlate with the drugs' affinities (radioligand displacement assays,  $\text{pK}_i$  Table 1). Spiperone and aripiprazole (highest affinities) display the longest RTs, while rotigotine (lowest affinity) shows the fastest dissociation from the  $\text{D}_2\text{R}$ . This correlation of binding kinetics and affinities at the  $\text{D}_2\text{R}$  was demonstrated

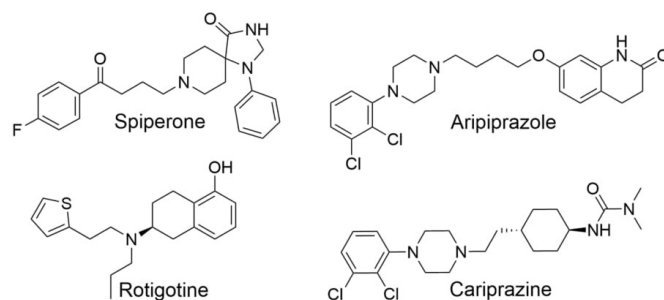


**Figure 2.** Chemical structures of the evaluated ligands.

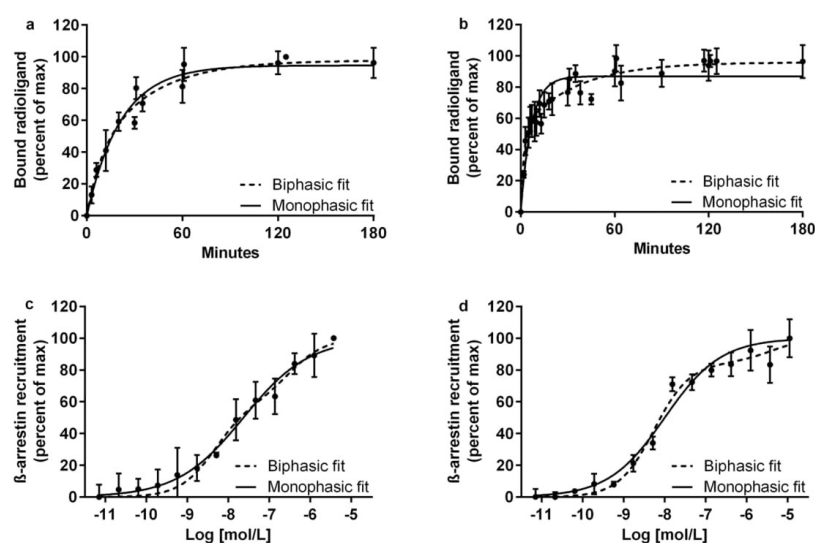


**Figure 3.** Dissociation profiles and  $\beta$ -arrestin recruitment of aripiprazole and cariprazine at the D<sub>3</sub>R. (a,b) Dissociation of aripiprazole (a) and cariprazine (b) from the D<sub>3</sub>R, determined by dilution assays. D<sub>3</sub>R membrane preparations were pre-incubated with the compounds. Dissociation was initiated with an excess of [<sup>3</sup>H]spiperone. Figure displays normalized values globally fitted for all experiments (n = 3/9, triplicates) given as mean with s.d. (c,d)  $\beta$ -arrestin activation of aripiprazole (c) and cariprazine (d) at the D<sub>3</sub>R. U2OS cells were incubated with partial agonists for 90 min. Data is normalized, globally fitted for all experiments (n = 2, duplicates) given as mean with s.d.

by Kapur and Seeman<sup>14</sup>. Spiperone, aripiprazole and cariprazine (slow  $k_{off}$ ) share a large, lipophilic aromatic motif, connected through a linker to a second motif with different hydrogen-bond acceptor and donor groups (Fig. 2), while rotigotine is missing this diverse motif. In the presented study the antagonist and the partial agonists display a slow dissociation, while the full agonist rotigotine shows fast dissociation from the D<sub>2</sub>R, which is supported by their structural and binding properties.

**D<sub>3</sub>R kinetic experiments.** The evaluation of  $k_{off}$  at the D<sub>3</sub>R reveals different dissociation behaviours of aripiprazole and cariprazine (Table 2, Fig. 3a,b). Cariprazine displays a rapid biphasic dissociation behaviour ( $p < 0.0001$ ) that is not sufficiently described by a monophasic fit. Dissociation of aripiprazole is slower and better described by a monophasic fit ( $p = 0.0925$ ). Evaluation of the antagonist spiperone also reveals a slow, but biphasic ( $p < 0.0001$ ) dissociation, while the agonist rotigotine displays a monophasic ( $p = 0.0688$ ) dissociation, not significantly faster than aripiprazole or spiperone. The biphasic dissociation of cariprazine is not altered by the

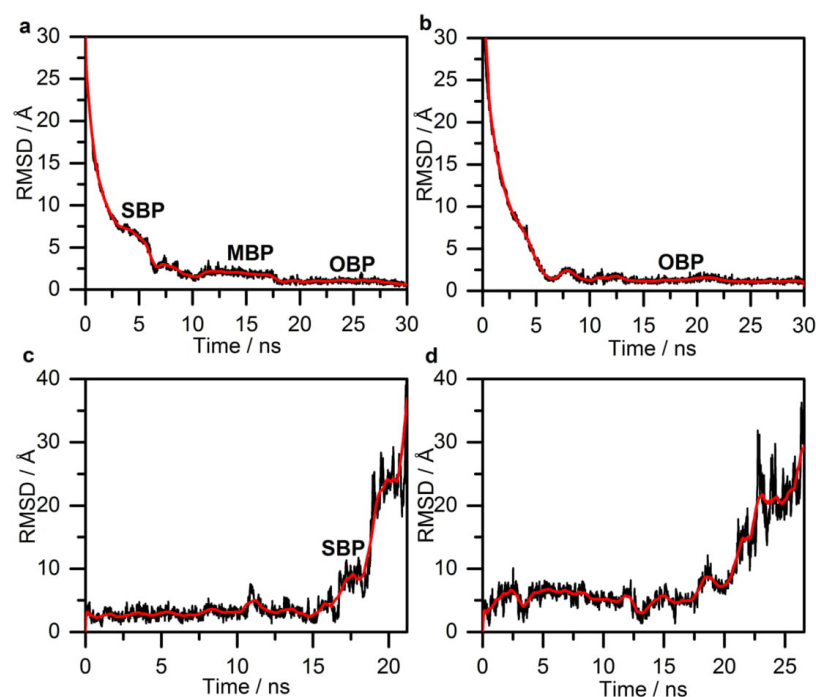


**Figure 4.** Ligand heavy atom RMSD during the binding (a: cariprazine, b: aripiprazole) and unbinding (c: cariprazine, d: aripiprazole) simulations. Black line corresponds to the calculated values, the smoothed curve is calculated as moving average for 100 points for better visualization. The separate phases of the binding are indicated on the graph.

addition of guanosine 5'-[ $\beta$ , $\gamma$ -imido]triphosphate (Gpp(NH)p), the absence of sodium in the buffer or the use of another radioligand ( $[^3\text{H}]$ raclopride).

**Functional binding assays at the D<sub>3</sub>R.**  $\beta$ -arrestin 2 recruitment assays result in EC<sub>50</sub> values of 23.7 nM for aripiprazole and 10.2 nM for cariprazine (monophasic fit). However, a biphasic fit of cariprazine is more appropriate ( $p = 0.0004$ ) with EC<sub>50</sub> values of 5.52 nM and 4.19  $\mu\text{M}$  (Fig. 3c,d). Both are partial agonist in the tested system with ca. 30% of E<sub>max</sub>. A statistically non-significant biphasic binding is observed for cariprazine in radioligand displacement studies with pK<sub>i</sub> of 8.71 and 11.91. In case of aripiprazole, the biphasic fit is not applicable.

**Molecular Modelling.** The root-mean-square deviation of atomic positions (RMSD) against the time-frame in binding trajectories are consistent with the observed biphasic kinetics of cariprazine (Fig. 4a) and the one-phase kinetics of aripiprazole (Fig. 4b). Upon reaching the receptor surface cariprazine contacts extracellular loop (ECL) 2 and ECL1, which are guiding it towards the entrance of the binding site. The 3–5 ns period (Fig. 4a) corresponds to the secondary binding pose (SBP), where cariprazine interacts with extracellular surface residues, mainly on ECL2, the top part of the transmembrane region (TM) 2 and TM5-7 (Fig. 5a). Key hydrogen-bonds (H-bonds) with Ser182<sup>ECL2</sup> and Glu2.65 and hydrophobic interactions (e.g. Val5.39, Pro5.36) contribute to the stabilization (Fig. 5e). Tyr7.35 helps to isolate the ligand from the orthosteric binding site. After 5 ns cariprazine rearranges in the receptor cavity, enters the orthosteric site, transiently stabilized in a metastable binding pose (MBP, 10–17.5 ns, Fig. 4a) then reaches the final, orthosteric binding pose (OBP, 20–30 ns, Fig. 4a). These two positions resemble regarding the orientation of the ligand (Fig. 5b,c), however the occupancy of the key H-bond interaction with Asp3.32 increases from 10% (MBP) to 99% (OBP). Hydrophobic interactions (e.g. Val3.33, Ile183<sup>ECL2</sup>, Phe6.51, Phe5.38, Leu2.64 and Tyr7.35) also contribute to the stabilization (Fig. 5e) of the binding mode. Similar to previous molecular dynamic (MD) studies of D<sub>3</sub>R ligands<sup>19</sup>, Tyr7.35 and the ECL2 residues Ser182, Ile183, Ser184 function as a lock, facilitating the entrance of the ligand into the binding pocket (Fig. 6). The recently published high resolution structure of the D<sub>2</sub>R confirms the impact of Ile184 (Ile183 in the D<sub>3</sub>R) on the binding kinetics of bivalent ligands (ligands bearing two pharmacophores connected by a linker<sup>13,20–22</sup>). Aripiprazole also first interacts with the ECL2 of the receptor, then forms a  $\pi$ - $\pi$  stacking interaction with Tyr7.35. The lock opens and the ligand enters the binding site. A stable intermediate state was not observed (Fig. 4b); the



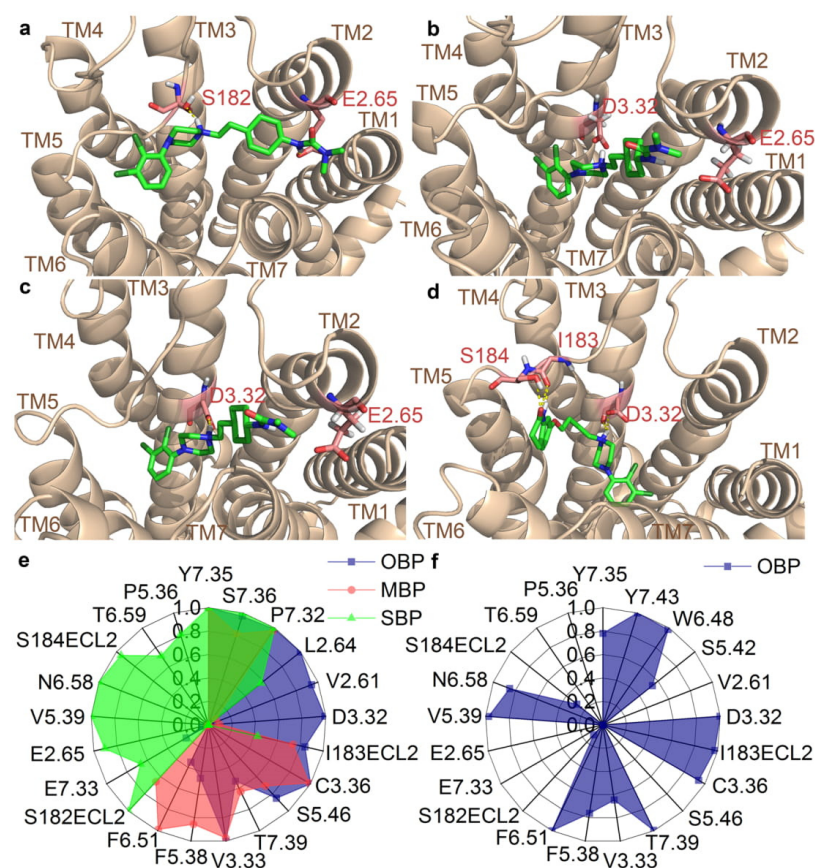


**Figure 5.** Binding poses and frequent interactions during binding simulations. (a–d) Cariprazine in the secondary binding pose (a, SBP), metastable binding pose (b, MBP) and the final binding pose (c, OBP) and aripiprazole's final binding pose (d, OBP). The complexes are visualized from the top, the protein is represented as ribbon, the ligands as green sticks and important residues as light red sticks. Hydrogen bonds are shown as dashed yellow lines. (e,f) Most frequent interactions of cariprazine in the SBP (e, green), MBP (e, red) and OBP (e, blue) and aripiprazole in the OBP (f, blue).

ligand proceeds till it reaches the OBP and forms the H-bond interaction with Asp3.32, which remains intact (10–30 ns). The orientation of the ligand (Fig. 5d) varies compared to cariprazine, but similar interactions were also detected (Fig. 5f). Both H-bonds (Asp3.32, Ile183<sup>ECL2</sup>) and hydrophobic interactions (e.g. Trp6.48, Phe6.51, Tyr7.43) stabilize its binding mode. Stability assessments and unbinding simulations suggest that aripiprazole might also reorient in the binding pocket to a similar pose as cariprazine.

Even though the unbinding simulations offer less reliable structural insight, the trajectories display some characteristic dissociation features. Cariprazine relocates into the SBP after 17 ns (Fig. 4c) and fully dissociates after 21 ns. During the unbinding of aripiprazole (Fig. 4d) we could not observe well defined stages, the higher fluctuations in the RMSD values show less stabilization and the shape of the graph resembles more a one-phase dissociation kinetics.

## Discussion

Cariprazine and aripiprazole display similar dissociation behaviours at the D<sub>2</sub>R, but differ at the D<sub>3</sub>R. Aripiprazole exhibits similar RT at the D<sub>3</sub>R and the D<sub>2</sub>R, whereas cariprazine shows the shortest RT and the most pronounced biphasic behaviour of the tested ligands at the D<sub>3</sub>R. This could influence cariprazine's *in vivo* action, as it can react rapidly to variations in the dopamine level. Recent research revealed that metastable receptor states may determine binding orientation of bivalent drugs in MD simulations<sup>23</sup> and may influence their

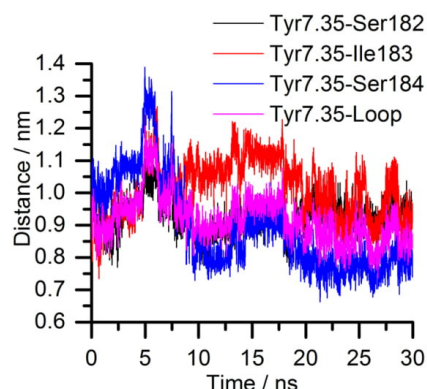


**Figure 6.** Tyr7.35 and ECL2 lock movement during the binding of cariprazine. Distances between the centre of masses of Tyr7.35 and ECL2 residues Ser182, Ile183, Ser184 and the centre of mass of the three residues together representing the loop position in the cariprazine binding trajectory to the D<sub>3</sub>R.

binding kinetics<sup>23</sup>. Our findings suggest that cariprazine's biphasic properties are connected to a metastable binding pose. Different binding poses may influence a biased agonism at the D<sub>3</sub>R, by stimulating different signalling pathways depending on the natural ligand's concentration. It has to be mentioned that there may be other explanations for the biphasic *in vitro* behaviour. Given the high affinity and the fast  $k_{off}$  from the D<sub>3</sub> receptor, the  $k_{on}$  should be fast, which could result in rebinding effects in the assay. To check this possibility, different concentrations of cariprazine (0.2 and 40 times  $K_i$  value,  $n = 1$ ) were evaluated, however, the biphasic nature of its dissociation remained. Although other models may also describe the obtained data, the combination of the experimental data and the MD simulations strengthen a biphasic *in vitro* dissociation profile of cariprazine and a pronounced interaction with different receptor sites. Various studies have shown that the  $\beta$ -arrestin pathway at the D<sub>2</sub>R plays an important role in clinical efficacy of antipsychotics. Genetic  $\beta$ -arrestin depletion led to a loss in antipsychotic activity of tested agents with an increase in motoric ADE<sup>24</sup>. A BRET assay revealed the antagonism of antipsychotic drugs, including aripiprazole, on the D<sub>2</sub>R mediated  $\beta$ -arrestin recruitment<sup>25</sup>. Given the biphasic nature of cariprazine's  $\beta$ -arrestin recruitment and dissociation from the D<sub>3</sub>R, increases in local dopamine concentration may not lead to a complete displacement of the ligand, but a certain amount will be able to act at the target for a longer period.

A recent review<sup>26</sup> criticizes the use of the RT as sole explanation of a drug's profile and claims for individual evaluation of its impact. In the case of antipsychotic agents however, the correlation between RT and drug profiles seems to be a reasonable hypothesis for different *in vivo* profiles<sup>9</sup>. Cariprazine displays a different dissociation profile than other tested ligands and shows concurring properties in functional assays and MD simulations at the D<sub>3</sub>R. Its profile differs especially from aripiprazole, also a highly active antipsychotic, only lacking the effectivity on the negative symptoms. Therefore, the characteristic receptor interaction may be one possible cause behind the efficacy of cariprazine on the negative symptoms of schizophrenia.

Although the clinical effects of cariprazine seem to correlate to its binding behaviour at the D<sub>3</sub>R, there may be additional factors. The translation of an *in vitro/in silico* biphasic behaviour to *in vivo* effects remains to be elucidated and requires more research on the origin of negative symptoms. However, with these findings, it is possible to rationally develop compounds with biphasic kinetics and characterize them *in vivo* regarding their effects on the negative symptomatic. Within this work, we show that:

- Cariprazine and aripiprazole share similar dissociation properties at the D<sub>2</sub>R
- Cariprazine and aripiprazole display different dissociation profiles at the D<sub>3</sub>R
- Cariprazine dissociates faster from the D<sub>3</sub>R than from the D<sub>2</sub>R
- Cariprazine exhibits biphasic kinetics at the D<sub>3</sub>R
- The biphasic behaviour is also observed in functional assays with cariprazine
- MD simulations support the experiments with structural interpretation.

Recent work<sup>13</sup> emphasizes the significance of evaluating and comparing binding modes to understand and advance drug development. By elucidating the binding profile of cariprazine the insights on receptor interaction at the D<sub>3</sub>R were broadened and future evaluation of novel antipsychotic drugs with special focus on the negative symptoms has gained an interesting aspect. By this, a next step in the understanding and improvement of antipsychotic therapy was made and future approaches may benefit from specialized agents for this diverse symptom complex.

## Methods

**Cell culture and membrane preparation of CHO cells expressing the hD<sub>2s</sub>R and the hD<sub>3</sub>R.** Cell culture and membrane preparations were performed as reported previously with modifications<sup>27</sup>. CHO cells stably expressing the human dopamine D<sub>2short</sub>R or D<sub>3</sub>R were cultured in DMEM (with 1% glutamine, 10% FBS, and 1% penicillin/streptomycin for D<sub>2</sub>, 1% glutamine, 10% dialysed FBS for D<sub>3</sub>). CHO-D<sub>2</sub> cells were collected in PBS buffer, CHO-D<sub>3</sub> cells in medium and centrifuged at  $3,000 \times g$  for 10 min at 4 °C. The pellet was resuspended in binding buffer (1 mM MgCl<sub>2</sub>, 1 mM CaCl<sub>2</sub>, 5 mM KCl, 120 mM NaCl and 50 mM Tris, pH 7.7), disrupted and centrifuged at  $23,000 \times g$  for 30 min (4 °C). The resulting pellet was stored in binding buffer at  $-80^{\circ}\text{C}$ .

**Radioligand displacement assays at the hD<sub>2</sub>R and the hD<sub>3</sub>R.** Displacement assays were performed as reported previously<sup>28</sup> with modifications. Briefly, membrane preparations (D<sub>2s</sub>R: 25 µg/well; D<sub>3</sub>R: 20 µg/well) were co-incubated with [<sup>3</sup>H]spiperone (0.2 nM) and the test ligand. Nonspecific binding (NSB) was measured with haloperidol (10 µM) and separation of bound radioligand was performed using VE-water. Assays ran in triplicates at least in three independent experiments. Data was analysed using non-linear regression and equation “one site competition”. The K<sub>i</sub> values were calculated from the IC<sub>50</sub> values using the Cheng-Prusoff equation<sup>29</sup>.

**Determination of the [<sup>3</sup>H]spiperone dissociation rate constants at the D<sub>2</sub>R and the D<sub>3</sub>R.** The k<sub>off</sub> of [<sup>3</sup>H]spiperone (RL) was measured, using an excess of haloperidol<sup>30</sup>. Cell preparations (D<sub>2s</sub>R: 25 µg/well; D<sub>3</sub>R: 20 µg/well) were incubated (120 min, 250 rpm) with 0.2 nM RL in 0.2 mL. The dissociation was initiated at different time points with an excess of haloperidol (0.4 mM stock, 15 µL to prevent dilution). Assays ran in quadruplicates with eleven time points with n = 4 at the D<sub>2</sub>R and n = 7 at the D<sub>3</sub>R. NSB was determined with haloperidol (10 µM), total binding with 0.2 nM RL for the total time of the experiments. Bound RL was separated as described above. Binding data was analysed using non-linear regression and fitting to “one phase exponential decay”.

**Determination of unlabelled ligands dissociation rate constants at the D<sub>2</sub>R and the D<sub>3</sub>R.** The k<sub>off</sub> of unlabelled ligands (UL) were measured indirectly by the dilution method, similar as described previously<sup>30,31</sup>. 50 µL of the membrane preparations (D<sub>2s</sub>R: 25 µg/well; D<sub>3</sub>R: 20 µg/well) were incubated with the UL at four times its K<sub>i</sub> value for 120 min. Afterwards the dissociation was initiated at different time points with an excess of RL (150 µL, 20 times its K<sub>D</sub> value). This dilution results in the majority of the receptors being occupied by RL at the end of the experiment. As the RL may only bind when the UL has dissociated, k<sub>obs</sub> of the RL reflects the k<sub>off</sub> of the UL (Supplementary Fig. S1). To ensure, that the association of the RL occurs without delay to the dissociation of the UL, the concentration of the RL has to be very high (e.g. 20 times K<sub>D</sub> value). This model assumes that RL and UL bind to the same binding site. Assays ran in triplicates with eight time points with at least n = 3 independent experiments. Total binding was measured in the absence of UL; at the end of the experiments 80–100% of the total binding were achieved (spiperone and rotigotine 70% at the D<sub>3</sub>R). Rotigotine was measured at 5 times its K<sub>i</sub> value at the D<sub>3</sub>R. NSB and separation are described above. The k<sub>off</sub> were obtained by applying non-linear regression and fitting to “one phase exponential association” or “two phase exponential association”. As this indirect method underlies model theories and assumptions the resulting k<sub>off</sub> are approximations that serve mainly as comparison criteria. The effects of Gpp(NH)p, the omitting of sodium-ions in the buffer and of using [<sup>3</sup>H]raclopride as RL were evaluated with the same method (n ≥ 2).

**Measurement of β-arrestin 2 activation at the D<sub>3</sub>R by aripiprazole and cariprazine.** The PathHunter® β-arrestin cXpress GPCR assay kit was used to measure β-arrestin recruitment at the D<sub>3</sub>R (protocol of agonists for aripiprazole and cariprazine). Briefly, U2OS cells were incubated at 37 °C for 48 h. Agonist dilutions were added to the respective wells and incubated for 90 min at 37 °C. Afterwards the detection reagent was added and incubated for 60 min at room temperature in the dark. Luminescence was read with the Infinite 1000 Reader (Tecan). Assays ran in duplicates with n = 2 independent experiments. Data was analysed using non-linear regression and fitting to equations “log(agonist) vs. normalized response - variable slope” and “biphasic”. For biphasic fitting “bottom” was constrained to zero, “top” to 100 and nH1/nH2 to 1.

**Molecular modelling approaches at the D<sub>3</sub>R.** MD simulations were performed on cariprazine and aripiprazole. The initial structures were constructed from the D<sub>3</sub>R X-Ray structure (Protein database entry code: 3PBL)<sup>32</sup>, mutated residues were transformed to their natural form, eticlopride was removed. The protein was embedded into a 1-palmitoyl-2-oleoyl-sn-glycero-3-phosphocholine (POPC) lipid bilayer, the complexes were solvated in TIP3P waters and neutralized with chloride ions. Parameterization was based on Amber ff14SB force field<sup>33</sup> and restrained electrostatic potential (RESP)<sup>34</sup> charges were calculated for the ligands. All preparatory steps were carried out with the default parameters in the BiKi Life Sciences suite<sup>35</sup>. The structures were minimized and equilibrated following the default protocol of the program package (see details in the Supplementary Information). Binding studies against the D<sub>3</sub>R were carried out applying BiKi Life Sciences MD Binding tool implemented in GROMACS-4.6.1<sup>36</sup> as published recently<sup>37</sup>. This approach is based on adaptive forces attracting the ligand into the predefined binding site, which residues were identified by NanoShaper<sup>38</sup> and refined by visual inspection (Supplementary Table S1). The additional attractive forces between the ligand and the binding site facilitate the ligand to overcome the barrier of entering the binding pocket; therefore reduce the timescale of the full binding event into a few 10 ns. The bias was switched off, when the ligand reached the 4 Å distance criteria from the backbone heavy atoms of Ser193. During the 20 replica production runs an 0.2 gaining factor was applied in the 30 ns long simulations in isothermal-isobaric (NPT) ensemble at 300 K and 1.013 bar pressure. The binding poses lacking hydrogen bond interaction with the conserved Asp110 were ruled out, the remaining unbiased trajectories were clustered with GROMACS g\_cluster tool by the single-linkage method (1.5 Å cut-off) and their stability was tested with scaled MD. The most stable pose was identified as final binding mode and the



interaction fingerprints were calculated by IChem<sup>39</sup> with default settings based on every 10<sup>th</sup> frame of the corresponding trajectories. The unbinding studies were based on scaled MDs with a scaling factor of 0.4 applying BiKiNetics tool<sup>40</sup>. The final binding mode of the MD binding simulations was the starting pose using structural restraints in canonical (NVT) ensemble at 300 K without the explicit membrane environment. The applied parameters are summarized in Supplementary Table S1. The ligands were considered fully dissociated, when the 6 Å solvation shell around them contained only water molecules.

**Data and statistical analysis.** *In vitro* assays were analysed with Prism 6 (GraphPad Software Inc., San Diego, CA) and are given as means  $\pm$  standard deviation (s.d.). In some instances the number of experiments was increased to characterize binding properties into detail (e.g. biphasic dissociation of cariprazine). This is marked in the tables. The signal of the indirect kinetic experiments and the  $\beta$ -arrestin assays were normalized (zero was set as zero) to allow comparison of different curve shapes. Significance of biphasic fitting over one-phasic fitting or “biphasic” over “log(agonist) vs. normalized response” was tested with the globalized data sets using the “extra sum-of-squares F Test” provided by GraphPad. Comparisons were considered significant if p-value was  $<0.05$  ( $\alpha = 0.05$ ). All *in vitro* assays were performed at room temperature.

**Materials and reagents.** [<sup>3</sup>H]Radioligands were purchased from Perkin Elmer (Waltham, USA). Cariprazine was synthesized at RCNS, Hungary. The authors confirm the identity and purity of the given compound. The  $\beta$ -arrestin kit was purchased from DiscoverX (Birmingham, UK).

**Data availability.** The datasets generated and analysed during the current study are available from the corresponding author on reasonable request.

## References

- Brisch, R. *et al.* The role of dopamine in schizophrenia from a neurobiological and evolutionary perspective: old fashioned, but still in vogue. *Front. Psychiatry* **5**, 47, <https://doi.org/10.3389/fpsy.2014.00047> (2014).
- Sokoloff, P. & Le Foll, B. The dopamine D3 receptor, a quarter century later. *Eur. J. Neurosci.* **45**, 2–19 (2017).
- Ágai-Csongor, É. *et al.* Discovery of cariprazine (RGH-188): a novel antipsychotic acting on dopamine D3/D2 receptors. *Bioorg. Med. Chem. Lett.* **22**, 3437–3440 (2012).
- Wesołowska, A., Partyka, A., Jastrzębska-Więsek, M. & Kołaczowski, M. The preclinical discovery and development of cariprazine for the treatment of schizophrenia. *Expert Opin. Drug Discov.* in press, 1471057; <https://doi.org/10.1080/17460441.2018.1471057> (2018).
- Németh, G. *et al.* Cariprazine versus risperidone monotherapy for treatment of predominant negative symptoms in patients with schizophrenia: a randomised, double-blind, controlled trial. *Lancet* **389**, 1103–1113 (2017).
- Copeland, R. A. Thermodynamics and Binding Kinetics in Drug Discovery [Keszler, G. M. & Swinney, D. C. (ed.)] *Thermodynamics and Kinetics of Drug Binding*, 157–167 (Wiley Online Library, 2015).
- Klein Herenbrink, C. *et al.* The role of kinetic context in apparent biased agonism at GPCRs. *Nat. Commun.* **7**, 10842, <https://doi.org/10.1038/ncomms10842> (2016).
- Carboni, L. *et al.* Slow dissociation of partial agonists from the D(2) receptor is linked to reduced prolactin release. *Int. J. Neuropsychopharmacol.* **15**, 645–656 (2012).
- Vauquelin, G., Bostoen, S., Vanderheyden, P. & Seeman, P. Clozapine, atypical antipsychotics, and the benefits of fast-off D2 dopamine receptor antagonism. *Naunyn-Schmiedeberg's Arch. Pharmacol.* **385**, 337–372 (2012).
- Hauser, A. S., Attwood, M. M., Rask-Andersen, M., Schiöth, H. B. & Gloriam, D. E. Trends in GPCR drug discovery: New agents, targets and indications. *Nat. Rev. Drug Discov.* **16**, 829–842 (2017).
- Roth, B. L., Sheffler, D. & Potkin, S. G. Atypical antipsychotic drug actions: unitary or multiple mechanisms for ‘atypicality’? *Clin. Neurosci. Res.* **3**, 108–117 (2003).
- Langlois, X. *et al.* Pharmacology of JNJ-37822681, a specific and fast-dissociating D2 antagonist for the treatment of schizophrenia. *J. Pharmacol. Exp. Ther.* **342**, 91–105 (2012).
- Wang, S. *et al.* Structure of the D2 dopamine receptor bound to the atypical antipsychotic drug risperidone. *Nature* **555**, 269–273 (2018).
- Kapur, S. & Seeman, P. Antipsychotic agents differ in how fast they come off the dopamine D2 receptors. Implications for atypical antipsychotic action. *J. Psychiatry. Neurosci.* **25**, 161–166 (2000).
- Leysen, J. E. & Gommeren, W. The dissociation rate of unlabelled dopamine antagonists and agonists from the dopamine-D2 receptor, application of an original filter method. *J. Recept. Res.* **4**, 817–845 (1984).
- Sibley, D. R., Mahan, L. C. & Creese, I. Dopamine receptor binding on intact cells. Absence of a high-affinity agonist-receptor binding state. *Mol. Pharmacol.* **23**, 295–302 (1983).
- Seeman, P. Targeting the dopamine D2 receptor in schizophrenia. *Expert Opin. Ther. Targets* **10**, 515–531 (2006).
- Wood, M., Dubois, V., Scheller, D. & Gillard, M. Rotigotine is a potent agonist at dopamine D1 receptors as well as at dopamine D2 and D3 receptors. *Br. J. Pharmacol.* **172**, 1124–1135 (2015).
- Thomas, T., Fang, Y., Yuriev, E. & Chalmers, D. K. Ligand binding pathways of clozapine and haloperidol in the dopamine D2 and D3 receptors. *J. Chem. Inf. Model.* **56**, 308–321 (2016).
- Bonifazi, A. *et al.* Novel bivalent ligands based on the sumanirole pharmacophore reveal Dopamine D2 Receptor (D2R) biased agonism. *J. Med. Chem.* **60**, 2890–2907 (2017).
- Lane, J. R., Sexton, P. M. & Christopoulos, A. Bridging the gap: Bitopic ligands of G-protein-coupled receptors. *Trends Pharmacol. Sci.* **34**, 59–66 (2013).
- Strasser, A., Wittmann, H.-J. & Seifert, R. Binding kinetics and pathways of ligands to GPCRs. *Trends Pharmacol. Sci.* **38**, 717–732 (2017).
- Lane, J. R. *et al.* Structure-based ligand discovery targeting orthosteric and allosteric pockets of dopamine receptors. *Mol. Pharmacol.* **84**, 794–807 (2013).
- Allen, J. A. *et al.* Discovery of  $\beta$ -arrestin-biased dopamine D2 ligands for probing signal transduction pathways essential for antipsychotic efficacy. *Proc. Natl. Acad. Sci. USA* **108**, 18488–18493 (2011).
- Masri, B. *et al.* Antagonism of dopamine D2 receptor/ $\beta$ -arrestin 2 interaction is a common property of clinically effective antipsychotics. *Proc. Natl. Acad. Sci. USA* **105**, 13656–13661 (2008).
- Folmer, R. H. A. Drug target residence time: a misleading concept. *Drug Discov. Today* **23**, 12–16 (2018).
- Sokoloff, P. *et al.* Pharmacology of human dopamine D3 receptor expressed in a mammalian cell line: comparison with D2 receptor. *Eur. J. Pharmacol.* **225**, 331–337 (1992).

28. Schübler, M., Sadek, B., Kottke, T., Weizel, L. & Stark, H. Synthesis, molecular properties estimations, and dual dopamine D2 and D3 receptor activities of benzothiazole-based ligands. *Front. Chem.* **5**, 64, <https://doi.org/10.3389/fchem.2017.00064> (2017).
29. Yung-Chi, C. & Prusoff, W. H. Relationship between the inhibition constant ( $K_i$ ) and the concentration of inhibitor which causes 50 per cent inhibition ( $IC_{50}$ ) of an enzymatic reaction. *Biochem. Pharmacol.* **22**, 3099–3108 (1973).
30. Bosma, R., Mocking, T. A. M., Leurs, R. & Vischer, H. F. Ligand-Binding Kinetics on Histamine Receptors [Tiligada, E. & Ennis, M. (ed.)] *Histamine Receptors as Drug Targets*, 115–155 (Springer Science+ Business Media LLC, New York, USA).
31. Swinney, D. C. *et al.* A study of the molecular mechanism of binding kinetics and long residence times of human CCR5 receptor small molecule allosteric ligands. *Br. J. Pharmacol.* **171**, 3364–3375 (2014).
32. Chien, E. Y. T. *et al.* Structure of the human dopamine D3 receptor in complex with a D2/D3 selective antagonist. *Science* **330**, 1091–1095 (2010).
33. Maier, J. A. *et al.* ff14SB: Improving the accuracy of protein side chain and backbone parameters from ff99SB. *J. Chem. Theor. Comp.* **11**, 3696–3713 (2015).
34. Bayly, C. I., Cieplak, P., Cornell, W. & Kollman, P. A. A well-behaved electrostatic potential based method using charge restraints for deriving atomic charges: the RESP model. *J. Phys. Chem.* **97**, 10269–10280 (1993).
35. Decherchi, S., Bottegoni, G., Spitaleri, A., Rocchia, W. & Cavalli, A. BiKi Life Sciences: a new suite for molecular dynamics and related methods in drug discovery. *J. Chem. Inf. Model.* **58**, 219–224 (2018).
36. Pronk, S. *et al.* GROMACS 4.5: A high-throughput and highly parallel open source molecular simulation toolkit. *Bioinformatics* **29**, 845–854 (2013).
37. Spitaleri, A., Decherchi, S., Cavalli, A. & Rocchia, W. Fast dynamic docking guided by adaptive electrostatic bias: the MD-Binding approach. *J. Chem. Theor. Comp.* **14**, 1727–1736 (2018).
38. Decherchi, S. & Rocchia, W. A general and robust ray-casting-based algorithm for triangulating surfaces at the nanoscale. *PLoS one* **8**, e59744 (2013).
39. Marcou, G. & Rognan, D. Optimizing fragment and scaffold docking by use of molecular interaction fingerprints. *J. Chem. Inf. Model.* **47**, 195–207 (2007).
40. Mollica, L. *et al.* Kinetics of protein-ligand unbinding via smoothed potential molecular dynamics simulations. *Sci. Rep.* **5**, 11539, <https://doi.org/10.1038/srep11539> (2015).

### Acknowledgements

The authors thank Andrea Cavalli and Sergio Decherchi (Istituto Italiano di Tecnologia (IIT)) for providing access to BiKi Life Sciences software and their suggestions, Didier Rognan for providing the license of IChem and the National Information Infrastructure Development (NIIF) Programme for providing us access to the supercomputers in Hungary. CHO-D<sub>3</sub> cells were a kind donation of Prof. Dr. Shine (Garvan Institute, Australia). CHO-D<sub>3</sub> cells were donated by Prof. Dr. Sokoloff (Centre Paul Broca de l'INSERM, France). AF and HS participate in the DFG GRK2158- "Natural products and natural product analogs against therapy-resistant tumors and microorganism". D.J.K., G.M.K. and H.S. participated in COST Action CM1207 – "GLISTEN: GPCR-ligand interactions, structures, and transmembrane signalling". D.J.K. and G.M.K. were supported by the National Brain Research Program (2017-1.2.1-NKP-2017-00002). H.S. was kindly supported by DFG INST208/664 and COST Action CA15135. The authors thank S. Hagenow, D. Reiner and M. Frank for scientific discussion.

### Author Contributions

A.F. designed, performed and interpreted the radioligand and  $\beta$ -arrestin assays and wrote the paper; D.J.K. performed and analysed the simulations and contributed to the paper; G.M.K. contributed to the design and interpretation of studies and the paper; H.S. contributed to the design and interpretation of studies and the paper. He also supervised the project. All authors reviewed the manuscript.

### Additional Information

**Supplementary information** accompanies this paper at <https://doi.org/10.1038/s41598-018-30794-y>.

**Competing Interests:** G.M.K. contributed to the discovery of cariprazine. The other authors declare no competing interests.

**Publisher's note:** Springer Nature remains neutral with regard to jurisdictional claims in published maps and institutional affiliations.



**Open Access** This article is licensed under a Creative Commons Attribution 4.0 International License, which permits use, sharing, adaptation, distribution and reproduction in any medium or format, as long as you give appropriate credit to the original author(s) and the source, provide a link to the Creative Commons license, and indicate if changes were made. The images or other third party material in this article are included in the article's Creative Commons license, unless indicated otherwise in a credit line to the material. If material is not included in the article's Creative Commons license and your intended use is not permitted by statutory regulation or exceeds the permitted use, you will need to obtain permission directly from the copyright holder. To view a copy of this license, visit <http://creativecommons.org/licenses/by/4.0/>.

© The Author(s) 2018

## Supplementary Information

## Binding kinetics of cariprazine and aripiprazole at the dopamine D<sub>3</sub> receptor

Annika Frank<sup>1</sup>, Dóra J. Kiss<sup>2,3</sup>, György M Keserű<sup>2\*</sup>, Holger Stark<sup>1\*</sup><sup>1</sup>Institute of Pharmaceutical and Medicinal Chemistry, Heinrich Heine University Düsseldorf, Düsseldorf, Germany<sup>2</sup>Medicinal Chemistry Research Group, Research Centre for Natural Sciences, Hungarian Academy of Sciences, Budapest, Hungary<sup>3</sup>ELTE Eötvös Loránd University, Doctoral School of Chemistry, Budapest, Hungary*Equilibration protocol for the MD simulations.*

The 5000 steps of steepest descent minimization were followed by three equilibration step in canonical (NVT) ensemble. The temperature was increased from 100 K to 300 K applying the velocity-rescaling temperature coupling available in the GROMACS program package. The backbone restraints were lifted off after the second NVT step. Each stage run for 0.1 ns with 2 fs time steps, except in the first stage a 1 fs time step was applied. The final equilibration step contained 1 ns run in NPT ensemble with 2 fs time steps at 300K and 1.013 bar pressure applying a Parrinello-Rahman barostat.

**Table S1:** Parameters applied during MD binding and unbinding simulations. Ser193 was set as switch off in the binding simulations

MD protocol	Residues
MD Binding attractive residues	V78 F106 V107 D110 V111 C114 T115 I183 F188 V189 S192 S193 S196 W342 F345 F346 H349 T368 T369 V373
BiKiNetics unrestrained residues	T36 V86 L89 E90 F106 V107 D110 V111 M112 M113 C114 T115 C181 S182 I183 S184 F188 V189 I190 S192 S193 V195 S196 W342 F345 F346 H349 T365 S366 T369 V373



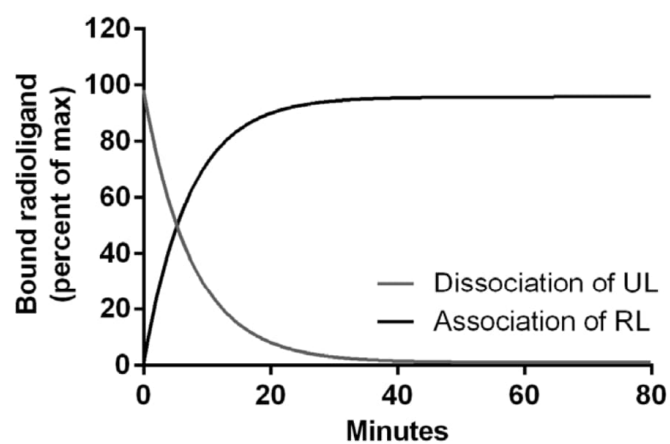


Figure S1: Principle of the dilution method.

#### Figure Legend

Figure S1: Principle of the dilution method. Receptor preparations are pre-incubated with the UL. Afterwards the dissociation is initiated with an excess of RL. As the RL may only bind, when the UL has dissociated the  $k_{obs}$  of the RL equals the  $k_{off}$  of the UL.

## 10 Conclusions and prospects

This work describes the pharmacological *in vitro* evaluation of novel scaffolds at aminergic GPCRs. Thereby, it raises new motivations for subsequent *in vivo* and *in silico* evaluation of these scaffolds.

So far, agents targeting the H<sub>4</sub>R provide only poor efficacy or drug-likeness and none have entered the market (Thurmond, 2015). In the presented work (chapter 3), an array of methanolic extracts, including a *Curcuma* rhizoma extract, were evaluated *in vitro* (Frank et al., 2017). Curcumin and two derivatives (Figure 16) emerged as ligands for the H<sub>4</sub>R, exhibiting moderate, but dose dependent activity in radioligand displacement assays and providing novel non-amine scaffolds for H<sub>4</sub>R ligands (Frank et al., 2017). Curcumin enjoys high popularity as a natural remedy for the treatment of inflammatory diseases, which is a research field closely connected to the H<sub>4</sub>R. Many efforts have been made to increase its status from food supplement to evidence-based clinical agent, but *in vivo* evidence of its anti-inflammatory action has not been convincingly presented so far. On the other hand, *in vitro* evidence for its action on various targets in the fields of inflammation is steadily growing, making it a hot topic in natural product research (Mirzaei et al., 2018; Qureshi et al., 2018; Shehzad et al., 2019). At the same time, criticism regarding false positive results is on the rise, as curcumin displays poor drug-likeness and belongs to a class of pan-assay interfering compounds (PAINS) (Nelson et al., 2017). Such problems may occur because of interferences with cells or spectroscopic instruments during assay readout. In this study, interferences of curcumin are not expected, as the readout is based on radiometric signals. A non-labeled ligand must compete with a radiolabelled ligand at the binding site, leaving small risk for false positive signals. Additionally, membrane preparations were used, reducing the risk of cell-based interference compromising the assay. Interestingly, the crude extract of *Curcuma longa* was more active than the pure components of the extract (Frank et al., 2017). This further suggests that the effects in the assay are not caused by assay interference of curcumin. Although curcumin depicts a ligand that needs to be evaluated carefully, within this study curcumin derivatives were determined to be potential non-amine H<sub>4</sub>R ligands, representing a promising new pharmacophore at this receptor. The lack of a basic amine in this structure gives indication for a novel binding mode or unreported binding pocket in the H<sub>4</sub>R. This would be a profitable prospect for additional research regarding curcumin's action in inflammatory diseases at the H<sub>4</sub>R. Functional assays on these derivatives could further elucidate the regulatory role of the H<sub>4</sub>R in inflammation.

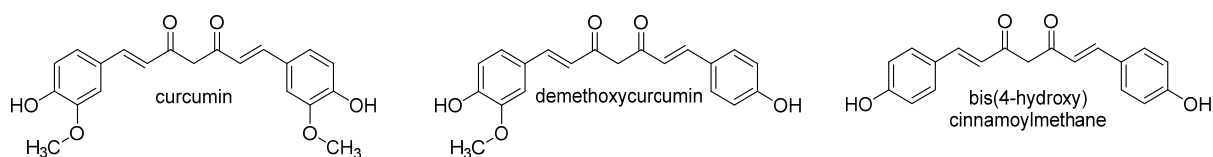


Figure 16: Structures of compounds of the methanolic extract of *Curcuma* rhizomes (chapter 3) (Frank et al., 2017).

## 10 Conclusions and prospects

The use of natural product inspired compounds was also successful in the design and evaluation of a small series of pyrrolo[2,3-*d*]pyrimidine derivatives as potential H<sub>3</sub>R ligands (chapter 4). The natural compound class of pyrrolo[2,3-*d*]pyrimidines is usually investigated for anti-infectious and -inflammatory properties (Jiang et al., 2019; Raju et al., 2019; Shah et al., 2018). Compound repositioning, by the combination of this scaffold with known H<sub>3</sub>R moieties, afforded novel H<sub>3</sub>R ligands with potentially extended pharmacological properties. This was realised by introducing lipophilic and basic moieties to the 7-position and 4-position respectively, enabling the possibility to use natural products as starting point for scaffold evaluation. The first series of novel pyrrolo[2,3-*d*]pyrimidines provided selective *in vitro* H<sub>3</sub>R affinity, which was complemented by the results of *in silico* experiments and presents a novel class of H<sub>3</sub>R lead compounds (chapter 4, lead A in Figure 17) (Espinosa-Bustos et al., 2018). Conducting a rationale-based drug optimization approach allowed for the design of a second series that convinced by increased H<sub>3</sub>R affinity and selectivity (chapter 5) (Frank et al., 2019). The effects of dehalogenation at 2-position and electron withdrawing moieties at a benzyl moiety in 7-position gave an impetus for prospective SAR studies (Frank et al., 2019). These ligands provide valuable insights for derivatization of similar H<sub>3</sub>R scaffolds in the future, as the changes did result in low nanomolar affinities (lead B in Figure 17) and the derivatization pattern of the benzyl followed a trend with increased binding affinity through higher electron-withdrawing capacities of the substitution. The presented series is rather small and lacks structural modifications that could improve binding affinities or could explore the derivatization possibilities of the scaffold. Implementation of piperidinyloxy groups as basic part or a shift of the lipophilic part to the 6-position present reasonable prospects for derivatization of this natural compound inspired class. The introduction of halogens, especially fluorine, into the agents provides interesting alterations to their pharmacokinetic and physicochemical properties (Hardman, 1991; Purser et al., 2008). Hence, evaluation of pharmacokinetic properties could be highly interesting and could be performed in a next step.

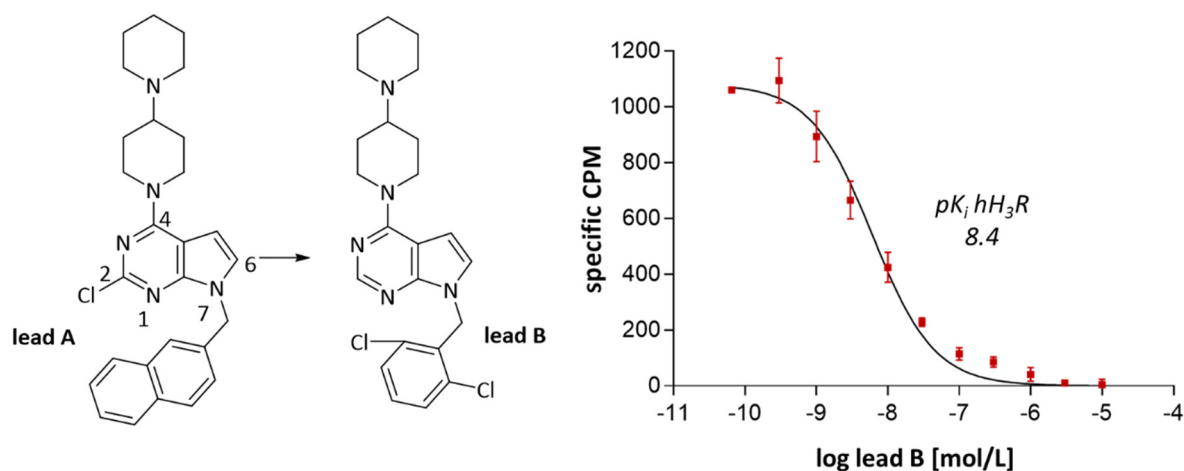


Figure 17: Scaffold optimization of natural product inspired compounds (chapter 4 and 5) and representative binding curve for the most active compound (lead B, chapter 5) (Espinosa-Bustos et al., 2018; Frank et al., 2019).

## 10 Conclusions and prospects

Potential lead compounds from *in vitro* affinity screenings need to be forwarded into *in vivo* evaluation and early preclinical *in vitro* evaluation regarding pharmacokinetic parameters, to improve the existing scaffolds. A series of (homo)piperidine ether derivative-based H<sub>3</sub>R ligands, inspired by pitolisant, was found to present selective H<sub>3</sub>R activity, which gave motivation for their subsequent *in vivo* evaluation as anti-epileptic agents (chapter 6) (Alachkar et al., 2018). Two compounds (**4** and **13** in the publication, Figure 18) emerged as successful, preclinical agents, when they were tested in epilepsy mouse models. Compound **4** displayed highest potential among the tested substances in maximal electroshock- and chemically (pentylenetetrazol) induced seizure models (Alachkar et al., 2018). An *in silico* ADME-Tox screening and *in vitro* evaluation of CYP interactions revealed satisfying pharmacokinetic properties, thereby substantiating a further evaluation of this novel agent (Alachkar et al., 2018). As stated in chapter 6, further *in vivo* studies with different species are necessary for the prospective evaluation of compound **4**. This work is an example for the benefits of early *in vitro* scaffold evaluation. The presented series was developed by optimizing previous research (Sadek et al., 2016a) on this scaffold class and allowed for the determined development and characterization of *in vivo* active ligands.

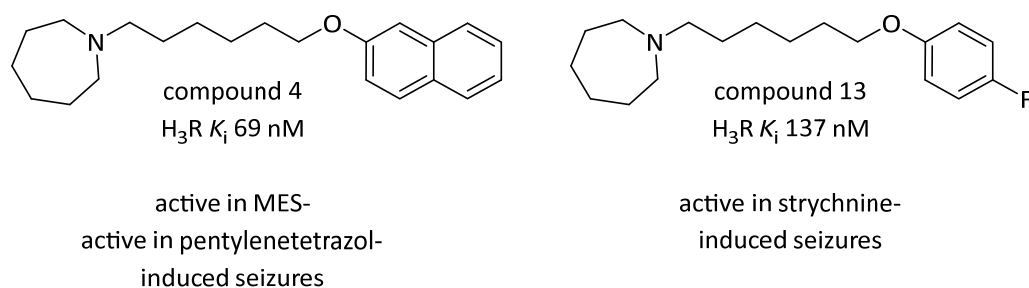


Figure 18: Chemical structures of the two most promising compounds in *in vivo* animal models for epilepsy (chapter 6) (Alachkar et al., 2018).

## 10 Conclusions and prospects

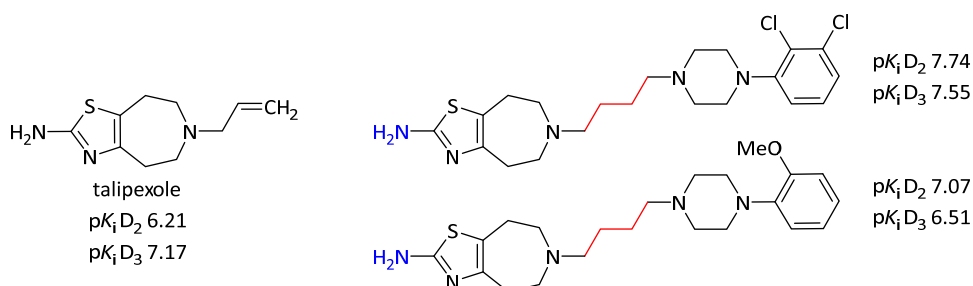


Figure 19: Chemical structures of talipexole, the most active compound bearing a 1-(2,3-dichlorophenyl)-piperazine and the compound bearing a (2-methoxyphenyl)piperazine (chapter 7) (Stank et al., 2019). The amino moiety (blue) is interesting for investigating bioisosteric replacement, while the linker length (red) is supposed to yield receptor subtype selectivity.

The previous scaffolds of this work bear only one pharmacophore, directed at one binding site. In contrast to that, a small series of bitopic  $D_2/D_3R$  ligands was synthesized and pharmacologically characterized, to address two binding sites with one novel scaffold (chapter 7) (Stank et al., 2019). The demand for subtype selective dopamine receptor ligands is on the rise and design of bitopic ligands with a defined linker length and two pharmacophores provides a valuable addition to recent attempts (Cao et al., 2016; Cao et al., 2018; Omran et al., 2018). Combining reported dopamine receptor preferring pharmacophores with a 5,6,7,8-tetrahydro-4*H*-thiazolo[4,5-*d*]azepin-2-amine, inspired by talipexole, yielded the presented small series of novel, bitopic ligands (chapter 7) (Stank et al., 2019). Novel hit compounds at  $D_2/D_3Rs$  were identified, with the most active compound (1-(2,3-dichlorophenyl)piperazine derivative, Figure 19), lacking receptor selectivity, but displaying increased affinity compared to talipexole (Stank et al., 2019). A deamination of the active 5,6,7,8-tetrahydro-4*H*-thiazolo[4,5-*d*]azepin-2-amine did not influence selectivity or even receptor affinity (Stank et al., 2019). An aminated (2-methoxyphenyl)piperazine (Figure 19) was not synthesized, as the presented series was not an iterative attempt (Stank et al., 2019). Therefore a general statement regarding the deamination of bioisosteric replacements in these ligands is not possible, but presents a reasonable approach for further derivatization. The linker length did not influence  $D_3R$  affinity of the presented (2-methoxyphenyl)piperazines, but prolongation of the dimethyl linker with tetramethyl and trimethyl groups resulted in slightly increased  $D_2R$  affinity (Stank et al., 2019). Previous results suggested more flexible bitopic ligands should be preferred by the  $D_3R$ 's SBP, given its different spatial orientation (Newman et al., 2012; Wang et al., 2018). A reasonable prospect for further elucidation on this topic might be the linker derivatization of the more active 1-(2,3-dichlorophenyl)piperazines or *in silico* evaluations that resolve the binding orientation of the presented ligands. Battiti and colleagues recently reported on the influence of chirality on the affinity of  $D_3R$  selective bitopic ligands (Battiti et al., 2019). Hence, the introduction of achiral 5,6,7,8-tetrahydro-4*H*-thiazolo[4,5-*d*]azepines provides further benefits. It has to be noted that a functional *in vitro* evaluation of these compounds was not performed yet, which would be necessary to assess clinical implication of such ligands.

## 10 Conclusions and prospects

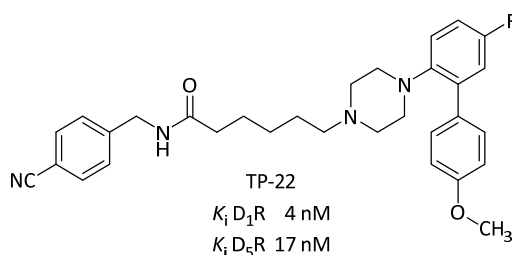


Figure 20: Chemical structure of TP-22 (chapter 8) (Carbone et al., 2019), including presented receptor affinities for the D<sub>1</sub>R and D<sub>5</sub>R subtype.

The involvement of serotonin and dopamine receptor subtypes and especially their interplay is the topic of general interest in neurological disorders given a high degree of overlap of the receptor's scaffolds. Evaluating *N*-(4-cyanobenzyl)-6-(4-(5-fluoro-4'-methoxy-[1,1'-biphenyl]-2-yl)piperazin-1-yl)hexanamide, a 5-HT<sub>7</sub>R agonist (Figure 20, TP-22), at the dopamine receptor subtypes revealed *in vitro*  $K_i$  values in the low nanomolar range at the D<sub>1</sub>R and D<sub>5</sub>R, with low affinities at D<sub>2</sub> and D<sub>3</sub>Rs (chapter 8) (Carbone et al., 2019). Further *in vitro* evaluation showed antagonist properties at D<sub>1</sub>Rs that complement its 5-HT<sub>7</sub> receptor activity (Carbone et al., 2019). In the presented study TP-22 increased the effects of methylphenidate in two animal models, which is surprising given its *in vitro* evaluation as D<sub>1</sub>R antagonist. Agonist behaviour on 5-HT receptor subtypes and antagonist properties at dopamine receptor subtypes are rarely reported. Animal models that evaluate the *in vivo* behaviour of TP-22 at dopamine receptor subtypes, especially D<sub>1</sub> and D<sub>5</sub>Rs, could elucidate this observation. A comparison of the RT at the dopamine and serotonin receptor subtypes could also be helpful to bring the different functionalities into accordance. Nevertheless, the presented results strengthen the importance of early *in vitro* evaluation of various receptor subtype affinities and binding modes to identify pharmacologically striking features that could ease preclinical transition of multi-target-directed ligands.

The DTRT evaluation promises improved translation of *in vitro* findings to *in vivo* behaviour (Daryaei, Tonge, 2019) and has been linked to clinical profiles in the case of D<sub>2</sub>R antagonists (Fyfe et al., 2019; Kapur, Seeman, 2000; 2001). Within the presented study (chapter 9) cariprazine (Vraylar®) showed a unique *in vitro* biphasic dissociation profile with a short RT (Figure 21A), among the four test compounds (Frank et al., 2018). The *in vitro* results were supported by *in silico* binding and unbinding evaluations and complemented by *in vitro* functional assays for  $\beta$ -arrestin recruitment (Frank et al., 2018). Aripiprazole, displayed different *in vitro* as well as *in silico* D<sub>3</sub>R binding and unbinding (Figure 21A) but no differences in functionality. Cariprazine was just recently approved as one of the first ligands for the use in schizophrenia with mainly negative symptoms (Ragguett, McIntyre, 2019). A bimolecular and rapid dissociation could enable the D<sub>3</sub>R to react to peaks in dopamine levels but still allow for a balanced D<sub>3</sub>R signaling that is discussed to be disturbed in negative symptoms (Frank et al.,



## 10 Conclusions and prospects

2018; Simpson et al., 2014). The differences in D<sub>3</sub>R RT and unbinding could explain the clinical variations of aripiprazole and cariprazine, as structural motifs ((2,3-dichloro)piperazines), receptor affinities as well as functional properties of the two ligands are otherwise comparable. However, this is speculative and follow-up studies will be necessary to test this hypothesis. Accordingly, two compounds, structurally related to cariprazine, were synthesized and are currently under evaluation for their RT (unpublished data). In addition to the identification of novel target-interactions of cariprazine the presented assay displays an innovative tool for the assessment of DTRTs. Prior RT evaluations of unlabelled ligands usually neglected drug-target interactions that involve more than one reaction step (Figure 21B). Especially the often used Motulsky and Mahan equation was until recently limited to monomolecular binding events. Given the reported SBP (Chien et al., 2010; Wang et al., 2018) for the D<sub>2</sub> and D<sub>3</sub>R this would be insufficient for describing all possible binding interactions. The published work (chapter 9) is one of the first indirect radioligand assays that addresses this issue. It was published at the same time as another method that used mathematical modifications of the Motulsky and Mahan equation for this intention (Guo et al., 2018). While the presented assay does not allow for evaluation of association times, it has a higher throughput than the method of Guo and colleagues (up to four compounds per plate instead of one) although the high amount of radiolabelled ligand (20 times K<sub>i</sub>) that is required to perform this assay, limits its cost effectiveness. This novel assay does not require RT characterization of the radiolabelled ligand, although it should bind sufficiently fast to the receptor. When comparing the total counts per minute of the radiolabelled ligand in presence of the fastest unlabelled ligand (cariprazine) and the radiolabelled ligand without presence of competitor, more radiolabelled ligand had bound at respective time points in case of the radiolabelled ligand without competitor. This supports a sufficiently fast association.

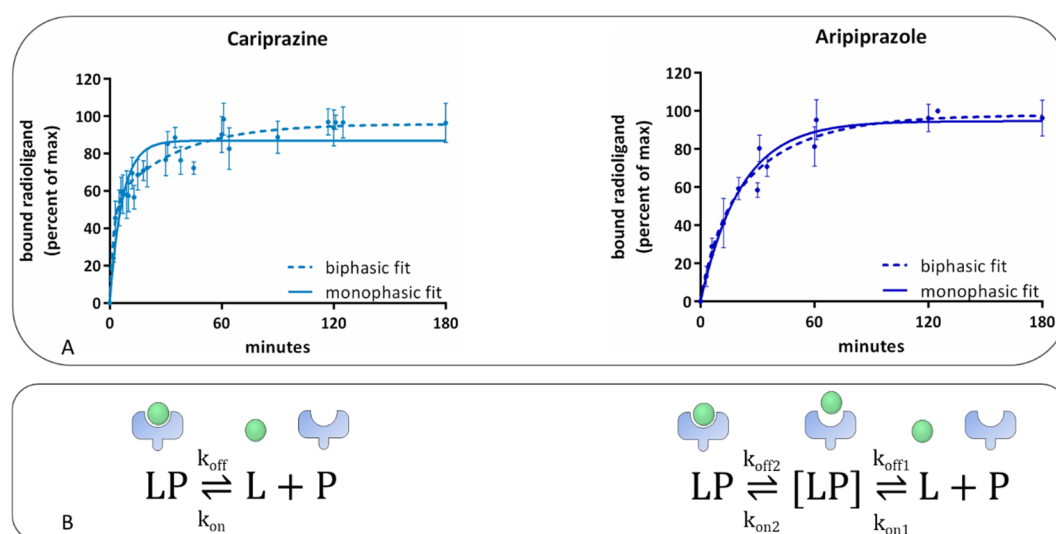


Figure 21: (A) Dissociation behaviour of cariprazine (left) and aripiprazole (right) at the D<sub>3</sub>R in vitro (chapter 9) (Frank et al., 2018). (B) Monomolecular drug-target interactions (left) against bimolecular target interactions (right). L: ligand; P: protein.

## 10 Conclusions and prospects

A general drawback of displacement assays is the simplified assumption that radiolabelled and unlabelled ligand bind exclusively to the same binding sites. Radiolabelling and subsequent RT evaluation of cariprazine could be helpful in additional studies, to definitely confirm the reported target-interactions. The presented publication is one of the first published results for DTRT investigations of unlabelled ligands at the D<sub>3</sub>R, where others investigated only radiolabelled compounds (Fasciani et al., 2018; Wood et al., 2015). Hence, this work not only sheds light on cariprazine's mode of action but also allows for future medium-throughput evaluation of unlabelled ligands at the D<sub>2</sub> and D<sub>3</sub>R. The results further implicate a role of the D<sub>3</sub>R in the treatment of negative symptoms in schizophrenia. To which extent dissociation kinetics do influence clinical profiles has to be evaluated in follow-up studies by comparing dissociation profiles of clinical agents that act as strongly on the negative symptoms as cariprazine. The *in vivo* evaluation of compounds that show a similar dissociation profile will hopefully yield experimental support for this hypothesis.

The presented results address recent issues of histamine, dopamine and serotonin receptor subtype targeting by exploring novel scaffolds, investigating pathway interactions and implementing new evaluation tools for a better *in vivo* translation of *in vitro* results. The evaluation of natural compounds and natural compound inspired scaffolds as histamine receptor ligands combines the fields of pharmaceutical biology and pharmaceutical chemistry and yielded novel compounds with improved binding affinities and previously unreported scaffolds. Furthermore, this work implemented a novel DTRT assay that is the first to describe D<sub>3</sub>R RT of unlabelled ligands and detected unreported binding interactions of a recently approved antipsychotic agent. By that, it supported mode of action evaluations for cariprazine and contributed to a better understanding in the treatment of negative symptoms.

## 11 List of abbreviations

5-HT<sub>7</sub>R: Serotonin 5-HT<sub>7</sub> receptor

ABS: Allosteric binding site

AC: Adenylyl cyclase

ADE: Adverse drug effects

ADHD: Attention deficit hyperactivity disorder

Asp: Aspartate

Ca<sup>2+</sup>: Calcium ions

cAMP: 3',5'-Cyclic adenosine monophosphate

CNS: Central nervous system

COMT: Catechol-O-methyltransferase

CYP: Cytochrome P450

D<sub>1</sub>R: Dopamine D<sub>1</sub> receptor

D<sub>2</sub>R: Dopamine D<sub>2</sub> receptor

D<sub>3</sub>R: Dopamine D<sub>3</sub> receptor

D<sub>4</sub>R: Dopamine D<sub>4</sub> receptor

D<sub>5</sub>R: Dopamine D<sub>5</sub> receptor

DAG: Diacylglycerol

DAT: Dopamine transporter

DB: Database

DDC: DOPA decarboxylase

DOPAC: Dihydroxyphenylacetic acid

DTRT: Drug-target residence time

ECL: Extracellular loop

e.g.: Exempli gratia

EMA: European Medicines Agency

EPS: Extrapyramidal side effects

FDA: U.S. Food and Drug Administration

Gα: G protein α-subunit

GABA: γ-Aminobutyric acid

## 11 List of abbreviations

---

GDP:	Guanosine diphosphate
G $\beta\gamma$ :	G protein $\beta\gamma$ -subunit
GIRK:	G protein-gated inwardly rectifying potassium
GPCR:	G protein-coupled receptor
GTP:	Guanosine triphosphate
H <sub>1</sub> R:	Histamine H <sub>1</sub> receptor
H <sub>2</sub> R:	Histamine H <sub>2</sub> receptor
H <sub>3</sub> R:	Histamine H <sub>3</sub> receptor
H <sub>4</sub> R:	Histamine H <sub>4</sub> receptor
ICL:	Intracellular loop
IP3:	Inositol (1,4,5)-trisphosphate
IUPHAR:	International Union of Basic and Clinical Pharmacology
K <sup>+</sup> :	Potassium ions
k <sub>obs</sub> :	Observed kinetic rate constant
k <sub>off</sub> :	Dissociation rate constant
k <sub>on</sub> :	Association rate constant
[L]:	Ligands concentration [mol/L]
MAO:	Monoamine oxidase
MAPK:	Mitogen-activated proteinkinase
OBS:	Orthosteric binding site
PD:	Parkinson's disease
PKA:	Proteinkinase A
PKC:	Proteinkinase C
PLC $\beta$ :	Phospholipase C- $\beta$
RLS:	Restless-legs syndrome
RT:	Residence time
SARs:	Structure-activity relationships
SBP:	Secondary binding pocket
SN:	Substantia nigra
t <sub>1/2</sub> asso:	Association half-life time
t <sub>1/2</sub> disso:	Dissociation half-life time

## 11 List of abbreviations

---

TH: Tyrosine-3-hydroxylase

TMD: Transmembrane domain

VMAT: Vesicular monoamine transporter

## 12 Research contributions

### Chapter 3

Frank A, Abu-Lafi S, Adawi A, Schwed JS, Stark H, Rayan A. From medicinal plant extracts to defined chemical compounds targeting the histamine H<sub>4</sub> receptor: Curcuma longa in the treatment of inflammation. *Inflammation Research* (2017), **66**: 923-929.

Research contribution: Pharmacological evaluation of majority of extracts and compounds at the H<sub>4</sub> receptor, interpretation of data and preparation of manuscript.

### Chapter 4

Espinosa-Bustos C, Frank A, Arancibia-Opazo S, Salas CO, Fierro A, Stark H. New lead elements for histamine H<sub>3</sub> receptor ligands in the pyrrolo[2,3-d]pyrimidine class. *Bioorganic & Medicinal Chemistry Letters* (2018), **28**: 2890-2893.

Research contribution: Pharmacological evaluation of compounds at the H<sub>3</sub> and H<sub>4</sub> receptor, interpretation of data and preparation of manuscript.

### Chapter 5

Frank A, Meza-Arriagada F, Salas CO, Espinosa-Bustos C, Stark H. Nature-inspired pyrrolo[2,3-d]pyrimidines targeting the histamine H<sub>3</sub> receptor. *Bioorganic & Medicinal Chemistry* (2019), **27**: 3194-3200.

Research contribution: Pharmacological evaluation of compounds at the H<sub>3</sub> and H<sub>4</sub> receptor, interpretation of data and preparation of manuscript.

### Chapter 6

Alachkar A, Łażewska D, Latacz G, Frank A, Siwek A, Lubelska A, Honkisz-Orzechowska E, Handzlik J, Stark H, Kieć-Kononowicz K, Sadek B. Studies on anticonvulsant effects of novel histamine H<sub>3</sub>R antagonists in electrically and chemically induced seizures in rats. *International Journal of Molecular Sciences* (2018), **19**: 3386, DOI: 10.3390/ijms19113386.

Research contribution: Statistical evaluation of *in vitro* compound data at the H<sub>3</sub> and H<sub>4</sub> receptor, interpretation of data and partial preparation of manuscript.



### Chapter 7

Stank L, Frank A, Hagenow S, Stark H. Talipexole variations as novel bitopic dopamine D<sub>2</sub> and D<sub>3</sub> receptor ligands, *MedChemComm* (2019): DOI: 10.1039/C9MD00379G.

Research contribution: Pharmacological evaluation of compounds at the D<sub>2</sub> and D<sub>3</sub> receptor, interpretation of data and partial preparation of manuscript.

### Chapter 8

Carbone C, Lo Russo SLM, Lacivita E, Frank A, Stark H, Alleva E, Saso L, Leopoldo M, Adriani W. Prior activation of 5-HT<sub>7</sub> receptors modulates the conditioned place preference with methylphenidate, *Frontiers in Behavioral Neuroscience* (2019), **13**: 208, DOI: 10.3389/fnbeh.2019.00208.

Research contribution: Pharmacological affinity evaluation of compounds at the D<sub>1</sub>, D<sub>2</sub>, D<sub>3</sub> and D<sub>5</sub> receptor, interpretation of data and partial preparation of manuscript.

### Chapter 9

Frank A, Kiss DJ, Keserű GM, Stark H. Binding kinetics of cariprazine and aripiprazole at the dopamine D<sub>3</sub> receptor. *Scientific Reports* (2018), **8**: 12509, DOI: 10.1038/s41598-018-30794-y.

Research contribution: Development and evaluation of a novel residence time assay at the D<sub>2</sub> and D<sub>3</sub> receptor, pharmacological evaluation of compounds at the D<sub>2</sub> and D<sub>3</sub> receptor and for  $\beta$ -arrestin recruitment at the D<sub>3</sub> receptor, interpretation of data and preparation of manuscript.

## 13 References for chapters 1-2 &amp; 10

- Abi-Dargham, A; Mawlawi, O; Lombardo, I; Gil, R; Martinez, D; Huang, Y; Hwang, D-R; Keilp, J; Kochan, L; van Heertum, R; Gorman, JM; Laruelle, M, **2002**. Prefrontal dopamine D1 receptors and working memory in schizophrenia. *Journal of Neuroscience*, **22**: 3708–3719.
- Abi-Dargham, A; Rodenhiser, J; Printz, D; Zea-Ponce, Y; Gil, R; Kegeles, LS; Weiss, R; Cooper, TB; Mann, JJ; van Heertum, RL; Gorman, JM; Laruelle, M, **2000**. Increased baseline occupancy of D2 receptors by dopamine in schizophrenia. *Proceedings of the National Academy of Sciences of the United States of America*, **97**: 8104–8109.
- Ahlskog, JE; Muentner, MD, **2001**. Frequency of levodopa-related dyskinesias and motor fluctuations as estimated from the cumulative literature. *Movement Disorders*, **16**: 448–458.
- Alachkar, A; Łażewska, D; Latacz, G; Frank, A; Siwek, A; Lubelska, A; Honkisz-Orzechowska, E; Handzlik, J; Stark, H; Kieć-Kononowicz, K; Sadek, B, **2018**. Studies on anticonvulsant effects of novel histamine H3R antagonists in electrically and chemically induced seizures in rats. *International Journal of Molecular Sciences*, **19**: 3386.
- Allen, JA; Yost, JM; Setola, V; Chen, X; Sassano, MF; Chen, M; Peterson, S; Yadav, PN; Huang, X-P; Feng, B; Jensen, NH; Che, X; Bai, X; Frye, SV; Wetsel, WC; Caron, MG; Javitch, JA; Roth, BL; Jin, J, **2011**. Discovery of  $\beta$ -arrestin-biased dopamine D2 ligands for probing signal transduction pathways essential for antipsychotic efficacy. *Proceedings of the National Academy of Sciences of the United States of America*, **108**: 18488–18493.
- Anichtchik, OV; Peitsaro, N; Rinne, JO; Kalimo, H; Panula, P, **2001**. Distribution and modulation of histamine H3 receptors in basal ganglia and frontal cortex of healthy controls and patients with Parkinson's disease. *Neurobiology of Disease*, **8**: 707–716.
- Aral, H; Kosaka, K; Iizuka, R, **1984**. Changes of biogenic amines and their metabolites in postmortem brains from patients with Alzheimer-type dementia. *Journal of Neurochemistry*, **43**: 388–393.
- Arrang, J-M; Garbarg, M; Schwartz, J-C, **1983**. Auto-inhibition of brain histamine release mediated by a novel class (H3) of histamine receptor. *Nature*, **302**: 832–837.
- Axe, FU; Bembenek, SD; Szalma, S, **2006**. Three-dimensional models of histamine H3 receptor antagonist complexes and their pharmacophore. *Journal of Molecular Graphics and Modelling*, **24**: 456–464.
- Ayano, G, **2016**. Dopamine: Receptors, functions, synthesis, pathways, locations and mental disorders: Review of literatures. *Journal of Mental Disorders and Treatment*, **2**: 120.
- Bach, NJ; Kornfeld, EC; Jones, ND; Chaney, MO; Dorman, DE; Paschal, JW; Clemens, JA; Smalstig, EB, **1980**. Bicyclic and tricyclic ergoline partial structures. Rigid 3-(2-aminoethyl) pyrroles and 3-and 4-(2-aminoethyl) pyrazoles as dopamine agonists. *Journal of Medicinal Chemistry*, **23**: 481–491.
- Bakker, RA; Wieland, K; Timmerman, H; Leurs, R, **2000**. Constitutive activity of the histamine H1 receptor reveals inverse agonism of histamine H1 receptor antagonists. *European Journal of Pharmacology*, **387**: R5-7.
- Barone, P; Lamb, J; Ellis, A; Clarke, Z, **2007**. Sumanitrol versus placebo or ropinirole for the adjunctive treatment of patients with advanced Parkinson's disease. *Movement Disorders*, **22**: 483–489.

- Battiti, FO; Cemaj, SL; Guerrero, AM; Shaik, AB; Lam, J; Rais, R; Slusher, BS; Deschamps, JR; Imler, GH; Newman, AH; Bonifazi, A, **2019**. The significance of chirality in drug design and synthesis of bitopic ligands as D3 receptor (D3R) selective agonists. *Journal of Medicinal Chemistry*, **62**: 6287–6314.
- Bereczki, D, **2010**. The description of all four cardinal signs of Parkinson's disease in a Hungarian medical text published in 1690. *Parkinsonism & Related Disorders*, **16**: 290–293.
- Berg, KA; Clarke, WP, **2018**. Making sense of pharmacology: Inverse agonism and functional selectivity. *International Journal of Neuropsychopharmacology*, **21**: 962–977.
- Bézard, E; Ferry, S; Mach, U; Stark, H; Leriche, L; Boraud, T; Gross, C; Sokoloff, P, **2003**. Attenuation of levodopa-induced dyskinesia by normalizing dopamine D3 receptor function. *Nature Medicine*, **9**: 762–767.
- Billups, D; Billups, B; Challiss, RAJ; Nahorski, SR, **2006**. Modulation of Gq-protein-coupled inositol trisphosphate and Ca<sup>2+</sup> signaling by the membrane potential. *Journal of Neuroscience*, **26**: 9983–9995.
- Blagg, J; Allerton, CMN; Batchelor, DVJ; Baxter, AD; Burring, DJ; Carr, CL; Cook, AS; Nichols, CL; Phipps, J; Sanderson, VG; Verrier, H; Wong, S, **2007**. Design and synthesis of a functionally selective D3 agonist and its in vivo delivery via the intranasal route. *Bioorganic & Medicinal Chemistry Letters*, **17**: 6691–6696.
- Blandina, P; Passani, MB. *Histamine Receptors: Preclinical and Clinical Aspects*, Blandina, P; Passani, MB (eds), part of the "The Receptors" book series (volume 28); Humana Press, Cham, Switzerland, 2016; ISBN: 978-3-319-40306-9.
- Bleicher, KH; Böhm, HJ; Müller, K; Alanine, AI, **2003**. Hit and lead generation: Beyond high-throughput screening. *Nature Reviews Drug Discovery*, **2**: 369–378.
- Boeckler, F; Gmeiner, P, **2006**. The structural evolution of dopamine D3 receptor ligands: Structure–activity relationships and selected neuropharmacological aspects. *Pharmacology & Therapeutics*, **112**: 281–333.
- Bongers, G; de Esch, I; Leurs, R. Molecular pharmacology of the four histamine receptors. In: *Histamine in Inflammation*, Thurmond, RL (eds), part of the "Advances in Experimental Medicine and Biology" book series (volume 709); Springer, Boston, MA, 2010; 11–19; ISBN: 978-1-4419-8055-8057.
- Bordet, R; Ridray, S; Carboni, S; Diaz, J; Sokoloff, P; Schwartz, J-C, **1997**. Induction of dopamine D3 receptor expression as a mechanism of behavioral sensitization to levodopa. *Proceedings of the National Academy of Sciences of the United States of America*, **94**: 3363–3367.
- Bosma, R; Mocking, TA; Leurs, R; Vischer, HF. Ligand-binding kinetics on histamine receptors. In: *Histamine Receptors as Drug Targets*, Tiligada, E; Ennis, M (eds), part of the "Methods in Pharmacology and Toxicology" book series; Humana Press, Cham, Switzerland, 2017; 115–155; ISBN: 978-1-4939-6843-5.
- Boyle, DL; DePrimo, SE; Calderon, C; Chen, D; Dunford, PJ; Barchuk, W; Firestein, GS; Thurmond, RL, **2019**. Toreforant, an orally active histamine H<sub>4</sub>-receptor antagonist, in patients with active rheumatoid arthritis despite methotrexate: Mechanism of action results from a phase 2, multicenter, randomized, double-blind, placebo-controlled synovial biopsy study. *Inflammation Research*, **68**: 261–274.

- Breinbauer, R; Vetter, IR; Waldmann, H, **2002**. From protein domains to drug candidates—natural products as guiding principles in the design and synthesis of compound libraries. *Angewandte Chemie International Edition*, **41**: 2878–2890.
- Butini, S; Nikolic, K; Kassel, S; Brückmann, H; Filipic, S; Agbaba, D; Gemma, S; Brogi, S; Brindisi, M; Campiani, G; Stark, H, **2016**. Polypharmacology of dopamine receptor ligands. *Progress in Neurobiology*, **142**: 68–103.
- Calabrese, F; Tarazi, FI; Racagni, G; Riva, MA, **2019**. The role of dopamine D3 receptors in the mechanism of action of cariprazine. *CNS Spectrums*: 10.1017/S109285291900083X.
- Cao, Y; Min, C; Acharya, S; Kim, KM; Cheon, SH, **2016**. Design, synthesis and evaluation of bitopic arylpiperazinephenyl-1, 2, 4-oxadiazoles as preferential dopamine D3 receptor ligands. *Bioorganic & Medicinal Chemistry*, **24**: 191–200.
- Cao, Y; Sun, N; Zhang, J; Liu, Z; Tang, Y-z; Wu, Z; Kim, KM; Cheon, SH, **2018**. Design, synthesis, and evaluation of bitopic arylpiperazine-phthalimides as selective dopamine D3 receptor agonists. *MedChemComm*, **9**: 1457–1465.
- Carbone, C; Lo Russo, SLM; Lacivita, E; Frank, A; Alleva, E; Stark, H; Saso, L; Leopoldo, M; Adriani, W, **2019**. Prior activation of 5-HT7 receptors modulates the conditioned place preference with methylphenidate. *Frontiers in Behavioral Neuroscience*, **13**: DOI: 10.3389/fnbeh.2019.00208.
- Carnicella, S; Drui, G; Boulet, S; Carcenac, C; Favier, M; Duran, T; Savasta, M, **2014**. Implication of dopamine D3 receptor activation in the reversion of Parkinson's disease-related motivational deficits. *Translational Psychiatry*, **4**: e401.
- Centonze, D; Usiello, A; Gubellini, P; Pisani, A; Borrelli, E; Bernardi, G; Calabresi, P, **2002**. Dopamine D2 receptor-mediated inhibition of dopaminergic neurons in mice lacking D2L receptors. *Neuropsychopharmacology*, **27**: 723–726.
- Cerveri, G; Gesi, C; Mencacci, C, **2019**. Pharmacological treatment of negative symptoms in schizophrenia: Update and proposal of a clinical algorithm. *Neuropsychiatric Disease and Treatment*, **15**: 1525–1535.
- Changeux, JP; Devillers-Thiery, A; Chemouilli, P, **1984**. Acetylcholine receptor: An allosteric protein. *Science*, **225**: 1335–1345.
- Chaudhuri, KR; Schapira, AHV, **2009**. Non-motor symptoms of Parkinson's disease: Dopaminergic pathophysiology and treatment. *The Lancet Neurology*, **8**: 464–474.
- Cherezov, V; Rosenbaum, DM; Hanson, MA; Rasmussen, SGF; Thian, FS; Kobilka, TS; Choi, H-J; Kuhn, P; Weis, WI; Kobilka, BK; Stevens, RC, **2007**. High-resolution crystal structure of an engineered human  $\beta$ 2-adrenergic G protein-coupled receptor. *Science*, **318**: 1258–1265.
- Chidiac, P; Hebert, TE; Valiquette, M; Dennis, M; Bouvier, M, **1994**. Inverse agonist activity of beta-adrenergic antagonists. *Molecular Pharmacology*, **45**: 490–499.
- Chien, EYT; Liu, W; Zhao, Q; Katritch, V; Han, GW; Hanson, MA; Shi, L; Newman, AH; Javitch, JA; Cherezov, V; Stevens, RC, **2010**. Structure of the human dopamine D3 receptor in complex with a D2/D3 selective antagonist. *Science*, **330**: 1091–1095.
- Choi, YK; Adham, N; Kiss, B; Gyertyán, I; Tarazi, FI, **2014**. Long-term effects of cariprazine exposure on dopamine receptor subtypes. *CNS Spectrums*, **19**: 268–277.

- Civelli, O; Bunzow, JR; Grandy, DK; Zhou, Q-Y; van Tol, HHM, **1991**. Molecular biology of the dopamine receptors. *European Journal of Pharmacology: Molecular Pharmacology*, **207**: 277–286.
- Connelly, WM; Shenton, FC; Lethbridge, N; Leurs, R; Waldvogel, HJ; Faull, RLM; Lees, G; Chazot, PL, **2009**. The histamine H4 receptor is functionally expressed on neurons in the mammalian CNS. *British Journal of Pharmacology*, **157**: 55–63.
- Copeland, RA; Pompliano, DL; Meek, TD, **2006**. Drug–target residence time and its implications for lead optimization. *Nature Reviews Drug Discovery*, **5**: 730–739.
- Corrêa, MF; dos Santos Fernandes, JP, **2015**. Histamine H4 receptor ligands: Future applications and state of art. *Chemical Biology & Drug Design*, **85**: 461–480.
- Daryaei, F; Tonge, PJ, **2019**. Pharmacokinetic–pharmacodynamic models that incorporate drug–target binding kinetics. *Current Opinion in Chemical Biology*, **50**: 120–127.
- Dauvilliers, Y; Schwartz, J-C; Davis, C; Dayno, J, **2019**. Efficacy and safety of pitolisant in patients with narcolepsy: A review of clinical trials. *Neurology*, **92**: P3.6-034 (15 Supplement).
- Davie, CA, **2008**. A review of Parkinson's disease. *British Medical Bulletin*, **86**: 109–127.
- de Lean, A de; Kilpatrick, BF; Caron, MG, **1982**. Dopamine receptor of the porcine anterior pituitary gland. Evidence for two affinity states discriminated by both agonists and antagonists. *Molecular Pharmacology*, **22**: 290–297.
- de Strooper, B, **2010**. Proteases and proteolysis in Alzheimer disease: A multifactorial view on the disease process. *Physiological Reviews*, **90**: 465–494.
- Demchyshyn, LL; McConkey, F; Niznik, HB, **2000**. Dopamine D5 receptor agonist high affinity and constitutive activity profile conferred by carboxyl-terminal tail sequence. *Journal of Biological Chemistry*, **275**: 23446–23455.
- DeWire, SM; Ahn, S; Lefkowitz, RJ; Shenoy, SK, **2007**.  $\beta$ -arrestins and cell signaling. *Annual Review of Physiology*, **69**: 483–510.
- Egan, M; Yaari, R; Liu, L; Ryan, M; Peng, Y; Lines, C; Michelson, D, **2012**. Pilot randomized controlled study of a histamine receptor inverse agonist in the symptomatic treatment of AD. *Current Alzheimer Research*, **9**: 481–490.
- Ehringer, H; Hornykiewicz, O, **1960**. Verteilung von Noradrenalin und Dopamin (3-Hydroxytyramin) im Gehirn des Menschen und ihr Verhalten bei Erkrankungen des extrapyramidalen Systems. *Klinische Wochenschrift*, **38**: 1236–1239.
- Elefsinioti, AL; Bagos, PG; Spyropoulos, IC; Hamodrakas, SJ, **2004**. A database for G proteins and their interaction with GPCRs. *BMC Bioinformatics*, **5**: DOI: 10.1186/1471-2105-5-208.
- Emanuel, MB, **1999**. Histamine and the antiallergic antihistamines: A history of their discoveries. *Clinical & Experimental Allergy*, **29**: Suppl 3: 1-11; discussion 12.
- Erdag, D; Merhan, O; Yildiz, B. Biochemical and pharmacological properties of biogenic amines. In: *Biogenic Amines*, Proestos, C (eds); IntechOpen, London, UK, 2018.
- Espinosa-Bustos, C; Frank, A; Arancibia-Opazo, S; Salas, CO; Fierro, A; Stark, H, **2018**. New lead elements for histamine H3 receptor ligands in the pyrrolo[2,3-d]pyrimidine class. *Bioorganic & Medicinal Chemistry Letters*, **28**: 2890–2893.
- Fahn, S, **2008**. The history of dopamine and levodopa in the treatment of Parkinson's disease. *Movement Disorders*, **23**: Suppl 3: S497-508.

- Fasciani, I; Pietrantoni, I; Rossi, M; Mannoury la Cour, C; Aloisi, G; Marampon, F; Scarselli, M; Millan, MJ; Maggio, R, **2018**. Distinctive binding properties of the negative allosteric modulator,[3H] SB269, 652, at recombinant dopamine D3 receptors. *European Journal of Pharmacology*, **819**: 181–189.
- Ferrada, C; Ferrè, S; Casadó, V; Cortès, A; Justinova, Z; Barnes, C; Canela, EI; Goldberg, SR; Leurs, R; Lluís, C; Franco, R, **2008**. Interactions between histamine H3 and dopamine D2 receptors and the implications for striatal function. *Neuropharmacology*, **55**: 190–197.
- Fischer, BA; Carpenter, WT, **2009**. Will the Kraepelinian dichotomy survive DSM-V? *Neuropsychopharmacology*, **34**: 2081–2087.
- Ford, CP, **2014**. The role of D2-autoreceptors in regulating dopamine neuron activity and transmission. *Neuroscience*, **282**: 13–22.
- Fox, SH; Katzenschlager, R; Lim, SY; Ravina, B; Seppi, K; Coelho, M; Poewe, W; Rascol, O; Goetz, CG; Sampaio, C, **2011**. The Movement Disorder Society evidence-based medicine review update: Treatments for the motor symptoms of Parkinson's disease. *Movement Disorders*, **26**: Suppl 3: S2-S41.
- Frank, A; Abu-Lafi, S; Adawi, A; Schwed, JS; Stark, H; Rayan, A, **2017**. From medicinal plant extracts to defined chemical compounds targeting the histamine H4 receptor: Curcuma longa in the treatment of inflammation. *Inflammation Research*, **66**: 923–929.
- Frank, A; Kiss, DJ; Keserű, GM; Stark, H, **2018**. Binding kinetics of cariprazine and aripiprazole at the dopamine D3 receptor. *Scientific Reports*, **8**: DOI:10.1038/s41598-018-30794-y.
- Frank, A; Meza-Arriagada, F; Salas, CO; Espinosa-Bustos, C; Stark, H, **2019**. Nature-inspired pyrrolo[2,3-d]pyrimidines targeting the histamine H3 receptor. *Bioorganic & Medicinal Chemistry*, **27**: 3194–3200.
- Frederick, AL; Stanwood, GD, **2009**. Drugs, biogenic amine targets and the developing brain. *Developmental Neuroscience*, **31**: 7–22.
- Fredriksson, R; Lagerström, MC; Lundin, LG; Schiöth, HB, **2003**. The G-protein-coupled receptors in the human genome form five main families. Phylogenetic analysis, paralogon groups, and fingerprints. *Molecular Pharmacology*, **63**: 1256–1272.
- Fronik, P; Gaiser, BI; Sejer Pedersen, D, **2017**. Bitopic ligands and metastable binding sites: Opportunities for G protein-coupled receptor (GPCR) medicinal chemistry. *Journal of Medicinal Chemistry*, **60**: 4126–4134.
- Fyfe, TJ; Kellam, B; Sykes, DA; Capuano, B; Scammells, PJ; Lane, JR; Charlton, SJ; Mistry, SN, **2019**. Structure-kinetic profiling of haloperidol analogues at the human dopamine D2 receptor. *Journal of Medicinal Chemistry*: accepted.
- Garcia-Ladona, FJ; Cox, BF, **2003**. BP 897, a selective dopamine D3 receptor ligand with therapeutic potential for the treatment of cocaine-addiction. *CNS Drug Reviews*, **9**: 141–158.
- Ghamari, N; Zarei, O; Arias-Montañó, J-A; Reiner, D; Dastmalchi, S; Stark, H; Hamzeh-Mivehroud, M, **2019a**. Histamine H3 receptor antagonists/inverse agonists: Where do they go? *Pharmacology & Therapeutics*, **200**: 69–84.
- Ghamari, N; Zarei, O; Reiner, D; Dastmalchi, S; Stark, H; Hamzeh-Mivehroud, M, **2019b**. Histamine H3 receptor ligands by hybrid virtual screening, docking, molecular dynamics simulations, and investigation of their biological effects. *Chemical Biology & Drug Design*, **93**: 832–843.



- Ghoshal, A; Kumar, A; Yugandhar, D; Sona, C; Kuriakose, S; Nagesh, K; Rashid, M; Singh, SK; Wahajuddin, M; Yadav, PN, **2018**. Identification of novel  $\beta$ -lactams and pyrrolidinone derivatives as selective Histamine-3 receptor (H3R) modulators as possible anti-obesity agents. *European Journal of Medicinal Chemistry*, **152**: 148–159.
- Gingrich, JA; Caron, MG, **1993**. Recent advances in the molecular biology of dopamine receptors. *Annual Review of Neuroscience*, **16**: 299–321.
- Goodchild, RE; Court, JA; Hobson, I; Piggott, MA; Perry, RH; Ince, P; Jaros, E; Perry, EK, **1999**. Distribution of histamine H3-receptor binding in the normal human basal ganglia: Comparison with Huntington's and Parkinson's disease cases. *European Journal of Neuroscience*, **11**: 449–456.
- Grady, EF; Bohm, SK; Bunnett, NW, **1997**. Turning off the signal: Mechanisms that attenuate signaling by G protein-coupled receptors. *American Journal of Physiology-Gastrointestinal and Liver Physiology*, **273**: G586-G601.
- Graham, JR; Wolff, HG, **1938**. Mechanism of migraine headache and action of ergotamine tartrate. *Archives of Neurology & Psychiatry*, **39**: 737–763.
- Grandy, DK; Marchionni, MA; Makam, H; Stofko, RE; Alfano, M; Frothingham, L; Fischer, JB; Burke-Howie, KJ; Bunzow, JR; Server, AC, **1989**. Cloning of the cDNA and gene for a human D2 dopamine receptor. *Proceedings of the National Academy of Sciences of the United States of America*, **86**: 9762–9766.
- Green, JP; Prell, GD; Khandelwal, JK; Blandina, P, **1987**. Aspects of histamine metabolism. *Agents and Actions*, **22**: 1–15.
- Griebel, G; Decobert, M; Jacquet, A; Beeské, S, **2012**. Awakening properties of newly discovered highly selective H3 receptor antagonists in rats. *Behavioural Brain Research*, **232**: 416–420.
- Gründer, G; Hippus, H; Carlsson, A, **2009**. The 'atypicality' of antipsychotics: A concept re-examined and re-defined. *Nature Reviews Drug Discovery*, **8**: 197–202.
- Guo, D; Hillger, JM; IJzerman, AP; Heitman, LH, **2014**. Drug-target residence time—A case for G protein-coupled receptors. *Medicinal Research Reviews*, **34**: 856–892.
- Guo, D; Peletier, LA; Bridge, L; Keur, W; de Vries, H; Zweemer, A; Heitman, LH; IJzerman, AP, **2018**. A two-state model for the kinetics of competitive radioligand binding. *British Journal of Pharmacology*, **175**: 1719–1730.
- Haas, HL; Panula, P, **2016**. Histamine receptors. *Neuropharmacology*, **106**: 1–164.
- Haas, HL; Sergeeva, OA; Selbach, O, **2008**. Histamine in the nervous system. *Physiological Reviews*, **88**: 1183–1241.
- Hancock, AA, **2006**. The challenge of drug discovery of a GPCR target: Analysis of preclinical pharmacology of histamine H3 antagonists/inverse agonists. *Biochemical Pharmacology*, **71**: 1103–1113.
- Harding, SD; Sharman, JL; Faccenda, E; Southan, C; Pawson, AJ; Ireland, S; Gray, AJG; Bruce, L; Alexander, SPH; Anderton, S; Bryant, C; Davenport, AP; Doerig, C; Fabbro, D; Levi-Schaffer, F; Spedding, M; Davies, JA, **2018**. The IUPHAR/BPS Guide to pharmacology in 2018: Updates and expansion to encompass the new guide to IMMUNOPHARMACOLOGY. *Nucleic acids research*, **46**: D1091-D1106.

- Hardman, DJ, **1991**. Biotransformation of halogenated compounds. *Critical Reviews in Biotechnology*, **11**: 1–40.
- Hauser, AS; Attwood, MM; Rask-Andersen, M; Schiöth, HB; Gloriam, DE, **2017**. Trends in GPCR drug discovery: New agents, targets and indications. *Nature Reviews Drug Discovery*, **16**: 829–842.
- Herring, WJ; Wilens, TE; Adler, LA; Baranak, C; Liu, K; Snavely, DB; Lines, CR; Michelson, D, **2012**. Randomized controlled study of the histamine H3 inverse agonist MK-0249 in adult attention-deficit/hyperactivity disorder. *The Journal of Clinical Psychiatry*, **73**: e891–e898.
- Hilger, D; Masureel, M; Kobilka, BK, **2018**. Structure and dynamics of GPCR signaling complexes. *Nature Structural & Molecular Biology*, **25**: 4–12.
- Hornykiewicz, O, **1966**. Dopamine (3-hydroxytyramine) and brain function. *Pharmacological Reviews*, **18**: 925–964.
- Hough, LB, **2001**. Genomics meets histamine receptors: New subtypes, new receptors. *Molecular Pharmacology*, **59**: 415–419.
- Hu, W; Chen, Z, **2017**. The roles of histamine and its receptor ligands in central nervous system disorders: An update. *Pharmacology & Therapeutics*, **175**: 116–132.
- Huang, ES, **2003**. Construction of a sequence motif characteristic of aminergic G protein-coupled receptors. *Protein Science*, **12**: 1360–1367.
- Ioan, BG; Manea, C; Hanganu, B; Statescu, L; Solovastu, LG; Manolescu, I, **2017**. The chemistry decomposition in human corpses. *Revista de Chimie*, **68**: 1352–1356.
- Ishikawa, M; Watanabe, T; Kudo, T; Yokoyama, F; Yamauchi, M; Kato, K; Kakui, N; Sato, Y, **2010**. Investigation of the histamine H3 receptor binding site. Design and synthesis of hybrid agonists with a lipophilic side chain. *Journal of Medicinal Chemistry*, **53**: 6445–6456.
- Jaber, M; Robinson, SW; Missale, C; Caron, MG, **1996**. Dopamine receptors and brain function. *Neuropharmacology*, **35**: 1503–1519.
- Jackson, DM; Westlind-Danielsson, A, **1994**. Dopamine receptors: Molecular biology, biochemistry and behavioural aspects. *Pharmacology & Therapeutics*, **64**: 291–370.
- Jairath, G; Singh, PK; Dabur, RS; Rani, M; Chaudhari, M, **2015**. Biogenic amines in meat and meat products and its public health significance: A review. *Journal of Food Science and Technology*, **52**: 6835–6846.
- Jiang, F; Zang, L; Miao, X; Jia, F; Wang, J; Zhu, M; Gong, P; Jiang, N; Zhai, X, **2019**. Design, synthesis and anti-inflammatory evaluation of novel pyrrolo [2, 3-d] pyrimidin derivatives as potent JAK inhibitors. *Bioorganic & Medicinal Chemistry*, **27**: 4089–4100.
- Jones, C; Kapur, S; Remington, G; Zipursky, RB, **2000**. Transient d2 dopamine receptor occupancy in low EPS-incidence drugs: PET evidence. *Biological Psychiatry*, **47**: S112.
- Kapur, S; Seeman, P, **2000**. Antipsychotic agents differ in how fast they come off the dopamine D2 receptors. Implications for atypical antipsychotic action. *Journal of Psychiatry and Neuroscience*, **25**: 161–166.
- Kapur, S; Seeman, P, **2001**. Does fast dissociation from the dopamine D2 receptor explain the action of atypical antipsychotics?: A new hypothesis. *American Journal of Psychiatry*, **158**: 360–369.

- Karcz, T; Handzlik, J; Łażewska, D; Kottke, T; Seifert, R; Kieć-Kononowicz, K, **2010**. Search for histamine H4 receptor ligands in the group of 4-methylpiperazino amide derivatives. *Inflammation Research*, **59**: Suppl 2: S243–245.
- Karlsson, P; Farde, L; Halldin, C; Sedvall, G, **2002**. PET study of D1 dopamine receptor binding in neuroleptic-naïve patients with schizophrenia. *American Journal of Psychiatry*, **159**: 761–767.
- Katritch, V; Cherezov, V; Stevens, RC, **2012**. Diversity and modularity of G protein-coupled receptor structures. *Trends in Pharmacological Sciences*, **33**: 17–27.
- Kebabian, JW; Petzold, GL; Greengard, P, **1972**. Dopamine-sensitive adenylate cyclase in caudate nucleus of rat brain, and its similarity to the “dopamine receptor”. *Proceedings of the National Academy of Sciences of the United States of America*, **69**: 2145–2149.
- Kim, YC; Alberico, SL; Emmons, E; Narayanan, NS, **2015**. New therapeutic strategies targeting D1-type dopamine receptors for neuropsychiatric disease. *Frontiers in Biology*, **10**: 230–238.
- Kiss, B; Horváth, A; Némethy, Z; Schmidt, É; Laszlovszky, I; Bugovics, G; Fazekas, K; Hornok, K; Orosz, S; Gyertyán, I; Agai-Csongor, E; Domány, G; Tihanyi, K; Adham, N; Szombathelyi, Z, **2010**. Cariprazine (RGH-188), a dopamine D3 receptor-preferring, D3/D2 dopamine receptor antagonist–partial agonist antipsychotic candidate: In vitro and neurochemical profile. *Journal of Pharmacology and Experimental Therapeutics*, **333**: 328–340.
- Klebe, G, **2000**. Recent developments in structure-based drug design. *Journal of Molecular Medicine*, **78**: 269–281.
- Klein Herenbrink, C; Sykes, DA; Donthamsetti, P; Canals, M; Coudrat, T; Shonberg, J; Scammells, PJ; Capuano, B; Sexton, PM; Charlton, SJ; Javitch, JA; Christopoulos, A; Lane, JR, **2016**. The role of kinetic context in apparent biased agonism at GPCRs. *Nature Communications*, **7**: 10842.
- Knab, AM; Lightfoot, JT, **2010**. Does the difference between physically active and couch potato lie in the dopamine system? *International Journal of Biological Sciences*, **6**: 133–150.
- Kollmeier, A; Francke, K; Chen, B; Dunford, PJ; Greenspan, AJ; Xia, Y; Xu, XL; Zhou, B; Thurmond, RL, **2014**. The histamine H4 receptor antagonist, JNJ 39758979, is effective in reducing histamine-induced pruritus in a randomized clinical study in healthy subjects. *Journal of Pharmacology and Experimental Therapeutics*, **350**: 181–187.
- Kollmeier, AP; Greenspan, A; Xu, XL; Silkoff, PE; Barnathan, ES; Loza, MJ; Jiang, J; Zhou, B; Chen, B; Thurmond, RL, **2018**. Phase 2a, randomized, double-blind, placebo-controlled, multicentre, parallel-group study of an H4R-antagonist (JNJ-39758979) in adults with uncontrolled asthma. *Clinical & Experimental Allergy*, **48**: 957–969.
- Koob, GF; Sanna, PP; Bloom, FE, **1998**. Neuroscience of addiction. *Neuron*, **21**: 467–476.
- Kovac, AL, **2000**. Prevention and treatment of postoperative nausea and vomiting. *Drugs*, **59**: 213–243.
- Kubes, P; Kanwar, S, **1994**. Histamine induces leukocyte rolling in post-capillary venules. A P-selectin-mediated event. *The Journal of Immunology*, **152**: 3570–3577.
- Kühhorn, J; Hübner, H; Gmeiner, P, **2011**. Bivalent dopamine D2 receptor ligands: Synthesis and binding properties. *Journal of Medicinal Chemistry*, **54**: 4896–4903.

- Lane, CAL; Hay, D; Mowbray, CE; Paradowski, M; Selby, MD; Swain, NA; Williams, DH, **2012**. Synthesis of novel histamine H4 receptor antagonists. *Bioorganic & Medicinal Chemistry Letters*, **22**: 1156–1159.
- Lane, JR; Chubukov, P; Liu, W; Canals, M; Cherezov, V; Abagyan, R; Stevens, RC; Katritch, V, **2013**. Structure-based ligand discovery targeting orthosteric and allosteric pockets of dopamine receptors. *Molecular Pharmacology*, **84**: 794–807.
- Langlois, X; Megens, A; Lavreysen, H; Atack, J; Cik, M; te Riele, P; Peeters, L; Wouters, R; Vermeire, J; Hendrickx, H; Macdonald, G; De Bruyn, M, **2012**. Pharmacology of JNJ-37822681, a specific and fast-dissociating D2 antagonist for the treatment of schizophrenia. *Journal of Pharmacology and Experimental Therapeutics*, **342**: 91–105.
- Laszy, J; Laszlovszky, I; Gyertyán, I, **2005**. Dopamine D3 receptor antagonists improve the learning performance in memory-impaired rats. *Psychopharmacology*, **179**: 567–575.
- Latorraca, NR; Venkatakrishnan, AJ; Dror, RO, **2017**. GPCR dynamics: Structures in motion. *Chemical Reviews*, **117**: 139–155.
- Lawler, CP; Prioleau, C; Lewis, MM; Mak, C; Jiang, D; Schetz, JA; Gonzalez, AM; Sibley, DR; Mailman, RB, **1999**. Interactions of the novel antipsychotic aripiprazole (OPC-14597) with dopamine and serotonin receptor subtypes. *Neuropsychopharmacology*, **20**: 612–627.
- Letavic, MA; Aluisio, L; Apodaca, R; Bajpai, M; Barbier, AJ; Bonneville, A; Bonaventure, P; Carruthers, NI; Dugovic, C; Fraser, IC; Kramer, ML; Lord, B; Lovenberg, TW; Li, LY; Ly, KS; Mcallister, H; Mani, NS; Morton, KL; Ndifor, A; Nepomuceno, SD; Pandit, CR; Sands, SB; Shah, CR; Shelton, JE; Snook, SS; Swanson, DM; Xiao, W, **2015**. Novel benzamide-based histamine h3 receptor antagonists: The identification of two candidates for clinical development. *ACS Medicinal Chemistry Letters*, **6**: 450–454.
- Leucht, C; Kitzmantel, M; Kane, J; Leucht, S; Chua, W, **2008**. Haloperidol versus chlorpromazine for schizophrenia. *Cochrane Database of Systematic Reviews*: (1), CD004278.
- Leurs, R; Vollinga, RC; Timmerman, H. The medicinal chemistry and therapeutic potentials of ligands of the histamine H3 receptor. In: *Progress in Drug Research/Fortschritte der Arzneimittelforschung/Progrès des Recherches Pharmaceutiques* (volume 45), Jucker, E (eds); Birkhäuser Basel, Basel, Switzerland, 1995; 107–165; ISBN: 978-3-0348-7164-8.
- Lieberman, A; Kupersmith, M; Estey, E; Goldstein, M, **1976**. Treatment of Parkinson's disease with bromocriptine. *New England Journal of Medicine*, **295**: 1400–1404.
- Lieberman, JA, **2004**. Dopamine partial agonists: A new class of antipsychotic. *CNS Drugs*, **18**: 251–267.
- Lim, HD; van Rijn, RM; Ling, P; Bakker, RA; Thurmond, RL; Leurs, R, **2005**. Evaluation of histamine H1-, H2-, and H3-receptor ligands at the human histamine H4 receptor: Identification of 4-methylhistamine as the first potent and selective H4 receptor agonist. *Journal of Pharmacology and Experimental Therapeutics*, **314**: 1310–1321.
- Lindemann, L; Hoener, MC, **2005**. A renaissance in trace amines inspired by a novel GPCR family. *Trends in Pharmacological Sciences*, **26**: 274–281.
- Lionta, E; Spyrou, G; Vassilatis, DK; Cournia, Z, **2014**. Structure-based virtual screening for drug discovery: Principles, applications and recent advances. *Current Topics in Medicinal Chemistry*, **14**: 1923–1938.

- Lipinski, CA; Lombardo, F; Dominy, BW; Feeney, PJ, **2001**. Experimental and computational approaches to estimate solubility and permeability in drug discovery and development settings. *Advanced Drug Delivery Reviews*, **46**: 3–26.
- Lipski, J; Nistico, R; Berretta, N; Guatteo, E; Bernardi, G; Mercuri, NB, **2011**. L-DOPA: A scapegoat for accelerated neurodegeneration in Parkinson's disease? *Progress in Neurobiology*, **94**: 389–407.
- Liu, C; Ma, X-J; Jiang, X; Wilson, SJ; Hofstra, CL; Blevitt, J; Pyati, J; Li, X; Chai, W; Carruthers, N; Lovenberg, TW, **2001**. Cloning and pharmacological characterization of a fourth histamine receptor (H4) expressed in bone marrow. *Molecular Pharmacology*, **59**: 420–426.
- Ludlow, RF; Verdonk, ML; Saini, HK; Tickle, IJ; Jhoti, H, **2015**. Detection of secondary binding sites in proteins using fragment screening. *Proceedings of the National Academy of Sciences of the United States of America*, **112**: 15910–15915.
- Luttrell, LM; Ferguson, S; Daaka, Y; Miller, WE; Maudsley, S; Della Rocca, GJ; Lin, F-T; Kawakatsu, H; Owada, K; Luttrell, DK; Caron, M; Lefkowitz, R, **1999**.  $\beta$ -Arrestin-dependent formation of  $\beta$ 2 adrenergic receptor-Src protein kinase complexes. *Science*, **283**: 655–661.
- Lynch, MR, **1992**. Schizophrenia and the D1 receptor: Focus on negative symptoms. *Progress in Neuro-psychopharmacology and Biological Psychiatry*, **16**: 797–832.
- Maas, JW, **1975**. Biogenic amines and depression: Biochemical and pharmacological separation of two types of depression. *Archives of General Psychiatry*, **32**: 1357–1361.
- Marinissen, MJ; Gutkind, JS, **2001**. G-protein-coupled receptors and signaling networks: Emerging paradigms. *Trends in Pharmacological Sciences*, **22**: 368–376.
- Masri, B; Salahpour, A; Didriksen, M; Ghisi, V; Beaulieu, JM; Gainetdinov, RR; Caron, MG, **2008**. Antagonism of dopamine D2 receptor/ $\beta$ -arrestin 2 interaction is a common property of clinically effective antipsychotics. *Proceedings of the National Academy of Sciences of the United States of America*, **105**: 13656–13661.
- McCall, RB; Lookingland, KJ; Bedard, PJ; Huff, RM, **2005**. Sumanitrole, a highly dopamine D2-selective receptor agonist: In vitro and in vivo pharmacological characterization and efficacy in animal models of Parkinson's disease. *Journal of Pharmacology and Experimental Therapeutics*, **314**: 1248–1256.
- McCorry, DC; Gray, RN, **2003**. Oral sumatriptan for acute migraine. *Cochrane Database of Systematic Reviews*: DOI: 10.1002/14651858.CD002915.
- McQuaid, LA; Latz, JE; Clemens, JA; Fuller, RW; Wong, DT; Mason, NR, **1989**. Substituted 5-amino-4, 5, 6, 7-tetrahydroindazoles as partial ergoline structures with dopaminergic activity. *Journal of Medicinal Chemistry*, **32**: 2388–2396.
- Meador-Woodruff, JH; Damask, SP; Wang, J; Haroutunian, V; Davis, KL; Watson, SJ, **1996**. Dopamine receptor mRNA expression in human striatum and neocortex. *Neuropsychopharmacology*, **15**: 17–29.
- Medina, VA; Brenzoni, PG; Lamas, DJ; Massari, N; Mondillo, C; Nunez, MA; Pignataro, O; Rivera, ES, **2011**. Role of histamine H4 receptor in breast cancer cell proliferation. *Frontiers in Bioscience (Elite edition)*, **3**: 1042–1060.
- Meiser, J; Weindl, D; Hiller, K, **2013**. Complexity of dopamine metabolism. *Cell Communication and Signaling*, **11**: DOI: 10.1186/1478-811X-11-34.

- Meltzer, HY; Li, Z; Kaneda, Y; Ichikawa, J, **2003**. Serotonin receptors: Their key role in drugs to treat schizophrenia. *Progress in Neuro-psychopharmacology and Biological Psychiatry*, **27**: 1159–1172.
- Meltzer, HY; Matsubara, S; Lee, JC, **1989**. The ratios of serotonin<sub>2</sub> and dopamine<sub>2</sub> affinities differentiate atypical and typical antipsychotic drugs. *Psychopharmacology Bulletin*, **25**: 390–392.
- Meltzer, HY; Stahl, SM, **1976**. The dopamine hypothesis of schizophrenia: A review. *Schizophrenia Bulletin*, **2**: 19–76.
- Meyler, WJ, **1996**. Side effects of ergotamine. *Cephalalgia*, **16**: 5–10.
- Millan, MJ; Di Cara, B; Dekeyne, A; Panayi, F; de Groote, L; Sicard, D; Cistarelli, L; Billiras, R; Gobert, A, **2007**. Selective blockade of dopamine D<sub>3</sub> versus D<sub>2</sub> receptors enhances frontocortical cholinergic transmission and social memory in rats: A parallel neurochemical and behavioural analysis. *Journal of Neurochemistry*, **100**: 1047–1061.
- Millan, MJ; Maiofiss, L; Cussac, D; Audinot, V; Boutin, J-A; Newman-Tancredi, A, **2002**. Differential actions of antiparkinson agents at multiple classes of monoaminergic receptor. I. A multivariate analysis of the binding profiles of 14 drugs at 21 native and cloned human receptor subtypes. *Journal of Pharmacology and Experimental Therapeutics*, **303**: 791–804.
- Milligan, G; Kostenis, E, **2006**. Heterotrimeric G-proteins: A short history. *British Journal of Pharmacology*, **147**: Suppl 1: S46–S55.
- Mirzaei, H; Masoudifar, A; Sahebkar, A; Zare, N; Sadri Nahand, J; Rashidi, B; Mehrabian, E; Mohammadi, M; Mirzaei, HR; Jaafari, MR, **2018**. MicroRNA: A novel target of curcumin in cancer therapy. *Journal of Cellular Physiology*, **233**: 3004–3015.
- Mishra, A; Singh, S; Shukla, S, **2018**. Physiological and functional basis of dopamine receptors and their role in neurogenesis: Possible implication for Parkinson's disease. *Journal of Experimental Neuroscience*, **12**: DOI: 10.1177/1179069518779829.
- Missale, C; Nash, SR; Robinson, SW; Jaber, M; Caron, MG, **1998**. Dopamine receptors: From structure to function. *Physiological Reviews*, **78**: 189–225.
- Mocking, TAM; Bosma, R; Rahman, SN; Verweij, EWE; McNaught-Flores, DA; Vischer, HF; Leurs, R. Molecular aspects of histamine receptors. In: *Histamine Receptors: Preclinical and Clinical Aspects*, Blandina, P; Passani, MB (eds), part of the "The Receptors" book series (volume 28); Humana Press, Cham, Switzerland, 2016; 1-49; ISBN: 978-3-319-40306-9.
- Mondovi, B; Fogel, WA; Federico, R; Calinescu, C; Mateescu, MA; Rosa, AC; Masini, E, **2013**. Effects of amine oxidases in allergic and histamine-mediated conditions. *Recent Patents on Inflammation & Allergy Drug Discovery*, **7**: 20–34.
- Moore, DJ; West, AB; Dawson, VL; Dawson, TM, **2005**. Molecular pathophysiology of Parkinson's disease. *Annual Review of Neuroscience*, **28**: 57–87.
- Morphy, R; Kay, C; Rankovic, Z, **2004**. From magic bullets to designed multiple ligands. *Drug Discovery Today*, **9**: 641–651.
- Morphy, R; Rankovic, Z, **2006**. The physicochemical challenges of designing multiple ligands. *Journal of Medicinal Chemistry*, **49**: 4961–4970.
- Murata, Y; Song, M; Kikuchi, H; Hisamichi, K; Xu, XL; Greenspan, A; Kato, M; Chiou, C-F; Kato, T; Guzzo, C; Thurmond, RL; Ohtsuki, M; Furue, M, **2015**. Phase 2a, randomized, double-blind,

- placebo-controlled, multicenter, parallel-group study of a H4R-antagonist (JNJ-39758979) in Japanese adults with moderate atopic dermatitis. *The Journal of Dermatology*, **42**: 129–139.
- Nakajima, S; Gerretsen, P; Takeuchi, H; Caravaggio, F; Chow, T; Le Foll, B; Mulsant, B; Pollock, B; Graff-Guerrero, A, **2013**. The potential role of dopamine D3 receptor neurotransmission in cognition. *European Neuropsychopharmacology*, **23**: 799–813.
- Nakamura, T; Itadani, H; Hidaka, Y; Ohta, M; Tanaka, K, **2000**. Molecular cloning and characterization of a new human histamine receptor, HH4R. *Biochemical and Biophysical Research Communications*, **279**: 615–620.
- Nelson, KM; Dahlin, JL; Bisson, J; Graham, J; Pauli, GF; Walters, MA, **2017**. The essential medicinal chemistry of curcumin. *Journal of Medicinal Chemistry*, **60**: 1620–1637.
- Newman, AH; Beuming, T; Banala, AK; Donthamsetti, P; Pongetti, K; LaBounty, A; Levy, B; Cao, J; Michino, M; Luedtke, RR; Javitch, JA; Shi, L, **2012**. Molecular determinants of selectivity and efficacy at the dopamine D3 receptor. *Journal of Medicinal Chemistry*, **55**: 6689–6699.
- Nicoud, MB; Formoso, K; Medina, VA, **2019**. Pathophysiological role of histamine H4 receptor in cancer: Therapeutic implications. *Frontiers in Pharmacology*, **10**: 556.
- Nieto-Alamilla, G; Márquez-Gómez, R; García-Gálvez, AM; Morales-Figueroa, GE; Arias-Montaña, JA, **2016**. The histamine H3 receptor: Structure, pharmacology, and function. *Molecular Pharmacology*, **90**: 649–673.
- Nomoto, M; Nishikawa, N; Nagai, M; Yabe, H; Nakatsuka, A; Moritoyo, H; Moritoyo, T; Kubo, M, **2009**. Inter- and intra-individual variation in L-dopa pharmacokinetics in the treatment of Parkinson's disease. *Parkinsonism & Related Disorders*, **15**: Suppl 1: S21-S24.
- Oda, T; Morikawa, N; Saito, Y; Masuho, Y; Matsumoto, S, **2000**. Molecular cloning and characterization of a novel type of histamine receptor preferentially expressed in leukocytes. *Journal of Biological Chemistry*, **275**: 36781–36786.
- O'Donnell, P; Grace, AA, **1998**. Dysfunctions in multiple interrelated systems as the neurobiological bases of schizophrenic symptom clusters. *Schizophrenia Bulletin*, **24**: 267–283.
- Okubo, Y; Suhara, T; Suzuki, K; Kobayashi, K; Inoue, O; Terasaki, O; Someya, Y; Sassa, T; Sudo, Y; Matsushima, E; Iyo, M; Tateno, Y; Toru, M, **1997**. Decreased prefrontal dopamine D1 receptors in schizophrenia revealed by PET. *Nature*, **385**: 634–636.
- Omran, A; Eslamimehr, S; Crider, AM; Neumann, WL, **2018**. Synthesis of 3-(3-hydroxyphenyl) pyrrolidine dopamine D3 receptor ligands with extended functionality for probing the secondary binding pocket. *Bioorganic & Medicinal Chemistry Letters*, **28**: 1897–1902.
- Palacios, JM; Camps, M; Cortes, R; Probst, A. Mapping dopamine receptors in the human brain. In: *Continuous Dopaminergic Stimulation in Parkinson's Disease*, Obeso, JA; Horowski, R; Marsden, CD (eds), part of the "Journal of Neural Transmission" book series (volume 27); Springer, Vienna, 1988; 227–235; ISBN: 978-3-7091-8954-2.
- Panula, P; Chazot, PL; Cowart, M; Gutzmer, R; Leurs, R; Liu, WLS; Stark, H; Thurmond, RL; Haas, HL, **2015**. International Union of Basic and Clinical Pharmacology. XCVIII. Histamine Receptors. *Pharmacological Reviews*, **67**: 601–655.
- Pilowsky, LS; Mulligan, RS; Acton, PD; Ell, PJ; Costa, DC; Kerwin, RW, **1997**. Limbic selectivity of clozapine. *The Lancet*, **350**: 490–491.



- Pilowsky, LS; Murray, RM; Kerwin, RW; Costa, DC; Ell, PJ; Verhoeff, N, **1992**. Clozapine, single photon emission tomography, and the D2 dopamine receptor blockade hypothesis of schizophrenia. *The Lancet*, **340**: 199–202.
- Pleuvry, BJ, **2004**. Receptors, agonists and antagonists. *Anaesthesia & Intensive Care Medicine*, **5**: 350–352.
- Povsic, TJ; Kohout, TA; Lefkowitz, RJ, **2003**.  $\beta$ -Arrestin1 mediates insulin-like growth factor 1 (IGF-1) activation of phosphatidylinositol 3-kinase (PI3K) and anti-apoptosis. *Journal of Biological Chemistry*, **278**: 51334–51339.
- Pullen, LC; Picone, M; Tan, L; Johnston, C; Stark, H, **2019**. Cognitive improvements in children with Prader-Willi Syndrome following pitolisant treatment-Patient reports. *The Journal of Pediatric Pharmacology and Therapeutics*, **24**: 166–171.
- Pulvirenti, L; Koob, GF, **2002**. Being partial to psychostimulant addiction therapy. *Trends in Pharmacological Sciences*, **23**: 151–153.
- Purser, S; Moore, PR; Swallow, S; Gouverneur, V, **2008**. Fluorine in medicinal chemistry. *Chemical Society Reviews*, **37**: 320–330.
- Pushpakom, S; Iorio, F; Eyers, PA; Escott, KJ; Hopper, S; Wells, A; Doig, A; Guilleams, T; Latimer, J; McNamee, C; Norris, A; Sanseau, P; Cavalla, D; Pirmohamed, M, **2018**. Drug repurposing: progress, challenges and recommendations. *Nature Reviews Drug Discovery*, **18**: 41-58.
- Qureshi, M; Al-Suhaimi, EA; Wahid, F; Shehzad, O; Shehzad, A, **2018**. Therapeutic potential of curcumin for multiple sclerosis. *Neurological Sciences*, **39**: 207–214.
- Ragguett, R-M; McIntyre, RS, **2019**. Cariprazine for the treatment of bipolar depression: A review. *Expert Review of Neurotherapeutics*, **19**: 317–323.
- Raible, DG; Lenahan, T; Fayvilevich, Y; Kosinski, R; Schulman, ES, **1994**. Pharmacologic characterization of a novel histamine receptor on human eosinophils. *American Journal of Respiratory and Critical Care Medicine*, **149**: 1506–1511.
- Raju, KS; AnkiReddy, S; Sabitha, G; Krishna, VS; Sriram, D; Reddy, KB; Sagurthi, SR, **2019**. Synthesis and biological evaluation of 1H-pyrrolo [2, 3-d] pyrimidine-1, 2, 3-triazole derivatives as novel anti-tubercular agents. *Bioorganic & Medicinal Chemistry Letters*, **29**: 284–290.
- Riess, O; Krüger, R, **1999**. Parkinson's disease—a multifactorial neurodegenerative disorder. *Journal of Neural Transmission. Supplementum*, **56**: 113–125.
- Rinne, JO; Anichtchik, OV; Eriksson, KS; Kaslin, J; Tuomisto, L; Kalimo, H; Röttä, M; Panula, P, **2002**. Increased brain histamine levels in Parkinson's disease but not in multiple system atrophy. *Journal of Neurochemistry*, **81**: 954–960.
- Rinne, UK; Mölsä, P, **1979**. Levodopa with benserazide or carbidopa in Parkinson disease. *Neurology*, **29**: 1584–1589.
- Rosethorne, EM; Charlton, SJ, **2011**. Agonist-biased signaling at the histamine H4 receptor: JNJ7777120 recruits  $\beta$ -arrestin without activating G proteins. *Molecular Pharmacology*, **79**: 749–757.
- Rudnick, G; Clark, J, **1993**. From synapse to vesicle: The reuptake and storage of biogenic amine neurotransmitters. *Biochimica et Biophysica Acta*, **1144**: 249–263.

- Ryoo, HL; Pierrotti, D; Joyce, JN, **1998**. Dopamine D3 receptor is decreased and D2 receptor is elevated in the striatum of Parkinson's disease. *Movement Disorders*, **13**: 788–797.
- Sabatucci, A; Tortolani, D; Dainese, E; Maccarrone, M, **2018**. In silico mapping of allosteric ligand binding sites in type-1 cannabinoid receptor. *Biotechnology and Applied Biochemistry*, **65**: 21–28.
- Sadée, W; Wang, D; Bilsky, EJ, **2005**. Basal opioid receptor activity, neutral antagonists, and therapeutic opportunities. *Life Sciences*, **76**: 1427–1437.
- Sadek, B; Saad, A; Latacz, G; Kuder, K; Olejarz, A; Karcz, T; Stark, H; Kieć-Kononowicz, K, **2016a**. Non-imidazole-based histamine H3 receptor antagonists with anticonvulsant activity in different seizure models in male adult rats. *Drug Design, Development and Therapy*, **10**: 3879–3898.
- Sadek, B; Saad, A; Sadeq, A; Jalal, F; Stark, H, **2016b**. Histamine H3 receptor as a potential target for cognitive symptoms in neuropsychiatric diseases. *Behavioural Brain Research*, **312**: 415–430.
- Sander, K; Kottke, T; Stark, H, **2008**. Histamine H3 receptor antagonists go to clinics. *Biological and Pharmaceutical Bulletin*, **31**: 2163–2181.
- Schildkraut, JJ; Kety, SS, **1967**. Biogenic amines and emotion. *Science*, **156**: 21–30.
- Schneider, CS; Mierau, J, **1987**. Dopamine autoreceptor agonists: Resolution and pharmacological activity of 2, 6-diaminotetrahydrobenzothiazole and an aminothiazole analog of apomorphine. *Journal of Medicinal Chemistry*, **30**: 494–498.
- Schreiber, SL, **2000**. Target-oriented and diversity-oriented organic synthesis in drug discovery. *Science*, **287**: 1964–1969.
- Schuetz, DA; de Witte,, WEA; Wong, YC; Knasmueller, B; Richter, L; Kokh, DB; Sadiq, SK; Bosma, R; Nederpelt, I; Heitman, LH; Segala, E; Amaral, M; Guo, D; Andres, D; Georgi, V; Stoddart, L; Hill, S; Cooke, R; De Graaf, C; Leurs, R; Frech, M; Wade, R; de Lange, E; IJzerman, A; Müller-Fahrnow, A; Ecker, G, **2017**. Kinetics for Drug Discovery: An industry-driven effort to target drug residence time. *Drug Discovery Today*, **22**: 896–911.
- Seeberger, LC; Hauser, RA, **2009**. Levodopa/carbidopa/entacapone in Parkinson's disease. *Expert Review of Neurotherapeutics*, **9**: 929–940.
- Seeman, P, **2006**. Targeting the dopamine D2 receptor in schizophrenia. *Expert Opinion on Therapeutic Targets*, **10**: 515–531.
- Seeman, P; Lee, T; Chau-Wong, M; Wong, K, **1976**. Antipsychotic drug doses and neuroleptic/dopamine receptors. *Nature*, **261**: 717–719.
- Seeman, P; Tallerico, T, **1998**. Antipsychotic drugs which elicit little or no parkinsonism bind more loosely than dopamine to brain D2 receptors, yet occupy high levels of these receptors. *Molecular Psychiatry*, **3**: 123–134.
- Segura-Aguilar, J; Paris, I; Muñoz, P; Ferrari, E; Zecca, L; Zucca, FA, **2014**. Protective and toxic roles of dopamine in Parkinson's disease. *Journal of Neurochemistry*, **129**: 898–915.
- Seppi, K; Weintraub, D; Coelho, M; Perez-Lloret, S; Fox, SH; Katzenschlager, R; Hametner, EM; Poewe, W; Rascol, O; Goetz, CG; Sampaio, C, **2011**. The Movement Disorder Society evidence-based medicine review update: Treatments for the non-motor symptoms of Parkinson's disease. *Movement Disorders*, **26**: Suppl 3: S42–S80.
- Shah, K; Lin, X; Queener, SF; Cody, V; Pace, J; Gangjee, A, **2018**. Targeting species specific amino acid residues: Design, synthesis and biological evaluation of 6-substituted pyrrolo [2, 3-d] pyrimidines

- as dihydrofolate reductase inhibitors and potential anti-opportunistic infection agents. *Bioorganic & Medicinal Chemistry*, **26**: 2640–2650.
- Shahid, M; Tripathi, T; Sobia, F; Moin, S; Siddiqui, M; Khan, RA, **2009**. Histamine, histamine receptors, and their role in immunomodulation: An updated systematic review. *The Open Immunology Journal*, **2**: 9–41.
- Shehzad, A; Islam, SU; Lee, YS. Curcumin and inflammatory brain diseases. In: *Curcumin for Neurological and Psychiatric Disorders*, Tahira Farooqui, T; Farooqui, AA (eds); Academic Press, Cambridge, MA, 2019; 437–458; ISBN: 978-0-12-815461-8.
- Shen, L-H; Liao, M-H; Tseng, Y-C, **2012**. Recent advances in imaging of dopaminergic neurons for evaluation of neuropsychiatric disorders. *Journal of Biomedicine and Biotechnology*, **2012**: DOI:10.1155/2012/259349.
- Shi, L; Javitch, JA, **2004**. The second extracellular loop of the dopamine D2 receptor lines the binding-site crevice. *Proceedings of the National Academy of Sciences of the United States of America*, **101**: 440–445.
- Shimamura, T; Shiroishi, M; Weyand, S; Tsujimoto, H; Winter, G; Katritch, V; Abagyan, R; Cherezov, V; Liu, W; Han, GW; Kobayashi, T; Stevens, R; Iwata, S, **2011**. Structure of the human histamine H1 receptor complex with doxepin. *Nature*, **475**: 65–70.
- Sibley, Lean, A de; Creese, I, **1982**. Anterior pituitary dopamine receptors. Demonstration of interconvertible high and low affinity states of the D-2 dopamine receptor. *Journal of Biological Chemistry*, **257**: 6351–6361.
- Simpson, EH; Winiger, V; Biezonski, DK; Haq, I; Kandel, ER; Kellendonk, C, **2014**. Selective overexpression of dopamine D3 receptors in the striatum disrupts motivation but not cognition. *Biological Psychiatry*, **76**: 823–831.
- Smit, MJ; Leurs, R; Alewijnse, AE; Blauw, J; van Nieuw Amerongen, GP; van de Vrede, Y; Roovers, E; Timmerman, H, **1996**. Inverse agonism of histamine H2 antagonist accounts for upregulation of spontaneously active histamine H2 receptors. *Proceedings of the National Academy of Sciences of the United States of America*, **93**: 6802–6807.
- Smits, RA; Leurs, R; de Esch, IJP, **2009**. Major advances in the development of histamine H4 receptor ligands. *Drug Discovery Today*, **14**: 745–753.
- Sokoloff, P; Giros, B; Martres, MP; Bouthenet, ML; Schwartz, JC, **1990**. Molecular cloning and characterization of a novel dopamine receptor (D3) as a target for neuroleptics. *Nature*, **347**: 146–151.
- Sriram, K; Insel, PA, **2018**. G protein-coupled receptors as targets for approved drugs: How many targets and how many drugs? *Molecular Pharmacology*, **93**: 251–258.
- Stahl, SM. *Stahl's Essential Psychopharmacology: Neuroscientific Basis and Practical Applications*; Cambridge University Press, 2013.
- Stahl, SM, **2016**. Parkinson's disease psychosis as a serotonin-dopamine imbalance syndrome. *CNS Spectrums*, **21**: 355–359.
- Stahl, SM, **2018**. Beyond the dopamine hypothesis of schizophrenia to three neural networks of psychosis: Dopamine, serotonin, and glutamate. *CNS Spectrums*, **23**: 187–191.

- Stank, L; Frank, A; Hagenow, S; Stark, H, **2019**. Talipexole variations as novel bitopic dopamine D2 and D3 receptor ligands. *MedChemComm*, **accepted**: DOI: 10.1039/C9MD00379G.
- Stark, H; Sippl, W; Ligneau, X; Arrang, JM; Ganellin, CR; Schwartz, JC; Schunack, W, **2001**. Different antagonist binding properties of human and rat histamine H3 receptors. *Bioorganic & Medicinal Chemistry Letters*, **11**: 951–954.
- Stille, G; Hippus, H, **1971**. Kritische Stellungnahme zum Begriff der Neuroleptika. *Pharmacopsychiatry*, **4**: 182–191.
- Swanson, DM; Wilson, SJ; Boggs, JD; Xiao, W; Apodaca, R; Barbier, AJ; Lovenberg, TW; Carruthers, NI, **2006**. Aplysamine-1 and related analogs as histamine H3 receptor antagonists. *Bioorganic & Medicinal Chemistry Letters*, **16**: 897–900.
- Syed, YY, **2016**. Pitolisant: First global approval. *Drugs*, **76**: 1313–1318.
- Syrovatkina, V; Alegre, KO; Dey, R; Huang, XY, **2016**. Regulation, signaling, and physiological functions of G-proteins. *Journal of Molecular Biology*, **428**: 3850–3868.
- Takahashi, H; Takano, H; Kodaka, F; Arakawa, R; Yamada, M; Otsuka, T; Hirano, Y; Kikyo, H; Okubo, Y; Kato, M; Obata, T; Ito, H; Suhara, T, **2010**. Contribution of dopamine D1 and D2 receptors to amygdala activity in human. *Journal of Neuroscience*, **30**: 3043–3047.
- Tarazi, FI; Zhang, K; Baldessarini, RJ, **2001**. Long-term effects of olanzapine, risperidone, and quetiapine on dopamine receptor types in regions of rat brain: Implications for antipsychotic drug treatment. *Journal of Pharmacology and Experimental Therapeutics*, **297**: 711–717.
- Thurmond, RL, **2015**. The histamine H4 receptor: From orphan to the clinic. *Frontiers in Pharmacology*, **6**: DOI: 10.3389/fphar.2015.00065.
- Thurmond, RL; Chen, B; Dunford, PJ; Eckert, W; Karlsson, L; La D, WP; Xu, XL; Greenspan, AJ, **2017**. Pharmacology and clinical activity of toreforant, a histamine H4 receptor antagonist. *Annals of Pharmacology and Pharmaceutics*, **2**: 1013.
- Thurmond, RL; Greenspan, A; Radziszewski, W; Xu, XL; Miao, Y; Chen, B; Ge, T; Zhou, B; Baker, DG; Pavlova, D; Ritchlin, CT; Tanaka, Y; Takeuchi, T; Smolen, JS, **2016**. Toreforant, a histamine H4 receptor antagonist, in patients with active rheumatoid arthritis despite methotrexate therapy: Results of 2 Phase II studies. *The Journal of Rheumatology*, **43**: 1637–1642.
- Torrent, A; Moreno-Delgado, D; Gómez-Ramírez, J; Rodríguez-Agudo, D; Rodríguez-Caso, C; Sánchez-Jiménez, F; Blanco, I; Ortiz, J, **2005**. H3 autoreceptors modulate histamine synthesis through calcium/calmodulin- and cAMP-dependent protein kinase pathways. *Molecular Pharmacology*, **67**: 195–203.
- Usiello, A; Baik, JH; Rougé-Pont, F; Picetti, R; Dierich, A; LeMeur, M; Piazza, PV; Borrelli, E, **2000**. Distinct functions of the two isoforms of dopamine D2 receptors. *Nature*, **408**: 199–203.
- Vauquelin, G; van Liefde, I, **2006**. Slow antagonist dissociation and long-lasting in vivo receptor protection. *Trends in Pharmacological Sciences*, **27**: 355–359.
- Venkatakrishnan, AJ; Deupi, X; Lebon, G; Tate, CG; Schertler, GF; Babu, MM, **2013**. Molecular signatures of G-protein-coupled receptors. *Nature*, **494**: 185-194.
- Vogel, R; Mahalingam, M; Lüdeke, S; Huber, T; Siebert, F; Sakmar, TP, **2008**. Functional role of the “ionic lock”—an interhelical hydrogen-bond network in family A heptahelical receptors. *Journal of Molecular Biology*, **380**: 648–655.

- Wadenberg, ML; Wiker, C; Svensson, TH, **2007**. Enhanced efficacy of both typical and atypical antipsychotic drugs by adjunctive  $\alpha 2$  adrenoceptor blockade: Experimental evidence. *International Journal of Neuropsychopharmacology*, **10**: 191–202.
- Wang, S; Che, T; Levit, A; Shoichet, BK; Wacker, D; Roth, BL, **2018**. Structure of the D2 dopamine receptor bound to the atypical antipsychotic drug risperidone. *Nature*, **555**: 269–273.
- Wang, X; Li, J; Dong, G; Yue, J, **2014**. The endogenous substrates of brain CYP2D. *European Journal of Pharmacology*, **724**: 211–218.
- Weis, WI; Kobilka, BK, **2018**. The molecular basis of G protein–coupled receptor activation. *Annual Review of Biochemistry*, **87**: 897–919.
- Wheatley, M; Wootten, D; Conner, MT; Simms, J; Kendrick, R; Logan, RT; Poyner, DR; Barwell, J, **2012**. Lifting the lid on GPCRs: The role of extracellular loops. *British Journal of Pharmacology*, **165**: 1688–1703.
- Witherow, DS; Garrison, TR; Miller, WE; Lefkowitz, RJ, **2004**.  $\beta$ -Arrestin inhibits NF- $\kappa$ B activity by means of its interaction with the NF- $\kappa$ B inhibitor I $\kappa$ B $\alpha$ . *Proceedings of the National Academy of Sciences of the United States of America*, **101**: 8603–8607.
- Wood, M; Dubois, V; Scheller, D; Gillard, M, **2015**. Rotigotine is a potent agonist at dopamine D1 receptors as well as at dopamine D2 and D3 receptors. *British Journal of Pharmacology*, **172**: 1124–1135.
- Young, RC; Mitchell, RC; Brown, TH; Ganellin, CR; Griffiths, R; Jones, M; Rana, KK; Saunders, D; Smith, IR; Sore, NE; Wilks, TJ, **1988**. Development of a new physicochemical model for brain penetration and its application to the design of centrally acting H2 receptor histamine antagonists. *Journal of Medicinal Chemistry*, **31**: 656–671.
- Zampeli, E; Tiligada, E, **2009**. The role of histamine H4 receptor in immune and inflammatory disorders. *British Journal of Pharmacology*, **157**: 24–33.

## 14 Acknowledgement

I am very grateful for the opportunities during my PhD studies and for the personal development I experienced in that time. I would like to thank my supervisor Prof Dr. Dr. h.c. Holger Stark for the opportunity to join his research group at the institute of “Pharmaceutical and Medicinal Chemistry” at the Heinrich Heine University. During my time, he was a constant source of professional expertise and new ideas for my projects and I could always seek his assistance in professional or organizational matters. I am especially grateful to him for enabling me to work within the GRK2158. The experiences and possibilities in that research environment enriched my PhD times not only interdisciplinary and interculturally but also on a personal level. In addition, I would like to thank him for the opportunity to regularly attend workshops, symposia and progress reports. I enjoyed them very much, as I got to discover many different places, expand my network and could improve on a professional level as well. Through numerous trips and exchange programs many fruitful cooperation’s have been formed that enriched my studies in his working group.

In that sense I would like to thank Prof. Dr. György Keserű for the opportunity to work with him and Dóra J. Kiss on the actions of cariprazine. The topic was highly interesting and I enjoyed the constructive, professional exchange. Furthermore, I would like to thank Dr. Christian Espinosa-Bustos for the cooperation on two projects, although we never managed to visit each other. Additional thanks for good cooperations go to Sandra Arancibia-Opazo, Cristian Salas, Angelica Fierro, Francisco Meza-Arriagada, Saleh Abu-Lafi, Azmi Adawi, Anwar Rayan, Alaa Alachkar, Dorota Łażewska, Gniewomir Latacz, Agata Siwek, Annamaria Lubelska, Ewelina Honkisz-Orzechowska, Jadwiga Handzlik, Katarzyna Kieć-Kononowicz, Bassem Sadek, Cristiana Carbone, Sara Lucia Maria Lo Russo, Enza Lacivita, Enrico Alleva, Luciano Saso, Marcello Leopoldo and Walter Adriani. For interesting and valuable lab rotations I would like to thank Prof. Dr. Evi Kostenis, Prof. Dr. Matthias Kassack and Prof. Dr. Thomas Müller, together with Dr. Lena Vogel, Dr. Alexandra Hamacher, Daniel Drießen and Nadine Horstick-Muche for my lab-rotations. I am grateful to Prof. Dr. Holger Gohlke, for co-reviewing this thesis and for the inspiring discussions we have had during my PhD time.

My PhD times were greatly improved by my colleagues that joined me in difficult times and celebrated the good times. I would like to thank Jens Hagenow, Milica Elek, Sicheng Zhong, Markus Falkenstein, Kiril Lutsenko, Sofia Slimi, Anna Affini, Lars Stank, Erika Plazas and Mariam Dubiel for a nice working atmosphere, much prosecco and professional as well as emotional support.

For an especially fun time in the practical course and in the GRK2158 my thanks go to Hjördis Brückmann. I enjoyed our time as co-assistants and learned a lot from you. Without you, my China-experience would not have been the same and I sincerely hope they send your powerbank back.

## 14 Acknowledgement

---

Although I enjoyed my time with Hjördis in the practical course a lot, I apologize to Dr. Aleksandra Zivkovic and thank her for keeping us two together, nonetheless. I thank her for all the practical skills and theoretical backgrounds she taught me, the support I experienced from her during my time and the fun we had in the practical course.

My sincere thanks go to Kathrin Grau, Stefanie Hagenow and David Reiner. Without your professional expertise, practical help and emotional support this work would have been a lot harder and I am deeply grateful for the time I got to spend with you. I thank you for all the long discussions, the practical suggestions, the assistance in the lab and even more, even longer discussions. You did not only improve my scientific progress but also supported me in many private situations. Thank you for emotional pep talks, lots of joy in the office/lab, honest opinions and the quality time we spent. Hopefully my next co-workers are as receptive as you when it comes to amusement parks, kitchen groups and musicals. Kathrin thank you for motivating me and listening to my stories about McMuffel. Steffi, thanks for introducing me to Siegrid, Faszien and the “joys” of jogging after work, but also for mousetastic adventures together with Jens. David, I thank you for our successful Christmas bakery, for introducing me to the Marlene, to boat owners and for always expanding my geography knowledge, although you knew it was hopeless.

My time in the university was greatly enriched by the GRK2158 as we joined in many lectures but also spent some quality time outside of lecture halls. Hence, I would like to thank Prof. Dr. Dr. h.c. Peter Proksch for initiating the GRK2158 and for providing us these experiences and opportunities. I would like to thank Dr. Martina Holz for the support in organizational matters but also for motivational support. Thanks for a joyful time, in and outside of the lectures, go to all student members of the GRK2158, but also the PI's that held motivation high. A special thanks goes to Nam Tran-Cong, Kim Le and Haiqian Yu for an unforgettable trip through China that I deeply enjoyed. Thanks Kim, for waiting with me, while sitting on the beach and enjoying the fireworks. Nam, please never eat Durian next to me again. Haiqian, thank you so much for guiding us over 3000 km and providing us with the best of foods from all of China.

For motivational support and nice talks between offices I would like to thank Christopher Pflieger, Anita Hübsch and Michelle Bonus.

I would like to thank my family. This work is whole-heartedly devoted to my parents, Angelika and Detlev Schank. Thank you for believing in me every day and for motivating me to always pursue my goals. Big thanks, for all the times you cheered me up and helped me to distract myself with family time, restaurants and musicals. I am grateful for your guidance and support in every step of my life. I thank Julius Schank, my brother, for spending quality time with me, motivating me and driving me home from university after long parties without questioning it. My thanks go to my grandparents,



## 14 Acknowledgement

---

Helma Schank, Josephine Gradt, Werner Schank and Hans Gradt for being role models and a constant source of motivation and inspiration. Further I would like to thank Martin, Elke, Kilian und Maximilian Schank as well as Helmut Gradt for their support.

I want to thank all of my close friends that stood by me and enriched my life after work. Thanks to Sanne Bähitz, Nicola Sellinger and Darius Rupalla for their company during my studies and for the resulting friendship. Sanne and Nicola, I thank you for the joy, the honest opinions and the backup I experience from you since a long time. Furthermore my gratitude goes towards Jana Esser. Thank you for keeping up with me and being the motivator I need. You contributed to my personal development to a great extent, although I hope you won't be the author of my memoirs. Lina Feder, I thank you for the friendship we maintained over the years, that resulted in so many good times but also helped me through rainy days. You helped me, when I needed emotional support in private matters and the job alike. I thank all the members of the Volksbühne Bergisch Neukirchen that accompanied me and cheered for me. Vanessa Schleimer, Katharina Siller, Michaela Willig, Birgit Celik, Anne-Claire Berger, Leonie Weber, Anna Feld, Daniela Magdeburg, Sonja Zarembo and Valerie Hohnl thank you for all the years of fun, support and motivation. Additionally, I would like to thank Kira, Nora and Patrick Kraft, Adam and Maggy Görtz, Marcin Golkowski, Julia Schakow, Sandra Gedrat, Stefan Seufert, Immo Weber, Cindy Frank, Patrick Lau, Christina Boenki, Jenny Wyborny, Silke Braun and Volker Frank for quality time and support.

A special thank you and heartfelt love goes to Lizzy and Askia for emotional support during studies and PhD times.

My biggest thank you goes to my beloved husband Marian Frank. I can't thank you enough for everything you did and keep doing for me. Thank you for proof-reading countless sentences during my PhD and for kicking my spirits when they were down. Be it work related or in our private life, you are my rock in the storm and the most valuable mouse detective in the whole wide world. Thank you for the love and support since the first day we met.

## **15 Declaration of academic honesty**

Ich, Frau Annika Frank, versichere an Eides statt, dass die vorliegende Dissertation mit dem Titel „From natural scaffolds to detailed drug-target interactions on biogenic amines“ von mir selbstständig und ohne unzulässige fremde Hilfe unter Beachtung der „Grundsätze zur Sicherung guter wissenschaftlicher Praxis an der Heinrich-Heine-Universität Düsseldorf“ erstellt worden ist. Außer den angegebenen Quellen und Hilfsmitteln wurden keine weiteren verwendet. Diese Dissertation wurde weder in gleicher noch in abgewandelter Form in einem anderen Prüfungsverfahren vorgelegt.

Düsseldorf, den 29.12.2019

Annika Frank

## 16 Curriculum vitae

### Contact information

Name	Annika Frank
Address	Kaarster Str. 115
City, State	41462 Neuss, Germany
Birthday, City	21.10.1990, Bergisch Gladbach, Germany
Email	A.Frank@hhu.de

### Education

[07/2016 to 12/2019]	PhD research at Heinrich Heine University, Institute of Pharmaceutical and Medicinal Chemistry, Düsseldorf  Project: From natural scaffolds to detailed drug-target interactions on biogenic amines
[since 05/2016]	Licensed pharmacists
[11/2015 to 04/2016]	Elective period at Bayer Animal Health GmbH, Monheim
[05/2015 to 10/2015]	Elective period at St. Cosmas Apotheke, Neuss
[04/2011 to 04/2015]	Heinrich Heine University Düsseldorf, Studies of Pharmacy 2015: Second degree of pharmaceutical education 2013: First degree of pharmaceutical education
[08/2001 to 08/2010]	Landrat-Lucas-Gymnasium, Leverkusen, Degree: Abitur

### Employment history

[07/2016 to currently]	Heinrich Heine University, Institute of Pharmaceutical and Medicinal Chemistry, Düsseldorf; scientific researcher
[11/2015 to 04/2016]	Bayer Animal Health GmbH, Formulation Development, Monheim; elective period
[05/2015 to 10/2015]	St. Cosmas Apotheke, Neuss; elective period

### Internships

[2014]	Scientific assistant at Heinrich Heine University, Institute of Pharmaceutical Technology, Düsseldorf
[07/2012 to 08/2012]	Pharmacy of Klinikum Leverkusen GmbH, Leverkusen
[08/2011 to 09/2011]	Sonnen Apotheke, Mettmann
[11/2010 to 12/2010]	Struwwelpeter-Apotheke, Leverkusen
[07/2010 to 08/2010]	Klinikum Leverkusen GmbH, Leverkusen
[03/2004 to 04/2004]	Bayer CropScience AG, Development, Ecotoxicology, Monheim

### Licenses, certificates

Pharmacist license

Work in heterogeneous teams (iGrad certificate)

Leading heterogeneous teams (iGrad certificate)

Projekte erfolgreich managen- Grundlagen des Projektmanagements (iGrad certificate)

Body language seminar (iGrad certificate)

### Professional affiliations

Member of the GRK2158 „Naturstoffe und Analoga gegen Therapie-resistente Tumore und Mikroorganismen: Neue Leitstrukturen und Wirkmechanismen“

04/2018 to 04/2019 student-speaker of GRK2158 PhD students

### Skills

GraphPad, Office, 3D Design software, *in vitro* assays, instrumental analytic, cell culture

### Languages

German (native), English (fluent), Spanish (basic knowledge)



---

Annika Frank

## 17 Published research

Peer reviewed and not

Frank A, Abu-Lafi S, Adawi A, Schwed JS, Stark H, Rayan A. From medicinal plant extracts to defined chemical compounds targeting the histamine H<sub>4</sub> receptor: Curcuma longa in the treatment of inflammation. *Inflammation Research* (2017), **66**: 923-929.

Frank A, Stark H. Another piece of puzzle in adjuvant treatment of inflammatory diseases with natural compounds. Science Trends. *ScienceTrends* (October 20, 2017); <https://sciencetrends.com/another-piece-puzzle-adjuvant-treatment-inflammatory-diseases-natural-compounds/>.

Brückmann H, Frank A, Reiner D, Stark H. Pharmakotherapie des Restless-Legs-Syndroms - eine detaillierte Betrachtung. *Pharmakon* (2018), **6**: 35-47.

Espinosa-Bustos C, Frank A, Arancibia-Opazo S, Salas CO, Fierro A, Stark H. New lead elements for histamine H<sub>3</sub> receptor ligands in the pyrrolo[2,3-d]pyrimidine class. *Bioorganic & Medicinal Chemistry Letters* (2018), **28**: 2890-2893.

Frank A, Kiss DJ, Keserű GM, Stark H. Binding kinetics of cariprazine and aripiprazole at the dopamine D<sub>3</sub> receptor. *Scientific Reports* (2018), **8**: 12509, DOI: 10.1038/s41598-018-30794-y.

Alachkar A, Łażewska D, Latacz G, Frank A, Siwek A, Lubelska A, Honkisz-Orzechowska E, Handzlik J, Stark H, Kieć-Kononowicz K, Sadek B. Studies on anticonvulsant effects of novel histamine H<sub>3</sub>R antagonists in electrically and chemically induced seizures in rats. *International Journal of Molecular Sciences* (2018), **19**: 3386, DOI: 10.3390/ijms19113386.

Frank A, Meza-Arriagada F, Salas CO, Espinosa-Bustos C, Stark H. Nature-Inspired pyrrolo[2,3-d]pyrimidines targeting the histamine H<sub>3</sub> receptor. *Bioorganic & Medicinal Chemistry* (2019), **27**: 3194-3200.

Drießen D, Stuhldreier F, Frank A, Stark H, Wesselborg S, Stork B, Müller TJJ. Novel meriolin derivatives as rapid apoptosis inducers. *Bioorganic & Medicinal Chemistry* (2019), **27**: 3463-3468.

Stank L, Frank A, Hagenow S, Stark H. Talipexole variations as novel bitopic dopamine D<sub>2</sub> and D<sub>3</sub> receptor ligands. *MedChemComm* (2019), epub, ahead of print: DOI: 10.1039/C9MD00379G.

Carbone C, Lo Russo SLM, Lacivita E, Frank A, Alleva E, Stark H, Saso L, Leopoldo M, Adriani W. Prior activation of 5-HT<sub>7</sub> receptors modulates the conditioned place preference with methylphenidate. *Frontiers in Behavioral Neuroscience* (2019), **13**: 208, DOI: 10.3389/fnbeh.2019.00208.

### ***Pending Publications***

Sadek B, Alachkar A, Ojha SK, Sadeq A, Adem A, Frank A, Stark H. Current issues and prospects of pentylenetetrazole-induced seizures and memory deficits in rodents - a clinically relevant experimental model for pharmacological studies. Submitted (2019).

### ***Poster***

Frank A, Stark H. A robust and versatile method for measuring dissociation kinetics of unlabelled ligands at the dopamine D<sub>2</sub> and D<sub>3</sub> receptors. *International Symposium on GPCRs and G Proteins*, Königswinter/Germany (Sept. 12-14, 2017).

Frank A, Stark H. Evaluation of ligand-target interactions at the sphingosine kinases 1, 2 and histamine H<sub>4</sub> receptors. *1<sup>st</sup> GRK2158 Symposium*, Düsseldorf/Germany (Sept. 20-23, 2017).

Zareba P, Bajda M, Lazewska D, Reiner D, Frank A, Stark H, Kieć-Kononowicz K, Malawska B. Cholinesterases inhibition of novel histamine H<sub>3</sub> receptor ligands as multifunctional ligands on Alzheimer's disease. *9<sup>th</sup> Polish Meeting on Medicinal Chemistry*, Lublin/Poland (Sept. 13-15, 2018).

Brückmann H, Zivkovic A, Frank A, Imeri F, Schwalm S, Lyck R, Engelhardt B, Pfeilschifter J, Huwiler A, Stark H. Modulation of S1P sphingolipid signaling. *2<sup>nd</sup> GRK2158 Symposium*, Beijing/China (Sept. 17-21, 2018).

Sadek B, Venkatachalam K, Zhong S, Frank A, Hagenow S, Reiner D, Stark H. The multi-targeting ligand ST-713 incorporating histamine H<sub>3</sub>R and dopamine D<sub>2</sub>R/D<sub>3</sub>R antagonist pharmacophores palliates autism like behavioral phenotypes in BTBR T<sup>+tf</sup>/J mice. *48th Annual Meeting of the European Histamine Research Society*, Krakow/Poland (May 15-18, 2019).

Frank A, Meza-Arriagada F, Salas CO, Espinosa-Bustos C, Stark H. From natural compounds to small molecules targeting the histamine H<sub>3</sub> receptors. *48th Annual Meeting of the European Histamine Research Society*, Krakow/Poland (May 15-18, 2019).

Frank A, Meza-Arriagada F, Salas CO, Espinosa-Bustos C, Stark H. Drug-optimization of nature-inspired heterocycles targeting the histamine H3 receptor. *3<sup>rd</sup> GRK2158 Symposium*, Düsseldorf/Germany (May, 25-26, 2019).

Lazewsak D, Zareba P, Hagenow S, Kaleta M, Wiecek M, Reiner D, Frank A, Malawska B, Stark H, Kieć-Kononowicz K. Azepanylhexoyl Derivatives – Histamine H3 receptor affinity, cholinesterase inhibitory activity and ADME/TOX prediction. *EFMC/ACSMEDI Medicinal Chemistry Frontiers 2019*, Krakow/Poland (June 10-13, 2019).

Elek M, Frank A, Djokovic N, Oljagic S, Zivkovic A, Nikolic K, Stark H. Pentafluorosulfanyl (SF5) moiety as promising substituent in synthesis and design of novel D2 and D3 receptors ligands. *Paul Ehrlich Euro-PhD Network & MuTaLig COST Action Meeting*, Catanzaro/Italy (June 13-15, 2019).

### **Oral Presentations**

Frank A, Stark H. Ligand-target interactions at the sphingosine kinases and histamine H4 receptors. *1<sup>st</sup> GRK2158 Symposium*, Düsseldorf/Germany (Sept. 20-23, 2017).

Frank A, Stark H. Drug-target residence time at GPCRs. *Institute Symposium*, Duesseldorf.

Frank A, Stark H. Natural compounds and small molecules targeting the histamine H4 receptor. *2<sup>nd</sup> GRK2158 Symposium*, Beijing/China (Sept. 17-21, 2018).

Reiner D, Frank A, Kiss DJ, Keserű GM, Stark H. Binding kinetics at histamine and dopamine receptor subtypes. *XVII Conference of the Polish Histamine Research Society "Biogenic Amines and Related Biologically Active Compounds"*, Lodz/Poland (Oct. 25-27, 2018).